

Universidade do Minho
Escola de Ciências

Diana Cláudia Martins da Costa Barros

**Transcriptomic and proteomic responses
to silver nanoparticles in aquatic microbes**

Transcriptomic and proteomic responses
to silver nanoparticles in aquatic microbes

Diana Cláudia Martins da Costa Barros

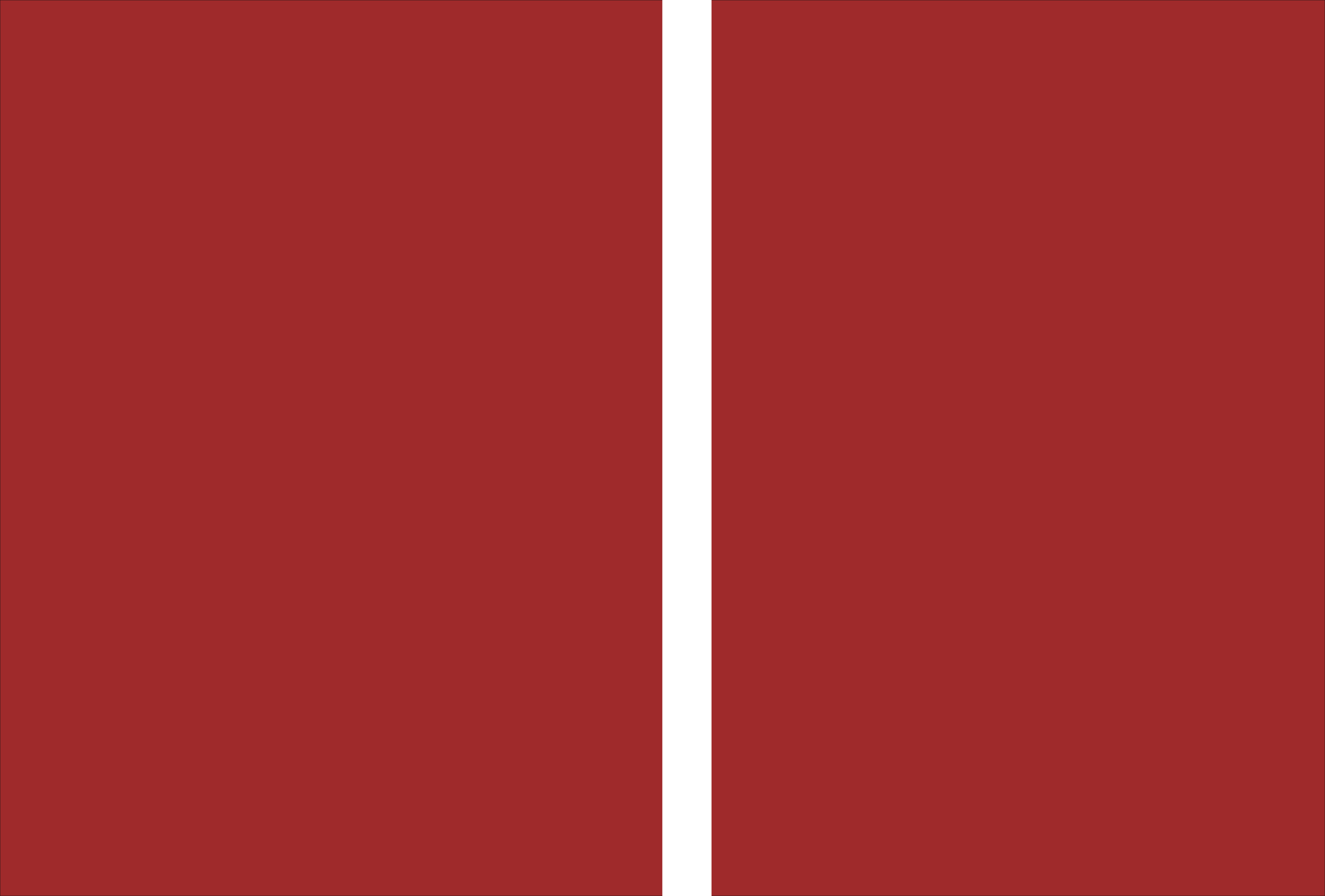
UMinho | 2019

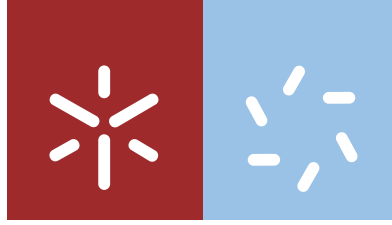
FCT
Fundação para a Ciência e a Tecnologia
MINISTÉRIO DA EDUCAÇÃO E CIÊNCIA

Cofinanciado por:



março de 2019





Universidade do Minho
Escola de Ciências

Diana Cláudia Martins da Costa Barros

**Transcriptomic and proteomic responses
to silver nanoparticles in aquatic microbes**

Tese de Doutoramento
Doutoramento em Biologia Molecular e Ambiental

Trabalho efetuado sob a orientação da
Professora Doutora Fernanda Cássio
da
Professora Doutora Cláudia Pascoal
e do
Professor Doutor Pedro M Santos

DECLARAÇÃO DE INTEGRIDADE

Declaro ter atuado com integridade na elaboração da presente dissertação. Confirmando que em todo o trabalho conducente à sua elaboração não recorri à prática de plágio ou a qualquer forma de falsificação de resultados.

Mais declaro que tomei conhecimento integral do Código de Conduta Ética da Universidade do Minho.

Universidade do Minho, Março de 2019

Nome completo: Diana Cláudia Martins da Costa Barros

Assinatura: Diana Cláudia Martins da Costa Barros

*Success is not final,
failure is not fatal,
it is the courage to continue
that counts*

Winston Churchill

Agradecimentos/acknowledgments

A tese aqui apresentada simboliza a superação de mais um desafio e é fruto do trabalho desenvolvido enquanto aluna de doutoramento ao longo de 4 anos (bem, na verdade foram 6). Confesso que foi um projecto bastante desafiador no qual aprendi sobre vários tópicos científicos e no qual adquiri habilidades e ferramentas para alcançar os objectivos propostos. No entanto, apesar de ser um marco importante no meu crescimento tanto pessoal como profissional, o esforço dedicado a esta tese não foi meramente individual. Como disse o poeta John Donne, “nenhum homem é uma ilha”, e portanto, a elaboração desta tese não teria sido possível sem a contribuição directa ou indirecta de diversas pessoas para as quais aqui ficam algumas merecidas palavras de reconhecimento.

Em primeiro lugar, gostaria de dirigir um agradecimento especial à minha orientadora, a Professora Doutora Fernanda Cássio, por mais uma vez me receber na sua equipa e aceitar a orientação deste trabalho. Agradeço os ensinamentos e disponibilidade, bem como a confiança que depositou em mim no decorrer destes anos. Também lhe fico grata pela compreensão demonstrada e palavras de carinho quando mais precisei.

À minha co-orientadora, a Professora Doutora Cláudia Pascoal, agradeço todo o apoio e disponibilidade demonstradas sempre que necessitei, assim como a colaboração no desenvolvimento e produção do trabalho científico desta tese.

Ao meu co-orientador, o Professor Doutor Pedro M Santos, que aceitou fazer parte deste projecto. Agradeço os ensinamentos e sugestões partilhados no decorrer deste percurso e principalmente a sua contribuição no trabalho desenvolvido no capítulo 2.

To Arunava I would like to address a very special acknowledgment. There aren't enough words to express my gratitude. Thanks for the endless support, all fruitful advices (scientific or not), everything you taught me, your friendship and for always being there.

Às anteriores e ao atual Directores do Departamento de Biologia da Universidade do Minho, a Prof^a Célia Pais, a Prof^a M^a João Sousa e o Prof. Hernâni Gerós, respectivamente, à anterior e atual Directoras do Centro de Biologia Molecular e Ambiental (CBMA), a Prof^a Cândida Lucas e a Prof^a Fernanda Cássio, respectivamente, e à anterior e atual Directoras do Programa Doutoral em Biologia Molecular e Ambiental (PDBMA), a Prof^a Manuela Côrte-Real e a Prof^a M^a João Sousa, por me receberem e fornecerem os recursos para o desenvolvimento do meu trabalho de doutoramento.

A todas as pessoas do Departamento de Biologia, em especial ao pessoal técnico pela disponibilidade e prontidão com que sempre me auxiliaram.

A todos os colegas com os quais partilhei o Lab. da Biodiversidade, a todos os que vieram e partiram e que de alguma forma acompanharam o meu percurso. Não vou enumerar pessoas, porque foram várias, e todas, de uma maneira ou de outra proporcionaram um ambiente de convívio e amizade. Muito obrigada a todos pelos bons momentos partilhados!

Agradeço também à minha família que, de uma forma ou de outra, ajudou a moldar-me ao longo de toda a minha vida.

Um agradecimento muito especial aos meus pais Victor e Madalena e à minha irmã Patrícia. Apesar de pouco compreenderem o que fazia, apoiaram-me incondicionalmente e ajudaram-me em tudo o que podiam, e sempre com um sorriso mesmo apesar dos atrasos e de todos os feriados e fins-de-semana passados a trabalhar. Obrigada por estarem sempre presentes e por me darem asas para voar e atingir os meus sonhos e objectivos. Obrigada por todo o vosso Amor e por nunca deixarem de acreditar em mim, mesmo quando eu própria mais duvidava. Mas, mais importante que o vosso apoio é deixar-vos orgulhosos com o resultado da oportunidade que me proporcionaram. AMO-VOS!!!

Por fim, um agradecimento muito especial ao meu Amor Hugo. Obrigada pelo carinho, dedicação, paciência e compreensão. Foi um longo caminho, cheio de altos e baixos, árduo e repleto de dúvidas mas, o teu apoio foi muito importante para enfrentar este grande desafio. Muito obrigada!

Este trabalho foi financiado principalmente pela Fundação para a Ciência e Tecnologia (FCT), Portugal, através da bolsa de doutoramento SFRH/BD/80407/2011 e dos projetos PTDC/AAC-AMB/121650/2010 (NANOECOTOX), PTDC/BIA-BMA/30922/2017 (EMERGEMIX) e NORTE-01-0145-FEDER-000009 (EcoAgriFood) financiados pela FCT e pelo Fundo Europeu de Desenvolvimento Regional (FEDER), através do COMPETE2020 - Programa Operacional Regional Competitividade e Internacionalização (POCI) e do Programa Operacional Regional Norte de Portugal (NORTE 2020). O trabalho foi também apoiado pelo programa estratégico UID/BIA/04050/2019 (POCI-01-0145-FEDER-007569) financiado por fundos através da FCT I.P. e pelo FEDER, através do COMPETE2020.

Abstract

Silver nanoparticles (AgNPs) are presently among the most widely used nanomaterials. With the extraordinary advances in nanotechnologies, enormous amounts are expected to be released into the environment and to reach freshwaters. The inherent antimicrobial properties of silver ions (Ag^+) has raised concern on whether natural microbiota can be affected in the same way as pathogenic microbes. Moreover, the mechanisms of toxicity of AgNPs remain unclear particularly the discrimination of the role of Ag^+ released from AgNPs in toxicity is not fully elucidated. We assessed the impacts of AgNPs and Ag^+ based on omic approaches and on the activities of selected antioxidant enzymes in two aquatic fungal ecotypes of *Articulospora tetracladia*, one isolated from a non-polluted stream (At72) and the other from a metal-polluted stream (At61), and in the bacterial strain *Pseudomonas* sp. M1 (PsM1), isolated from a metal-polluted stream. At72 was the most sensitive to AgNPs, whereas PsM1 was the most tolerant one. These results were supported by data from NP characterization, which showed increased particle stability and less agglomeration in the presence of At72 than in the presence of the other tested microbes. Our results also reinforced the role of antioxidant enzymes against oxidative stress induced by both Ag forms; enzyme activities were higher i) in At72 than in At61 and ii) against Ag^+ than AgNPs. Omic responses to equitoxic and environmentally realistic levels of AgNPs and Ag^+ suggested different mechanisms of toxicity since distinct profiles of protein and gene expression were unveiled. In addition, gene ontology enrichment analysis further unravelled the biological processes associated with different adaptive responses in the metabolic, energetic and stress pathways which allowed discerning the effects of AgNPs from those of Ag^+ . For instance, proteomics revealed that DNA repair, vesicle-mediated transport and protein degradation were the processes more associated with At72 responses, while redox homeostasis, energy production, ascospore formation and nucleic acids metabolism were mainly associated with the responses of At61. In PsM1, chaperones, transmembrane transporters, as well as proteins related to biofilm formation and pathogenesis were pointed as potential biomarkers of the stress induced by Ag^+ and/or AgNPs. On the other hand, transcriptomics strongly suggested cellular membranes as the major targets of AgNPs and Ag^+ and highlighted the processes of energy production and of steroid metabolism in response to AgNPs and Ag^+ , respectively. Furthermore, the negligible amount of Ag^+ released from AgNPs suggests that toxicity of AgNPs was mainly attributed to the particulate form of silver.

Resumo

As nanopartículas de prata (AgNPs) estão atualmente entre os nanomateriais mais amplamente usados. Com o desenvolvimento das indústrias com base nanotecnológica, é esperado que quantidades elevadas de nanomateriais sejam libertadas no ambiente, das quais uma fração considerável deverá atingir os ecossistemas de água doce. As propriedades antimicrobianas inerentes aos iões de prata (Ag^+), levaram ao aumento das preocupações sobre a possibilidade da microbiota natural poder ser afetada da mesma forma que os microrganismos patogénicos. Além disso, os mecanismos de toxicidade das AgNPs ainda não estão bem esclarecidos, particularmente a questão da discriminação do papel dos Ag^+ lixiviados das nanopartículas na toxicidade. Neste estudo, os impactos das AgNPs e Ag^+ foram avaliados com base em abordagens ómicas e nas atividades de enzimas antioxidantes em dois ecótipos do fungo aquático *Articulospora tetracladia*, uma estirpe isolada de um rio não poluído (At72) e outra de um rio poluído com metais (At61), e na estirpe bacteriana *Pseudomonas* sp. M1 (PsM1), isolada de um rio poluído com metais. At72 foi o mais sensível a AgNPs, enquanto PsM1 foi a mais tolerante. Os resultados foram sustentados por dados da caracterização das NPs, que mostraram maior estabilidade de partículas e menor aglomeração na presença de At72 que na presença dos outros microrganismos. Os resultados reforçaram o papel das enzimas antioxidantes contra o stresse oxidativo induzido por ambas as formas de Ag; as atividades enzimáticas foram maiores i) em At72 do que em At61 e ii) contra Ag^+ do que AgNPs. As respostas ómicas a níveis equitóxicos dos compostos e em concentrações ambientalmente realistas de AgNPs e Ag^+ sugeriram diferentes mecanismos de toxicidade, uma vez que revelaram perfis distintos de expressão proteica e génica. Além disso, a análise de enriquecimento de ontologia génica desvendou processos biológicos associados a diferentes respostas adaptativas nas vias metabólica, energética e de stresse, o que permitiu discernir os efeitos das AgNPs dos de Ag^+ . Por exemplo, a proteómica revelou que a reparação do ADN, o transporte vesicular e a degradação proteica foram os processos mais associados às respostas de At72, enquanto a homeostasia redox, a produção de energia, a formação de ascósporos e o metabolismo dos ácidos nucleicos foram principalmente associados às respostas de At61. Em PsM1, as chaperonas, os transportadores transmembranares, assim como as proteínas relacionadas com a formação de biofilme e patogénese são apontados como potenciais biomarcadores do stresse induzido por Ag^+ e/ou AgNPs. Por outro lado, a transcriptómica apontou as membranas celulares como os alvos principais das AgNPs e Ag^+ e destacou os processos de produção de energia e do metabolismo de esteroides na resposta à exposição a AgNPs e Ag^+ , respectivamente. Além disso, a insignificante quantidade de Ag^+ libertada das AgNPs sugeriu que a toxicidade das AgNPs esteve principalmente associada à forma particulada da prata.

Table of Contents

Chapter 1

General introduction	1
1.1. Nanoscience and nanotechnology: history and current advances	3
1.2. Environmental exposure of NPs	7
1.2.1. Emission to environmental compartments	7
1.2.2. Accumulation of NPs in aquatic environments	8
1.2.3. Exposure of aquatic life to NPs	10
1.3. The importance of freshwaters	11
1.4. Toxicity of NPs to freshwater biota	13
1.4.1. Short-term versus long-term effects	13
1.4.2. Sensitivity of freshwater organisms to NPs	14
1.4.3. Action mechanisms of NPs	17
1.5. Oxidative stress biomarkers: enzymatic and non-enzymatic	24
1.6. Emerging field of environmental “OMICs”	26
1.6.1. Proteomics	28
1.6.2. Transcriptomics	30
1.7. Aim and outline of the thesis	32
References	33

Chapter 2

<i>Proteomics and antioxidant enzymes reveal different mechanisms of toxicity induced by ionic and nanoparticulate silver in bacteria</i>	49
Abstract	51
2.1. Introduction	52
2.2. Materials and methods	54
2.2.1. Bacterial exposure to Ag ⁺ and AgNPs	54
2.2.2. Characterization of nanoparticles and quantification of dissolved silver	55
2.2.3. Preparation of cell-free extracts and protein quantification	56
2.2.4. Antioxidant enzyme activities	56
2.2.5. Protein denaturation, SDS-PAGE and gel staining	57
2.2.6. SWATH-MS analysis	58
2.2.7. Statistical analyses	59

2.3. Results	60
2.3.1. Characterization of AgNPs and quantification of dissolved Ag ⁺	60
2.3.2. Effects of Ag ⁺ and AgNPs on the growth of <i>Pseudomonas</i> sp. M1	61
2.3.3. Effects of Ag ⁺ and AgNPs on the activity of antioxidant enzymes	62
2.3.4. Effects of Ag ⁺ and AgNPs on the proteome of <i>Pseudomonas</i> sp. M1	63
2.3.5. Relationships between oxidative stress enzymes and related proteins	65
2.4. Discussion	66
References	71

Chapter 3

Proteomic and antioxidant enzymatic responses to nanoparticulate and ionic silver unravel distinct mechanisms of toxicity in two aquatic fungal ecotypes **77**

Abstract	79
3.1. Introduction	80
3.2. Materials and methods	82
3.2.1. Fungal ecotypes	82
3.2.2. Preparation of AgNP suspensions and Ag ⁺ solution	82
3.2.3. Characterization of nanoparticles	82
3.2.4. Quantification of silver	83
3.2.5. Exposure conditions and effective sublethal concentrations	83
3.2.6. Fungal biomass, preparation of mycelia-free extract and protein quantification	84
3.2.7. Antioxidant enzyme activities	84
3.2.8. Denaturation of proteins and SDS-PAGE	85
3.2.9. SWATH-MS analysis	86
3.2.10. Statistical analyses	87
3.3. Results	88
3.3.1. Characterization of AgNPs and quantification of Ag	88
3.3.2. Effects of AgNPs and Ag ⁺ on the fungal growth	89
3.3.3. Effects of AgNPs and Ag ⁺ on antioxidant enzymatic biomarkers	89
3.3.4. Effects of AgNPs and Ag ⁺ on fungal proteomes	90
3.3.5. Relationship between proteomic and enzymatic responses to oxidative stress	97
3.4. Discussion	99
References	104

Chapter 4	
<i>Transcriptomics reveal different mechanisms of toxicity to nanoparticulate and ionic silver in aquatic fungi</i>	109
Abstract	111
4.1. Introduction	112
4.2. Materials and methods	113
4.2.1. Preparation of AgNPs	113
4.2.2. Fungal growth	113
4.2.3. RNA extraction	114
4.2.4. Library preparation and sequencing	114
4.2.5. Transcriptome assembly and annotation	114
4.3. Results and discussion	115
4.3.1. Transcriptome sequencing and assembly	115
4.3.2. Transcriptional responses to AgNPs and Ag ⁺	116
References	123
Chapter 5	
<i>General discussion and future perspectives</i>	129
General discussion and future perspectives	131
References	140
Appendix	145

List of Figures

Chapter 1		
Figure 1.1	Applications of nanoparticles	4
Figure 1.2	Top-down and bottom-up approaches in nanotechnology	5
Figure 1.3	Toxicity of AgNPs as a function of nanoparticle size	20
Figure 1.4	Nanoparticle interaction with cells: intracellular targets and nanotoxicological mechanisms	21
Figure 1.5	Interactions of toxicants, nanoparticles and organisms	24
Figure 1.6	Milestones of the development of HTS over the last decades	28
Chapter 2		
Figure 2.1	Effects of AgNPs or Ag ⁺ on the specific growth rate of <i>Pseudomonas</i> sp. M1	61
Figure 2.2	Activities of SOD, GST, GPx and CAT in <i>Pseudomonas</i> sp. M1	63
Figure 2.3	Heatmap and clustering analysis of the proteins with significant variation and Gene Ontology enrichment analysis in <i>Pseudomonas</i> sp. M1	64
Figure 2.4	PCA of proteins involved in antioxidant activities and activities of antioxidant enzymes in <i>Pseudomonas</i> sp. M1	65
Chapter 3		
Figure 3.3	Activities of SOD, GST, GPx and CAT in fungi	90
Figure 3.2	Venn diagram of proteins significantly altered and percentage of significantly altered proteins, which content increased or decreased in fungi	91
Figure 3.4	Heatmap and clustering analysis of the proteins with significant variation and Gene Ontology enrichment analysis in At72	93-94
Figure 3.4	Heatmap and clustering analysis of the proteins with significant variation and Gene Ontology enrichment analysis in At72	95-96
Figure 3.5	PCA of proteins involved in antioxidant activities and activities of antioxidant enzymes in fungi	98
Chapter 4		
Figure 4.1	Differential gene expression profile	116
Figure 4.2	Clusters of differential expressed genes	117-118
Figure 4.5	Histograms of gene ontology classification	119
Chapter 5		
Figure 5.1	Total number of identified and significantly altered proteins	134
Figure 5.2	Heatmaps of the proteins with significant variation	135
Figure 5.3	Most relevant biological processes highlighted by GO enrichment analysis of the proteins with significant variation	137

List of Tables

Chapter 1

Table 6.1	Enzymatic and non-enzymatic antioxidant systems	25
------------------	---	----

Chapter 2

Table 2.7	Characterization of AgNPs (HDD, Pdl and zeta potential) and quantification of Ag	61
------------------	--	----

Table 2.2	EC ₁₀ and EC ₂₀ of AgNPs and of Ag ⁺ in <i>Pseudomonas</i> sp. M1	62
------------------	--	----

Chapter 3

Table 3.1	Characterization of AgNPs (HDD, Pdl and zeta potential) and quantification of Ag	88
------------------	--	----

Table 3.2	EC ₂₀ of AgNPs and of Ag ⁺ in fungi (At72 and At61)	89
------------------	---	----

Appendix

Chapter 2

1	Table S2.1 Enzyme activity fold-changes of SOD, GST, GPx and CAT in <i>Pseudomonas</i> sp. M1	147
2	Detailed information regarding protein identification by mass spectrometry in <i>Pseudomonas</i> sp. M1	148-150
3	Figure S2.1 Effects of the Ag ⁺ -ligand cysteine on growth of <i>Pseudomonas</i> sp. M1 in MM medium	151
4	Figure S2.2 Percentages of significantly altered proteins in <i>Pseudomonas</i> sp. M1	152
5	Figure S2.3 Protein networks in <i>Pseudomonas aeruginosa</i> adapted from STRING database	153
6	Table S2.2 Total identified proteins by SWATH-MS/MS from SDS-PAGE in <i>Pseudomonas</i> sp. M1	154-160

Chapter 3

7	Figure S3.1 Effects of AgNPs or Ag ⁺ on the specific growth rate of fungi	161
8	Figure S3.2 Fungal biomass produced by fungi in presence of nitrate	162
9	Table S3.1 Specific activities of SOD, GST, GPx and CAT in fungi	163
10	Detailed information regarding protein identification by mass spectrometry in fungi	164-166
11	Table S3.2 Total identified proteins by SWATH-MS/MS from SDS-PAGE in At72	167-187
12	Table S3.3 Total identified proteins by SWATH-MS/MS from SDS-PAGE in At61	188-216

Chapter 4

13	Table S4.1 Transcriptome sequencing, filtering and rRNA reads metrics	217
14	Description of clusters from Figure 4.2	218
15	Table S4.2 Gene ontology enrichment of differentially expressed genes	219-221
16	Figure S4.1 Heatmap of gene ontology enrichment of differentially expressed genes	222
17	Figure S4.2 Histograms of gene ontology classification	223

Chapter 1

General introduction

1.1. Nanoscience and nanotechnology: history and current advances

The word “nano” has become increasingly familiar, but even those who do not know its meaning recognize that it refers to something very small. It derives from the Greek “*nanus*”, signifying “dwarf” and was officially endorsed in 1960 as a standard unit prefix by the International System (SI).

The technology at extremely small scale, i.e. at the nanoscale, involves physical, chemical and biological knowledge and it is based on the manipulation of individual atoms and molecules to design and create particles, materials, structures, devices and systems whose size and/or shape range between 1-100 nm. The underlying science is called nanoscience.

Richard Zsigmondy, the 1925 Nobel Prize Laureate in Chemistry, was the first to coin the concept of “nanometer” to characterize/measure the size of particles such as gold (Au) colloids using a microscope (Zsigmondy 1909). In 1959, at the American Physical Society meeting at Caltech, Richard P. Feynman, who won the Nobel Prize in Physics in 1965, planted the seeds of a new era in science and technology. In his famous lecture entitled “*There’s Plenty of Room at the Bottom*” he introduced the concept of manipulating matter at the atomic level (Feynman 1960), but only over a decade later the term “nanotechnology” was coined for the first time by Norio Taniguchi (Taniguchi 1974). In 1981 the development of the scanning tunnelling microscope allowed to “see” individual atoms, and nanotechnology was publicly disseminated by Kim Eric Drexler, who used the term in his book “*Engines of Creation: The Coming Era of Nanotechnology*” (Drexler 1986).

Although handling of nanoscale materials (NMs) or particles (NPs) has occurred throughout human history (e.g. iron oxide nanoparticles in Maya blue paint during ~800 AD, José-Yacamán et al 1996; gold-silver alloyed nanoparticles in the Roman Lycurgus during ~400 AD, Freestone et al 2007), it dramatically increased during the industrial revolution.

Nanotechnology is rapidly maturing with more than 1000 claimed nanoproducts and nanodevices already in the market (Wilson 2012). The unique properties of nanoscale products are being extensively exploited for commercial applications and for novel performance that benefits society. Thanks to both academia and industry efforts, nanoscale-based products are linked to numerous areas including medicine (Dong and Feng 2007), cosmetics (Lens 2009), renewable energies (Wei et al 2008), environmental remediation (Tungittiplakorn et al 2004), and electronic devices (Kachynski et al 2008) (Fig.

1.1). Overall, although the meaning of nanotechnology varies from field to field, a search in the scope of “nano” yields more than 350,000 research and review articles (Scopus.com, March 2019).

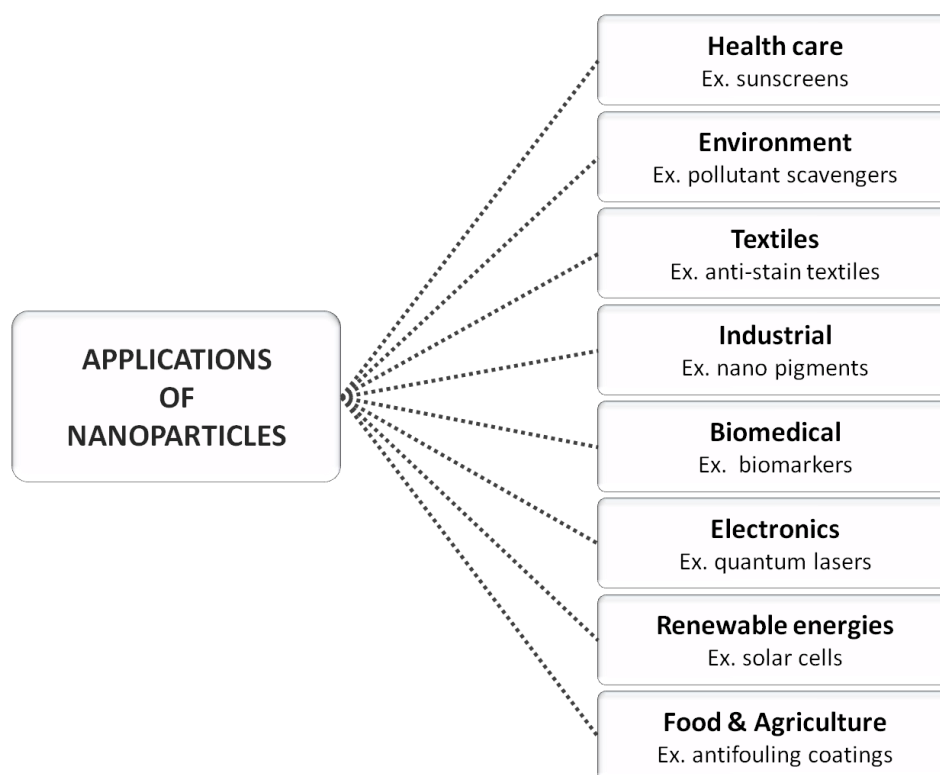


Figure 1.1 Applications of nanoparticles (adapted from Tsuzuki 2009).

Nanotechnology is commonly employed to create materials with fundamentally new properties and functions. However, in opposite to NPs purposely created by humans (anthropogenic), they can also be produced in many natural processes including dust storms, photochemical and biogenic reactions, volcanic eruptions, forest fires, and rock erosion.

To date, several methods can be applied to create NPs, however they are divided into two main approaches namely the top-down approach and the bottom-up approach (Fig. 1.2). Based on the operation, protocol and reaction conditions these are further divided into various classes. The top-down synthesis employs a destructive methodology in which larger structures are reduced in size to the nanoscale while maintaining their original properties without atomic-level control (e.g. laser ablation).

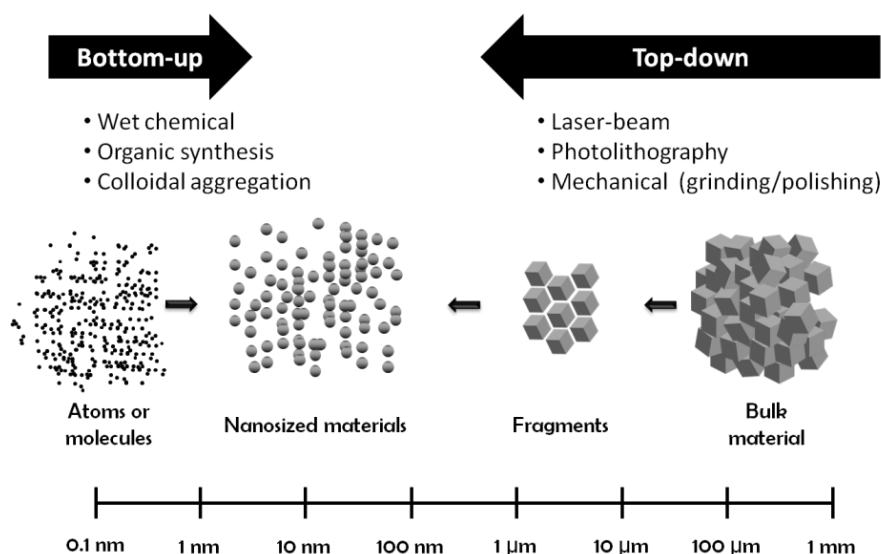


Figure 1.2 Top-down and bottom-up approaches in nanotechnology (adapted from Adams et al 2013, Runowski 2014 and Khan et al 2017).

The process of engineering NPs from relatively simpler substances such as atoms or molecular components through assembly constitutes the bottom-up approach, also designated as “molecular nanotechnology” or “molecular manufacturing” (Khan et al 2017). Biogenic and environmental friendly bottom-up synthesis of NPs was also proposed, attracting many scientists due to the feasibility and less toxic nature of processes, which are considered further economical. These green processes take advantage of biological systems such as bacteria, yeast, fungi, plants and even human cells to accomplish the synthesis of NPs (Parveen et al 2016).

The main differences between NPs and their bulk or dissolved counterparts are the increased surface area per unit mass and discontinuous behaviour of delocalized surface electrons by quantum confinement effects. These factors induce changes in chemical, mechanical, optical, electric, and magnetic properties causing significantly different reactivity/behaviour of nanomaterials (Buzea et al 2007).

According to the physico-chemical properties of NPs, different characterization techniques involving different methods and instruments have been developed. These are mainly divided into morphological, structural, particle size/surface area and optical characterization. For morphological analysis of NPs, the most relevant are microscopic techniques such as polarized optical microscopy (POM) and scanning/transmission electron microscopy (SEM/TEM, respectively). To study structural properties of NPs, common

techniques are X-ray diffraction (XRD), energy dispersive X-ray (EDX), X-ray photoelectron spectroscopy (XPS), infrared (IR), Raman spectroscopy, Brunauer-Emmett-Teller (BET) and Zeta size analyser. The size of NPs is estimated by SEM, TEM, XRD, atomic force microscopy (AFM) and dynamic light scattering (DLS). Optical properties of NPs including absorption, reflectance, luminescence and phosphorescence are usually examined in ultraviolet-visible (UV-Vis), photoluminescence (PL) and null ellipsometer instruments. The UV/Vis- diffuse reflectance spectrometer (DRS) can also be used to measure the optical absorption, transmittance and reflectance of NPs. In addition, for elemental composition analysis, inductively coupled plasma mass or optical emission spectrometry (ICP-MS or ICP-OES) and flame-atomic absorption spectroscopy (flame-AAS) are usually employed. Detailed information can be found in Khan et al (2017). Nevertheless, a combination of multiple techniques as well as the development of new ones might be required for complete and consistent characterization of NPs and reduction of sampling errors in complex matrixes.

Classification of NPs usually relies on their dimensionality, morphology, composition, uniformity and agglomeration, however, a distinction between fixed nanometer-scale NPs and free NPs should not be dismissed. Regarding dimensionality, depending on the overall shape, nano-based products can be zero-dimensional (0D, e.g. quantum dots - QDs), 1D (e.g. nanowires), 2D (e.g. nanodisks) or 3D (e.g. nanoflowers). Often, only 1D or 2D are at the nanoscale (e.g. quantum wells or nanowires), but occasionally all three dimensions are at the nanoscale (e.g. QDs or nanocrystals). NPs morphology takes into account general aspect ratio, differentiating between particles with high- or low-aspect ratio together with sphericity and flatness characteristics. Concerning composition, NPs can be of single-composition most of which are synthesized or of several constituent materials often found in nature in agglomerates. With regard to uniformity and agglomeration NPs can occur as dispersed aerosols, as suspensions/colloids or in an agglomerate state (Tiwari et al 2012). Based on physical and chemical characteristics, NPs are also categorized into carbon-based (e.g. fullerenes and carbon nanotubes - CNTs), metal (e.g. gold and silver), including metal oxides and zerovalent metals, ceramics (e.g. nanotrusses), semiconductor (e.g. QDs), polymeric (e.g. dendrimers) and lipid-based (e.g. lipidic nano-pores) NPs.

1.2. Environmental exposure to NPs

1.2.1. Emission to environmental compartments

Concern about the potential human and environmental health risks of NPs began in the early 2000s due to the increasing application of engineered nanoparticles (ENPs) in industrial and commercial products, which led to a diversification in emission sources into the environment. Environmental scientists have been challenged in multiple ways ranging from NP characterization and fate in complex matrixes to individual and effects of NPs in mixtures in the existing environmental compartments.

With regard to emission scenarios, NPs can enter the environment along their life cycle in three phases: 1) during production of raw material or nano-based products; 2) during use; and 3) after disposal of NP-containing products. However, it is estimated that most of the NPs are emitted during use phase or after disposal (Keller et al 2013). These emissions can occur either directly to the environment or indirectly via a technical system such as wastewater treatment plants (WWTPs) or landfills. In addition, emissions can be controlled by ageing or weathering, the fate of the NP during use, and the waste management system (Bundschuh et al 2018). Current material flow analysis models indicate that most of the NPs derived from consumer products will be released into sewer systems and reach WWTPs or eventually directly discharged into receiving waters (Gottschalk and Nowack 2011). However, global estimation of NP emissions (release pattern and mass) largely depends on their type and application. For instance, the dominating emission pathways of titanium dioxide NPs (TiO₂NPs), which are mostly used in cosmetics and in housing and construction, occur via wastewater. During wastewater treatment, TiO₂NPs accumulate in sewage sludge and are ultimately deployed onto soils and landfills. Zinc oxide NPs (ZnONPs), which are mainly employed in cosmetics, electronics and medicine are, like for TiO₂NPs, emitted via wastewater. ZnONPs accumulate in sediments, in natural and urban soil and at landfills (Mueller and Nowack 2008). CNTs and silver NPs (AgNPs) are both predominantly released via production and use. AgNPs have been included in numerous consumer products, including textiles, medical products, domestic appliances, food containers, cosmetics, paints and others mainly due to the antimicrobial properties of silver (Swathy et al 2014). The release of AgNPs into the environment occurs mainly via wastewaters and effluents. Then, AgNPs are retained in sewage sludge which can often be

used as fertilizer for agricultural soils. With surface runoff AgNPs can then be transferred to aquatic system. WWTP sludge can also be sent to landfills resulting in AgNPs entering into aquatic systems (Blaser et al 2008). Around 90% of CTNs, which are used in electronic devices and thermal materials, are accumulated in landfills followed by ca. 10% in soils and <1% in sediments and air (Sun et al 2016).

Overall assessment of ENP emissions shows that landfills (about 63-91%) and soils (around 8-28%) take the largest portion followed by emissions into the aquatic environment and air (7 and 1.5%, respectively, of the production volumes; Keller et al 2013). The detection of nanoscale palladium particles unintentionally produced was also reported (Prichard and Fisher 2012). In addition, the emission of NPs can also be intentional due to their direct application in environmental compartments (e.g. nanopesticides into agricultural fields, Kah 2015). Detection of NPs in aquatic ecosystems has however been hindered by the lack of appropriate analytical techniques (von der Kammer et al 2012) challenging nanoecotoxicologists by limiting their studies on the fate and behaviour of NPs in surface waters.

1.2.2. Accumulation of NPs in aquatic environments

NPs surreptitiously enter the environment through water, soil and air during various human activities; however, after emission, aquatic ecosystems are likely to serve as terminal repositories with an average reported concentration around 10^7 - 10^8 L⁻¹ (Lau 2011). Moreover, the occurrence of NPs in surface waters can also be due to natural biogenesis (e.g. AgNPs by *Fusarium oxysporum*, Durán et al 2005). Because natural NPs (NNPs) and ENPs share similarities, NNPs behaviour may provide evidences of the fate of ENPs after their release in surface waters. Depending on the type of NP, advanced models estimate NP concentrations in surface waters to be lower (ng L⁻¹ or µg L⁻¹ range). For instance, analytical studies revealed that concentrations of TiO₂NPs in surface water are between 3 ng L⁻¹ and 1.6 µg L⁻¹. For AgNPs, the mean of AgNP concentration in surface waters of European Union (EU) was estimated in 1.5 ng/L (Q_{0.15} 0.4 µg/L to Q_{0.85} 2.8 ng/L) in 2014 (Sun et al 2016). However, these models hardly consider NP-specific fate mechanisms. Once in the environment, NPs are subject to transformations that can affect their stability, mobility, behaviour, and ultimately, their fate. Such transformations are likely to be influenced by NP surface properties (e.g. area and charge) as well as by

environmental conditions (e.g. pH, ionic strength or the presence of organic matter) (Wagner et al 2014). For instance, high ionic strength results in aggregation of NPs that may decrease their toxicity to organisms (Jin et al 2010). Other NP inherent factors such as size, shape, crystal structure and coating should also be considered. The most important processes affecting the fate of NPs in aquatic ecosystems are agglomeration and aggregation, dissolution, redox reactions and transformation into new solid phases (Klaine et al 2008, Nowack and Bucheli 2007). Agglomeration or aggregation of NPs leads to larger particles that may be removed from the water column and transported to the sediments. Bioavailability of NPs and their dissolution behaviour may also be different for larger agglomerated particles (Jiang et al 2009). Transformations such as aggregation, oxidation and dissolution are the most reported changes for AgNPs (Behra et al 2013). For example, charge stabilized AgNPs (i.e. citrate-coated) are more unstable than sterically stabilized AgNPs (i.e. polyvinylpyrrolidone: PVP or polyethylene glycol: PEG) (Tejamaya et al 2012) and thus, present different toxicity (see Angel et al 2013). Furthermore, interaction of NPs with many inorganic (e.g. Cl^- , S^{2-}) and organic (e.g. humic substances) ligands can enhance or reduce their toxicity to aquatic organisms (e.g. see Choi et al 2009).

As soon as NPs are released into the environment, they start to transform into other species, which can coexist in the environment and jointly pose a risk to biota (e.g. for AgNPs, Zhang et al 2018). In addition to fate and behaviour, the environmental transformation of NPs is also intimately related to alterations in NPs bioavailability and transport which can in turn influence their uptake by organisms and potential toxicity. For instance, the residence times of AgNPs can increase in the presence of organic constituents in aquatic ecosystems (Cumberland and Lead 2009), but by preventing their attachment to organisms acting as a physical barrier, organic constituents can decrease the toxicity of AgNPs (Gao et al 2012). This demonstrates the influence of environmental conditions of aquatic ecosystems on the bioavailability and toxicity of NPs.

Moreover, NPs are more stable in freshwater than in seawater. Due to high natural organic matter (NOM) content, many NPs, particularly metal and metal oxide NPs, are less likely to aggregate. As with aggregation, sedimentation occurs also more quickly in seawater than in other natural waters. Consequently, particles are likely to remain suspended for extended lengths of time leading to higher exposure of freshwater species (Garner and Keller 2014). Dissolution of NPs can decrease their hydrodynamic diameter and in turn

increase their toxicity (Li et al 2010). However, this process is slower in freshwaters meaning that NPs remain suspended in nano form for significant periods of time leading to high exposure of aquatic species to particulate rather than dissolved NPs. Apart from few exceptions (e.g. AgNPs), NPs tend to sediment quickly in freshwaters leading to high exposure of benthic species to particulate rather than dissolved NPs (Gerner and Keller 2014). An exception are ZnONPs which are predicted to dissolve rapidly in seawater and freshwater.

1.2.3. Exposure of aquatic life to NPs

Once in aquatic compartments, the uptake of NPs by aquatic organisms can occur directly from water (either from sediments or suspended particulate matter) or indirectly via diet from food sources. Routes for uptake of NPs are further defined by the organism's physiology and the ability of NPs to overcome the cells forming the environment-organism barriers.

For example, fish and molluscs can uptake NPs through the respiratory system (e.g. gills). Although cellular uptake of NPs is difficult to confirm *in vivo*, it was demonstrated to occur for AgNPs in rainbow trout (*Oncorhynchus mykiss*, Farkas et al 2011). After incorporation, NPs may even translocate within the body to various organs and tissues (Farkas et al 2011, Kashiwada 2006). Filter feeders (e.g. crustaceans, forage fishes and aquatic molluscs) can be particularly exposed to dispersed NPs in the water column, mainly if NPs are incorporated into aggregates compared to those freely suspended since capture and ingestion is more efficient (Ward and Kach 2009). Considering the common phenomenon of NP agglomeration/aggregation and sedimentation in aquatic ecosystems, organisms living in sediments or feeding on biofilms may be particularly prone to NP exposure and further uptake (Ferry et al 2009).

Uptake of NPs by organisms takes place by absorption into cells, consequently, uptake mechanisms should be considered at the cellular level. In unicellular organisms, the cell itself comprises the environment-organism barrier so that uptake by the cell is equivalent to organism uptake; however, in organisms such as algae, plants, bacteria and fungi, the cell wall is an additional barrier to the entry of NPs compared to animal cells. In the absence of specific cell wall damage, NPs smaller than the largest pore can pass through the cell wall and reach the plasma membrane, which is also semipermeable. In case of

damage in cell wall, by close association of NPs, the cell membrane is also reached, and so, internalization into cells may occur (Rodea-Palomares et al 2011, Etxeberria et al 2006). Uptake of AgNPs by bacteria has been shown by TEM demonstrating the feasibility of NPs penetration through living semipermeable membrane (Xu et al 2004). Moreover, size-dependent uptake of AgNPs was demonstrated in *Daphnia magna* (Zhao and Wang 2012). Particular attention should be also given to the accumulation of NPs and further NP transfer between tissues or along the food chain. In aquatic ecosystems containing sediments, microbial biofilms, primary producers, filter feeders, grazers and omnivores, the most effective sink for NPs are filter feeders followed by biofilms (Ferry et al 2009). Trophic transfer of NPs from algae to daphnids (Bouldin et al 2008) and to clams (Croteau et al 2011), as well as from daphnids to fish (Zhu et al 2010) was shown for metal-based QDs, ZnONPs and TiO₂NPs, respectively, evidencing diet as a pathway through which organisms accumulate/incorporate NPs. Transfer of QDs to organisms at higher trophic level through dietary uptake was also reported (e.g. from rotifers to ciliated protozoans, Holbrook et al 2008). Bioaccumulation of NPs can also result in biomagnification, a process through which concentration of xenobiotics increases in organisms from lower to higher trophic levels within the food web. Werlin et al (2011) reported biomagnification in protozoa fed on bacteria previously exposed to QDs confirming the dietary exposure as the via of NP transfer. Even in the absence of biomagnification, aquatic organisms can accumulate large amounts of NPs and eventually become a significant dietary source of NPs to their predators. Bioaccumulation is also a direct way to assess the processes that influence bioavailability, and so, determining the bioavailability, uptake and intracellular accumulation of NPs in aquatic organisms is essential for the evaluation of their toxicity to aquatic life and transfer along the food chain.

1.3. The importance of freshwaters

Freshwaters constitute a valuable natural resource providing a broad variety of goods and services for humans including wastes dilution, cooling water supply for power generation and other industrial processes (Postel and Carpenter 1997). Ecosystem services in freshwaters depend greatly on a vast range of organisms that are threatened by several anthropogenic stressors. The impact of biodiversity loss and alterations in the composition

of biotic communities on ecosystem functioning is currently a hot topic (Hooper et al 2005). For instance, fish and shellfish yields depend heavily on sustained production of diverse benthic prey species (Huner 1995, New and Valenti 2000). Many crayfish species, which are involved in processes such as burrowing and mixing of sediments, nutrient cycling, breaking down dead organic matter, and grazing on submerged macrophytes, link sedimentary habitats with overlying waters (Covich et al 1999, Hobbs 2001).

Organic matter turn-over is another example of an ecosystem service particularly provided by forest streams in which riparian vegetation, microbial and invertebrate activities as well as physico-chemical characteristics of the stream water are integrated (Gessner et al 1999), allowing the assessment of structural and functional integrity of these systems (Gessner and Chauvet 2002). Organic matter turn-over is mainly driven by invertebrate shredders, fungi and bacteria (Gessner et al 1999). Fungi, particularly aquatic hyphomycetes, are recognised to dominate plant litter decomposition at early stages and increase litter palatability for invertebrate shredders (Krauss et al 2011, Suberkropp 1998). Aquatic hyphomycetes are ubiquitous and possess morphological and physiological adaptations to lotic environments that dictate their success as colonizers and decomposers of plant litter. For instance, they produce a vast range of extracellular enzymes, with cellulolytic, pectinolytic and proteolytic activity, which are instrumental in the acquisition of carbon (C), nitrogen (N), and phosphorus (P) compounds for microbial processes, such as growth and reproduction (e.g. Arnosti et al 2014), and the cycling of elements at the ecosystem level (Frossard et al 2012, Lin and Webster 2014).

In addition, the organisms belonging to these ecosystems are also involved in processes, such as biofiltration and detoxification. Without recycling, organic matter can accumulate and potentially lead to deoxygenation (i.e. through microbial respiration), which can cause rapid deterioration of water quality with consequences to organisms and processes in which they are involved (Manning et al 2017). Clearly, the disruption of key biological processes such as nutrient acquisition, growth and reproduction of freshwater biota can lead to changes in stream food webs, nutrient cycling and the overall flow of energy in ecosystems.

1.4. Toxicity of NPs to freshwater biota

1.4.1. Short-term versus long-term effects

As previously mentioned, NPs released into the environment undergo several transformations that may, in turn, influence their toxicity. Moreover, when assessing the impacts of NPs, another important factor to take into consideration is the exposure time, and so, in addition to adjusting the duration of the experiment to the tested organism and measured endpoint, it is also necessary to take into account whether it will be a short- or a long-term exposure assay since short-term effects of NPs may differ under long-term conditions. For instance, Kim et al (2017) reported an increase in aggregation and dissolution of copper oxide NPs (CuONPs) and ZnONPs with exposure time (i.e. 24, 48 and 72h). However, increased toxicity to *D. magna* with time was only verified for CuONPs. Another study reported that long-term exposure to AgNPs lowered the inhibitory concentration by 1-2 orders of magnitude than that observed by short-term exposure under similar AgNP concentrations in *Nitrosomonas europaea* (Barker et al 2018). On the other hand, because of NPs agglomeration in aquatic environments, benthic organisms can encounter NPs that settled at the bottom of water bodies (Ferry et al 2009, Schug et al 2014) and consequently be particularly affected by them.

Studies with TiO₂NPs have shown that these NPs have low toxicity or are safe to aquatic organisms during short-term exposure (e.g. Huang et al 2009); however, others raised the importance of performing longer exposure experiments. Long-term exposure of zebrafish gills to TiO₂NPs decreased the Na⁺ K⁺-ATPase activity in the gills, intestine and brain of the rainbow trout (Griffitt et al 2009a, Federici et al 2007). Inhibition of biomass production by aquatic fungal populations exposed to CuONPs was also reported to be time-dependent (Pradhan et al 2014). Pradhan et al (2011) demonstrated an inhibition of plant litter decomposition and biomass of freshwater microbial decomposers by AgNPs and CuONPs in a time-dependent manner. The mortality of the invertebrate *Allogamus ligonifer* exposed to CuONPs or AgNPs also increased with exposure time (Pradhan et al 2012, Batista 2017). Another aspect to take into consideration is that accumulation/adsorption of NPs to food or to different organisms is more certainly to occur at longer exposure time, which can lead to biomagnification of NPs. Longer exposure time can also lead to the acclimatization or adaptation of the organism (or community) resulting in increased tolerance (Vinebrooke

et al 2004). Consequently, an increase in organisms (or community) tolerance might result in shifts in community composition because sensitive species can be replaced by tolerant ones (Blanck 2002). Some investigators justify the assay of toxicity during shorter time as a way to prevent changes in community structure. This was the case of Tlili et al (2016) who assessed the toxicity of AgNPs on plant litter degrading fungi and bacteria in streams and reported an inhibition of biomass production by both microbial decomposers. Short-term effects of AgNPs in periphyton community that plays a key role as primary producers in stream ecosystems were found on respiration, photosynthesis and activity of extracellular enzymes (Gil-Allué et al 2015).

Overall, there is evidence that longer exposure is the most adequate for risk assessment of NPs on aquatic organisms; however, depending on the goal of the experiment, information from shorter time assays might be also important. On the other hand, investigations covering multiple years of exposure (repeated or not) are required to properly assess the potential long-term implications, particularly for slightly soluble or insoluble NPs that may accumulate in certain environmental compartments (e.g. sediments) over time.

1.4.2. Sensitivity of freshwater organisms to NPs

Living organisms constitute a vast diversity of taxonomy, life history, physiology, morphology, behaviour, and geographical distribution. These biological differences mean that different species respond differently to a given compound at a given concentration (i.e. different species have different sensitivities).

Because a certain chemical will not cause the same toxicity in all species, tests are performed to assess if a toxicant causes acute lethal effects (i.e. mortality) or sublethal effects (e.g. changes in growth or reproduction) or none effect. These toxicological bioassays use various measures of toxicity including: no observed effect concentration (NOEC), minimum inhibitory concentration (MIC), lowest observed effect concentration (LOEC), median lethal dose (LD50), median lethal concentration (LC50), half maximal effective concentration (EC50). Most studies report median L(E)C50 data, except for bacteria where MIC values are considered more relevant for indicating the antimicrobial properties of NPs. According to EU-Directive 93/67/EEC, the classification of NPs to different hazard categories is based on the lowest median L(E)C50 value of the three key environmental organisms: algae, crustaceans and fish (CEC 1996). The lowest median

L(E)C50 value $<1 \text{ mg L}^{-1}$ classifies chemical as very toxic to aquatic organisms; $1 - 10 \text{ mg L}^{-1}$ = toxic to aquatic organisms; $10 - 100 \text{ mg L}^{-1}$ = harmful to aquatic organisms; $>100 \text{ mg L}^{-1}$ = not classified (CEC1996). Sanderson et al (2003) and Blaise et al (2008) suggested an additional category “extremely toxic” for L(E)C50 value $< 0.1 \text{ mg L}^{-1}$.

Acute toxicity of NPs was already reported in a vast range of aquatic organisms and is generally higher for organisms from lower trophic levels (e.g. invertebrate filter-feeders) compared to higher trophic levels (e.g. fish) (Griffitt et al 2008). Adam et al (2015) conducted a broad study including several species to assess the toxicity of ZnO and CuO NPs. Regarding ZnONPs, results showed that freshwater algae was the most sensitive ($\text{EC}_{50} < 0.07 \text{ mg L}^{-1}$); without a clear pattern for the other tested taxonomic groups that exhibited a wide toxicity range for L(E)C50: bacteria ($0.04 - 803.5 \text{ mg L}^{-1}$), protozoa ($4 - 10 \text{ mg L}^{-1}$), yeast ($97.2 - 105.3 \text{ mg L}^{-1}$), nematoda ($1.8 - 789.0 \text{ mg L}^{-1}$), crustacea ($0.2 - 17.7 \text{ mg L}^{-1}$), fish ($1.4 - 18.5 \text{ mg L}^{-1}$) and amphibia (8.3 mg L^{-1}). For CuONPs a wide toxicity (L(E)C50) range was shown depending on the taxonomic group: bacteria ($3.7 - 63.1 \text{ mg L}^{-1}$), algae ($0.7 - 57.0 \text{ mg L}^{-1}$), protozoa ($97.9 - 129.0 \text{ mg L}^{-1}$), yeasts ($10.7 - 16.5 \text{ mg L}^{-1}$), crustacea ($0.01 - 9.8 \text{ mg L}^{-1}$) and fish (193.3 mg L^{-1}). These authors also found that toxicity of ZnONPs was similar to that of bulk ZnO, whereas CuONPs toxicity was higher than their bulk counterparts but lower than that of the corresponding salt (CuCl_2). According to the EU-Directive 93/67/EEC (CEC 1996), CuONPs are considered toxic whereas ZnONPs are considered very toxic. Bondarenko et al (2013) summarized the ecotoxicity of Ag, CuO and ZnO NPs, and indicated that crustaceans, algae and fish were more sensitive compared to bacteria, yeast and mammalian cells. Regarding AgNPs, crustaceans are the most sensitive, with median L(E)C50 value of 0.01 mg L^{-1} ; followed by algae (median L(E)C50 = 0.36 mg L^{-1}), fish (median L(E)C50 = 1.36 mg L^{-1}), nematodes (median L(E)C50 = 3.34 mg L^{-1}), bacteria (median L(E)C50 = 7.10 mg L^{-1}), yeast (median L(E)C50 = 7.90 mg L^{-1}) and protozoa (median L(E)C50 = 38 mg L^{-1}). AgNPs are classified as very toxic by the EU-Directive 93/67/EEC (CEC 1996) whereas extremely toxic according to Sanderson et al (2003) and Blaise et al (2008). Generally, the sensitivity pattern of different organisms to metal NPs largely follows the pattern of their sensitivity to the respective metal ions; however, in the case of Ag, differences between the L(E)C50 values of NPs and ions were ca. 10-15 times (Bondarenko et al 2013).

Responses of aquatic organisms at the community level are required to predict the risks of these chemicals to aquatic ecosystems since the disappearance of sensitive species can lead to alterations in ecosystem functions and increase the sensitivity of the community to an additional perturbation. As a consequence, the ability of these communities to respond to future disturbances would decrease (Paine et al 1998). On the other hand, communities subjected to long-term stressors, such as metal, may develop resistance to such toxicants (Habi and Daba 2009). By inhabiting such polluted ecosystems, these communities evolve mechanisms (e.g. bioaccumulation, biomineralization, biosorption, and biotransformation) to resist/tolerate such environments (Rani and Goel 2009, Zolgharnein et al 2010, Ayangbenro and Babalola 2017). For instance, CuONPs were less toxic to fungi isolated from metal-polluted streams than to fungi from non-polluted streams (Pradhan et al 2015); however, CuONPs had impacts on the structure of aquatic microbial communities (Pradhan et al 2011). The increased resistance to a certain stressor can also lead to intolerance to another (e.g. Kashian et al 2007), suggesting a potential fitness cost related to tolerance gains (Wilson 1988).

It may also happen that communities become tolerant to two toxicants after being exposed to one but not to the other. This mechanism termed co-tolerance is more likely to occur when the toxicants have similar modes of action or when they induce similar detoxification mechanisms (Blanck et al 1988). For instance, it has been observed co-tolerance between metals, such as copper and zinc, nickel and silver (Soldo and Behra 2000), or between copper and zinc in communities of periphyton (Tlili et al 2011); however, negative co-tolerance can also occur (e.g. between copper or zinc and arsenic, Tlili et al 2011).

Tolerance to higher levels of metals displayed by aquatic microorganisms such as fungi (Guimarães-Soares et al 2007, Azevedo et al 2009) and bacteria (Habi and Daba 2009, Zolgharnein et al 2010) has been reported. The exhibited higher tolerance to these toxicants is associated with the development of several adaptive mechanisms (e.g. extracellular complexation, Gadd 1999; efflux pumps, Einicker-Lamas et al 2003; intracellular complexation, Guimarães-Soares et al 2007) by tolerant organisms. If these mechanisms involved in metal detoxification help organisms to survive in metal contaminated environments, maybe they can use these mechanisms to defend themselves

against metal NPs. Indeed, Chae et al (2009) found induction of genes related to metal detoxification in the fish *Japanese Medaka* exposed to AgNPs.

1.4.3. Action mechanisms of NPs

Currently, assessing the safety of NPs has become a worldwide issue due to the high dissemination of nano-based products. The existing quantitative nanoecotoxicological data on single model organisms, classifies NPs from “extremely toxic” to “harmful” (Kahru and Dubourguier 2010); however, for risk assessment and regulatory purposes, nanoecotoxicological information is required at all levels (i.e. single organisms, simplified communities and whole ecosystems). The NP unique properties (including the shape, size, surface charge, composition and the NPs stability) influence how NPs interact with cells and cellular components (e.g. nucleic acids, proteins, fatty acids and carbohydrates) and, thus, their overall potential toxicity. With regard to their bulk form, NPs can be more (e.g. in the freshwater green microalgae *Pseudokirchneriella subcapitata*, Aruoja et al 2009) or less (e.g. in the aquatic bacterium *Vibrio fischeri* and in the aquatic crustaceans *D. magna* and *Thamnocephalus platyurus*, Heinlaan et al 2008) toxic. Surface area, which is strongly increased for NPs compared to microscale particles of similar chemical composition and surface reactivity are considered as the principal indicators of NPs reactivity, and together with chemistry, particle size (Hartmann et al 2010), particle shape (Dai et al 2015) and zeta potential (El Badawy et al 2011) are among the most relevant variables affecting the toxicity of NPs.

The primary sites for interaction of NPs with cells are cell membranes or cell walls, which constitute important defence barriers to the external environment and the entrance of NPs. However, between the accepted forms of contact of NPs with cells (e.g. electrostatic attraction, Li et al 2015; van der Waals forces, Armentano et al 2014; receptor-ligand interactions, Gao et al 2014; and hydrophobic interactions, Luan et al 2016) and their self-oxidative nature, NPs can adsorb on the outer membrane or the cell wall and cause damage to these structures just by direct contact, without the need to penetrate into the cells (Wang et al 2017). For instance, direct contact and adsorption of cells on TiO₂NPs can cause a loss of membrane integrity (Seil and Webster 2012). NPs react with cells and induce their pro-oxidant effects primarily by generating reactive oxygen species (ROS) that damage cell walls or membranes, diffuse into intracellular space and interfere with the

integrity and permeability of the cell membrane/wall (Zhang et al 2013). Then, internalization of NPs due to loss of proton motive force and increased membrane permeability can occur (Sirelkhatim et al 2015). Altered permeability allowing inflow of NPs into the cells is commonly attributed as a toxicity mechanism of several NPs, such as AgNPs (Marambio-Jones et al 2010), ZnONPs (Sirelkhatim et al 2015) or aluminium oxide NPs (Al_2O_3 NPs, Beyth et al 2015). Kloepper et al (2005) also demonstrated by spectroscopic and electron microscopic analysis that QDs with less than 5 nm in diameter can enter bacterial cells possibly by means of oxidative damage to the cell wall and cell membrane. Moreover, internalization may also occur through cell wall pores, while potential entry routes of NPs through bilayer lipid membranes occur by endocytic processes, embedded transport carrier proteins or ion channels (Navarro et al 2008).

Once inside the cells, interaction of NPs with biomolecules starts when NPs come into contact with biological fluids leading to changes in their physico-chemical properties (e.g. zeta potential and size). For instance, NPs can be coated with biomolecules forming a corona where NP size and surface properties can determine the amount and type of bound biomolecules (Lundqvist et al 2008). Different surface coatings as well as different cell types were shown to influence AgNPs-induced cytotoxicity (Suresh et al 2012). Biomolecules such as extracellular proteins and polysaccharides present in bacterial biofilms have also been shown to adsorb to AgNPs (Khan et al 2011a, b). It was however been proposed that cellular interaction with particle's corona is determined by the coating, which defines its surface charge, stability and hydrodynamic size, whereas the structure and size of the NP solely determines the corona nature (Colvin and Kulinowski 2007). The corona formation can also affect the biological functioning of the bound biomolecules (e.g. conformational changes in proteins, Cedervall et al 2007). For instance, the interaction of NPs with intracellular proteins, particularly sulphur containing membrane proteins and DNA, can interfere with cell division leading to cell death which is one mechanism of NPs toxicity (Chen and Schluesener 2008). On the other hand, protein conformational changes induced by NPs may in turn affect downstream protein-protein interactions, cellular signalling and also DNA transcription, a crucial process for enzyme synthesis. Gheshlaghi et al (2008) reported an inhibition of tubulin polymerization due to conformational changes induced by TiO_2 NPs which impaired cell division, cellular transport and cell migration. In addition, protein conformational changes in the active site can lead to loss of enzyme

activity (Karajanagi et al 2004). Turci et al (2010) reported an irreversible conformational change of albumin and lactoperoxidase after their adsorption on silica NPs. Almost all types of NPs interact with proteins but, actin was identified as one of the most commonly bound protein (Ehrenberg and McGrath 2005). This suggests that NPs inhibit actin function including vesicle and organelle transport, cell signalling, maintenance of cell junctions, cell motility among others. The formation of protein aggregates induced by cerium dioxide (CeO₂) NPs, QDs and CNTs was also reported (Linse et al 2007).

On the other hand, biomolecules can also be modified by ROS (e.g. O₂⁻, OH[·], H₂O₂) which can be formed directly or through released ions from NPs. These high-energy species can attack nucleic acids, lipids, proteins and other biomolecules (Pradhan et al 2015, Halliwell and Gutteridge 1999). The consequent damage includes damage to DNA, protein oxidation, depolarization of mitochondrial membrane, lipid peroxidation, impairment of the electron transport chain and activation of an NADPH-like system (Xia et al 2006). Oxidative stress (OS) can indeed be a driver for many NP-induced effects as ROS generation is considered one of the most frequently reported effects of NP-associated toxicity (Manke et al 2013). The increased cellular OS was manifested in reduced levels of antioxidants GSH and α-tocopherol whereas membrane integrity was detected via release of lactate dehydrogenase (LDH) from the cells (by silica and cerium oxide NPs, Lin et al 2006a,b). On the other hand, DNA damage, including single- and double-strand breakages (SSBs and DSBs), can lead to cell cycle arrest or apoptosis (by ZnONPs, Lin et al 2009). Perturbation of intracellular calcium [Ca²⁺] was also observed which may be associated with metabolic and energetic imbalance as well as with cellular dysfunction (by ZnONPs, Huang et al 2010).

Another mechanism that has been widely attributed to several NPs is the release of toxic ions from their surface, mainly when the thermodynamic properties favour particles dissolution in a suspending medium or biological environment (Xia et al 2008). In fact, many authors consider that toxicity of some NPs is due to the released ions and not to NPs themselves. For instance, in the case of AgNPs, some authors have demonstrated that released Ag ions explained a large proportion of the observed toxicity for various aquatic organisms (Gil-Allué et al 2015, Völker et al 2015). However, others contradict these findings, highlighting more severe effects of AgNPs than those that could be explained exclusively by the released ions (Nair et al 2013, Tlili et al 2016). On the other hand,

Sotiriou and Pratsinis (2010) showed that Ag^+ dominated the toxicity of AgNPs less than 10 nm, whereas for larger particles (>10 nm) the toxicity of the released Ag^+ and AgNPs was comparable (Fig. 1.3).

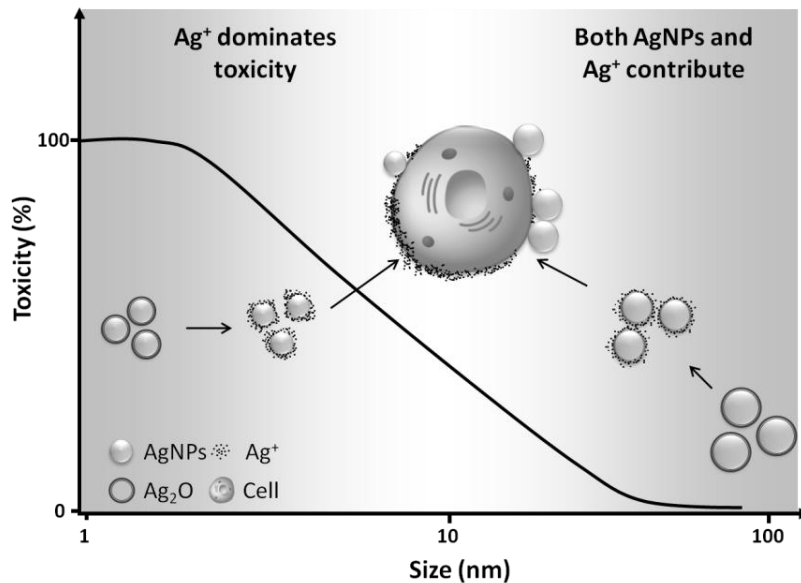


Figure 1.3 Toxicity of AgNPs as a function of nanoparticle size (adapted from Sotiriou and Pratsinis 2011).

Omic analysis point to distinct mechanisms of toxicity of NPs. For instance, Griffitt et al (2009b) found different transcriptional responses among various NMs (Ag and Cu) and between nanoparticulate and soluble species suggesting that each exposure produced different biological responses in zebrafish. Different gene expression profiles under AgNPs and Ag^+ (AgNO_3) exposure were also revealed in *D. magna* suggesting different modes of toxicity between NPs and released ions (Poynton et al 2012). A different response pattern between CuONPs and Cu ions was also shown by distinct protein regulation and gene expression (in marine mussels, Gomes et al 2014; in zebrafish gills, Griffitt et al 2009b). Similarly, different mechanisms of action were also revealed for ZnONPs through gene expression analysis (Nair and Chung 2015, Su et al 2015). Nonetheless, it is also probable that NPs and released ions share common mechanisms of action (Völker et al 2013). Hence, it is problematic to draw a generic conclusion regarding the relevance of toxic ions released from NPs relative to the effects induced by the NPs themselves. For instance, Kim

et al (2017) reported greater lipid peroxidation induced by CuONPs than by Cu ions and converse results for ZnONPs.

For NPs that do not release toxic ions, the attachment or adsorption to the organisms' outer surface is suggested as potential toxicity trigger. This mechanism was attributed for instance to TiO₂NPs and Fe₃O₄NPs that physically inhibited moulting and ultimately induced death of daphnids (Dabrunz et al 2011, Baumann et al 2014); TiO₂NPs were also able to alter daphnids swimming behaviour (Noss et al 2013).

Toxicants such as NPs that do not interact or bind to a single type of macromolecule can disturb multiple pathways, influence various cellular processes and interact with several cellular targets (Fröhlich 2012); however, different NPs can damage various processes (Fig. 1.4). Some of the main reported cellular targets are membranes, mitochondria, nucleus, lysosomes, vesicles and golgi apparatus (Elsaesser and Howard 2012).

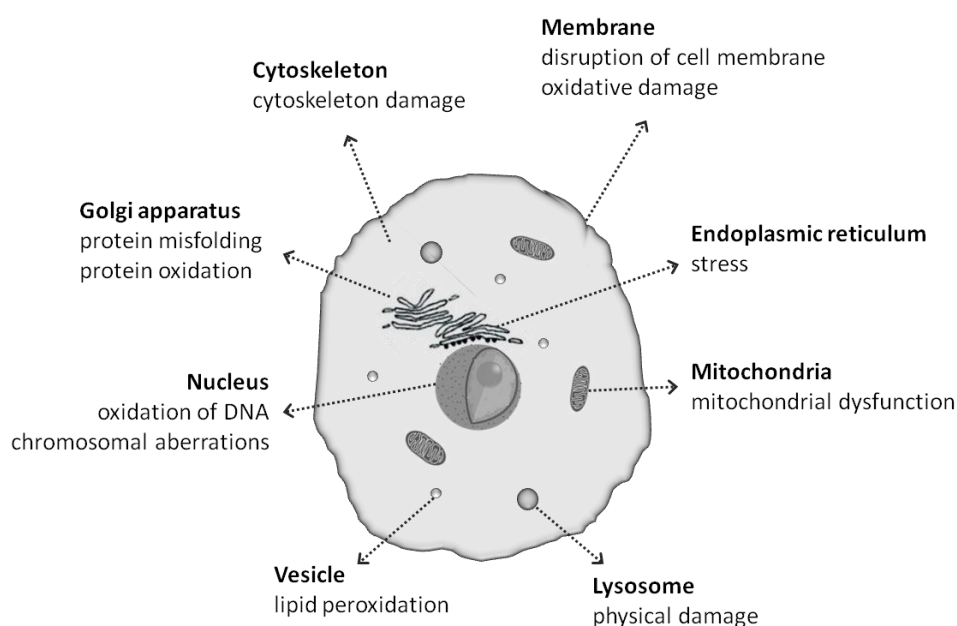


Figure 1.4 Nanoparticle interaction with cells: intracellular targets and nanotoxicological mechanisms (adapted from Elsaesser and Howard 2012).

Mitochondria as the cell energy stations are the major targets of fullerenes (Foley et al 2002) and CNTs (Zhu et al 2006); however, TiO₂NPs (Xia et al 2006) and AgNPs (Hussain et al 2005) also seem to be able to affect mitochondrial function, leading to apoptosis.

AgNPs are able to cause mechanical disruption by disturbing the respiratory chain, increasing mitochondrial membrane permeability (Piao et al 2011), while silicon dioxide NPs (SiO₂NPs), which were identified inside these organelles, are reported to cause direct injury to mitochondrial membranes (Sun et al 2011). Cytotoxicity can in turn be aggravated by mitochondria increasing the levels of intracellular ROS. Lysosomes are also a preferential target for many NPs, since these intracellular compartments take up NPs by endocytosis (Faklaris et al 2009, Goya et al 2008). NPs are then stored in these structures where they are either digested or excreted (Greulich et al 2011).

Accumulation and storage of NPs has been reported to cause lysosomal destabilization and permeabilization of its membranes (by ZnONPs in Cho et al 2011, by TiO₂NPs in Jin et al 2008) as well as morphological damage such as swelling of lysosomes (QDs, Funnell and Maysinger 2006). The inhibition of lysosomes functioning can in turn be accompanied by autophagy (Stern and Johnson 2008). DNA damage can be a result of smaller NPs entering the nucleus either by diffusion through nuclear pores or via receptor mediated transport mechanisms (Pante and Kann et al 2002); although localization in the nucleus is not essential since NPs can also get access to DNA due to rupture of the nuclear membrane during mitosis. Many NPs, including Ag (Kim et al 2011), ZnONPs (Sharma et al 2011), TiO₂NPs (Shukla et al 2011) and CuNPs (Wang et al 2012), induce genotoxicity mostly by ROS generation and oxidative DNA-damage whose effects consist of point mutations and double-strand breaks.

Accumulation and storage of NPs has been reported to cause lysosomal destabilization and permeabilization of its membranes (by ZnONPs in Cho et al 2011, by TiO₂NPs in Jin et al 2008) as well as morphological damage such as swelling of lysosomes (QDs, Funnell and Maysinger 2006). The inhibition of lysosomes functioning can in turn be accompanied by autophagy (Stern and Johnson 2008). DNA damage can be a result of smaller NPs entering the nucleus either by diffusion through nuclear pores or via receptor mediated transport mechanisms (Pante and Kann et al 2002); although localization in the nucleus is not essential since NPs can also get access to DNA due to rupture of the nuclear membrane during mitosis. Many NPs, including Ag (Kim et al 2011), ZnONPs (Sharma et al 2011), TiO₂NPs (Shukla et al 2011) and CuNPs (Wang et al 2012), induce genotoxicity mostly by ROS generation and oxidative DNA-damage whose effects consist of point mutations and double-strand breaks. Other examples indicative of genotoxicity comprise the up-

regulation of DNA repair enzymes (AgNPs, Ahamed et al 2008) or interaction with pathways of nucleotide excision repair (NER) and base excision repair (BER) impairing the ability for DNA repair (TiO₂NPs, Jugan et al 2012), the formation of histone aggregates (AuNPs, Sule et al 2008), interfering with the export of mRNA, affecting the process of translation (AgNPs, AshaRani et al 2009), interaction with the mitotic spindle, microtubule, centrosomes and condensed chromatin (CNTs, Sargent et al 2012), and the formation of clusters of topoisomerase which can affect the transcription process (SiO₂NPs, Chen and Mikecz 2005).

Other cellular processes also affected by NPs are the bacterial replication (AgNPs, Seil and Webster 2012) or cell differentiation, adhesion and spreading of bacteria (silica nanowires, Fernando et al 2018). In a review by Fröhlich (2017), several pathways indicative of NPs toxicity according to changes in mRNA expression, proteome and metabolome include: growth inhibition, cell cycle, apoptosis, morphogenesis, differentiation, signal transduction, membrane and vesicular trafficking, cytoskeleton rearrangement, phagocytosis and endocytosis, stress response, antioxidant activity, endoplasmic reticulum stress and metabolic processes related to energy production, carbohydrates, lipids, amino acids and nucleic acids.

There are also other relevant mechanisms whose effects can have implications in population development, suggesting potentially transgenerational effects. For instance, zebrafish exposed to CuONPs exhibited a delayed or impaired hatching process due to inhibition of proteolytic activity of hatching enzyme 1 (Muller et al 2015). Nair et al (2011) also reported reproductive failure due to activation of gonadotrophin releasing hormone in *Chironomus riparius* exposed to AgNPs (Nair et al 2011). In addition, algae (Zou et al 2016) and aquatic plants exposed to AgNPs showed alterations in photosynthetic pigment composition and effects in photosystem II (Jiang et al 2017). It has also been pointed that NPs may have the potential to function as carriers for other pollutants (Moore 2006, Zhang et al 2007); this concern is raised due to the occurrence of mixtures of chemical stressors in aquatic and terrestrial ecosystems. The “Trojan horse” designation was indeed applied to carbon-based NPs potential to increase metal ions uptake (Boncel et al 2015). Similarly, TiO₂NPs adsorbed perfluorooctanesulfonate (a persistent organic pollutant) facilitate its accumulation in fish (Qiang et al 2016) and increased the uptake of Cu ions in *D. magna*

(Fan et al 2011). Other types of interactions of toxicants with NPS and organisms may also occur (Fig. 1.5).

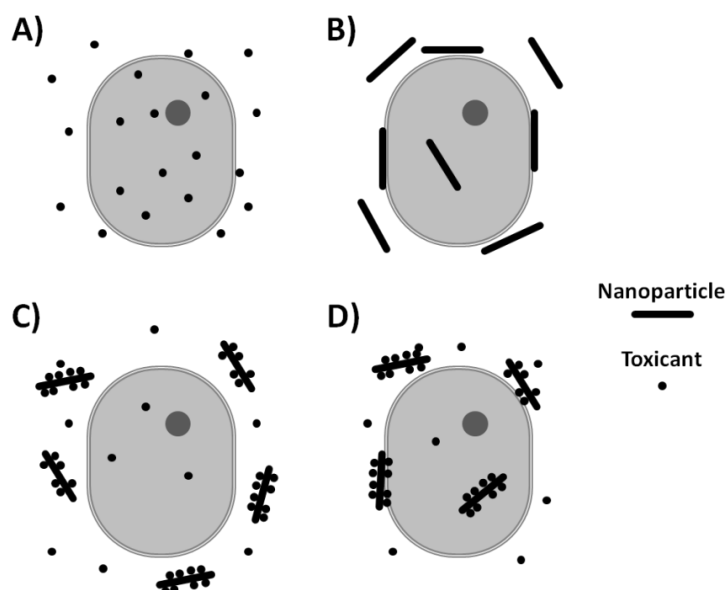


Figure 1.5 Interactions of toxicants, nanoparticles and organisms. A) Adsorption and uptake of toxicant, B) adsorption and uptake of nanoparticles, C) adsorption of toxicant onto nanoparticles and reduction in toxicant uptake by organism and D) adsorption of nanoparticles with adsorbed toxicant and possible uptake of toxicant-nanoparticles (adapted from Nowack and Bucheli 2007).

1.5. Oxidative stress biomarkers: enzymatic and non-enzymatic

The term biomarker was adopted by environmental scientists to refer changes at any level of biological organization (i.e. sub-organismal, organismal, population, community, or ecosystem) as well as aberrations in organisms (including cultured cells and tissues) to estimate either exposure to xenobiotics or resultant effects. However, the most common usage of the term has been for biochemical, physiological, or histological changes at the sub-organism or organismal level (Huggett et al 2018).

Furthermore, biomarkers effective and reliable application requires several criteria. To fulfil these criteria, biomarkers must have biological significance, be more sensitive than conventional endpoints, be sensitive to many different contaminants, and be easy and inexpensive to use (Feige et al 2013).

Classification of biomarkers can vary according to the field or author (e.g. see Sharma et al 2013, Mishra and Verma 2010). Huggett and his colleagues (2018) addressed the following

types: physiological and nonspecific, metabolic, DNA alterations, histopathological, immunological and proteins.

One of the most commonly used biomarker to assess the stress caused by xenobiotics is the production of increased levels of ROS. During normal respiration, ROS can act as second messengers, stimulating cell proliferation; however, under exposure to environmental stressors such as xenobiotic NPs, ROS can accumulate to toxic levels (Pradhan et al 2015), leading to OS, which in turn may damage cellular components (e.g. proteins, lipids and DNA; Halliwell and Gutteridge 1999). In this sense, organisms have developed enzymatic and non-enzymatic antioxidant systems (Table 1.1) to deal with the OS and to maintain cellular homeostasis (Doyotte et al 1997).

Table 1.1 Enzymatic and non-enzymatic antioxidant systems.

Antioxidant systems	
Enzymatic	Non-enzymatic
Superoxide dismutase (SOD)	Glutathione (GSH)
Catalase (CAT)	Ascorbic acid (vitamin C)
Ascorbate peroxidase (APx)	Ubiquinol (coenzyme Q)
Glutathione reductase (GR)	α -Tocopherol (vitamin E)
Monodehydroascorbate reductase (MDAR)	Lipoic acid
Glutathione peroxidase (GPx)	Uric acid
Glutathione S-transferase (GST)	β -Carotene
	Retinol (vitamin A)

Key examples of enzymatic antioxidants include superoxide dismutase (SOD), catalase (CAT), glutathione peroxidase (GPx), glutathione S-transferase (GST), glutathione reductase (GR) and the neuronal enzyme acetylcholinesterase (AChE) (Fridovich 1986, Doyotte et al 1997, Gagnaire et al 2008). The majority of these enzymes belong to the ascorbate-glutathione cycle, and maintain the essential pool of reduced glutathione (GSH) to control cellular redox state, as GSH scavenges ROS or xenobiotics to detoxify cells (Penninckx 2002, Huang et al 2010). SODs are a group of metalloenzymes (e.g. CuZnSOD, MnSOD and FeSOD) that catalyse the detoxification of $O_2^{\cdot-}$ into H_2O_2 which is then removed by CAT or GPx which is also able to catalyse the reduction of other peroxides using GSH as the electron donor. GST, an enzyme of phase II biotransformation process, can employ GSH in the reduction of a broad range of organic hydroperoxides except for H_2O_2 (Hayes and

Pulford 1995). GR sustains a proper GSH/GSSG ratio and reduces oxidized GSH. Finally, AChE is able to hydrolyse the neurotransmitter acetylcholine into choline and acetic acid, allowing cholinergic neurons to return into their resting state after activation (Gagnaire et al 2008).

The most relevant non-enzymatic antioxidants are substances of low molecular weight consisting of free radical scavengers such as vitamin C and E, carotenoids, ascorbate, glutathione (GSH), whose function is to remove ROS (de Zwart et al 1999).

Additionally, once ROS increased levels can damage cellular macromolecules such as proteins, lipids and DNA; other biomarkers of OS should be assessed: lipid peroxidation (e.g. quantification of malondialdehyde - MDA formation, Janero 1990), DNA damage (e.g. occurrence of DNA strand breaks, Jena 2012) and protein oxidation (e.g. quantification of carbonyl derivatives of proteins, especially the oxidation products of phenylalanine and tyrosine amino acids, Witko-Sarsat et al 1996). In aquatic fungi, the exposure to CuONPs led to an increase in intracellular accumulation of ROS and to plasma membrane damage as well as to DNA strand breaks and increase in activities of SOD, GPx and GR (Pradhan et al 2015).

Other biomarker of OS that has been used extensively especially for assessing metal toxicity is a group of proteins called metallothioneins (MTs, Andrews 2000). MTs consist of low molecular weight, cysteine-rich proteins with metal-chelating and ROS-scavenging properties (Kinningham and Kasarskis 1998). In *Caenorhabditis elegans* under exposure to AgNPs, MTs showed protective effect (Meyer et al 2010). MTs were also reported to bind silver ions (Stillman 1999), be induced by silver exposure (Ringwood et al 2009), and protect from silver toxicity (Liu et al 1991).

1.6. Emerging field of environmental “OMICS”

Principles, methodology and techniques of toxicity testing have been changing in the last few years. The introduction of quantitative analysis of molecular and functional changes in multiple levels of biological organization was critical and has led to the development of the field of toxicogenomics, where the suffix “omics” stands for “as whole” and refers to a field of study in biology ending in -omics namely genomics, transcriptomics, proteomics and

metabolomics; the suffix “ome” is used to address the objects of study of such fields such as the genome, transcriptome, proteome and metabolome, respectively.

Toxicogenomics specifically refers to the interaction between genes and environmental stressors and, as a consequence, it gave rise to the concept of systems toxicology (Waters and Fostel 2004). Systems toxicology changed the current approach of relying almost exclusively on traditional toxicology testing of high-dose phenotypic responses and comprises several potential applications in different fields of ecotoxicology. Some of the most promising include the mode of action (MOA) profiling of toxicants, the assessment of exposure to environmental stressors, the identification of particularly sensitive subsets of ecological populations, and the discovery of molecular biomarkers.

Testing of NPs have also been applying systems toxicology approaches with the possibility of identifying new targets and markers for NPs toxicity as exposure to NPs occurs at lower levels than those used in conventional testing. On one hand, testing realistic exposure levels can lead to no phenotypic changes but, on the other hand, the application of higher doses may result in different cell response. By the use of omics, adverse effects of low particle concentrations on cells may be detected even before phenotypic changes occur. Also, the omic techniques have lower interference with NPs avoiding false positive or negative results so frequently reported with conventional biomarkers due to interference by color, chemical activity, light scattering, etc (e.g. Fröhlich 2013).

Omic technologies required the development of high-throughput sequencing (HTS) approaches (Fig. 1.6), which have become commercially available since the beginning of the 21st century, and replaced the traditional whole-genome Sanger sequencing by faster and more readily methods, generating higher throughput while simultaneously reducing manpower and cost (Metzker 2010).

It is, however, important to realise that not all omic techniques can be interpreted equally and that each analytical technique offers different advantages and limitations, and so, there is often a trade-off between the technique and the experimental goals.

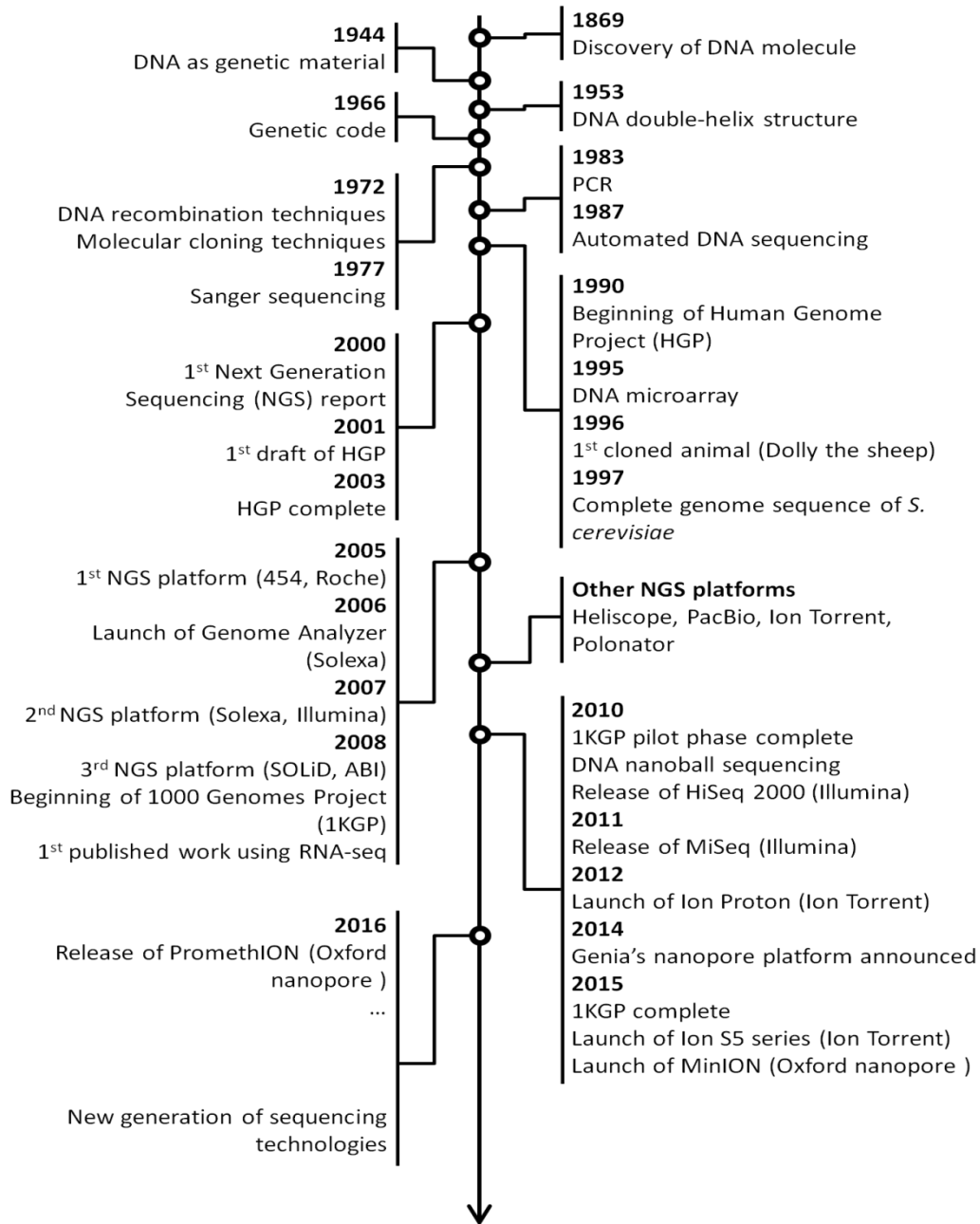


Figure 1.6 Milestones of the development of HTS over the last decades, which enabled current advances in systems biology research (adapted from Pareek et al 2011 and Besser et al 2018).

1.6.1. Proteomics

Proteomics is the large-scale study of a proteome, which is defined as a total set of proteins expressed in particular conditions by a genome in a cell, tissue, or organism (Anderson and Anderson 1998). Because organism's genome is more or less constant, it is more complex to study the proteome as it differs from cell to cell and from time to time. Moreover, the 4-nucleotide codes of DNA and/or mRNA are translated into a code of 20

amino acids, a huge increase in potential complexity needs to be considered when moving from studying the genome and/or transcriptome to the proteome. In addition, varying lengths of primary sequence polypeptides fold into one of a startlingly large number of possible conformations and chemical modifications (e.g. phosphorylation, glycosylation and ubiquitination) together with occurrence of multiple isoforms of the same protein due to alternative splicing can also derive in great diversity of the synthesised proteins. Besides confirming the presence of a certain protein, proteomics provide information regarding protein abundance, post-translational modifications, protein interactions and networks in biological processes.

Some considerations in proteomics include protein concentration, sample purification and protein digestion, plus affinity capture and sample fractionation to reduce the complexity of the target fluid. Two main approaches are used for fractionation and visualization of protein extracts: 1) two-dimensional gel electrophoresis (2-DE), in which proteins are separated in a polyacrylamide matrix according to their isoelectric point and molecular mass, followed by identification with mass spectrometry (MS); and 2) gel-free methodologies, involving chromatography-based multidimensional separation of proteins (e.g. capillary liquid chromatography), coupled to automated MS (Baggerman et al 2005).

Liquid chromatography coupled to tandem mass spectrometry (LC-MS/MS) has become the method of choice for the identification and quantification of proteins and proteomes (Aebersold and Mann 2003, Han et al 2008, Walther and Mann 2010), especially after the introduction of soft ionization techniques such as matrix assisted laser desorption ionization (MALDI) and electrospray ionization (ESI), at the end of the 1980s (Karas and Hillenkamp 1988, Fenn et al 1989). Most approaches to protein identification rely on proteolysis (e.g. with trypsin) of the separated protein, since its molecular weight is insufficiently discriminating. Then, often without any further separation the resulting peptides are analysed. Other methods for sample preparation include GeLC-MS/MS, liquid digestion (LD) followed by LC-MS and an adaptation of the in-gel digestion method, termed short-GeLC which was proposed to be a faster and more reproducible sample preparation method for quantitative approaches (Anjo et al 2015). In-gel digestion provides a simple and cost-effective procedure for sample pre-fractionation with appealing features such as the ability to remove digestion interfering contaminants, visual quality control of the samples (if combined with MS-compatible staining) and the possibility of application to a

variety of samples, including challenging ones (e.g. membrane proteins) (Granvogl et al 2007, Switzar et al 2013, Vowinckel et al 2014).

Mass spectrometers are highly sensitive and accurate for the determination of molecular masses of different types of molecules and consist of three functional units: the ion source which ionizes neutral analytes (e.g. a protein or a peptide), the mass analyser which separates the resulting ions according to their mass-to-charge ratio (m/z), and the ion detector that creates a mass spectrum, characteristic of the molecular mass and/or structure, that can be recorded and processed by a computer. The combination of different types of mass analysers in combination with MALDI- or ESI has resulted in a wide variety of different mass spectrometric instrumentation (e.g. MALDI-TOF, MALDI-TOF/TOF, ESI-Q-TOF and ESI-ion trap). In addition, the coupling of two mass selective devices for tandem MS (MS/MS) has also led to the expansion of the field's applications.

SWATH-MS method is a particularly promising quantitative method due to its ability to combine protein identification data obtained with data-independent acquisition (DIA) to accurately quantify peptides at large scale (Gillet et al 2012). It achieves essentially complete peptide fragment-ion coverage for precursors using a quadrupole-time-of-flight mass spectrometer (QqTOF, Chernushevich et al 2001).

Each analytical technique offers advantages and limitations in terms of instrument sensitivity, resolution, mass accuracy, dynamic range and throughput (Nadler et al 2017).

1.6.2. Transcriptomics

Transcriptomics is the study of the transcriptome, which is the complete set of RNA molecules (i.e. transcripts) that are produced by the genome, under specific physiological conditions in a cell, tissue, or organism. The transcriptome analysis gives indication on how genes are regulated, providing information on the identity and quantity of expressed transcripts, including the messenger RNA (mRNA), non-coding RNAs and small RNAs, supports gene annotation and allows the detection of not annotated genes (Creecy and Conway 2015).

Several technologies have been developed to deduce and quantify the transcriptome, including hybridization- or sequence-based approaches. Hybridization-based approaches are high-throughput and relatively inexpensive being cDNA microarrays analysis the most established hybridization-based technique. It was developed in the mid-1990s and typically

involves the incubation of fluorescently labelled cDNA with custom-made microarrays (Lowe et al 2017). However, hybridization-dependent methods require previous knowledge about the genome sequence to design the array probes or have to rely on some degree of homology between related species. These methods show limited detection range due to the saturation of the signal and high background levels derived from cross-hybridization events (Okoniewski and Miller 2006, Royce et al 2007). In addition, hybridization-based approaches can often require complicated normalization methods since comparing expression levels across different experiments may be difficult.

In contrast to microarrays methods, sequence-based approaches can directly determine the cDNA sequence using high-throughput sequencing to record all transcripts. RNA-Seq (RNA sequencing), also called whole transcriptome shotgun sequencing (WTSS, Lawley et al 2013), is the key contemporary technique developed in the 2000s and emerged as the method of choice for measuring transcriptomes of organisms. It can be used to analyse alternative gene spliced transcripts, post-translational modifications, gene fusion, mutations/single-nucleotide polymorphisms (SNPs) and changes in gene expression over time, or differences in gene expression in different conditions (Lowe et al 2017) without sophisticated normalization of data sets (Mortazavi et al 2008, Wilhelm et al 2008). Key advantages over microarray transcriptomes are the quantification of both low- and high-abundance RNAs and smaller input RNA amounts (nanograms vs micrograms for microarrays) allowing examination of structures down to the single-cell level when combined with linear amplification of cDNA (Hashimshony et al 2012, Svensson et al 2018). Standard RNA-Seq pipelines use next-generation sequencing (NGS) for targeting messenger RNA (mRNA). To that end, the total extracted RNA sample must be depleted of ribosomal (rRNA) and transfer RNA (tRNA) fraction, which are predominant and will compete for sequencing reagents (Wang et al 2009). The library preparation of RNA samples usually involves fragmentation and RNA conversion to a pool of cDNA fragments with the required adapters attached to one or both ends (Martin and Wang 2011, Schroeder et al 2006). Using HTS, short sequences, from one end i.e. (single-end sequencing) or both ends (i.e. pair-end sequencing), are obtained from each cDNA. Following sequencing, the resulting short sequences called reads are either aligned with the reference genome or reference transcriptome, or assembled *de novo* without the genomic sequence to produce a genome-scale transcription map that consists of both the

transcriptional structure and/or level of expression for each gene (Martin and Wang 2011). The generated reads are typically around 100 bp in length, but can range from 30 bp to over 10,000 bp, depending on the DNA-sequencing technology used (e.g. Illumina, 454, PacBio or Ion Torrent; Quail et al 2012, Liu et al 2012). Unlike hybridization-based approaches, RNA-Seq is not limited to detect transcripts that correspond to existing genomic sequence and so is particularly attractive for non-model organisms with genomic sequences that are yet to be determined (Vera et al 2008).

Environmental application of transcriptomic technologies allows the identification of novel transcriptional networks in complex systems that respond to and counteract biotic and abiotic stresses. For instance, distinct transcriptional profiles associated with drought and salinity stresses were identified by comparative analysis of a range of chickpea lines at different developmental stages (Garg et al 2016).

A known limitation of transcriptomics is the fact that changes in mRNA expression may not influence the phenotype directly, and so it has been attracting much criticism concerning the inadequacy to detect genes with high influence on adaptive responses to the environment.

1.7. Aim and outline of the thesis

AgNPs are currently among the most used NMs increasing the chance of their release into aquatic ecosystems where AgNPs can exert toxic effects on biota, with consequences for food-webs, nutrient cycling and overall flow of energy in those ecosystems. However, the question regarding whether toxicity of AgNPs is specifically related to NP properties or mediated by dissolved released Ag^+ is still strongly debated. Often, assessed endpoints such as growth, reproduction or survival reveal neither subtle nor adaptive responses leading to false conclusions. With omic technologies, alterations in biological pathways at the genome-scale can be screened, improving the knowledge of molecular mechanisms and the estimation of possible adverse effects by environmental stressors such as AgNPs. In this study, the potential impacts of AgNPs on aquatic microbes with ecological relevance in freshwater ecosystems, namely fungi and bacteria were assessed. Responses to AgNPs were investigated at the individual and cellular level in microbes with different background under the hypothesis that microbes collected from polluted streams would be less

susceptible to toxicants than those collected from clean streams. To better understand the effects of AgNPs on the microbes, silver concentration was quantified and NP characterization was done under experimental conditions.

Chapter 1 provides an overview on the current knowledge regarding the nanoscale world briefly portraying several aspects of NPs, such as specific characteristics and classification, detection and characterization techniques, as well as synthesis approaches. Particular attention was given to the impacts of AgNPs on aquatic microorganisms from freshwater ecosystems. The relevance of environmental omics was also addressed. In the three subsequent chapters, proteomic (Chapters 2 and 3) and transcriptomic (Chapter 4) approaches were employed to gain insight into the mode of action of AgNPs. To that end, microcosm experiments were conducted to assess the impacts of AgNPs on aquatic microbes with different background: the bacterial strain *Pseudomonas* sp. M1, isolated from sediments in a polluted stream (Chapter 2), and two ecotypes of the aquatic fungus *Articulospora tetracladia*, one isolated from a non-polluted stream (At72) and the other from a metal-polluted stream (At61) (Chapter 3). Microorganisms were exposed to AgNPs (20 nm; citrate-coated) and to Ag⁺ at concentrations inhibiting 20% of biomass production (EC₂₀) at early exponential phase of growth. Effects were assessed based on the variations in the overall proteome as well as in the activities of selected antioxidant enzymes. The knowledge based on proteomics obtained in previous chapters was then complemented in Chapter 4 using a transcriptomic approach. To that end, similar exposure conditions were applied to the fungal ecotype from the non-polluted stream (At72), and the effects were examined on biochemical signals associated with the responses of this fungus by analysing the transcriptome, identifying the biological processes activated or repressed after short-term exposure to AgNPs and/or to Ag⁺. Chapter 5 integrates the major outcomes and the main conclusions are presented to provide a global perspective of the work and possible lines for future research.

References

- Aebersold R and Mann M. 2003. Mass spectrometry-based proteomics. *Nature*. 422: 198-207.
- Adam N, Schmitt C, De Bruyn L, Knapen D and Blust R. 2015. Aquatic acute species sensitivity distributions of ZnO and CuO nanoparticles. *Sci. Total Environ*. 526: 233-242.

- Adams FC and Barbante C. 2013. Nanoscience, nanotechnology and spectrometry. *Spectrochim. Acta B*. 86: 3-13.
- Ahamed M, Karns M, Goodson M, Rowe J, Hussain SM, Schlager JJ and Hong Y. 2008. DNA damage response to different surface chemistry of silver nanoparticles in mammalian cells. *Toxicol. Appl. Pharmacol.* 233: 404-410.
- Anderson NL and Anderson NG. 1998. Proteome and proteomics: new technologies, new concepts, and new words. *Electrophoresis*. 19: 1853-1861.
- Andrews GK. 2000. Regulation of metallothionein gene expression by oxidative stress and metal ions. *Biochem. Pharmacol.* 59: 95-104.
- Angel BM, Batley GE, Jarolimek CV and Rogers NJ. 2013. The impact of size on the fate and toxicity of nanoparticulate silver in aquatic systems. *Chemosphere*. 93: 359-365.
- Armentano I, Arciola CR, Fortunati E, Ferrari D, Mattioli S, Amoroso CF, Rizzo J, Kenny JM, Imbriani M and Visai L. 2014. The interaction of bacteria with engineered nanostructured polymeric materials: a review. *Scientific World J.* Article ID 410423.
- Arnosti C, Bell C, Moorhead DL, Sinsabaugh RL, Steen AD, Stromberger M, Wallenstein M and Weintraub MN. 2014. Extracellular enzymes in terrestrial, freshwater, and marine environments: perspectives on system variability and common research needs. *Biogeochemistry*. 117: 5-21.
- Aruoja V, Dubourguier HC, Kasemets K and Kahru A. 2009. Toxicity of nanoparticles of CuO, ZnO and TiO₂ to microalgae *Pseudokirchneriella subcapitata*. *Sci. Total Environ.* 407: 1461-1468.
- AshaRani PV, Low Kah Mun G, Hande MP and Valiyaveetil S. 2009. Cytotoxicity and genotoxicity of silver nanoparticles in human cells. *ACS Nano*. 3: 279-290.
- Ayangbenro AS and Babalola OO. 2017. A New Strategy for Heavy Metal Polluted Environments: A Review of Microbial Biosorbents. *Int. J. Environ. Res. Public Health*. 14: 94.
- Azevedo M-M, Almeida B, Ludovico P and Cássio F. 2009. Metal stress induces programmed cell death in aquatic fungi. *Aquat. Toxicol.* 92: 264-270.
- Baalousha M, Cornelis G, Kuhlbusch TAJ, Lynch I, Nickel C, Peijnenburg W and van den Brink NW. 2016. Modeling nanomaterial fate and uptake in the environment: current knowledge and future trends. *Environ. Sci. Nano*. 3: 323-345.
- Baggerman G, Vierstraete E, De Loof A and Schoofs L. 2005. Gel-based versus gel-free proteomics: a review. *Comb. Chem. High Throughput Screen.* 8: 669-677.
- Batista D. 2017. Impacts of silver nanoparticles and increased temperature on aquatic invertebrate shredders. In: *Impacts of Silver Nanoparticles in Freshwater Detrital Food-Webs in a Warming Scenario (Doctoral thesis)*. School of Sciences. University of Minho, Braga. P: 95-125.
- Baumann J, Koser J, Arndt D and Filser J. 2014. The coating makes the difference: acute effects of iron oxide nanoparticles on *Daphnia magna*. *Sci. Total Environ.* 484: 176-184.
- Behra R, Sigg L, Clift MJD, Herzog F, Minghetti M, Johnston B, Petri-Fink A and Rothen-Rutishauser B. 2013. Bioavailability of silver nanoparticles and ions: from a chemical and biochemical perspective. *J. Royal Soc. Interface*. 10: 20130396.
- Besser J, Carleton HA, Gerner-Smidt P, Lindsey RL, Trees E. 2018. Next-generation sequencing technologies and their application to the study and control of bacterial infections. *Clin. Microbiol. Infect.* 24: 335-341.
- Beyth N, Hourri-Haddad Y, Domb A, Khan W and Hazan R. 2015. Alternative antimicrobial approach: Nano-Antimicrobial Materials. *Evid.-Based Complementary Altern. Med.* Article ID 246012.

- Blaise C, Gagné F, Férard JF and Eullaffroy P. 2008. Ecotoxicity of selected nano-materials to aquatic organisms. *Environ. Toxicol.* 23: 591-598.
- Blanck H, Wangberg SA and Molander S. 1988. Pollution-induced community tolerance – a new ecotoxicological tool. In: Cairns J, Pratt JR (Eds) *Functional Testing of Aquatic Biota for Estimating Hazards of Chemicals*. American Society for Testing and Materials. Philadelphia, PA, USA. pp 219-230.
- Blanck H. 2002. A Critical Review of Procedures and Approaches Used for Assessing Pollution-Induced Community Tolerance (PICT) in Biotic Communities. *Hum. Ecol. Risk Assess.* 8: 1003-1034.
- Blaser SA, Scheringer M, MacLeod M and Hungerbühler K. 2008. Estimation of cumulative aquatic exposure and risk due to silver: contribution of nano-functionalized plastics and textiles. *Sci. Total Environ.* 390: 396-409.
- Boncel S, Kyziol-Komosinska J, Krzyewska I and Czupiol J. 2015. Interactions of carbon nanotubes with aqueous/aquatic media containing organic/inorganic contaminants and selected organisms of aquatic ecosystems - A review. *Chemosphere.* 136: 211-221.
- Bondarenko O, Juganson K, Ivask A, Kasemets K, Mortimer M and Kahru A. 2013. Toxicity of Ag, CuO and ZnO nanoparticles to selected environmentally relevant test organisms and mammalian cells in vitro: a critical review. *Arch. Toxicol.* 87: 1181-1200.
- Bouldin JL, Ingle TM, Sengupa A, Alexander R, Hannigan RE and Buchanan RA. 2008. Aqueous toxicity and food chain transfer of quantum dotsTM in freshwater algae and *Ceriodaphnia dubia*. *Environ. Toxicol. Chem.* 27: 1958-1963.
- Bundschuh M, Filser J, Lüderwald S, McKee MS, Metreveli G, Schaumann GE, Schulz R and Wagner S. 2018. Nanoparticles in the environment: where do we come from, where do we go to? *Environ. Sci. Eur.* 30: 6.
- Buzea C, Pacheco II and Robbie K. 2007. Nanomaterials and nanoparticles: Sources and toxicity. *Biointerphases.* 2: MR17-MR71.
- CEC (1996) CEC (Commission of the European Communities) technical guidance document in support of commission directive 93/67/EEC on risk assessment for new notified substances. Part II, Environmental Risk Assessment. Office for official publications of the European Communities, Luxembourg.
- Cedervall T, Lynch I, Lindman S, Berggård T, Thulin E, Nilsson H, Dawson KA and Linse S. 2007. Understanding the nanoparticle-protein corona using methods to quantify exchange rates and affinities of proteins for nanoparticles. *Proc. Natl. Acad. Sci. USA.* 104: 2050-2055.
- Chae YJ, Pham CH, Lee J, Bae E, Yi J, Gu MB. 2009. Evaluation of the toxic impact of silver nanoparticles on Japanese medaka (*Oryzias latipes*). *Aquat. Toxicol.* 94: 320-327.
- Chen M and von Mikecz A. 2005. Formation of nucleoplasmic protein aggregates impairs nuclear function in response to SiO₂ nanoparticles. *Exp. Cell Res.* 305: 51-62.
- Chen X and Schluesener H. 2008. Nanosilver: a nanoparticle in medical application. *Toxicol. Lett.* 176: 1-12.
- Chernushevich IV, Loboda AV and Thomson BA. 2001. An introduction to quadrupole-time-of-flight mass Spectrometry. *J. Mass Spectrom.* 36: 849-865.
- Cho WS, Duffin R, Howie SE, Scotton CJ, Wallace WA, Macnee W, Bradley M, Megson IL and Donaldson K. 2011. Progressive severe lung injury by zinc oxide nanoparticles; the role of Zn²⁺ dissolution inside lysosomes. *Part. Fibre Toxicol.* 8: 27.

- Choi O, Clevenger TE, Deng B, Surampalli RY, Ross LJ and Hu Z. 2009. Role of sulfide and ligand strength in controlling nanosilver toxicity. *Water Res.* 43: 1879-1886.
- Colvin VL and Kulinowski KM. 2007. Nanoparticles as catalysts for protein fibrillation. *PNAS.* 104: 8679-8680.
- Covich AP, Palmer MA and Crowl TA. 1999. The role of benthic invertebrate species in freshwater ecosystems. *BioScience.* 49: 119-127.
- Creecy JP and Conway T. 2015. Quantitative bacterial transcriptomics with RNA-seq. *Curr. Opin. Microbiol.* 23: 133-140.
- Croteau MN, Dybowska AD, Luoma SN and Valsami-Jones E. 2011. A novel approach reveals that zinc oxide nanoparticles are bioavailable and toxic after dietary exposures. *Nanotoxicology.* 5: 79-90.
- Cumberland SA and Lead JR. 2009. Particle size distribution of silver nanoparticles at environmental relevant conditions. *J. Chromatogr.* 1216: 9099-9105.
- Dabrunz A, Duester L, Prasse C, Seitz F, Rosenfeldt RR, Schilde R, Schaumann GE and Schulz R. 2011. Biological surface coating and molting inhibition as mechanisms of TiO₂ nanoparticle toxicity in *Daphnia magna*. *PLoS ONE* 6: e20112.
- Dai L, Banta GT, Selck H and Forbes VE. 2015. Influence of copper oxide nanoparticle form and shape on toxicity and bioaccumulation in the deposit feeder, *Capitella teleta*. *Mar. Environ. Res.* 111: 99-106.
- de Zwart LL, Meerman JHN, Commandeur JNM and Vermeulen NPE. 1999. Biomarkers of free radical damage. Applications in experimental animals and in humans. *Free Radicals Biol. Med.* 26: 202-226.
- Dong Y and Feng S-S. 2007. In vitro and in vivo evaluation of methoxy polyethylene glycol polylactide (mPEG-PLA) nanoparticles for small-molecule drug chemotherapy. *Biomaterials* 28: 4154-60.
- Doyotte A, Cossu C, Jacquin MC, Babut M and Vasseur P. 1997. Antioxidant enzymes, glutathione and lipid peroxidation as relevant biomarkers of experimental or field exposure in the gills and the digestive gland of the freshwater bivalve *Unio tumidus*. *Aquatic. Toxicol.* 39: 93-110.
- Drexler KE (foreword by Minsky M). 1986. *Engines of Creation: The Coming Era of Nanotechnology*. New York. Anchor Press/Doubleday.
- Durán N, Marcato PD, Alves OL, Souza GIHD and Esposito E. 2005. Mechanistic aspects of biosynthesis of silver nanoparticles by several *Fusarium oxysporum* strains. *J. Nanobiotechnology.* 3: 8.
- Ehrenberg M and McGrath JL. 2005. Binding between particles and proteins in extracts: implications for microrheology and toxicity. *Acta Biomater.* 1: 305-315.
- Einicker-Lamas M, Morales MM, Miranda K, Garcia-Abreu J, Oliveira AJ, Silva FL and Oliveira MM. 2003. P-glycoprotein-like protein contributes to cadmium resistance in *Euglena gracilis*. *J. Comp. Physiol. B.* 173: 559-564.
- El Badawy AM, Silva RG, Morris B, Scheckel KG, Suidan MT and Tolaymat TM. 2011. Surface Charge-Dependent Toxicity of Silver Nanoparticles. *Environ. Sci. Technol.* 45: 283-287.
- Elsaesser A and Howard CV. 2012. Toxicology of nanoparticles. *Adv. Drug Deliv. Rev.* 64: 129-137.
- Etxeberría E, Gonzalez P, Baroja-Fernandez E and Romero JP. 2006. Fluid phase endocytic uptake of artificial nano-spheres and fluorescent quantum dots by Sycamore cultured cells. *Plant Signal. Behav.* 1: 196-200.

- Faklaris O, Joshi V, Irinopoulou T, Tauc P, Girard H, Gesset C, Sennour M, Thorel A, Arnault JC, Boudou JP, Curmi PA and Treussart F. 2009. Photoluminescent diamond nanoparticles for cell labelling: study of the uptake mechanism in mammalian cells. *ACS Nano*. 3: 3955-3962.
- Fan WH, Cui MM, Liu H, Wang CA, Shi ZW, Tan C and Yang XP. 2011. NanoTiO₂ enhances the toxicity of copper in natural water to *Daphnia magna*. *Environ. Pollut.* 159: 729-734.
- Farkas J, Christian P, Gallego-Urrea JA, Roos N, Hassellöv M, Tollefsen KE and Thomas KV. 2011. Uptake and effects of manufactured silver nanoparticles in rainbow trout (*Oncorhynchus mykiss*) gill cells. *Aquat. Toxicol.* 101: 117-125.
- Federici G, Shaw BJ and Handy RD. 2007. Toxicity of titanium dioxide nanoparticles to rainbow trout (*Oncorhynchus mykiss*): gill injury, oxidative stress, and other physiological effects. *Aquat. Toxicol.* 84: 415-430.
- Feige U, Morimoto RI, Yahara I and Polla B S. 1996. *Stress Inducible Cellular Responses*. Basel, Boston, Berlin: Birkhäuser.
- Fenn JB, Mann M, Meng CK, Wong SF and Whitehouse CM. 1989. Electrospray ionization for mass spectrometry of large biomolecules. *Science*. 246: 64-71.
- Fernando SSN, Gunasekara TDCP and Holton J. 2018. Antimicrobial Nanoparticles: applications and mechanisms of action. *Sri Lankan Journal of Infectious Diseases*. 8: 2-11.
- Ferry JL, Craig P, Hexel C, Sisco P, Frey R, Pennington PL, Fulton MH, Scott IG, Decho AW, Kashiwada S, Murphy CJ and Shaw TJ. 2009. Transfer of gold nanoparticles from the water column to the estuarine food web. *Nat. Nanotechnol.* 4: 441-444.
- Feynman RP. 1960. There's plenty of room at the bottom. *Eng. Sci.* 22: 22-36.
- Foley S, Crowley C, Smahi M, Bonfils C, Erlanger BF, Seta P and Larroque C. 2002. Cellular localisation of a water-soluble fullerene derivative. *Biochem. Biophys. Res. Commun.* 294: 116-119.
- Freestone I, Meeks N, Sax M and Higgitt C. 2007. The Lycurgus cup - A roman nanotechnology. *Gold Bull.* 40: 270-277.
- Fridovich I. 1978. The biology of oxygen radicals. *Science*. 201: 875-880.
- Fridovich I. 1986. Biological effects of the superoxide radical. *Arch. Biochem. Biophys.* 24: 1-11.
- Fröhlich E. 2017. Role of omics techniques in the toxicity testing of nanoparticles. *J. Nanobiotechnol.* 15: 84.
- Fröhlich E. 2013. Cellular targets and mechanisms in the cytotoxic action of non-biodegradable engineered nanoparticles. *Curr. Drug. Metab.* 14: 976-988.
- Fröhlich E. 2012. The role of surface charge in cellular uptake and cytotoxicity of medical nanoparticles. *Int. J. Nanomed.* 7: 5577-5591.
- Frossard A, Gerull L, Mutz M and Gessner MO. 2012. Fungal importance extends beyond litter decomposition in experimental early-successional streams. *Environ. Microbiol.* 14: 2971-2983.
- Funnell WRJ and Maysinger D. 2006. Three-dimensional reconstruction of cell nuclei, internalized quantum dots and sites of lipid peroxidation. *J. Nanobiotechnol.* 4: 10.
- Gadd GM. 1999. Fungal production of citric and oxalic acid: importance in metal speciation, physiology and biochemical processes. *Adv. Microb. Physiol.* 41: 47-92.
- Gagnaire B, Geffard O, Xuereb B, Margoum C and Garric J. 2008. Cholinesterase activities as potential biomarkers: characterization in two freshwater snails, *Potamopyrgus antipodarum* (Mollusca, Hydrobiidae, Smith 1889) and *Valvata piscinalis* (Mollusca, Valvatidae, Müller 1774). *Chemosphere*. 71: 553-560.

- Gao J, Powers K, Wang Y, Zhou H, Roberts MS and Moudgil BM. 2012. Influence of Suwannee River humic acid on particles and toxicity of silver nanoparticles. *Chemosphere*. 89: 96-101.
- Gao W, Thamphiwatana S, Angsantikul P and Zhang L. 2014. Nanoparticle approaches against bacterial infections. *Wires Nanomed. Nanobi.* 6: 532-547.
- Garg R, Shankar R, Thakkar B, Kudapa H, Krishnamurthy L, Mantri N, Varshney RK, Bhatia S and Jain M. 2016. Transcriptome analyses reveal genotype- and developmental stage-specific molecular responses to drought and salinity stresses in chickpea. *Sci. Rep.* 6: 19228.
- Garner K and Keller A. 2014. Emerging patterns for engineered nanomaterials in the environment: A review of fate and toxicity studies. *J. Nanopart. Res.* 16: 2503.
- Gessner MO and Chauvet E. 2002. A case for using litter breakdown to assess functional stream integrity. *Ecol. Appl.* 12: 498-510.
- Gessner MO, Chauvet E and Dobson M. 1999. A perspective on leaf litter breakdown in streams. *Oikos*. 85: 377-384.
- Gheshlaghi ZN, Riazi GH, Ahmadian S, Ghafari M and Mahinpour R. 2008. Toxicity and interaction of titanium dioxide nanoparticles with microtubule protein. *Acta Biochim. Biophys. Sin.* 40: 777-782.
- Gil-Allué C, Schirmer K, Tlili A, Gessner MO and Behra R. 2015. Silver nanoparticle effects on stream periphyton during short-term exposures. *Environ. Sci. Technol.* 49: 1165-1172.
- Gillet LC, Navarro P, Tate S, Rost H, Selevsek N, Reiter L, Bonner R and Aebersold R. 2012. Targeted Data Extraction of the MS/MS Spectra Generated by Data-independent Acquisition: A New Concept for Consistent and Accurate Proteome Analysis. *Mol. Cell. Proteomics*. 11: O111.016717.
- Gomes T, Chora S, Pereira CG, Cardoso C and Bebianno MJ. 2014. Proteomic response of mussels *Mytilus galloprovincialis* exposed to CuO NPs and Cu²⁺: An exploratory biomarker discovery. *Aquat. Toxicol.* 155: 327-336.
- Gottschalk F and Nowack B. 2011. The release of engineered nanomaterials to the environment. *J. Environ. Monitor.* 13: 1145-1155.
- Goya GF, Marcos-Campos I, Fernandez-Pacheco R, Saez B, Godino J, Asin L, Lambea J, Tabuenca P, Mayordomo JI, Larrad L, Ibarra MR and Tres A. 2008. Dendritic cell uptake of iron-based magnetic nanoparticles. *Cell. Biol. Int.* 32: 1001-1005.
- Granvogl B, Ploscher M and Eichacker LA. 2007. Sample preparation by in-gel digestion for mass spectrometry-based proteomics. *Anal. Bioanal. Chem.* 389: 991-1002.
- Greulich C, Diendorf J, Simon T, Eggeler G, Epple M and Koller M. 2011. Uptake and intracellular distribution of silver nanoparticles in human mesenchymal stem cells. *Acta Biomater.* 7: 347-354.
- Griffitt RJ, Hyndman K, Denslow ND and Barber DS. 2009a. Sources fate and effects of engineered nanomaterials in the aquatic environment. *Toxicol. Sci.* 107: 404-412.
- Griffitt RJ, Hyndman K, Denslow ND and Barber DS. 2009b. Comparison of molecular and histological changes in zebrafish gills exposed to metallic nanoparticles. *Toxicol. Sci.* 107: 404-415.
- Griffitt RJ, Luo J, Bonzongo JC and Barber DS. 2008. Effects of particle composition and species on toxicity of metallic nanomaterials in aquatic organisms. *Environ. Toxicol. Chem.* 27: 1972-1978.

- Guimarães-Soares L, Pascoal C and Cássio F. 2007. Effects of heavy metals on the production of thiol compounds by the aquatic fungi *Fontanospora fusiramosa* and *Flagellospora curta*. *Ecotoxicol. Environ. Saf.* 66: 36-43.
- Habi S and Daba H. 2009. Plasmid Incidence, Antibiotic and Metal Resistance among *Enterobacteriaceae* Isolated from Algerian Streams. *Pak. J. Biol. Sci.* 12: 1474-1482.
- Halliwell B and Gutteridge JM. 1999. *Free Radicals in Biology and Medicine*. 4th edition, New York, Oxford University Press.
- Han X, Aslanian A and Yates JR 3rd. 2008. Mass spectrometry for proteomics. *Curr. Opin. Chem. Biol.* 12: 483-490.
- Hartmann NB, Kammer FVD, Hofmann T, Baalousha M, Ottofuelling S and Baun A. 2010. Algal testing of titanium dioxide nanoparticles - Testing considerations, inhibitory effects and modification of cadmium bioavailability. *Toxicology*. 269: 190-197.
- Hashimshony T, Wagner F, Sher N and Yanai I. 2012. CEL-Seq: single-cell RNA-Seq by multiplexed linear amplification. *Cell Rep.* 2: 666-673.
- Hayes JD and Pulford DJ. 1995. The glutathione S-transferase supergene family: regulation of GST and the contribution of the isoenzymes to cancer chemoprotection and drug resistance. *Crit. Rev. Biochem. Mol. Biol.* 30: 445-600.
- Heinlaan M, Ivask A, Blinova I, Dubourguier HC and Kahru A. 2008. Toxicity of nanosized and bulk ZnO, CuO and TiO₂ to bacteria *Vibrio fischeri* and crustaceans *Daphnia magna* and *Thamnocephalus platyurus*. *Chemosphere*. 71: 1308-1316.
- Hobbs HH. 2001. Decapoda. In: *Ecology and Classification of North American Freshwater Invertebrates* (ed Thorp JH and Covich AP), San Diego, California, Academic Press.
- Hodes G. 2007. When small is different: some recent advances in concepts and applications of nanoscale phenomena. *Adv. Mater.* 19: 639-655.
- Holbrook RD, Murphy KE, Morrow JB and Cole KD. 2008. Trophic transfer of nanoparticles in a simplified invertebrate food web. *Nat. Nanotechnol.* 3: 352-355.
- Hooper DU, Chapin III FS, Ewell JJ, Hector A, Inchausti P, Lavorel S, Lawton JH, Lodge DM, Loreau M, Naeem S, Schmid B, Setälä H, Symstad AJ, Vandermeer J and Wardle DA. 2005. Effects of biodiversity on ecosystem functioning: a consensus of current knowledge. *Ecol. Monogr.* 75: 3-35.
- Huang CC, Aronstam RS, Chen DR and Huang YW. 2010. Oxidative stress, calcium homeostasis, and altered gene expression in human lung epithelial cells exposed to ZnO nanoparticles. *Toxicol. In Vitro.* 24: 45-55.
- Huang GY, Wang YS, Sun CC, Dong JD and Sun ZX. 2010. The effect of multiple heavy metals on ascorbate, glutathione and related enzymes in two mangrove plant seedlings (*Kandelia candel* and *Bruguiera gymnorrhiza*). *Oceanol. Hydrobiol. Stud.* 39: 11-25.
- Huang S, Chueh PJ, Lin YW, Shih TS and Chuang SM. 2009. Disturbed mitotic progression and genome segregation are involved in cell transformation mediated by nano-TiO₂ long-term exposure. *Toxicol. Appl. Pharmacol.* 241: 182-194.
- Huggett RJ, Klmerle RA, Mehrle Jr PM and HL Bergman. 2018. *Biomarkers: Biochemical, Physiological, and Histological Markers of Anthropogenic Stress*. CRC Press.
- Huner JV. 1995. An Overview of the status of freshwater crawfish culture. *J. Shellfish Res.* 14: 539-543.
- Hussain SM, Hess KL, Gearhart JM, Geiss KT and Schlager JJ. 2005. In vitro toxicity of nanoparticles in BRL 3A rat liver cells. *Toxicol. In Vitro.* 19: 975-983.

- Janero DR. 1990. Malondialdehyde and thiobarbituric acid-reactivity as diagnostic indices of lipid peroxidation and peroxidative tissue injury. *Free Radicals Biol. Med.* 9: 515-540.
- Jena NR. 2012. DNA damage by reactive species: Mechanisms, mutation and repair. *J. Biosci.* 37: 503-517.
- Jiang HS, Yin LY, Ren NN, Zhao ST, Li Z, Zhi YW, Shao H, Li W and Gontero B. 2017. Silver nanoparticles induced reactive oxygen species via photosynthetic energy transport imbalance in an aquatic plant. *Nanotoxicology.* 11: 157-167.
- Jiang JK, Oberdorster G and Biswas P. 2009. Characterization of size, surface charge, and agglomeration state of nanoparticle dispersion for toxicological studies. *J. Nanoparticle Res.* 11: 77-89.
- Jin CY, Zhu BS, Wang XF and Lu QH. 2008. Cytotoxicity of titanium dioxide nanoparticles in mouse fibroblast cells. *Chem. Res. Toxicol.* 21: 1871-1877.
- Jin X, Li M, Wang J, Marambio-Jones C, Peng F, Huang X, Damoiseaux R and Hoek EMV. 2010. High-throughput screening of silver nanoparticle stability and bacterial inactivation in aquatic media: Influence of specific ions. *Environ. Sci. Technol.* 44: 7321-7328.
- Johnson RK, Wiederholm T and Rosenberg DM. 1992. Freshwater biomonitoring using individual organisms, populations, and species assemblages of benthic macroinvertebrates. In: *Freshwater Biomonitoring and Benthic Macroinvertebrates* (ed Rosenberg DM and Resh VH), New York, Chapman and Hall.
- José-Yacamán M, Rendon L, Arenas J, Serra Puche MC. 1996. Maya blue paint: An ancient nanostructured material. *Science.* 273: 223-225.
- Jugan ML, Barillet S, Simon-Deckers A, Herlin-Boime N, Sauvaigo S, Douki T and Carriere M. 2012. Titanium dioxide nanoparticles exhibit genotoxicity and impair DNA repair activity in A549 cells. *Nanotoxicology.* 6: 501-513.
- Kachynski AV, Kuzmin AN, Nyk M, Roy I and Prasad PN. 2008. Zinc oxide nanocrystals for nonresonant nonlinear optical microscopy in biology and medicine. *J. Phys. Chem. C.* 112: 10721-10724.
- Kah M. 2015. Nanopesticides and nanofertilizers: emerging contaminants or opportunities for risk mitigation? *Front Chem* 3: 64.
- Kahru A and Dubourguier H-C. 2010. From ecotoxicology to nanoecotoxicology. *Toxicology.* 269: 105-119.
- Karajanagi SS, Vertegel AA, Kane RS and Dordick JS. 2004. Structure and Function of Enzymes Adsorbed onto Single-Walled Carbon Nanotubes. *Langmuir.* 20: 11594-11599.
- Karas M and Hillenkamp F. 1988. Laser desorption ionization of proteins with molecular masses exceeding 10,000 daltons. *Anal. Chem.* 60: 2299-2301.
- Kashian DR, Zuellig RE, Mitchell KA and Clements WH. 2007. The cost of tolerance: sensitivity of stream benthic communities to UV-B and metals. *Ecol. Appl.* 17: 365-375.
- Kashiwada S. 2006. Distribution of nanoparticles in the see-through medaka (*Oryzias latipes*). *Environ. Health Perspect.* 114: 1697-1702.
- Keller AA, McFerran S, Lazareva A and Suh S. 2013. Global life cycle releases of engineered nanomaterials. *J. Nanopart. Res.* 15: 1692.
- Khan SS, Mukherjee A and Chandrasekaran N. 2011a. Impact of exopolysaccharides on the stability of silver nanoparticles in water. *Water Res.* 45: 5184-5190.

- Khan SS, Srivatsan P, Vaishnavi N, Mukherjee A and Chandrasekaran N. 2011b. Interaction of silver nanoparticles (SNPs) with bacterial extracellular proteins (ECPs) and its adsorption isotherms and kinetics. *J. Hazard. Mater.* 192: 299-306.
- Khan I, Saeed K and Khan I. 2017. Nanoparticles: Properties, applications and toxicities. *Arab. J. Chem.* <https://doi.org/10.1016/j.arabjc.2017.05.011>
- Kim HR, Kim MJ, Lee SY, Oh SM and Chung KH. 2011. Genotoxic effects of silver nanoparticles stimulated by oxidative stress in human normal bronchial epithelial (BEAS-2B) cells. *Mutat. Res.* 726: 129-135.
- Kim SY, Samanta P, Yoo JS, Kim WK and Jung JH. 2017. Time-dependent toxicity responses in *Daphnia magna* exposed to CuO and ZnO nanoparticles. *Bull. Environ. Contam. Toxicol.* 98: 502-507.
- Kiningham K and Kasarskis E. 1998. Antioxidant functions of metallothioneins. *J. Trace Elem. Exp. Med.* 11: 219-226.
- Klaine SJ, Alvarez PJJ, Batley GE, Fernandes TF, Handy RD, Lyon DY, Mahendra S, McLaughlin MJ and Lead JR. 2008. Nanomaterials in the environment: Behavior, fate, bioavailability, and effects. *Environ. Toxicol. Chem.* 27: 1825-1851.
- Kloepfer JA, Mielke RE and Nadeau JL. 2005. Uptake of CdSe/ZnS quantum dots into bacteria via purine-dependent mechanisms. *Appl. Environ. Microbiol.* 71: 2548-2557.
- Krauss GJ, Sole M, Krauss G, Schlosser D, Wesenberg D and Bärlocher F. 2011. Fungi in freshwaters: ecology, physiology and biochemical potential. *FEMS Microbiol. Rev.* 35: 620-651.
- Lau BLT. 2011. Understanding how nanoparticles behave in natural and engineered waters. *J. Am. Water Works Assoc.* 103: 20-22.
- Lawley B, Sims IM and Tannock GW. 2013. Whole-transcriptome shotgun sequencing (RNA-seq) screen reveals upregulation of cellobiose and motility operons of *Lactobacillus ruminis* L5 during growth on tetrasaccharides derived from barley β -glucan. *Appl. Environ. Microbiol.* 79: 5661-5669.
- Lens M. 2009. Use of fullerenes in cosmetics. *Recent Pat. Biotechnol.* 3: 118-123.
- Li H, Chen Q, Zhao J and Urmila K. 2015. Enhancing the antimicrobial activity of natural extraction using the synthetic ultrasmall metal nanoparticles. *Sci. Rep.* 5:11033
- Li X, Lenhart JJ and Walker HW. 2010. Dissolution-accompanied aggregation kinetics of silver nanoparticles. *Langmuir.* 26: 16690-16698.
- Lin L and Webster JR. 2014. Detritus decomposition and nutrient dynamics in a forested headwater stream. *Ecol. Model.* 293: 58-68.
- Lin W, Xu Y, Huang C-C, Ma Y, Shannon KB, Chen D-R and Huang Y-W. 2009. Toxicity of nano- and micro-sized ZnO particles in human lung epithelial cells. *J. Nanopart. Res.* 11: 25-39.
- Lin W, Huang YW, Zhou XD and Ma Y. 2006a. In vitro toxicity of silica nanoparticles in human lung cancer cells. *Toxicol. Appl. Pharmacol.* 217: 252-259.
- Lin W, Huang YW, Zhou XD and Ma Y. 2006b. Toxicity of cerium oxide nanoparticles in human lung cancer cells. *Int. J. Toxicol.* 25: 451-457.
- Linse S, Cabaleiro-Lago C, Xue WF, Lynch I, Lindman S, Thulin E, Radford SE and Dawson KA. 2007. Nucleation of protein fibrillation by nanoparticles. *Proc. Natl. Acad. Sci. U S A.* 104: 8691-8696.
- Liu J, Kershaw WC and Klaassen CD. 1991. The protective effect of metallothionein on the toxicity of various metals in rat primary hepatocyte culture. *Toxicol. Appl. Pharmacol.* 107: 27-34.

- Liu L, Li Y, Li S, Hu N, He Y, Pong R, Lin D, Lu L and Law M. 2012. Comparison of next-generation sequencing systems. *J. Biomed. Biotechnol.* 2012: 251364.
- Lowe R, Shirley N, Bleackley M, Dolan S and Shafee T. 2017. Transcriptomics technologies. *PLoS Comput. Biol.* 13: e1005457.
- Luan B, Huynh T and Zhou R. 2016. Complete wetting of graphene by biological lipids. *Nanoscale.* 8: 5750-5754.
- Lundqvist M, Stigler J, Elia G, Lynch I, Cedervall T and Dawson KA. 2008. Nanoparticle size and surface properties determine the protein corona with possible implications for biological impacts. *PNAS.* 105: 14265-14270.
- Manke A, Wang L and Rojanasakul Y. 2013. Mechanisms of Nanoparticle-Induced Oxidative Stress and Toxicity. *BioMed Res. Int.* Article ID 942916.
- Manning DWP, Rosemond AD, Gulis V, Benstead JP and Kominoski JS. 2018. Nutrients and temperature additively increase stream microbial respiration. *Glob. Chang. Biol.* 24: 233-247.
- Marambio-Jones C and Hoek EM. 2010. A review of the antibacterial effects of silver nanomaterials and potential implications for human health and the environment. *J. Nanopart. Res.* 12: 1531-1551.
- Martin JA and Wang Z. 2011. Next-generation transcriptome assembly. *Nat. Rev. Genet.* 12: 671-682.
- Metzker ML. 2010. Sequencing technologies - the next generation. *Nat. Rev. Genet.* 11: 31-46.
- Millennium Ecosystem Assessment (MEA). 2003. *Ecosystems and Human Well-being: A Framework for Assessment.* Island Press, Washington DC.
- Meyer JN, Lord CA, Yang XY, Turner EA, Badireddy AR, Marinakos SM, Chilkoti A, Wiesner MR and Auffan M. 2010. Intracellular uptake and associated toxicity of silver nanoparticles in *Caenorhabditis elegans*. *Aquat. Toxicol.* 100: 140-150.
- Mishra A and Verma M. 2010. Cancer biomarkers: are we ready for the prime time? *Cancers.* 2: 190-208.
- Moore MN. 2006. Do nanoparticles present ecotoxicological risks for the health of the aquatic environment? *Environ. Int.* 32: 967-976.
- Mortazavi A, Williams BA, McCue K, Schaeffer L, Wold B. 2008. Mapping and quantifying mammalian transcriptomes by RNA-Seq. *Nat. Methods.* 5: 621-628.
- Mueller NC and Nowack B. 2008. Exposure modeling of engineered nanoparticles in the environment. *Environ. Sci. Technol.* 42: 4447-4453.
- Muller EB, Lin SJ and Nisbet RM. 2015. Quantitative adverse outcome pathway analysis of hatching in zebrafish with CuO nanoparticles. *Environ. Sci. Technol.* 49: 11817-11824.
- Nadler WM, Waidelich D, Kerner A, Hanke S, Berg R, Trumpp A and Rösli C. 2017. MALDI versus ESI: The Impact of the Ion Source on Peptide Identification. *J. Proteome Res.* 16: 1207-1215.
- Nair PMG and Chung IM. 2015. Alteration in the expression of antioxidant and detoxification genes in *Chironomus riparius* exposed to zinc oxide nanoparticles. *Comp. Biochem. Phys. B.* 190: 1-7.
- Nair PMG, Park SY and Choi J. 2013. Evaluation of the effect of silver nanoparticles and silver ions using stress responsive gene expression in *Chironomus riparius*. *Chemosphere.* 92: 592-599.
- Nair PMG, Park SY, Lee SW and Choi J. 2011. Differential expression of ribosomal protein gene, gonadotrophin releasing hormone gene and Balbiani ring protein gene in silver nanoparticles exposed *Chironomus riparius*. *Aquat. Toxicol.* 101: 31-37.

- Navarro E, Baun A, Behra R, Hartmann NB, Filser J, Miao A-J, Quigg A, Santschi PH and Sigg L. 2008. Environmental behavior and ecotoxicity of engineered nanoparticles to algae, plants, and fungi. *Ecotoxicology*. 17: 372-386.
- New MB and Valenti WC. 2000. Freshwater prawn culture: the farming of *Macrobrachium rosenbergii*. Oxford, Blackwell Science.
- Noss C, Dabrunz A, Rosenfeldt RR, Lorke A and Schulz R. 2013. Three-dimensional Analysis of the Swimming Behavior of *Daphnia magna* Exposed to Nanosized Titanium Dioxide. *PLoS ONE*. 8: e80960.
- Nowack B and Bucheli TD. 2007. Occurrence, behavior and effects of nanoparticles in the environment. *Environmental Pollution*. 150: 5-22.
- Okoniewski MJ and Miller CJ. 2006. Hybridization interactions between probesets in short oligo microarrays lead to spurious correlations. *BMC Bioinformatics* 7: 276.
- Paine RT, Tegner MJ and Johnson EA. 1998. Compounded perturbations yield ecological surprises. *Ecosystems*. 1: 535-545.
- Pante N and Kann M. 2002. Nuclear pore complex is able to transport macromolecules with diameters of 39 nm. *Mol. Biol. Cell*. 13: 425-434.
- Pareek CS, Smoczynski R, Tretyn A. 2011. Sequencing technologies and genome sequencing. *J. Appl. Genet*. 52: 413-435.
- Parveen K, Banse V and Ledwani L. 2016. Green synthesis of nanoparticles: their advantages and disadvantages. *AIP Conf. Proc.* 1724, 020048. <http://dx.doi.org/10.1063/1.4945168>.
- Penninckx MJ. 2002. An overview on glutathione in *Saccharomyces* versus non-conventional yeasts. *FEMS Yeast Res.* 2: 295-305.
- Piao MJ, Kang KA, Lee IK, Kim HS, Kim S, Choi JY, Choi J and Hyun JW. 2011. Silver nanoparticles induce oxidative cell damage in human liver cells through inhibition of reduced glutathione and induction of mitochondria-involved apoptosis. *Toxicol. Lett.* 201: 92-100.
- Postel SL and Carpenter SR. 1997. Freshwater ecosystem services. In: *Nature's Services: Societal Dependence on Natural Ecosystems* (ed Daily GC), Washington, DC, Island Press.
- Poulton SW and Raiswell R. 2005. Chemical and physical characteristics of iron oxides in riverine and glacial meltwater sediments. *Chem. Geol.* 218: 203-221.
- Poynton HC, Lazorchak JM, Impellitteri CA, Blalock BJ, Rogers K, Allen HJ, Loguinov A, Heckrnan JL and Govindasmaway S. 2012. Toxicogenomic responses of nanotoxicity in *Daphnia magna* exposed to silver nitrate and coated silver nanoparticles. *Environ. Sci. Technol.* 46: 6288-6296.
- Pradhan A, Seena S, Pascoal C and Cássio F. 2011. Can metal nanoparticles be a threat to microbial decomposers of plant litter in streams? *Microb. Ecol.* 62: 58-68.
- Pradhan A, Seena S, Pascoal C and Cássio F. 2012. Copper oxide nanoparticles can induce toxicity to the freshwater shredder *Allogamus ligonifer*. *Chemosphere*. 89: 1142-1150.
- Pradhan A, Seena S, Dobritzsch D, Helm S, Gerth K, Dobritzsch M, Krauss G-J, Schlosser D, Pascoal C and Cássio F. 2014. Physiological responses to nanoCuO in fungi from non-polluted and metal-polluted streams. *Sci. Total Environ.* 466–467: 556-563.
- Pradhan A, Seena S, Schlosser D, Gerth K, Helm S, Dobritzsch M, Krauss G-J, Dobritzsch D, Pascoal C and Cássio F. 2015. Fungi from metal-polluted streams may have high ability to cope with the oxidative stress induced by copper oxide nanoparticles. *Environ. Toxicol. Chem.* 34: 923-930.
- Prichard HM and Fisher PC. 2012. Identification of platinum and palladium particles emitted from vehicles and dispersed into the surface environment. *Environ. Sci. Technol.* 46: 3149-3154.

- Qiang LW, Pan XY, Zhu LY, Fang SH and Tian SY. 2016. Effects of nano-TiO₂ on perfluorooctanesulfonate bioaccumulation in fishes living in different water layers: implications for enhanced risk of perfluorooctanesulfonate. *Nanotoxicology*. 10: 471-479.
- Quail MA, Smith M, Coupland P, Otto TD, Harris SR, Connor TR, Bertoni A, Swerdlow HP and Gu Y. 2012. A tale of three next generation sequencing platforms: comparison of Ion Torrent, Pacific Biosciences and Illumina MiSeq sequencers. *BMC Genomics*. 13: 341.
- Rani A and Goel R. 2009. Strategies for Crop Improvement in Contaminated Soils Using Metal Tolerant Bioinoculants. In: Khan MS, Zaidi A and Mussarat J (Eds) *Microbial Strategies for Crop Improvement*. Springer, Berlin. 105-132.
- Ringwood AH, McCarthy M, Bates TC and Carroll DL. 2010. The effects of silver nanoparticles on oyster embryos. *Mar. Environ. Res.* 69: S49-S51.
- Rodea-Palomares I, Boltes K, Fernández-Piñas F, Leganés F, García-Calvo E, Santiago J and Rosal R. 2011. Physicochemical characterization and ecotoxicological assessment of CeO₂ nanoparticles using two aquatic microorganisms. *Toxicol. Sci.* 119: 135-145.
- Royce TE, Rozowsky JS and Gerstein MB. 2007. Toward a universal microarray: prediction of gene expression through nearest-neighbor probe sequence identification. *Nucleic Acids Res.* 35: e99.
- Runowski M. 2014. Nanotechnology - nanomaterials, nanoparticles and multifunctional core/shell type nanostructures. *Chemik*. 68: 766-775.
- Sanderson H, Johnson DJ, Wilson CJ, Brain RA and Solomon KR. 2003. Probabilistic hazard assessment of environmentally occurring pharmaceuticals toxicity to fish, daphnids and algae by ECOSAR screening. *Toxicol. Lett.* 144: 383-395.
- Sargent LM, Hubbs AF, Young SH, Kashon ML, Dinu CZ, Salisbury JL, Benkovic SA, Lowry DT, Murray AR, Kisin ER, Siegrist KJ, Battelli L, Mastovich J, Sturgeon JL, Bunker KL, Shvedova AA and Reynolds SH. 2012. Single-walled carbon nanotube-induced mitotic disruption. *Mutat. Res.* 745: 28-37.
- Schroeder A, Mueller O, Stocker S, Salowsky R, Leiber M, Gassmann M, Lightfoot S, Menzel W, Granzow M and Ragg T. 2006. The RIN: an RNA integrity number for assigning integrity values to RNA measurements. *BMC Mol. Biol.* 7: 1.
- Schug H, Isaacson CW, Sigg L, Ammann AA, Schirmer K. 2014. Effect of TiO₂ nanoparticles and UV radiation on extracellular enzyme activity of intact heterotrophic biofilms. *Environ. Sci. Technol.* 48: 11620-11628.
- Seil JT and Webster TJ. 2012. Antimicrobial applications of nanotechnology: methods and literature. *Int. J. Nanomed.* 7: 2767-2781.
- Sharma S, Moon CS, Khogali A, Haidous A, Chabenne A, Ojo C, Jelebinkov M, Kurdi Y and Ebadi M. 2013. Biomarkers in Parkinson's disease (recent update). *Neurochem. Int.* 63: 201-229.
- Sharma V, Anderson D and Dhawan A. 2011. Zinc oxide nanoparticles induce oxidative stress and genotoxicity in human liver cells (HepG2). *J. Biomed. Nanotechnol.* 7: 98-99.
- Shukla RK, Sharma V, Pandey AK, Singh S, Sultana S and Dhawan A. 2011. ROS-mediated genotoxicity induced by titanium dioxide nanoparticles in human epidermal cells. *Toxicol. in vitro.* 25: 231-241.
- Sirelkhatim A, Mahmud S, Seeni A, Kaus NHM, Ann LC, Bakhori SKM, Hasan H and Mohamad D. 2015. Review on Zinc Oxide nanoparticles: Antibacterial activity and toxicity mechanism. *Nano-Micro Lett.* 7: 219-242.

- Soldo D and Behra R. 2000. Long-term effects of copper on the structure of freshwater periphyton communities and their tolerance to copper, zinc, nickel and silver. *Aquat. Toxicol.* 47: 181-189.
- Sotiriou GA, Pratsinis SE. 2011. Engineering nanosilver as an antibacterial, biosensor and bioimaging material. *Curr. Opin. Chem. Eng.* 1: 3-10.
- Svensson V, Vento-Tormo R and Teichmann SA. 2018. Exponential scaling of single-cell RNA-seq in the past decade. *Nat. Protoc.* 13: 599-604.
- Stern ST and Johnson DN. 2008. Role for nanomaterial-autophagy interaction in neurodegenerative disease. *Autophagy.* 4: 1097-1100.
- Stillman MJ. 1999. Spectroscopic studies of copper and silver binding to metallothioneins. *Met. Based Drugs.* 6: 277-290.
- Su GY, Zhang XW, Giesy JP, Musarrat J, Saquib Q, Alkhedhairy AA and Yu HX. 2015. Comparison on the molecular response profiles between nano zinc oxide (ZnO) particles and free zinc ion using a genome-wide toxicogenomics approach. *Environ. Sci. Pollut. Res.* 22: 17434-17442.
- Suberkropp K. 1998. Microorganisms and organic matter decomposition. In: Naiman RJ, Bilby RE (Eds) *River ecology and management: lessons from the Pacific Coastal Ecoregion*. Springer, New York, pp 120-143.
- Sule N, Singh R and Srivastava D. 2008. Alternative Modes of Binding of Recombinant Human Histone Deacetylase 8 to Colloidal Gold Nanoparticles. *J. Biomed. Nanotechnol.* 4: 463-468.
- Sun L, Li Y, Liu X, Jin M, Zhang L, Du Z, Guo C, Huang P and Sun Z. 2011. Cytotoxicity and mitochondrial damage caused by silica nanoparticles. *Toxicol. in vitro.* 25: 1619-1629.
- Sun TY, Bornhoft NA, Hungerbuhler K, Nowack B. 2016. Dynamic probabilistic modeling of environmental emissions of engineered nanomaterials. *Environ. Sci. Technol.* 50: 4701-4711.
- Suresh AK, Pelletier DA, Wang W, Morrell-Falvey JL, Gu B and Doktycz MJ. 2012. Cytotoxicity induced by engineered silver nanocrystallites is dependent on surface coatings and cell types. *Langmuir.* 28: 2727-2735.
- Swathy JR, Sankar MU, Chaudhary A, Aigal S, Anshup and Pradeep T. 2014. Antimicrobial silver: An unprecedented anion effect. *Sci. Rep.* 4: 7161.
- Switzar L, Giera M and Niessen WM. 2013. Protein digestion: an overview of the available techniques and recent developments. *J. Proteome Res.* 12: 1067-1077.
- Taniguchi N. 1974. On the Basic Concept of 'Nano-Technology'. *Proc. Intl. Conf. Prod. Eng. Tokyo, Part II, Japan Society of Precision Engineering.*
- Tejamaya M, Roemer I, Merrifield RC, Lead JR. 2012. Stability of Citrate, PVP, and PEG Coated Silver Nanoparticles in Ecotoxicology Media. *Environ. Sci. Technol.* 46: 7011-7017.
- Tiwari JN, Tiwari RN and Kim KS. 2012. Zero-dimensional, one-dimensional, two-dimensional and three-dimensional nanostructured materials for advanced electrochemical energy devices. *Prog. Mater. Sci.* 57: 724-803.
- Tlili A, Marechal M, Berard A, Volat B and Montuelle B. 2011. Enhanced co-tolerance and co-sensitivity from long-term metal exposures of heterotrophic and autotrophic components of fluvial biofilms. *Sci. Total Environ.* 409: 4335-4343.
- Tlili A, Cornut J, Behra R, Gil-Allué C and Gessner MO. 2016. Harmful effects of silver nanoparticles on a complex detrital model system. *Nanotoxicology.* 10: 728-735.
- Tsuzuki T. 2009. Commercial scale production of inorganic nanoparticles. *Int. J. Nanotechnol.* 6: 567-578.

- Tungittiplakorn W, Lion LW, Cohen C and Kim JY. 2004. Engineered polymeric nanoparticles for soil remediation. *Environ. Sci. Technol.* 38: 1605-1610.
- Turci F, Ghibaudi E, Colonna M, Boscolo B, Fenoglio I and Fubini B. 2010. An integrated approach to the study of the interaction between proteins and nanoparticles. *Langmuir.* 26: 8336-8346.
- Vera C, Wheat CW, Fescemyer HW, Frilander MJ, Crawford DL, Hanski I and Marden JH. 2008. Rapid transcriptome characterization for a nonmodel organism using 454 pyrosequencing. *Mol. Ecol.* 17: 1636-1647.
- Vinebrooke RD, Cottingham KL, Norberg J, Scheffer M, Dodson SI, Maberly SC and Sommer U. 2004. Impacts of multiple stressors on biodiversity and ecosystem functioning: the role of species co-tolerance. *Oikos.* 104: 451-457.
- Völker C, Kampken I, Boedicker C, Oehlmann J and Oetken M. 2015. Toxicity of silver nanoparticles and ionic silver: comparison of adverse effects and potential toxicity mechanisms in the freshwater clam *Sphaerium corneum*. *Nanotoxicology.* 9: 677-685.
- Völker C, Oetken M and Oehlmann J. 2013. The biological effects and possible modes of action of nanosilver. *Rev. Environ. Contam. Toxicol.* 233:81–106
- von der Kammer F, Ferguson PL, Holden PA, Masion A, Rogers KR, Klaine SJ, Koelmans AA, Horne N and Unrine JM. 2012. Analysis of engineered nanomaterials in complex matrices (environment and biota): general considerations and conceptual case studies. *Environ. Toxicol. Chem.* 31: 32-49.
- Vowinckel J, Capuano F, Campbell K, Deery M, Lilley KS and Ralser M. 2014. The beauty of being (label)-free: sample preparation methods for SWATH-MS and next-generation targeted proteomics. *F1000 Res.* 2: 272.
- Wagner S, Gondikas A, Neubauer E, Hofmann T and von der Kammer F. 2014. Spot the difference: Engineered and natural nanoparticles in the environment-release, behavior, and fate. *Angew. Chem. Int. Ed.* 53: 12398-12419.
- Walther TC and Mann M. 2010. Mass spectrometry-based proteomics in cell biology. *J. Cell Biol.* 190: 491-500.
- Wang L, Hu C and Shao L. 2017. The antimicrobial activity of nanoparticles: present situation and prospects for the future. *Int. J. Nanomed.* 12: 1227-1249.
- Wang Z, Li N, Zhao J, White JC, Qu P and Xing B. 2012. CuO nanoparticle interaction with human epithelial cells: cellular uptake, location, export, and genotoxicity. *Chem. Res. Toxicol.* 25: 1512-1521.
- Wang Z, Gerstein M and Snyder M. 2009. RNA-Seq: a revolutionary tool for transcriptomics. *Nat. Rev. Genet.* 10: 57-63.
- Ward JE and Kach DJ. 2009. Marine aggregates facilitate ingestion of nanoparticles by suspension-feeding bivalves. *Mar. Environ. Res.* 68: 137-142.
- Waters MD and Fostel JM. 2004. Toxicogenomics and systems toxicology: aims and prospects. *Nat. Rev. Genet.* 5: 936-948.
- Wei D, Unalan HE, Han DX, Zhang QX, Niu L, Amaratunga G and Ryhanen T. 2008. A solid-state dye-sensitized solar cell based on a novel ionic liquid gel and ZnO nanoparticles on a flexible polymer substrate. *Nanotechnology.* 19: 424006.
- Wigginton NS, Haus KL and Hochella MF. 2007. Aquatic environmental nanoparticles. *J Environ Monit.* 9: 1306-1316.

- Wilhelm BT, Marguerat S, Watt S, Schubert F, Wood V, Goodhead I, Penkett CJ, Rogers J, Bähler J. 2008. Dynamic repertoire of a eukaryotic transcriptome surveyed at single-nucleotide resolution. *Nature*. 453: 1239-1243.
- Wilson JB. 1988. The cost of heavy-metal tolerance: An example. *Evolution*. 42: 408-413.
- Wilson W. 2012. Consumer products inventory Project on Emerging Nanotechnologies, a project of the Woodrow Wilson International Center for Scholars.
- Witko-Sarsat V, Friedlander M, Capeilliere-Blandin C, Nguyen-Khoa T, Nguyen AT, Zingraff J, Jungers P, Descamps-Latscha B. 1996. Advanced oxidation protein products as a novel marker of oxidative stress in uremia. *Kidney Int*. 49: 1304-1313.
- Xia T, Kovoichich M, Liong M, Mädler L, Gilbert B, Shi H, Yeh JI, Zink JI and Nel AE. 2008. Comparison of the mechanism of toxicity of zinc oxide and cerium oxide nanoparticles based on dissolution and oxidative stress properties. *ACS Nano*. 2: 2121-2134.
- Xia T, Kovoichich M, Brant J, Hotze M, Sempf J, Oberley T, Sioutas C, Yeh JI, Wiesner MR and Nel AE. 2006. Comparison of the Abilities of Ambient and Manufactured Nanoparticles To Induce Cellular Toxicity According to an Oxidative Stress Paradigm. *Nano Lett*. 6: 1794-1807.
- Xu X-HN, Brownlow WJ, Kyriacou SV, Wan Q and Viola JJ. 2004. Real-time probing of membrane transport in living microbial cells using single nanoparticle optics and living cell imaging. *Biochemistry*. 43: 10400-10413.
- Zhang W, Xiao B and Fang T. 2018. Chemical Transformation of Silver Nanoparticles in Aquatic Environments: Mechanism, Morphology and Toxicity. *Chemosphere*. 191: 324-334.
- Zhang W, Li Y, Niu JF and Chen YS. 2013. Photogeneration of reactive oxygen species on uncoated silver, gold, nickel, and silicon nanoparticles and their antibacterial effects. *Langmuir*. 29: 4647-4651.
- Zhang XZ, Sun HW, Zhang ZY, Niu Q, Chen YS and Crittenden JC. 2007. Enhanced bioaccumulation of cadmium in carp in the presence of titanium dioxide nanoparticles. *Chemosphere*. 67: 160-166.
- Zhao C-M and Wang W-X. 2012. Size-dependent uptake of silver nanoparticles in *Daphnia magna*. *Environ. Sci. Technol*. 46: 11345-11351.
- Zhu XS, Wang JX, Zhang XZ, Chang Y and Chen YS. 2010. Trophic transfer of TiO₂ nanoparticles from daphnia to zebrafish in a simplified freshwater food chain. *Chemosphere*. 79: 928-933.
- Zhu Y, Zhao Q, Li Y, Cai X and Li W. 2006. The interaction and toxicity of multi-walled carbon nanotubes with *Stylonychia mytilus*. *J. Nanosci. Nanotechnol*. 6: 1357-1364.
- Zolgharnein H, Karami K, Assadi MM and Sohrab AD. 2010. Investigation of Heavy Metals Biosorption on *Pseudomonas aeruginosa* Strain MCCB 102 Isolated from the Persian Gulf. *Asian J. Biotechnol*. 2: 99-109.
- Zou XY, Li PH, Huang Q and Zhang HW. 2016. The different response mechanisms of *Wolfa globosa*: light-induced silver nanoparticle toxicity. *Aquat. Toxicol*. 176: 97-105.
- Zsigmondy R. 1909. Colloids and the Ultra Microscope. *J. Am. Chem. Soc*. 31: 951-95.

Chapter 2

Proteomics and antioxidant enzymes reveal different mechanisms of toxicity induced by ionic and nanoparticulate silver in bacteria

Abstract

The increased use of silver nanoparticles (AgNPs) raises concerns about their impacts on aquatic ecosystems. Impacts of Ag⁺ and AgNPs were assessed on proteomic and antioxidant enzymatic responses of *Pseudomonas* sp. M1. The effects of Ag⁺ on bacterial growth were stronger than those of AgNPs (EC₂₀=107.1 µg L⁻¹ for Ag⁺; EC₂₀=307.2 µg L⁻¹ for AgNPs), indicating lower toxicity of the latter. At EC₂₀, the activities of antioxidant enzymes increased more under exposure to Ag⁺ than to AgNPs, particularly for superoxide dismutase and glutathione peroxidase (stimulation of 667% and 433%, respectively). A total of 166 proteins were identified by SWATH-MS; among these, only 59 had their content significantly altered by one or both forms of silver. Exposure to AgNPs resulted in an increase of about 54% of these proteins, whereas 54% decreased under exposure to Ag⁺. Gene Ontology enrichment analysis revealed that protein folding and transmembrane transport were the most relevant processes affected by Ag⁺ exposure, whereas AgNPs mostly affected translation. Also, results suggest that each form of silver induced different adaptive responses. Furthermore, the low levels of Ag⁺ released from AgNPs (<0.1%) support a minor role of dissolved silver in AgNP toxicity to *Pseudomonas* sp. M1.

Keywords: Silver nanoparticles, antioxidant enzymes, proteomics, *Pseudomonas* sp. M1.

2.1. Introduction

The developments in nanotechnology over the past decade increased concerns about the environmental impacts of engineered nanoparticles (ENPs). Silver nanoparticles (AgNPs) are among the most widely used ENPs (Vance et al 2015). Due to their broad-spectrum antimicrobial properties, AgNPs have been used extensively in textiles and therapeutics (Nair and Laurencin 2007, Zhang et al 2009). About 20-130 tons of ionic silver (Ag^+) were predicted to reach EU freshwaters per year, mainly due to ionic leaching of AgNPs from biocidal plastics and textiles (Blaser et al 2008). The industrial production of AgNPs was predicted to become ca. 20 tons per year (European Commission 2012), of which about 30% can be released to the aquatic environment (Kaegi et al 2010). The environmental concentrations of AgNPs in freshwaters are predicted to be lower than $1 \mu\text{g L}^{-1}$, but may increase up to 100 times in wastewater effluents (Tiede et al 2010; Gottschalk et al 2013). Furthermore, the possibility of attaining higher AgNP-concentrations due to accidental spills cannot be ignored. Hence, AgNPs have been considered emerging chemical contaminants in aquatic environments and recommended for environmental risk assessment (OECD 2010).

The prime challenge regarding the assessment of ENP toxicity in aquatic biota is still the establishment of standard nano-specific protocols (Handy et al 2012), including sample preparation and test conditions, to achieve reproducible results and to effectively link the toxicological information to the physicochemical properties of ENPs (but see test guidelines, OECD 2014).

Many studies have reported toxic effects of AgNPs to freshwater organisms, including bacteria, algae, fungi, invertebrates and fish (Kumar et al 2014; Sohn et al 2015; Tlili et al 2016), but little is known on the mechanisms underlying such effects. Some studies indicate that the bioavailable Ag^+ released from AgNPs, contributes to toxicity (Fabrega et al 2011; Wang et al 2012). Speciation of released Ag^+ in aquatic environments might be a key factor influencing toxicity, and may occur via interactions with natural ligands forming AgCl , Ag_2O , Ag_2S , and other silver(I) complexes (Behra et al 2013; Reidy et al 2013; Zhang et al 2016; McGillicuddy et al 2017). Lubick (2008) showed that some algal species are more sensitive to AgNPs than to free Ag^+ , but when cysteine (a metal chelator) is added, the toxicity of both silver forms is reduced due to complexation of Ag^+ . More recently, it

was shown that actual Gibbs free energy can be used to accurately calculate the equilibrium concentrations of AgNPs and released Ag^+ and precisely determine the real transformation, fate, and ecotoxicity of AgNPs in aquatic environments (Zhang et al 2016). Heterotrophic bacteria play a crucial role in stream ecosystem processes, and they can be affected by acute and chronic exposure to AgNPs (Pradhan et al 2011; Tlili et al 2016). Very small particle size AgNPs can exhibit higher toxicity to prokaryotic cells than Ag^+ or other forms of Ag (Cumberland and Lead 2009, Choi and Hu 2009). Chronic exposure to Ag^+ , released from AgNPs at very low concentrations, may also heighten the silver tolerance/resistance in bacteria (Silver 2003). Interactions with and adhesion of AgNPs to the bacterial surface can alter cell wall structure, and induce intracellular generation of reactive oxygen species (ROS), disruption of the plasma membrane, changes in protein interactions, and interference with DNA replication, and damage macromolecules (lipids, proteins, DNA and RNA) (Reidy et al 2013; Zhang et al 2016).

Environmental stress biomarkers and omics are among the most promising next generation toxicity assessment tools, enhancing measurements of direct and highly sensitive responses to emerging environmental contaminants at the cellular and sub-cellular levels. Freshwater microbes and invertebrates are reported to trigger antioxidant defence mechanisms in response to exposure to metals or metal-based ENPs; these include changes in the activities of antioxidant enzymes such as catalase (CAT), superoxide dismutase (SOD), glutathione peroxidase (GPx), and glutathione-S-transferase (GST) (Azevedo et al 2007; Pradhan et al 2015; Pradhan et al 2016), suggesting a role as oxidative stress biomarkers. These enzymes are closely associated with the ascorbate-glutathione cycle, in which the reduced form of glutathione (GSH) is converted to its oxidized form (GSSG), thus maintaining a high GSH:GSSG ratio. This is crucial for regulating the cellular redox state and preventing cellular damage by oxidative stress (Pradhan et al 2015; Pradhan et al 2016). Proteomics can be used to unravel the dynamics of proteins in targeted organisms in response to environmental stressors, eventually revealing biomarkers of specific stressors (Nesatyy and Suter 2007; Ge et al 2013). Proteomics have been applied to environmentally relevant microbes, including aquatic bacteria, to reveal the mechanisms underlying the responses to anthropogenic stressors such as phenol, mancozeb and 2,4-dichlorophenoxyacetic acid (Teixeira et al 2005; Santos and Sá-Correia 2007; Santos et al 2009), making this approach valuable to determine the effects of

emerging chemical contaminants. Adverse effects of AgNPs on *Pseudomonas* (e.g. *P. aeruginosa*, *P. putida*, *P. chlororaphis*) have been reported (Kalishwaralal et al 2010; Dimkpa et al 2011; Yuan et al 2017; Yan et al 2018), but the mechanisms of toxicity have rarely been investigated.

The aim of this study was to investigate the impacts of AgNPs and its ionic precursor (Ag^+) on *Pseudomonas* sp. M1. This strain was chosen because of its heterotrophic nature and ability to biodegrade several environmental contaminants, including phenols, terpenes and other recalcitrant compounds (Santos and Sá-Correia 2007, Santos and Sá-Correia 2009). To gain insights into the mechanisms underlying the impacts of Ag^+ and AgNPs on *Pseudomonas* sp. M1 and its ability to deal with these toxicants, we determined i) dose-response curves using bacterial growth as endpoint, ii) antioxidant enzymatic responses, and iii) proteomic responses. We hypothesized that i) *Pseudomonas* sp. M1 would exhibit more tolerance to AgNPs than to Ag^+ , ii) the response profiles of antioxidant enzymes would potentially indicate the oxidative stress induced by the two silver forms, and iii) proteomic profiles would portray the key signature proteins in response to Ag^+ and AgNPs. Moreover, we aim to elucidate the role of dissolved ionic silver released from AgNPs in the overall toxicity effects as well as their underlying mechanisms.

2.2. Materials and methods

2.2.1. Bacterial exposure to Ag^+ and AgNPs

Pseudomonas sp. M1 is an oxidase-positive strain, isolated from sediments of the Rhine River (Wageningen, Netherlands; Iurescia et al 1999) and phylogenetically close to the environmental strain *P. citronellolis* (Santos et al 2007). *Pseudomonas* sp. M1 cells were cultivated at 30 °C and maintained in *Pseudomonas* Isolation Agar (PIA) plates. For the exposure experiments, liquid cultures were prepared in sterile 250-mL Erlenmeyer flasks (pre-silanized to avoid adherence of metals/ENPs to the surface) with 50 mL of mineral medium (MM) as described by Hartmans et al (1989) and supplemented with 0.4% lactate as sole carbon source, under orbital shaking (200 rpm; Certomat BS 3, B. Braun Biotech International) at 30 °C. The inoculum consisted of bacterial cells grown to an optical density (OD_{600}) between 0.6-0.8 to reach the exponential growth phase, and diluted in fresh MM containing lactate to obtain an initial OD_{600} of 0.15.

An aqueous suspension of citrate-coated AgNPs (1 g L^{-1}) was purchased from NanoSys GmbH (Wolfhalden, Switzerland). The AgNO_3 (> 99%) and other chemicals were purchased from Sigma-Aldrich (St. Louis, MO, USA), unless specified. The stock suspension of AgNPs (100 mg L^{-1}) was prepared in filtered ($0.2\text{-}\mu\text{m}$ pore-size membrane; Millipore, Billerica, MA) ultrapure water (Milli-Q, $18.2 \text{ M}\Omega\text{-cm}$) and stored in the dark. The stock solution of AgNO_3 was prepared by suspending the powder in autoclaved ($121 \text{ }^\circ\text{C}$, 20 min) ultrapure water.

The estimations of the effective concentrations (EC_{10} and EC_{20}), using growth as endpoint, were performed by exposing *Pseudomonas* sp. M1 cells to increasing concentrations of AgNPs ($\leq 1000 \text{ }\mu\text{g L}^{-1}$) and to their ionic precursor (Ag^+ in AgNO_3 ; $\leq 300 \text{ }\mu\text{g L}^{-1}$) for 90 min (at $30 \text{ }^\circ\text{C}$, 200 rpm). For enzymatic and proteomic assays, cells at mid-exponential phase (Santos and Sá-Correia 2007, Santos and Sá-Correia 2009) were exposed to toxicants (under same conditions). For enzymatic assays, cells were incubated with or without i) Ag^+ at concentrations similar to EC_{10} and EC_{20} and ii) AgNPs at concentrations similar to EC_{10} and EC_{20} for AgNPs and the concentrations used for exposure to Ag^+ . For proteomic analysis, the cells were incubated under similar conditions with or without Ag^+ or AgNPs at the concentrations of their respective EC_{20} .

A complementary test was carried out with cysteine (L-Cystein, $\geq 98\%$, Sigma-Aldrich), a strong Ag^+ chelating agent, to better understand the actual role of released Ag^+ in AgNP-induced toxicity. The effects of $500 \text{ }\mu\text{M}$ of cysteine (see Tlili et al 2016) on the growth of *Pseudomonas* sp. M1 in mineral medium with 0.4% lactate ($30 \text{ }^\circ\text{C}$ for 90 min) was assessed in the presence or absence of Ag^+ (at EC_{20}) or AgNPs (at EC_{20}).

2.2.2. Characterization of nanoparticles and quantification of dissolved silver

The stock suspension of AgNPs was characterized by UV-vis spectrophotometer (UV-1700 PharmaSpec, Shimadzu, Kyoto, Japan). The hydrodynamic size distribution, dispersity and stability of nanoparticles in the aqueous stock suspension before the experiment, and in the exposure medium at the beginning and end of the experiment were monitored by dynamic light scattering (DLS) and zeta potential using a zetasizer (Malvern, Zetasizer Nano ZS, Malvern Instruments Limited, UK).

Total and dissolved Ag^+ derived from AgNPs in the growth medium containing AgNPs were quantified at the beginning and at the end of the experiment by inductively coupled

plasma mass spectrometry (Thermo X7 Q-ICP-MS, Thermo Scientific) at the Scientific and Technological Research Assistance Centre (C.A.C.T.I., University of Vigo, Spain).

Bacterial cells were removed from the medium by centrifugation (5000 × g, 5 min). Total Ag concentration (isotope ¹⁰⁹Ag) in the medium was determined in cell-free supernatant diluted with HNO₃ (2%). The quantification of dissolved Ag⁺ from AgNPs was performed in cell-free supernatant after ultrafiltration for 30 min (3220 × g, 3 times) using Amicon Ultra-15 centrifugal filter units (Merck Millipore, Germany; 3 kDa of molecular weight cut-off, corresponding to < 2 nm of estimated pore size) followed by acidification with HNO₃ (1.68% final concentration).

2.2.3. Preparation of cell-free extracts and protein quantification

Cells of *Pseudomonas* sp. M1 were harvested by centrifugation (15000 × g for 10 min at 4 °C). For the assessment of the activities of antioxidant enzymes, cells were washed twice with ice-cold washing buffer (10 mM tris-HCl, pH 7.0, 0.25 M sucrose) and resuspended into the sonication buffer (10 mM tris-HCl, pH 7.0). For the proteomic analysis, the 10 mM tris-HCl pH 7.4 with 0.25 M sucrose was used as washing buffer, whereas sucrose was not present in the sonication buffer. Cells were disrupted by ultrasonication at 20 KHz (15 min, cycles of 3-sec burst with a 9-sec interval, in ice) using a 13-mm probe and Ultrasonic Processor GEX 400 (Sonics and Materials Inc, CT, USA). Unbroken cells were removed by centrifugation (5000 × g for 15 min at 4 °C), and cell-free extracts were obtained by centrifugation at 16000 × g for 30 min at 4 °C followed by a filtration (0.2-µm; Millipore, Billerica, MA). The extract was stored at -80 °C until use.

Protein concentration in the cell-free extracts was determined by the modified Lowry method (Peterson 1983), using bovine serum albumin (BSA) as protein standard.

2.2.4. Antioxidant enzyme activities

Antioxidant enzyme activities from unexposed cells were compared with those exposed to Ag⁺ or AgNPs by spectrophotometry (SpectraMax Plus 384 Microplate Reader, Molecular Devices, CA, USA). The activity of SOD was assessed based on its ability to inhibit superoxide radical dependent reactions using the Ransod Kit (Randox Laboratories Limited, Crumlin, UK). Briefly, 10 µL of the cell-free extract was added to 165 µL of reaction mixture containing 0.05 mM xanthine, 0.025 mM 2-(4-iodophenyl)-3-(4-nitrophenol)-5-

phenyltetrazolium chloride (INT) dissolved in 40 mM 3-(cyclohexylamino)-1-propanesulfonic acid (pH 10.2) and 0.94 mM of ethylenediaminetetraacetic acid (EDTA). The formation of superoxide radicals from xanthine started after addition of 25 μL of xanthine oxidase (80 U L^{-1}).

The activity of CAT was determined as described by Clairborne (1985). The 25 μL cell-free extract was added to a 275 μL reaction mixture, comprising 0.05 M potassium phosphate buffer pH 7.0 and 30 mM H_2O_2 . The decrease in absorbance due to dismutation of H_2O_2 was detected at 240 nm ($\epsilon = 0.04 \text{ mM}^{-1} \text{ cm}^{-1}$). CAT activity was calculated from the slope of the H_2O_2 absorbance curve and normalized to the protein concentration.

The GPx activity was determined according to Flohé and Günzler (1984) with slight modifications (Pradhan et al 2016). The cell-free extract (10 μL) was added to a reaction mixture (290 μL) containing 0.05 M potassium phosphate buffer (pH 7.0), 1 mM EDTA, 1 mM NaN_3 , 1 mM GSH (reduced glutathione), 0.24 mM reduced form of nicotinamide adenine dinucleotide phosphate (NADPH), 0.25 mM H_2O_2 and 0.2 U glutathione reductase (GR, from yeast). H_2O_2 served as substrate while NaN_3 blocked the activity of catalase. The oxidation of NADPH was detected at 340 nm ($\epsilon = 6.2 \text{ mM}^{-1} \text{ cm}^{-1}$) when GR reduced the GSSG (oxidized glutathione) to GSH. The activity of GPx was calculated from slope of the NADPH absorbance curve and normalized to the protein concentration.

The activity of GST in *Pseudomonas* sp. M1 was determined according to Habig et al (1974), by measuring the formation of 1-glutathion-2,4-dinitrobenzene, resulted from the conjugation of GSH with 1-chloro-2,4-dinitrobenzene (CDNB). The cell-free extract (50 μL) was added to 250 μL of reaction mixture containing 0.1 M potassium phosphate buffer (pH 6.5), 1.5 mM of CDNB and 1.5 mM of GSH. The activity of GST was calculated from the slope of the absorbance curve at 340 nm ($\epsilon = 9.6 \text{ mM}^{-1} \text{ cm}^{-1}$) and normalized to protein concentration.

2.2.5. Protein denaturation, SDS-PAGE and gel staining

Prior to protein identification, volumes equivalent to 200 μg of total protein from each sample were incubated for 60 min at room temperature with urea loading buffer containing 9 M urea, 50 mM Tris at pH 8.8, 10% (v/v) glycerol, 10% (w/v) SDS, 0.002% (w/v) bromophenol blue and 20 mM dithiothreitol (DTT). A second incubation was done for 60 min at room temperature with the same buffer containing 20 mM acrylamide. Then,

samples were loaded on SDS-polyacrylamide gels and subjected to electrophoretic separation. Finally, gels were stained with Coomassie Brilliant Blue G-250 solution. Detected protein bands were excised, sliced into small pieces and used for protein identification.

2.2.6. SWATH-MS analysis

After denaturation, the proteins were alkylated with acrylamide and subjected to in gel digestion with trypsin (0.01 mg mL^{-1}) by using the short-GeLC approach (Anjo et al 2014). The formed peptides were subjected to SPE using OMIX tips with C18 stationary phase (Agilent Technologies) as recommended by the manufacturer and then resuspended in $30 \mu\text{L}$ of mobile phase containing iRT peptides (Biognosys AG) as internal standards. Five μL of each replicate sample was combined to obtain one pooled sample per experimental condition (in a total of four pools), to be used for protein identification and SWATH-MS (Sequential Windowed data independent Acquisition of the Total High-resolution Mass Spectra)-library generation.

Samples were analyzed on a Triple TOFTM 5600 System (ABSciex®) in two phases: information-dependent acquisition (IDA) of the pooled samples for protein identification, and SWATH acquisition of each individual sample for protein quantification (see details in Appendix 2). A specific library of precursor masses and fragment ions was created by combining all files from the IDA experiments, and used for subsequent SWATH processing. Libraries were obtained using Protein Pilot™ software (v5.1, ABSciex®) searching against a database composed by the genus *Pseudomonas* from the SwissProt database (release at June 2015).

SWATH data processing was performed using SWATH™ processing plug-in for PeakView™ (v2.0.01, ABSciex®). Briefly, peptides were selected automatically from the library and up to 15 peptides with up to 5 fragment ions were chosen per protein. Quantitation was attempted for all proteins in library file that were identified below 5% local False Discovery Rate (FDR) from ProteinPilot™ searches, by extracting the peak areas of the target fragment ions of those peptides using an extracted-ion chromatogram (XIC) window of 5 minutes with 20 mDa XIC width.

Peptides that met 1% FDR threshold in at least three out of the four biological replicates were retained, and the levels of the proteins were estimated by summing all the respective

transitions and peptides that met the criteria (adapted from Collins et al 2013). For comparisons between experiments, protein levels were normalized to the total intensity. Detailed process and description can be found in Appendix 2.

2.2.7. Statistical analyses

The effective concentrations of Ag^+ and AgNPs inducing 10% or 20% of decrease (EC_{10} and EC_{20} with the respective 95% C.I.) in bacterial growth were calculated using PriProbit 1.63 (Sakuma 1998). Data in percentage was arcsine square root transformed to achieve normal distribution and homoscedasticity before analyses of variance (Zar 2010).

The effects of cysteine and the form of silver (Ag^+ or AgNPs) were tested by two-way analyses of variance (ANOVA), followed by Dunnett's post-hoc tests to identify treatments that differed significantly from the control. Two-way ANOVAs were also used to test for the effects of AgNPs or Ag^+ concentrations on antioxidant enzymes. One-way ANOVAs were used to test for the effects of each form of silver (Ag^+ or AgNPs) on the protein contents. Analyses were done in Prism 7.0 for Windows (GraphPad software Inc., CA, USA). Fold changes of statistically significant proteins (one-way ANOVA, $P < 0.05$) were determined by Log₂ transformation of the ratio of protein levels under exposure to Ag^+ or AgNPs versus control conditions.

Heatmap and clustering analyses of significantly altered proteins were performed using GProX (version 1.1.15, Rigbolt et al 2011). The proteins displayed in the heatmap were clustered according to their behavioural profiles. Clustering was performed using the unsupervised clustering fuzzy c-means algorithm implemented in the Mfuzz package (Kumar and Futschik 2007), a soft clustering algorithm, noise-robust and well-fitted to the protein profile data. Gene Ontology (GO) enrichment analysis was performed and the most representative biological processes associated with each cluster were highlighted. GO annotations for the 59 statistically altered proteins were performed using the Blast2GO (version 4.1.9) where protein sequences were loaded as a Sequences (FASTA) file. The BLAST was performed against the non-redundant (nr) protein database NCBI using the BLASTP method. GO annotations were exported for the Biological Process category and imported to the GProX software to perform the enrichment analysis. Each cluster was tested for overrepresented GO compared with the cluster 3 (background) using the

Binomial statistical test with Benjamini-Hochberg adjustment ($P < 0.05$). Significant effects were determined by PERMANOVA.

Principal component analysis (PCA) was applied to coordinate the alterations in the proteins and the activities of antioxidant enzymes (SOD, CAT, GST and GPx) according to the treatments (control, Ag^+ and AgNPs). The proteins related to the stress response used in PCA were catalase-peroxidase (KatG) and alkyl hydroperoxide reductase subunit C (AhpC). Significant effects were determined by PERMANOVA. The PCA was performed in PAST 3.14 for Windows (Copyright Hammer & Harper, Ohio, U.S.; Hammer et al 2001).

2.3. Results

2.3.1. Characterization of AgNPs and quantification of dissolved Ag^+

The AgNPs in mineral medium showed a peak at 419 nm by UV-vis spectrophotometer. At the beginning of the experiment, AgNPs at the highest concentration showed two peaks of hydrodynamic diameter (HDD) of smaller (average HDD < 45 nm; area intensity of 8.3%) and larger size range (average HDD < 310 nm; area intensity of 91.7%; Table 2.1). The peak with larger hydrodynamic size range was probably the consequence of AgNP agglomeration due to interactions with the medium components. After 90 min of exposure to AgNPs, only one peak was observed and the size of larger particles increased indicating increased NP agglomeration. The zeta potential of the AgNPs (-20.9 mV), the conductivity and the electrophoretic mobility did not change after 90 min of exposure (initial vs final conductivity: 7.38 ± 0.09 vs 7.41 ± 0.03 mS cm^{-1} ; and mobility: -1.39 ± 0.05 vs -1.39 ± 0.04 $\mu\text{m cm Vs}^{-1}$).

Changes in total silver quantification by ICP-MS in mineral medium either at the initial time (T0) or at the end of the experiment (T1 = 90 min) were not apparent (18.90 ± 0.71 $\mu\text{g L}^{-1}$ at T0 and 21.68 ± 3.03 $\mu\text{g L}^{-1}$ at T1; Table 2.1). Dissolved Ag^+ quantification by ICP-MS revealed that, at the beginning of the exposure (T0), the concentration of Ag^+ originating from the dissolution of AgNPs to the mineral medium (300 $\mu\text{g L}^{-1}$ in 50 mL) was 0.30 ± 0.07 $\mu\text{g L}^{-1}$; however, at the end of the experiment (T1), the concentration of dissolved Ag^+ was lower than at T0 (< 0.2 $\mu\text{g L}^{-1}$; the detection limit was 0.06 $\mu\text{g L}^{-1}$).

Table 2.1 Zeta potential, polydispersity index (Pdl) and hydrodynamic diameter (HDD) of AgNPs and total and dissolved Ag concentration in mineral medium with 0.4% lactate before (T0) and after 90 min (T1) of exposure to AgNPs at concentrations inhibiting 20% (EC₂₀) of the growth of *Pseudomonas* sp. M1. Mean \pm SD, n = 3.

Time	Zeta potential (mV)	Pdl	Peak 1		Peak 2		Total Ag ($\mu\text{g L}^{-1}$)	Dissolved Ag ($\mu\text{g L}^{-1}$)
			HDD (nm)	Area Intensity (%)	HDD (nm)	Area Intensity (%)		
T0	-20.9 \pm 0.7	0.56 \pm 0.12	307.4 \pm 36	91.7 \pm 2	42.2 \pm 27	8.3 \pm 2	18.90 \pm 0.71	0.30 \pm 0.07
T1	-20.9 \pm 0.6	0.50 \pm 0.31	657.8 \pm 33	100 \pm 0	-	-	21.68 \pm 3.03	<0.20 \pm 0.00

2.3.2. Effects of Ag⁺ and AgNPs on the growth of *Pseudomonas* sp. M1

The specific growth rate of *Pseudomonas* sp. M1 was 0.80 h⁻¹; the growth was inhibited by the exposure to Ag⁺ and AgNPs. The increase in the concentration of Ag⁺ or AgNPs resulted in a dose-dependent reduction of the specific growth rate (Fig. 2.1).

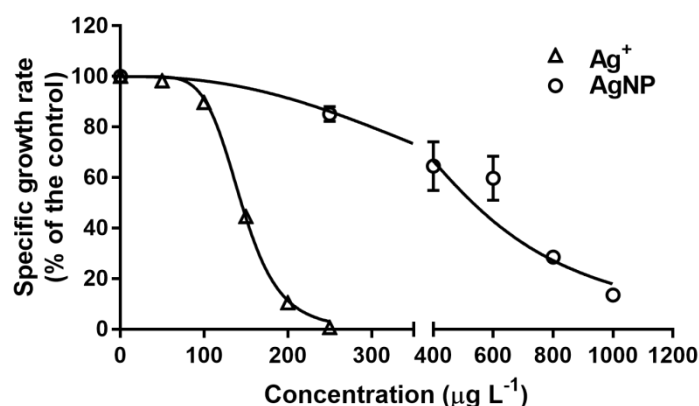


Figure 2.1 Effects of AgNPs (circles) or Ag⁺ (triangles) on the specific growth rate of *Pseudomonas* sp. M1. Data are percentage of the specific growth rate of the control culture in mineral media with lactate at 30 °C. Mean \pm SEM, n = 3.

Inhibitory effects of Ag⁺ on the bacterial growth were more pronounced than those of AgNPs, because EC₁₀ and EC₂₀ of Ag⁺ were \sim 4.4 and \sim 2.9 times lower than that of AgNPs, respectively (Table 2.2).

The role of Ag⁺ in the AgNP toxicity was further analysed by testing the effects of both forms of silver in the presence of an Ag⁺ ligand (cysteine). Exposure to cysteine alone did not affect the bacterial growth ($P > 0.05$; Appendix 3). In the absence of cysteine, exposure to Ag⁺ or AgNPs at EC₂₀ significantly inhibited bacterial growth ($P < 0.005$; Appendix 3).

Table 2.2 Concentrations of Ag⁺ and AgNPs inhibiting 10% (EC₁₀) and 20% (EC₂₀) of the growth of *Pseudomonas* sp. M1 grown in mineral medium with 0.4% lactate at 30 °C for 90 min (95% C.I. in parenthesis).

Stressor	EC ₁₀ (µg L ⁻¹)	EC ₂₀ (µg L ⁻¹)
Ag ⁺	51.2 (5.3-75.3)	107.1 (36.9-138.1)
AgNPs	225.7 (105.9-312.3)	307.2 (179.6-395.3)

The presence of cysteine did not alter the effect of AgNPs on *Pseudomonas* sp. M1 ($P>0.05$), but alleviated the negative effect of Ag⁺ showing no difference in bacterial growth from control ($P>0.05$; Appendix 3).

2.3.3. Effects of Ag⁺ and AgNPs on the activity of antioxidant enzymes

After 90 min of exposure of *Pseudomonas* sp. M1 to Ag⁺ or AgNPs, the activities of all tested antioxidant enzymes, except for GST, increased significantly with concentration (two-way ANOVA, $P<0.05$) of both silver forms (Fig. 2.2, Appendix 1). SOD and GPx activities increased significantly ($P<0.05$) under Ag⁺ or AgNPs exposure, particularly at the highest concentrations (Fig. 2.2A and 2.2B). GST activity did not differ significantly from control (Fig. 2.2A and 2.2B). At the same concentration (50 or 100 µg L⁻¹), stimulation of SOD and GPx activities by Ag⁺ was stronger than by AgNPs (Fig. 2.2). When the enzyme activities were compared at the exposure concentrations closer to EC₁₀ (50 µg L⁻¹ for Ag⁺; 200 µg L⁻¹ for AgNPs), only SOD and GPx activities were significantly higher than in control upon exposure to Ag⁺ (303.6% and 295.2%, respectively; Fig. 2.2A), whereas AgNPs strongly induced the activities of GPx (310.8%), SOD (283.2%) and CAT (268.7%) (Fig. 2.2B). When the cells were exposed to 100 µg L⁻¹ of Ag⁺ (nearby EC₂₀ of Ag⁺: 107.1 µg L⁻¹), maximum activity was observed for SOD (667.1%) followed by GPx (418.3%) and CAT (274.3%) (Fig. 2.2A). At 300 µg L⁻¹ of AgNPs (EC₂₀ of AgNPs: 307.2 µg L⁻¹), the activity of SOD was highest (583.4%) followed by that of GPx (433.8%), whereas CAT activity decreased (135.5%) to the control level (Fig. 2.2B).

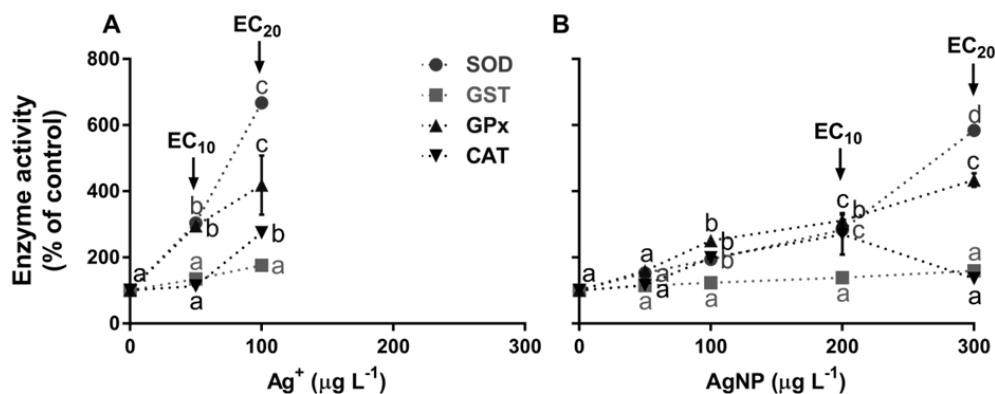


Figure 2.2 Activities of SOD, GST, GPx and CAT in *Pseudomonas sp. M1* exposed at (A) EC₁₀ and EC₂₀ of Ag⁺ and (B) at EC₁₀ and EC₂₀ of AgNPs and at concentrations used for Ag⁺. Values are percentage of respective control. Mean ± SEM, n = 3. Different letters indicate significant differences ($P < 0.05$).

2.3.4. Effects of Ag⁺ and AgNPs on the proteome of *Pseudomonas sp. M1*

After 90 min of exposure of *Pseudomonas sp. M1* to both forms of silver at concentrations (100 µg L⁻¹ of Ag⁺ and 300 µg L⁻¹ of AgNPs) similar to their respective EC₂₀ on bacterial growth (EC₂₀ = 107.1 µg L⁻¹ for Ag⁺ and EC₂₀ = 307.2 µg L⁻¹ for AgNPs), a total of 166 proteins were identified through SWATH-MS (Appendix 6). Out of these, the contents of 59 proteins (35.5%) were significantly altered after exposure to Ag⁺ or AgNPs (one-way ANOVA, $P < 0.05$; Appendix 6). Among these 59 proteins, 27 increased and 32 decreased after exposure to Ag⁺, whereas the opposite was found under AgNP exposure (i.e. 27 decreased and 32 increased) (Appendix 4). Moreover, the majority (74.6%) of the proteins whose contents were significantly altered showed a similar pattern (22 proteins increased; 22 proteins decreased) under exposure to both Ag forms. The average fold change of positively altered proteins was higher under exposure to Ag⁺ (0.89-fold for Ag⁺ vs 0.58-fold for AgNPs) whereas the opposite was found for negatively altered proteins (-0.71-fold for Ag⁺ vs -1.87-fold for AgNPs).

A heatmap analysis showed the dynamic profiles of the proteins significantly altered (in the control and under exposure to Ag⁺ and to AgNPs; Fig. 2.3A). Proteins were clustered according to their behavioural profiles and 4 clusters were generated (Fig. 2.3B). Cluster 1 was represented by 13 proteins, which increased under exposure to AgNPs (average fold change: 0.61) and decreased under exposure to Ag⁺ (average fold change: -0.29), except for 3 proteins (Appendix 6).

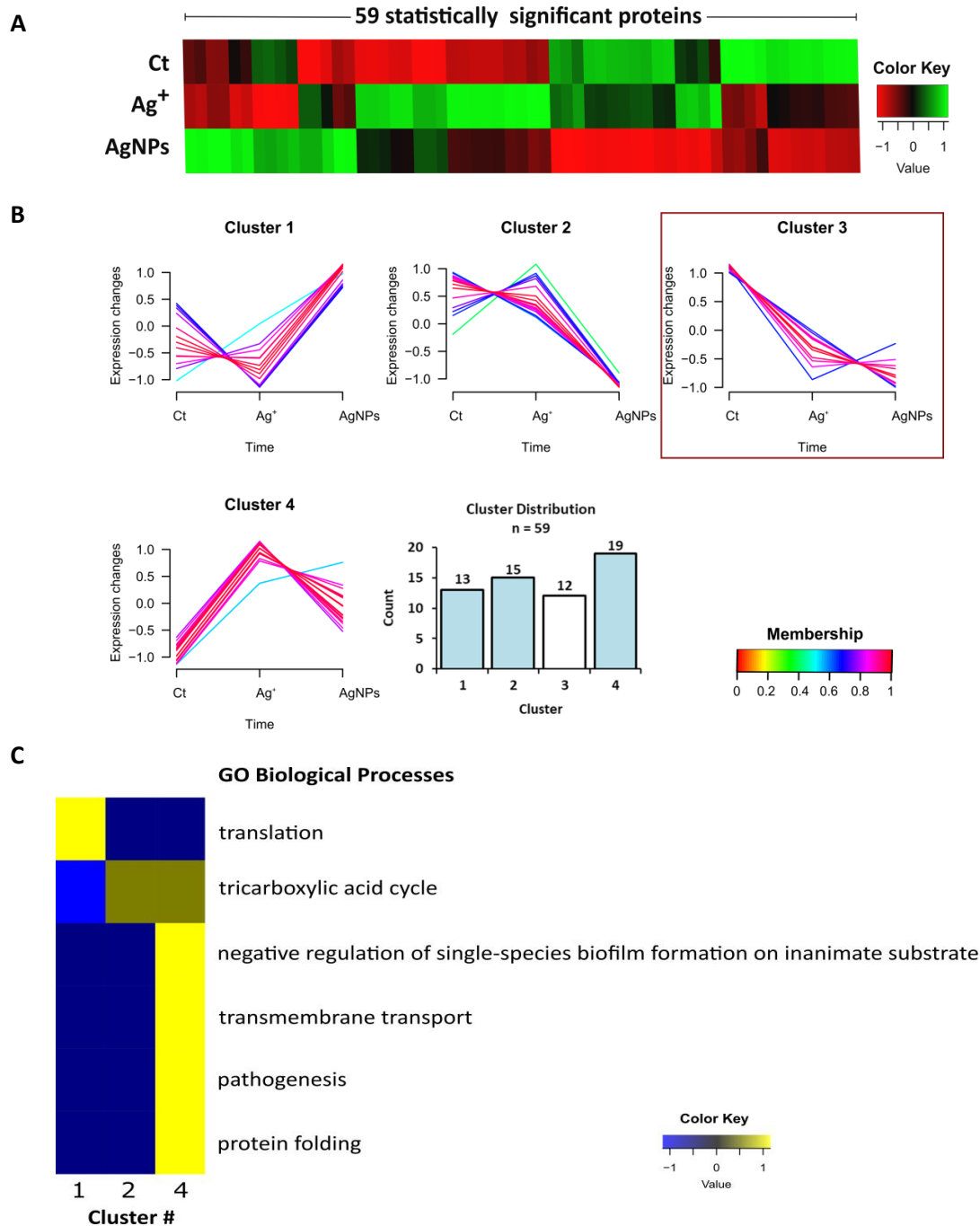


Figure 2.3 Heatmap and clustering analysis of the proteins with significant variation in *Pseudomonas* sp. M1 and GO enrichment analysis. The heatmap (A) shows the dynamic profiles of the 59 statistically significant proteins across the different experimental conditions (Control, Ct; Ag⁺ or AgNPs, NP). The unsupervised clustering analysis (B) was performed considering standardization of the 59 altered proteins. An upper and lower ratio limit of log₂ (2) and log₂ (0.5) was used for inclusion into a cluster, and the 59 proteins were partitioned into 4 groups where membership value represents how well the protein profile fit the average cluster profile. (C) Overrepresented biological processes of each cluster. Each cluster from (B) was tested for overrepresented GO compared with the cluster 3 using a Binomial statistical test with Benjamini-Hochberg adjustment ($p < 0.05$).

The contents of all proteins in cluster 2 (15 proteins) decreased under AgNP exposure (average: -1.44-fold), while under Ag⁺ exposure, 5 proteins increased (average fold change: 0.38) and 10 proteins decreased (average: -0.27). All proteins in cluster 3 (12 proteins) decreased significantly by Ag exposure (average: -2.39-fold by AgNPs and -1.43-fold by Ag⁺). Both silver forms stimulated (average: 0.56-fold by AgNPs and 1.05-fold by Ag⁺) the proteins from cluster 4 (19 proteins).

2.3.5. Relationships between oxidative stress enzymes and related proteins

The PCA of overall responses of antioxidant enzymes and proteins involved in antioxidant activities in *Pseudomonas* sp. M1 under exposure to EC₂₀ of Ag⁺ or AgNPs showed that PC1 and PC2 explained 70.8% and 19.6% of the total variance, respectively (Fig. 2.4). Exposure of the cells to Ag⁺ and AgNPs led to significant effects on the activities of antioxidant enzymes and the contents of proteins with antioxidant activities (PERMANOVA, $P < 0.05$). The PCA showed a clear discrimination between controls and treatments with Ag⁺ or AgNPs along the PC1 based on the responses of oxidative stress biomarkers. PC2 segregated Ag⁺ from AgNPs. With the exception of AhpC, all oxidative stress biomarkers were positively associated with Ag⁺ or AgNPs. CAT and KatG were closely associated with each other and were positively correlated to Ag⁺, whereas GPx, SOD and GST were associated with both treatments.

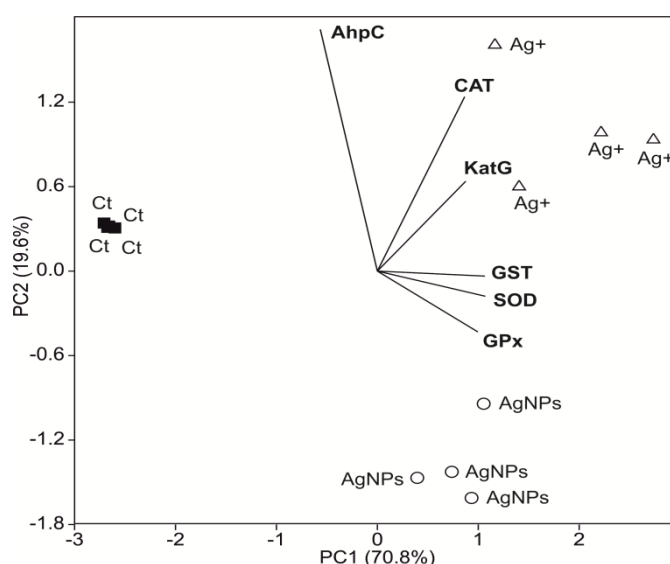


Figure 2.4 Principal component analysis (PCA) of proteins involved in antioxidant activities (AhpC and KatG) and activities of antioxidant enzymes (SOD, GST, GPx and CAT) in cells of *Pseudomonas* sp. M1 unexposed or exposed for 90 min to AgNPs or Ag⁺ at EC₂₀. Ct: control; AgNPs: 300 µg L⁻¹ (~EC₂₀); Ag⁺: 100 µg L⁻¹ (~EC₂₀).

2.4. Discussion

Our study showed that short-term exposure to both Ag^+ and AgNPs had negative impacts on the growth of *Pseudomonas* sp. M1, and the effects of Ag^+ were more pronounced than those of AgNPs. This different sensitivity of the bacterium to Ag^+ or AgNPs is in agreement with previous findings in aquatic microbes and other species of *Pseudomonas* (Pradhan et al 2011; Bondarenko et al 2013). Short- and long-term exposure (30 min - 24 h) to AgNPs led to toxic effects on aquatic Gram-positive and Gram-negative bacteria (Fabrega et al 2011) although effective concentrations varied widely (45 ng - 100 mg). Physicochemical properties of ENPs, as well as the exposure time and species sensitivity (Fabrega et al 2011) can contribute to explain such differences. The responses of *Pseudomonas* sp. M1 to each silver form may be different from other strains or species due to putative adaptation to stressors existing in its natural habitat (Rhine River), which has been reported to be occasionally contaminated with metals and organic micropollutants (Japenga et al 1990; Middelkoop 2000; Vega and Weng 2013). However, adaptive mechanisms of the strain might be specific to the stressors existing in the environment, while the bacterial sensitivity to other stressors might have not been altered. The isolation site of *Pseudomonas* sp. M1 was not contaminated by silver (Japenga et al 1990; Middelkoop 2000; Vega and Weng 2013). Smaller size AgNPs (1-10 nm) can exhibit toxicity to *P. aeruginosa* by i) impairing membrane permeability and respiration, ii) interacting with sulphur- and phosphorus-containing macromolecules, leading to cellular damage, and iii) releasing Ag^+ leading to additional bactericidal effects (Morones et al 2005). In our study, it is conceivable that the actual toxic effects of AgNPs or Ag^+ on *Pseudomonas* sp. might have been underestimated in the presence of Cl^- in the culture medium. The increased AgNP agglomeration might be the consequence of interactions with the medium components. Therefore, possible interactions between Cl^- and Ag^+ released from AgNPs or AgNO_3 cannot be discarded (Behra et al 2013). However, we want to point out that the dissolution of Ag^+ was considerably low at the beginning of our experiment (~0.1%) and decreased further probably due to Ag^+ biosorption to cells. This suggests low contribution of Ag^+ to the AgNP-induced stress. Moreover, the outcome of the complementary test with cysteine (Appendix 3), a strong Ag^+ ligand, further supported that AgNPs induced a direct toxicity on *Pseudomonas* sp. M1.

Common mechanisms of AgNPs in bactericidal activities involve: i) cell wall disruption, ii) interaction with thiol-containing enzymes or peptides, iii) interaction with 30S ribosome and inhibition of protein synthesis, and iv) inhibition of DNA synthesis and induction of apoptosis (Bao et al 2015; Dubey et al 2015). Our study showed that the short-term exposure of *Pseudomonas* sp. M1 to Ag^+ or AgNPs stimulated the activities of antioxidant enzymes involved in ascorbate-glutathione cycle, suggesting an attempt of cells to cope with the oxidative stress. The strong response of SOD suggested its crucial role in early defence against ROS, protecting the cells from Ag^+ - or AgNP-induced superoxide anion radical ($\bullet\text{O}_2^-$), by catalyzing its dismutation into H_2O_2 (Kumar et al 2014; Pradhan et al 2015). Chronic exposure to AgNPs ($0.1\text{-}0.25\text{ mg L}^{-1}$) increased mRNA of SOD gene in the gill tissue of freshwater fish (Johari et al 2016). However, the exposure to higher concentrations of AgNPs ($1\text{-}1.5\text{ mg L}^{-1}$) inhibited SOD activities in *P. aeruginosa* and *P. chlororaphis* disrupting the antioxidant defence (Dimkpa et al 2011; Yuan et al 2017). In our study, the induced activities of GPx and CAT by exposure to both Ag forms suggested an efficient cellular detoxification mechanism by scavenging peroxides/hydroperoxides. GPx activity induced by CuONPs was higher in fungi isolated from metal-polluted streams compared to fungi from non-polluted streams, explaining the increase in their tolerance to CuONPs (Pradhan et al 2015). Higher GPx activity may lead to the scarcity of GSH (reduced glutathione) by its conversion to GSSG (oxidized form), affecting the GSH-pool required for cell protection against oxidative stress. Indeed, a considerable decrease in GSH (up to 80%) with exposure to AgNPs (1 mg L^{-1}) induced cytotoxicity in bacteria (Yuan et al 2017). In our study, CAT activity increased at EC_{20} of Ag^+ and EC_{10} of AgNPs. A decrease in CAT activity was observed in *P. aeruginosa* upon longer exposure (12h) to higher AgNP concentrations (1 mg L^{-1} , Yuan et al 2017), but not under short exposure (1h) of *P. chlororaphis* to AgNPs (1.5 mg L^{-1} , Dimkpa et al 2011). In our study, GST activity was not triggered by either form of Ag, probably due to the efficient functioning of other antioxidant enzymes in cellular detoxification. The observed positive association between GPx and SOD activities under AgNP exposure suggested the contribution of these enzymes to cope with ROS. The more pronounced activities of antioxidant enzymes under Ag^+ exposure were consistent with the higher toxicity of the ionic form.

Our study provided evidence that Ag^+ and AgNPs affected cellular targets and biological processes in *Pseudomonas* sp. M1. Out of 59 proteins, the contents of which were

significantly altered after exposure to either Ag^+ or AgNPs, 15 proteins showed different patterns against each Ag form. The proteomic profiles through GO enrichment analysis based on protein clustering further allowed the exploration of biological processes in *Pseudomonas* sp. M1, and provided the mechanistic insight of the stress induced by Ag^+ or AgNPs (Fig. 2.3C). The most overrepresented process (12 proteins) under exposure to Ag^+ or AgNPs was the translation, in which 8 proteins increased after exposure to AgNPs but decreased under Ag^+ exposure (cluster 1, Fig. 2.3C). These proteins were mainly structural constituents of ribosomes which mediate the assembly of small or large ribosomal subunits (e.g. 30S ribosomal protein S8, RpsH; see Appendix 6) and/or tRNA bindings (e.g. 30S ribosomal protein S10, RpsJ; see Appendix 6). These findings indicated that ionic and nanoparticulate forms of Ag interacted differently with this particular group of proteins. The remaining 4 proteins (clusters 2 and 3) were elongation factors (EFs; e.g. Tsf and Tuf, see Appendix 6), which decreased under AgNPs more than under Ag^+ exposure. The decrease in the content of many elongation factors, including Efp, Tsf and Tuf1 (e.g. in *Pseudomonas* sp. M1 under exposure to phenol, Santos et al 2007; in *P. stutzeri* exposed to FeNPs, Saccà et al 2014), may indicate a compromised protein synthesis due to the stress caused by the nanoparticulate form of Ag. A strong functional association between proteins were obtained in *P. aeruginosa* using STRING database (von Mering et al 2007), selecting the networks of the proteins altered by Ag^+ or AgNPs in *Pseudomonas* sp. M1 (Appendix 5). Moreover, if polypeptide chain elongation process was affected by AgNPs, defective proteins would be produced and, hence, the performance of the cellular machinery responsible for maintaining protein homeostasis may be altered. In fact, we found an increase in the content of ribosomal constituents under AgNPs exposure which could represent the attempt of cells to counteract incorrect protein formation. Although the process of amino acid synthesis was not featured by GO enrichment analysis, the content of related proteins (e.g. LeuC, LeuD and LeuB; cluster 3) decreased under exposure to AgNPs more than to Ag^+ , affecting the synthesis of proteins and leucine-based enzyme activities. Indeed, very strong functional association between LeuD and LeuB was obtained in *P. aeruginosa* using STRING database when the interaction networks among the proteins altered by Ag^+ or AgNPs in *Pseudomonas* sp. M1 were selected (Appendix 5). A decrease in the content of proteins involved in amino acid metabolism by Ag^+ and graphene-based AgNPs was reported in *P. aeruginosa* (He et al 2014). GO enrichment analysis further

supported these findings, demonstrating the importance of other proteins in *Pseudomonas* sp. M1, particularly those associated with the process of protein folding (cluster 4, Fig. 2.3C) under Ag^+ exposure. This process is accomplished by chaperones, a group of ubiquitous stress responsive proteins that act as main responsible for proteostasis. Among the functions ensured by these proteins are the prevention of misfolding and promotion of refolding and proper assembly of unfolded polypeptides generated under stress conditions (e.g. GroEL, see Appendix 6) or the binding to nascent proteins assisting in their correct folding (e.g. DnaK, Appendix 6). STRING analysis of *P. aeruginosa* based on the proteins altered by Ag^+ in *Pseudomonas* sp. M1 showed strong interactions between GroEL and DnaK (Appendix 5). An increase in GroEL content was also reported in *P. stutzeri* after exposure to FeNPs (Saccà et al 2014). DnaK can play a protective role against many stressors, including AgNPs, diminishing the antimicrobial effects and increasing the tolerance of *P. aeruginosa* (Markowska et al 2014). Cells of *Pseudomonas* sp. M1 present low levels of these chaperones, but their levels increase under stress, contributing to its tolerance and survival in stressful conditions (Santos et al 2007). Thus, in our study, the increased content of these proteins suggests their involvement in preventing protein misfolding under the stress induced by Ag in *Pseudomonas* sp. M1.

Two of the differentially altered proteins by either forms of Ag had antioxidant roles (KatG and AhpC, see Appendix 6) helping to maintain cell-redox homeostasis. Moreover, the activities of CAT and the alterations in the protein content of KatG (1.58-fold for Ag^+ vs 0.74-fold for AgNPs) were closely associated with each other and positively correlated to Ag^+ . This suggests that more hydroperoxides were induced by exposure to Ag^+ and that CAT played a crucial role in the cellular detoxification in *Pseudomonas* sp. M1. Increased expression level of catalase (KatA, 1.69-fold) after exposure (24 h) to AgNPs (at 1.2 mg L^{-1}) was also reported in *P. aeruginosa* (Yan et al 2018). AhpC is a key component of a large family of thiol-specific antioxidant proteins known by scavenging reactive oxygen, nitrogen and sulphur species and organic hydroperoxides by reducing to dithiol forms. An increase in the content of AhpC can explain the tolerance of organisms to multiple stressors (Santos et al 2007; Mishra et al 2009), as observed in *Pseudomonas* sp. after 24 h exposure to $100 \mu\text{g L}^{-1}$ of AgNPs (Soni et al 2014). In our study, the content of AhpC decreased under the exposure to both forms of Ag, mainly under AgNP exposure (-0.38-fold for Ag^+ ; -2.68-fold for AgNPs), probably due to shorter exposure to higher concentration of nanoparticles.

Cosgrove et al (2007) reported a greater catalase expression provoked by a mutation in AhpC, suggesting its compensatory role in oxidative stress. Hence, it is possible that the decrease in the AhpC had occurred in *Pseudomonas* to privilege other antioxidant enzymes against Ag-induced oxidative stress.

In *Pseudomonas* sp. M1, the content of most proteins associated with the tricarboxylic acid cycle (clusters 2 and 4, Fig. 2.3C) increased under Ag⁺ exposure, but decreased under AgNP exposure (e.g. aconitate hydratase B - AcnB and isocitrate dehydrogenase [NADP] - Icd), suggesting that different pathways of carbohydrate and energy metabolism were affected by Ag⁺ and AgNPs. STRING analysis also showed a strong interaction between AcnB and Icd (Appendix 5). The exposure to graphene-based AgNPs altered the content of proteins involved in carbohydrate and energy metabolism in *P. aeruginosa* (He et al 2014). A decrease in AcnB by other metal-NPs was also reported in *P. stutzeri* (Saccà et al 2014). In contrast, the increase in the content of those proteins under Ag⁺ exposure in *Pseudomonas* sp. M1 suggested an adaptive mechanism in energy consumption and carbohydrate metabolism under Ag stress.

Transmembrane transport was another overrepresented process displayed by GO analysis in *Pseudomonas* sp. M1 (cluster 4) in which proteins (e.g. membrane protein, porins and outer membrane protein W, see Appendix 6) increased under Ag⁺ exposure more strongly than under AgNP exposure. This indicates that these proteins were mainly targeted by Ag⁺, affecting the membrane transport and facilitating Ag⁺ entrance into bacterial cells.

The processes of pathogenesis and of negative regulation of single-species biofilm formation were also revealed by GO enrichment analysis (cluster 4, Fig. 2.3C). Although no designation related to this process (as biological process annotated in UniProt) has been attributed to the proteins belonging to cluster 4, there is evidence that virulence factors related to pathogenesis can also be encoded in the genomes of non-pathogenic bacteria (Niu et al 2013). Moreover, Pitondo-Silva et al (2016) demonstrated a co-occurrence of resistance to antibiotics and heavy metals associated with the presence of virulence genes in *P. aeruginosa*, although the influence of other genes and/or mechanisms related to metal resistance could not be discarded. The process of biofilm formation, whose role in protecting bacteria from antibiotics is well known (Høiby et al 2010), was negatively regulated in *Pseudomonas* sp. M1 in our study. Singh et al (2015) demonstrated that AgNPs affect the *P. aeruginosa* biofilm by disabling the quorum sensing, a communication

process used by the strain to regulate virulence and biofilm formation. Because biofilm formation requires considerable amount of energy in producing extracellular polymeric substances (Hall-Stoodley et al 2004, López et al 2010), cells of *Pseudomonas* sp. M1 may have prioritized mechanisms/processes (e.g. pathogenesis/virulence) to save energy to deal with the stress induced by both silver forms.

References

- Anjo SI, Santa C and Manadas B. 2014. Short GeLC-SWATH: a fast and reliable quantitative approach for proteomic screenings. *Proteomics*. 15: 757-762.
- Azevedo M-M, Carvalho A, Pascoal C, Rodrigues F and Cássio F. 2007. Responses of antioxidant defenses to Cu and Zn stress in two aquatic fungi. *Sci. Total. Environ.* 377: 233-243.
- Bao H, Yu X, Xu C, Li X, Li Z, Wei D and Liu Y. 2015. New toxicity mechanism of silver nanoparticles: promoting apoptosis and inhibiting proliferation. *PLoS One*. 10: e0122535.
- Behra R, Sigg L, Clift MJ, Herzog F, Minghetti M, Johnston B, Petri-Fink A, Rothen-Rutishauser B. 2013. Bioavailability of silver nanoparticles and ions: from a chemical and biochemical perspective. *J. R. Soc. Interface*. 10: 20130396.
- Blaser SA, Scheringer M, MacLeod M and Hungerbühler K. 2008. Estimation of cumulative aquatic exposure and risk due to silver: contribution of nano-functionalized plastics and textiles. *Sci. Total. Environ.* 390: 396-409.
- Bondarenko O, Ivask A, Kähkönen A, Kurvet I and Kahru A. 2013. Particle-cell contact enhances antibacterial activity of silver nanoparticles. *PLoS One*. 8: e64060.
- Clairborne A. 1985. Catalase activity. In: Greenwald, R.A. (Ed.), *CRC Handbook of Methods in Oxygen Radical Research*. CRC Press, Boca Raton, FL.
- Collins BC, Gillet LC, Rosenberger G, Röst HL, Vichalkovski A, Gstaiger M and Aebersold R. 2013. Quantifying protein interaction dynamics by SWATH mass spectrometry: application to the 14-3-3 system. *Nat. Methods*. 10: 1246-1253.
- Choi OK and Hu ZQ. 2009. Nitrification inhibition by silver nanoparticles. *Wat. Sci. Technol.* 59: 1699-1702.
- Cosgrove K, Coutts G, Jonsson IM, Tarkowski A, Kokai-kun JF, Mond JJ and Foster SJ. 2007. Catalase (KatA) and alkyl hydroperoxide reductase (AhpC) have compensatory roles in peroxide stress resistance and are required for survival, persistence and nasal colonization in *Staphylococcus aureus*. *J. Bacteriol.* 189: 1025-1035.
- Cumberland S and Lead J. 2009. Particle size distributions of silver nanoparticle at environmentally relevant conditions. *J. Chromatogr. A*. 1216: 9099-9105.
- Dimkpa CO, Calder C, Gajjar P, Merugu S, Huang W, Britt DW, McLean JE, Johnson WP and Anderson AJ. 2011. Interaction of silver nanoparticles with an environmentally beneficial bacterium, *Pseudomonas chlororaphis*. *J. Hazard. Mater.* 188: 428-435.
- Dubey P, Matai I, Kumar SU, Sachdev A, Bhushan B and Gopinath P. 2015. Perturbation of cellular mechanistic system by silver nanoparticle toxicity: Cytotoxic, genotoxic and epigenetic potentials. *Adv. Colloid Interface Sci.* 221: 4-21.

- European Commission 2012. Commission staff working paper. Types and uses of nanomaterials, including safety aspects. Accompanying the Communication from the Commission to the European Parliament, the Council and the European Economic and Social Committee on the Second Regulatory Review on Nanomaterials.
- Fabrega J, Luoma SN, Tyler CR, Tamara S, Galloway TS and Lead JR. 2011. Silver nanoparticles: behaviour and effects in the aquatic environment. *Environ. Int.* 37: 517-531.
- Flohé L and Günzler WA. 1984. Assays of glutathione peroxidase. *Methods Enzymol.* 105: 114-121.
- Ge P, Hao P, Cao M, Guo G, Lv D, Subburaj S, Li X, Yan X, Xiao J, Ma W and Yan Y. 2013. iTRAQ-based quantitative proteomic analysis reveals new metabolic pathways of wheat seedling growth under hydrogen peroxide stress. *Proteomics.* 13: 3046-3058.
- Gottschalk F, Kost E and Nowack B. 2013. Engineered nanomaterials in water and soils: a risk quantification based on probabilistic exposure and effect modeling. *Environ. Toxicol. Chem.* 32: 1278-1287.
- Habig WH, Pabst MJ and Jakoby WB. 1974. Glutathione S-transferases – first enzymatic step in mercapturic acid formation. *J. Biol. Chem.* 249: 7130-7139.
- Hall-Stoodley L, Costerton JW and Stoodley P. 2004. Bacterial biofilms: from the natural environment to infectious diseases. *Nature Rev. Microbiol.* 2: 95-108.
- Hammer Ø, Harper DAT and Ryan PD. 2001. PAST: Paleontological Statistics Software Package for Education and Data Analysis. *Palaeontol. Electron.* 4: p9.
- Handy RD, van den Brink N, Chappell M, Muhling M, Behra R, Dusinska M, Simpson P, Ahtiainen J, Jha AN, Seiter J, Bednar A, Kennedy A, Fernandes TF and Riediker M. 2012. Practical considerations for conducting ecotoxicity test methods with manufactured nanomaterials: what have we learnt so far? *Ecotoxicology.* 21: 933-972.
- Hartmans S, Smits JP, van der Werf MJ, Volkering F and de Bont JAM. 1989. Metabolism of styrene oxide and 2-phenylethanol in the styrene-degrading *Xanthobacter* strain 124X. *Appl. Environ. Microbiol.* 55: 2850-2855.
- He T, Liu H, Zhou Y, Yang J, Cheng X and Shi H. 2014. Antibacterial effect and proteomic analysis of graphene-based silver nanoparticles on a pathogenic bacterium *Pseudomonas aeruginosa*. *BioMetals.* 27: 673-682.
- Højiby N, Bjarnsholt T, Givskov M, Molin S and Ciofu O. 2010. Antibiotic resistance of bacterial biofilms. *Int. J. Antimicrob. Agents.* 35: 322-332.
- Iurescia S, Marconi AM, Tofani D, Gambacorta A, Paterno A, Devirgiliis C, van der Werf MJ and Zennaro E. 1999. Identification and sequencing of beta-myrcene catabolism genes from *Pseudomonas* sp. Strain M1. *Appl. Env. Microbiol.* 65: 2871-2876.
- Japenga J, Zschuppe KH, DeGroot AJ and Salomons W. 1990. Heavy metals and organic micropollutants in flood plain of the River Waal, a distributary of the River Rhine, 1958-1981. *Neth. J. Agric. Sci.* 38: 381-397.
- Johari SA, Kalbassi MR, Lee SB, Dong MS and Yu IJ. 2016. Silver nanoparticles affects the expression of biomarker genes mRNA in rainbow trout (*Oncorhynchus mykiss*). *Comp. Clin. Pathol.* 25: 85-90.
- Kaegi R, Sinnet B, Zuleeg S, Hagendorfer H, Mueller E, Vonbank R, Boller M and Burkhardt M. 2010. Release of silver nanoparticles from outdoor facades. *Environ. Pollut.* 158: 2900-2905.
- Kalishwaralal K, BarathManiKanth S, Pandian SRK, Deepak V, Gurunathan S. 2010. Silver nanoparticles impede the biofilm formation by *Pseudomonas aeruginosa* and *Staphylococcus epidermidis*. *Colloids Surf. B.* 79: 340-344.

- Kumar N, Palmer GR, Shah V and Walker VK. 2014. The effect of silver nanoparticles on seasonal change in arctic tundra bacterial and fungal assemblages. *PLoS One*. 9: e99953.
- Kumar L and Futschik ME. 2007. Mfuzz: a software package for soft clustering of microarray data. *Bioinformatics*. 2: 5-7.
- Lok C-N, Ho C-M, Chen R, He Q-Y, Yu W-Y, Sun H, Tam PK-H, Chiu J-F and Che C-M. 2006. Proteomic Analysis of the Mode of Antibacterial Action of Silver Nanoparticles. *J. Proteome Res*. 5: 916-924.
- López D, Vlamakis H and Kolter R. 2010. Biofilms. *Cold Spring Harbor Perspectives in Biology*. 2: a000398.
- Lubick N. 2008. Nanosilver toxicity: ions, nanoparticles or both? *Environ. Sci. & Technol*. 42: 8617.
- Markowska K, Grudniak AM, Krawczyk K, Wróbel I and Wolska KI. 2014. Modulation of antibiotic resistance and induction of a stress response in *Pseudomonas aeruginosa* by silver nanoparticles. *J. Med. Microbiol*. 63: 849-854.
- McGillicuddy E, Murray I, Kavanagh S, Morrison L, Fogarty A, Cormican M, Dockery P, Prendergast M, Rowan N and Morris D. 2017. Silver nanoparticles in the environment: Sources, detection and ecotoxicology. *Sci. Total. Environ*. 575: 231-246.
- Middelkoop H. 2000. Heavy metal pollution of the river Rhine and Meuse floodplains in the Netherlands. *Neth. J. Geosci*. 79: 411-428.
- Mishra Y, Chaurasia N and Rai LC. 2009. AhpC (alkyl hydroperoxide reductase) from *Anabaena* sp. PCC 7120 protects *Escherichia coli* from multiple abiotic stresses. *Biochem. Biophys. Res. Commun*. 381: 606-611.
- Morones JR, Elechiguerra JL, Camacho A, Holt K, Kouri JB, Ramirez JT and Yacaman MJ. 2005. The bactericidal effect of silver nanoparticles. *Nanotechnology*. 16: 2346-2353.
- Nair LS and Laurencin CT. 2007. Biodegradable polymers as biomaterials. *Prog. Polym. Sci*. 32: 762-798.
- Nesatyy VJ and Suter MJF. 2007. Proteomics for the analysis of environmental stress responses in organisms. *Environ. Sci. Technol*. 41: 6891-6900.
- Niu C, Yu D, Wang Y, Ren H, Jin Y, Zhou W, Li B, Cheng Y, Yue J, Gao Z and Liang L. 2013. Common and pathogen-specific virulence factors are different in function and structure. *Virulence*. 4: 473-482.
- OECD. 2014. Ecotoxicology and environmental fate of manufactured nanomaterials: test guidelines. Series on the Safety of Manufactured Nanomaterials. No. 40. ENV/JM/MONO Organisation for Economic Co-operation and Development, Paris.
- OECD. 2010. Guidance Manual for the testing of manufactured nanomaterials: OECD's sponsorship programme, ENV/JM/MONO (2009) 20REV. OECD Environment, Health and Safety Publications, Series on the Safety of Manufactured Nanomaterials No. 25, Organisation for Economic Co-operation and Development, Paris.
- Peterson GL. 1983. Determination of total protein. *Meth. Enzymol*. 91: 95-121.
- Pitondo-Silva A, Gonçalves GB and Stehling EG. 2016. Heavy metal resistance and virulence profile in *Pseudomonas aeruginosa* isolated from Brazilian soils. *APMIS*. 124: 681-688.
- Pradhan A, Silva CO, Silva C, Pascoal C and Cássio F. 2016. Enzymatic biomarkers can portray nanoCuO-induced oxidative and neuronal stress in freshwater shredders. *Aquat. Toxicol*. 180: 227-235.
- Pradhan A, Seena S, Schlosser D, Gerth K, Helm S, Dobritsch M, Krauss G-J, Dobritsch D, Pascoal C and Cássio F. 2015. Fungi from metal-polluted streams may have high ability to cope with the

- oxidative stress induced by copper oxide nanoparticles. *Environ. Toxicol. and Chem.* 34: 923-930.
- Pradhan A, Seena S, Pascoal C and Cássio F. 2011. Can metal nanoparticles be a threat to microbial decomposers of plant litter in streams? *Microb. Ecol.* 62: 58-68.
- Reidy B, Haase A, Luch A, Dawson KA and Lynch I. 2013. Mechanisms of silver nanoparticle release, transformation and toxicity: a critical review of current knowledge and recommendations for future studies and applications. *Materials.* 6: 2295-2350.
- Rigbolt KT, Vanselow JT and Blagoev B. 2011. GProX, a user-friendly platform for bioinformatics analysis and visualization of quantitative proteomics data. *Mol. Cell. Proteomics.* 10: O110.007450.
- Saccà ML, Fajardo C, Martinez-Gomariz M, Costa G, Nande M and Martin M. 2014. Molecular Stress Responses to Nano-Sized Zero-Valent Iron (nZVI) Particles in the Soil Bacterium *Pseudomonas stutzeri*. *PLoS One.* 9: e89677.
- Sakuma M. 1998. Probit analysis of preference data. *Appl. Entomol. Zool.* 33: 339-347.
- Santos PM, Roma V, Benndorf D, von Bergen M, Harms H and Sá-Correia I. 2007. Mechanistic insights into the global response to phenol in the phenol-biodegrading strain *Pseudomonas* sp. M1, revealed by quantitative proteomics. *OMICS.* 11: 233-251.
- Santos PM and Sá-Correia I. 2009. Adaptation to β -myrcene catabolism in *Pseudomonas* sp. M1: An expression proteomics analysis. *Proteomics.* 9: 5101-5111.
- Santos PM and Sá-Correia I. 2007. Characterization of the unique organization and co-regulation of a gene cluster required for phenol and benzene catabolism in *Pseudomonas* sp. M1. *J. Biotech.* 131: 371-378.
- Santos PM, Simões T and Sá-Correia I. 2009. Insights into yeast adaptive response to the agricultural fungicide mancozeb: a toxicoproteomics approach. *Proteomics.* 9: 657-670.
- Silver S. 2003. Bacterial silver resistance: molecular biology. *FEMS Microbiol. Rev.* 27: 341-353.
- Singh BR, Singh BN, Singh A, Khan W, Naqvi AH and Singh HB. 2015. Mycofabricated biosilver nanoparticles interrupt *Pseudomonas aeruginosa* quorum sensing systems. *Sci. Rep.* 5: 13719.
- Sohn EK, Johari SA, Kim TG, Kim JK, Kim E, Lee JH, Chung YS and Yu IJ. 2015. Aquatic Toxicity Comparison of Silver Nanoparticles and Silver Nanowires. *BioMed. Res. Int.* 2015: 893049.
- Soni D, Bafana A, Gandhi D, Sivanesan S and Panday RA. 2014. Stress response of *Pseudomonas* species to silver nanoparticles at the molecular level. *Environ. Toxicol. Chem.* 33: 2126-2132.
- Teixeira MC, Santos PM, Fernandes AR and Sá-Correia I. 2005. Proteome analysis of the yeast response to the herbicide 2,4-dichlorophenoxyacetic acid. *Proteomics.* 5: 1889-1901.
- Tiede K, Boxall ABA, Wang X, Gore D, Tiede D, Baxter M, David H, Tear SP and Lewis J. 2010. Application of hydrodynamic chromatography-ICP-MS to investigate the fate of silver nanoparticles in activated sludge. *J. Anal. At. Spectrom.* 25: 1149-1154.
- Tlili A, Cornut J, Behra R, Gil-Allué C and Gessner MO. 2016. Harmful effects of silver nanoparticles on a complex detrital model system. *Nanotoxicology.* 10: 728-735.
- Vance ME, Kuiken T, Vejerano EP, McGinnis SP, Hochella Jr. MF, Rejeski D and Hull MS. 2015. Nanotechnology in the real world: Redeveloping the nanomaterial consumer products inventory. *Beilstein J. Nanotechnol.* 6: 1769-1780.
- Vega FA and Weng LP. 2013. Speciation of heavy metals in River Rhine. *Water Res.* 47: 363-372.

- von Mering C, Jensen LJ, Kuhn M, Chaffron S, Doerks T, Krüger B, Snel B and Bork P. 2007. STRING 7 - recent developments in the integration and prediction of protein interactions. *Nucleic Acids Res.* 35: D358-D362.
- Wang Z, Chen JW, Li XH, Shao JP and Peijnenburg WJGM. 2012. Aquatic toxicity of nanosilver colloids to different trophic organisms: contributions of particles and free silver ion. *Environ. Toxicol. Chem.* 31: 2408-2413.
- Yan X, He B, Liu L, Qu G, Shi J, Hu L, Jiang G. 2018. Antibacterial mechanism of silver nanoparticles in *Pseudomonas aeruginosa*: proteomics approach. *Metallomics.* 10: 557-564.
- Yuan YG, Peng QL and Gurunathan S. 2017. Effects of silver nanoparticles on multiple drug-resistant strains of *Staphylococcus aureus* and *Pseudomonas aeruginosa* from mastitis-infected goats: An Alternative Approach for Antimicrobial Therapy. *Int. J. Mol. Sci.* 18: 569.
- Zar JH. 2010. *Biostatistical analysis*, Englewood-Cliffs, Prentice-Hall.
- Zhang C, Hu Z and Deng B. 2016. Silver nanoparticles in aquatic environments: Physiochemical behavior and antimicrobial mechanisms. *Water Res.* 88: 403-427.
- Zhang F, Wu X, Chen Y and Lin H. 2009. Application of silver nanoparticles to cotton fabric as an antibacterial textile finish. *Fibers Polym.* 10: 496-501.

Chapter 3

Proteomic and antioxidant enzymatic responses to nanoparticulate and ionic silver unravel distinct mechanisms of toxicity in two aquatic fungal ecotypes

Submitted

Barros D, Pradhan A, Pascoal C, Cássio F. 2019. Proteomic and antioxidant enzymatic responses to nanoparticulate and ionic silver unravel distinct mechanisms of toxicity in two aquatic fungal ecotypes

Abstract

Antimicrobial properties of silver have led to the incorporation of silver nanoparticles (AgNPs) into several consumer products raising concern about their risks to non-target aquatic microorganisms. Impacts of AgNPs and Ag⁺ on two aquatic fungal ecotypes of *Articulospora tetracladia*, collected from metal-polluted (At61) and non-polluted (At72) streams, were assessed based on antioxidant enzymatic and proteomic responses. The At61 showed more tolerance to AgNPs than At72. Antioxidant enzyme activities were induced by AgNPs or Ag⁺ in both fungal ecotypes; the activities increased more in At72 under exposure to Ag⁺. Proteomic responses to the Ag forms revealed that 41.3% and 27.3% of total altered proteins were common in At72 and At61, respectively. In At72, gene ontology enrichment analyses indicated that Ag⁺ increased the levels of proteins involved in proteostasis and decreased the levels of proteins involved in vesicle-mediated transport; whereas the key group of proteins induced by AgNPs had crucial functions in DNA repair and energy production. In At61, AgNPs increased the levels of proteins involved in protein biosynthesis and energy production, while both Ag forms increased the content of proteins related to cell-redox and protein homeostasis, ascospore formation, fatty acid biosynthesis and nucleic acids metabolism. Both Ag forms induced stress-responsive proteins, which was consistent with the responses of enzymes involved in oxidative stress. Overall, our results unravel distinct mechanisms of toxicity to nanoparticulate and ionic silver in aquatic fungi with different background. The distinct mechanisms of action should be taken into consideration when implementing risk assessment methodologies for emergent chemical contaminants.

Keywords: silver nanoparticles, aquatic fungal ecotypes, polluted and non-polluted streams, antioxidant enzymes, proteomics

3.1. Introduction

Current development in nanotechnology has led to the discharge of engineered nanomaterials (ENMs) into various environmental compartments, including surface waters (Liu and Cohen 2014). ENMs are emerging contaminants in freshwaters (Boxall 2012), with potential risk to aquatic organisms. Silver nanoparticles (AgNPs) are among the most widespread ENMs due to their broad-spectrum antimicrobial properties and are vastly used in textiles, paints, cosmetics, tissue engineering, therapeutics and biomedical applications (Salata 2004, Blaser et al 2008, Zhang et al 2009, Marambio-Jones and Hoek 2010). The global production of AgNPs was estimated to be 20-500 tons annually (Mueller and Nowack 2008, European Commission 2012). About 25-30% of the marketed AgNPs are predicted to be discharged and reach the freshwaters, which might be a challenge for freshwater biota and the processes they govern (Blaser et al 2008, Kaegi et al 2010). The predicted environmental concentrations of AgNPs in surface waters range between 10^{-3} and 10^{-1} $\mu\text{g L}^{-1}$, and higher concentrations can be found in runoffs from wastewaters, outdoor facades or accidental spills (Mueller and Nowack 2008, Kaegi et al 2010, Tiede et al 2010, Gottschalk et al 2013).

AgNPs can exhibit adverse impacts on several freshwater organisms, including algae, bacteria, fungi, nematodes, cladocerans and fishes (Navarro et al 2008, Pradhan et al 2011, Gottschalk et al 2013, Barros et al 2019). However, the complexity of the AgNP effects in natural environments has limited the establishment of well-directed and species-specific toxicity assessment guidelines (but see OECD 2014). Moreover, the mode of toxicity induced by AgNPs remain unclear, as some studies suggest that the toxicity can be related to speciation of the dissolved Ag^+ from nanoparticles (Navarro et al 2008, Jo et al 2012; Behra et al 2013), while others have shown toxicity of AgNPs, independent of Ag^+ , to freshwater organisms (Poynton et al 2012, Tlili et al 2016). The exposure of aquatic organisms to ionic silver is known to induce intracellular accumulation of reactive oxygen species (ROS), leading to oxidative stress (He et al 2012, van Aerle et al 2013). Consequently, cellular macromolecules such as proteins, lipids and DNA are damaged by the induced ROS (Bai et al 2003). The activities of antioxidant enzymes are considered early warning biomarkers of oxidative stress induced by ionic and nanoparticulate forms of metals including silver in freshwater organisms (Pradhan et al 2015, Pradhan et al 2016, Barros et al 2019). Most of

the antioxidant enzymes belong to the ascorbate-glutathione cycle and play crucial roles in regulation of the cellular redox state and prevention of the cellular damage, by maintaining a high ratio between reduced (GSH) and oxidized glutathione (GSSG) (Huang et al 2010). The key antioxidant enzymes are: i) superoxide dismutase (SOD), which catalyses the dismutation of the superoxide ($O_2^{\bullet-}$) radical into either molecular oxygen (O_2) or hydrogen peroxide (H_2O_2); ii) catalase (CAT), which detoxifies H_2O_2 ; iii) glutathione peroxidase (GPx), which catalyses the reduction of H_2O_2 and other peroxides, using GSH as the electron donor; and iv) glutathione S-transferase (GST), which catalyses the conjugation of GSH with xenobiotics.

On the other hand, the advances in sensitive gel-electrophoretic and mass spectrometric techniques coupled with computerized analysis have allowed to identify proteins as possible biomarkers of stress and paved the way to reveal mechanisms of action (Minden 2012, Bouatra et al 2013). Several studies on the cellular stress response and functional proteins have shown that there is a convergence towards a common set of stress-induced proteins in widely diverse taxa (Kültz 2005, Petrak et al 2008, Wang et al 2009). Therefore, application of enzymatic stress biomarkers and proteomics might be a useful approach to reveal the mechanisms of AgNP toxicity (Barros et al 2019).

Aquatic fungi are a dominant group of microbes in streams, playing a key role in organic matter decomposition in trophic networks (Pascoal et al 2005a). Although, these fungi are generally sensitive to water quality (e.g. Pascoal et al 2005b), they occur in metal-polluted streams probably by developing specific adaptive responses against ionic or nanoparticulate form of metals (Guimarães-Soares et al 2007, Azevedo et al 2009, Pradhan et al 2015).

The aim of this study was to investigate whether metal adapted fungi can exhibit tolerance to metal ions and /or metal nanoparticles by triggering specific responses to stressor exposure. To that end, we examined the impacts of AgNPs on two fungal ecotypes of *Articulospora tetracladia*, one collected from a metal-polluted (At61) stream and the other from a non-polluted (At72) stream. We assessed the i) dose-response effects on fungal growth, ii) antioxidant enzymatic responses, and iii) proteomic responses. We hypothesized that i) AgNPs and Ag^+ would induce toxicity to *A. tetracladia* by inhibiting biomass production, ii) the fungal ecotype from the non-polluted stream would be more sensitive than the one from the metal-polluted stream, and iii) the proteomic profiles would match

with those of antioxidant enzymes and would reveal distinct functional responses to each form of Ag.

3.2. Materials and methods

3.2.1. Fungal ecotypes

Two aquatic fungal intraspecific ecotypes were used: i) *Articulospora tetracladia* UMB-072.01 (At72), isolated from foam at Maceira, a non-polluted stream in Peneda-Gerês National Park, Portugal, and ii) *A. tetracladia* UMB-061.01 (At61), isolated from decomposing leaves at a metal-polluted site of the Este River, near the industrial park of the city of Braga, Portugal. At the polluted site, the reported metal concentrations in the sediment fraction (<63 μm , volatile matter content: 12.3 w%) were Cu: 518.1, Cd: 0.14 and Pb: 16.4 g kg^{-1} of volatile dry weight (Soares et al 1999). Further details about the sampling sites can be found elsewhere (Pascoal et al 2005b). The aquatic hyphomycetes were cultivated at 18°C and maintained on malt extract agar (ME, 1% w/v; agar, 1% w/v).

3.2.2. Preparation of AgNP suspensions and Ag⁺ solution

A commercial stock suspension of citrate-coated AgNPs (1 g L^{-1} , NanoSys GmbH, Wolfhalden, Switzerland) was used to prepare the working stock of AgNPs (0.1 g L^{-1}) in sterile (121°C, 20 min) ultrapure water (Milli-Q, 18.2 M Ω -cm) followed by filtration (0.2- μm pore-size membrane, Millipore, Billerica, MA). The working stock solution of Ag⁺ was prepared (0.1 g L^{-1}) freshly by dissolving the AgNO₃ salt (> 99%, Sigma-Aldrich, St. Louis, MO, USA) in sterile ultrapure water followed by filtration. All the other chemicals used in this study were purchased from Sigma-Aldrich, unless specified.

3.2.3. Characterization of nanoparticles

Zeta potential and dynamic light scattering (DLS) were used (Zetasizer Nano ZS, Malvern Instruments Limited, UK) to determine the stability, dispersity and hydrodynamic size distribution of AgNPs in the i) working stock (aqueous) suspension and ii) malt extract medium at the beginning and end of the 3-day exposure period.

3.2.4. Quantification of silver

Inductively Coupled Plasma Mass Spectrometer (Thermo X7 Q-ICP-MS, Thermo Scientific) was used to quantify silver and Ag^+ released by dissolution from AgNPs in the malt extract medium at the beginning and end of the 3-day exposure period. Fungal mycelia were removed from the malt extract medium by centrifugation ($5000 \times g$, 5 min). The dissolved Ag^+ in the medium that derived from AgNPs was quantified in biomass-free supernatant after centrifugal ultrafiltration ($3220 \times g$, 30 min; repeated thrice) using Amicon Ultra-15 centrifugal filter units (3 kDa of molecular weight cut-off, corresponding to < 2 nm of estimated pore size; Merck Millipore, Germany) followed by acidification with nitric acid (1.68% final concentration). The retrieved mycelia was weighed and washed thrice with 2 mL of L-cysteine solution (0.5 mM in sterile ultrapure water, Milli-Q, $18.2 \text{ M}\Omega\text{-cm}$) to remove and quantify the adsorbed silver as Ag^+ after acidification as mentioned above. Finally, the mycelia was soaked in 5% nitric acid, washed with sterile ultrapure water thrice and lyophilized for 48h and weighed (drymass) again, then mineralized in furnace at $550 \text{ }^\circ\text{C}$ (12h) followed by digestion with 2% nitric acid to determine the Ag accumulated in fungi. The Ag or Ag^+ quantifications were performed at the Scientific and Technological Research Assistance Centre (C.A.C.T.I., University of Vigo, Spain).

3.2.5. Exposure conditions and effective sublethal concentrations

To establish the exposure concentrations for assessing the responses of proteome and antioxidant enzymes, the EC_{20} , an effective sublethal concentration of AgNPs or Ag^+ on the growth of each fungal ecotype was determined. To that end, one agar plug (12-mm diameter, 5-mm depth; MEA 1%) of 20 day-old culture of each fungus was homogenized (Ultraturrax, IKA, Staufen, Germany) in 1 mL of sterilized (121°C , 20 min) liquid malt extract medium (ME 1%), and 1 mL of the homogenate was transferred aseptically into 250-mL Erlenmeyer flasks containing 100 mL of 1% sterile ME. After 48h of fungal growth ($18 \text{ }^\circ\text{C}$, 140 rpm), each fungal culture was exposed to increasing concentrations of AgNPs (0, 0.5, 1, 3, 6 and 8 mg L^{-1}) or Ag^+ (0, 0.05, 0.1, 0.2, 0.4 and 0.6 mg L^{-1}). Fungal cultures were then incubated for 3 days (to reach mid-exponential growth phase) on a shaker ($18 \text{ }^\circ\text{C}$, 140 rpm). Experiments were run in triplicates.

For antioxidant enzymatic assays, fungal cultures at mid exponential growth phase were unexposed (controls) or exposed for 3 days to i) AgNPs at EC_{20} , ii) Ag^+ at EC_{20} , and iii) AgNPs

at the concentrations corresponding to the EC₂₀ of Ag⁺. For proteomic analysis, the fungi were unexposed (controls) or exposed for 3 days to either AgNPs or Ag⁺ at the respective EC₂₀.

3.2.6. Fungal biomass, preparation of mycelia-free extract and protein quantification

For biomass quantification, fungal mycelia were harvested by filtration (5 µm pore size; Millipore, Billerica, MA, USA), washed with Milli Q water, then dried at 80 °C to constant mass (48 ± 8 h), and weighed to the nearest 0.001 g.

For preparation of mycelia-free extract, fungal biomass was harvested by centrifugation (5000 × g for 5 min at 4 °C), dipped in liquid nitrogen and stored at -80 °C until used. For assessing the activities of antioxidant enzymes and proteomic analysis, harvested mycelia were washed twice with 100 mM potassium phosphate (K₂HPO₄ + KH₂PO₄, pH 7.4) buffer (1:8, w:v) at 4°C and ground with liquid nitrogen in a cooled mortar. Ground mycelium was then resuspended in the extraction solution containing 100 mM potassium phosphate buffer (pH 7.4), 2 mM ethylenediaminetetraacetic acid (EDTA) and 1 mM phenylmethylsulfonyl fluoride (PMSF) at 4°C and homogenized (Ultraturrax, IKA, Staufen, Germany). Mycelia-free extracts were obtained after centrifugation of the homogenates (10000 × g for 10 min at 4°C) followed by a filtration (0.2 µm; Millipore, Billerica, MA). For the proteomic analysis, the extracted protein suspensions were concentrated using trichloroacetic acid + deoxycholate / acetone precipitation. The concentration of total intracellular protein in mycelia-free extracts was determined by the modified Lowry method (Peterson 1983), using a protein standard (bovine serum albumin).

3.2.7. Antioxidant enzyme activities

The activities of antioxidant enzymes were measured in mycelia-free extracts from fungi unexposed or exposed to nanoparticulate and ionic silver using a spectrophotometer (SpectraMaxPlus 384 Microplate Reader, Molecular Devices, CA, USA) following the adaptation to other microorganism described elsewhere (Barros et al 2019).

In brief, the SOD activity was assessed with Ransod Kit (Randox Laboratories Limited, Crumlin, UK) based on the ability of this enzyme to inhibit superoxide radical dependent reactions. The reaction mixture comprised of 0.05 mM xanthine, 0.025 mM 2-(4-iodophenyl)-3-(4-nitrophenol)-5-phenyltetrazolium chloride (INT) dissolved in 40 mM 3-

(cyclohexylamino)-1-propanesulfonic acid (pH 10.2) and 0.94 mM EDTA and the mycelia-free extract (1:20 v/v). Formation of superoxide radicals started with the addition of xanthine oxidase (final concentration 10 U L⁻¹), which reacted with INT to produce a red formazan dye (detected at 505 nm). One unit (U) of SOD activity was defined as the amount required for 50% inhibition of this reaction. The activity was normalized to protein concentration.

Modified method of Clairborne (1985) was used to determine the CAT activity (Barros et al 2019). The reaction mixture contained 50 mM potassium phosphate buffer (pH 7.0), 30 mM H₂O₂ and the mycelia-free extract (1:12 v/v). The dismutation of H₂O₂ was detected as the decrease in absorbance (240 nm, $\epsilon = 0.04 \text{ mM}^{-1} \text{ cm}^{-1}$) and the CAT activity was calculated from the slope of the absorbance curve of H₂O₂ and normalized to the protein concentration. The activity of GPx was determined according to Flohé and Günzler (1984) with slight modification (see Barros et al 2019). The reaction mixture comprised of 50 mM potassium phosphate buffer (pH 7.0), 1 mM EDTA, 1 mM GSH (reduced glutathione), 1 mM of NaN₃ (CAT inhibitor), 0.24 mM reduced nicotinamide adenine dinucleotide phosphate (NADPH), 0.25 mM H₂O₂ (substrate), 0.2 U GR (glutathione reductase from yeast) and the mycelia-free extract (1:30 v/v).. The GR reduced GSSG (oxidized glutathione) to GSH while the NADPH was oxidised (340 nm, $\epsilon = 6.2 \text{ mM}^{-1} \text{ cm}^{-1}$).GPx activity was computed from the slope of the NADPH absorbance curve and normalized to the protein concentration.

The GST activity was determined based on the method developed by Habig et al (1974), with slight adaptation (Barros et al 2019). The reaction mixture contained 100 mM potassium phosphate buffer (pH 6.5), 1.5 mM 1-chloro-2,4-dinitrobenzene (CDNB), 1.5 mM GSH and the mycelia-free extract (1:6 v/v). The formation of 1-glutathion-2,4-dinitrobenzene, resulted from the conjugation of GSH with CDNB was monitored (340 nm, $\epsilon = 9.6 \text{ mM}^{-1} \text{ cm}^{-1}$). GST activity was calculated from the slope of the absorbance curve and normalized to protein concentration.

3.2.8. Denaturation of proteins and SDS-PAGE

A denaturation step was performed before identification of the fungal proteins following the method described by Barros et al (2019). Briefly, an incubation of total protein per sample (volumes equivalent to 200 μg) was carried out for 60 min at room temperature with urea loading buffer (9 M of urea, 50 mM of Tris at pH 8.8, 20 mM dithiothreitol, 10% w/v SDS, 10% v/v glycerol and 0.002% w/v bromophenol blue). This was followed by an

additional incubation (60 min at room temperature) with the same buffer containing 20 mM acrylamide and SDS-polyacrylamide gel electrophoretic separation of the samples was performed followed by Coomassie Brilliant Blue G-250 staining. The bands containing total proteins were excised, sliced into small pieces of the gel and used for protein identification at the Center for Neuroscience and Cell Biology, University of Coimbra, Portugal.

3.2.9. SWATH-MS analysis

The Sequential Windowed data independent Acquisition of the Total High-resolution Mass Spectra (SWATH-MS) analysis was performed with an adaptation of the process described by Barros et al (2019). In brief, the gel pieces were first destained using a destaining solution (50 mM ammonium bicarbonate and 30% acetonitrile) followed by washing step with deionized water, then dehydrated and subjected to in gel digestion (with 0.01 $\mu\text{g } \mu\text{L}^{-1}$ of trypsin) by using the short-GeLC approach (Anjo et al 2014). The formed peptides were subjected to solid phase extraction using OMIX tips containing C18 stationary phase (Agilent Technologies), as per the manufacturer's recommendation, and then resuspended to 40 μL of mobile phase containing iRT peptides (Biognosys AG) as internal standards. The replicate samples were combined (10 μL of each) to obtain one pooled sample per experimental condition (in a total of four pools) and used for protein identification and SWATH-MS-library generation. Triple TOFTM 5600 System (ABSciex[®]) was used for the sample analyses in two phases: i) information-dependent acquisition (IDA) of the pooled sample for protein identification, and ii) SWATH acquisition of each individual sample for protein quantification. All files from the IDA experiments were combined to create a specific library of precursor masses and fragment ions, and the library was used for subsequent SWATH processing. Libraries were obtained using Protein PilotTM software (v5.1, ABSciex[®]) searching against the SwissProt database (released in March 2016).

SWATHTM processing plug-in for PeakViewTM (v2.0.01, ABSciex[®]) was used to perform the SWATH data processing. Peptides (≤ 15 peptides per protein with ≤ 5 fragment ions) were chosen automatically from the library and SWATHTM quantitation was attempted for all the proteins in the library file, identified $< 5\%$ local False Discovery Rate (FDR) from ProteinPilotTM searches, by extracting the peak areas of the target fragment ions of those peptides using an extracted-ion chromatogram (XIC) window of 5 min with 100 ppm XIC width.

All the peptides that met 1% FDR threshold (in at least 3 out of 4 replicates) were retained; the protein levels were estimated by summing all the respective transitions from all the filtered peptides for a given protein (an adaptation of Collins et al 2013). The protein levels were normalized to the total intensity for performing the comparisons between treatments (see Appendix 10 and Barros et al 2019 for details).

3.2.10. Statistical analyses

The effective concentrations of Ag⁺ and AgNPs decreasing 20% of fungal growth (EC₂₀, 95% C.I.) were calculated using PriProbit 1.63. To achieve normal distribution and homoscedasticity, the data in percentage were transformed to arcsine square root. One-way analyses of variance (ANOVAs) were used to test for the effects of the Ag form (at EC₂₀ or at the same concentration) on the activities of antioxidant enzymes from fungi. One-way ANOVAs were also used to test for the effects of the Ag forms on alterations in protein content. Tukey's post-hoc multiple comparisons were used to identify significant differences. These analyses were performed in Prism 7.0 (for Windows, GraphPad software Inc., CA, USA).

Heatmaps and cluster analyses of quantified proteins from each fungal ecotype were performed using GProX v 1.1.15 (Rigbolt et al 2011). The proteins shown in the heat maps were clustered by their behavioural profiles. For clustering, the unsupervised clustering fuzzy *c*-means algorithm implemented in the Mfuzz package (Kumar and Futschik 2007) was used which is a soft clustering algorithm, noise-robust and well-fitted to the protein profile data. The most representative biological processes associated with each cluster were featured based on UniProt Gene Ontology (GO) database, followed by enrichment analysis within GProX, using a binomial statistical test with Benjamini-Hochberg adjustment ($P < 0.05$). This analysis required a comparison between the cluster representing the group of proteins, the amount of which decreased under exposure to Ag⁺ and AgNPs in relation to control (cluster 5 in At72 and cluster 4 in At61) and the other clusters.

A Principal Component Analysis (PCA) was performed to associate the responses of antioxidant enzymes with the protein contents in fungi unexposed or exposed to Ag⁺ and AgNPs. Significant effects were tested by permutational multivariate analysis of variance (PERMANOVA). The PCA was done in PAST 3.14 for Windows (<http://folk.uio.no/ohammer/past>; Hammer et al 2001).

3.3. Results

3.3.1. Characterization of AgNPs and quantification of Ag

At the beginning (T0) and end (T1) of the experiment, the average hydrodynamic diameter (HDD) of AgNPs did not vary (T0: 31.9 nm, T1: 32.1 nm; 100% intensity) in aqueous suspensions; the polydispersity index was lower (Pdl: <0.29) and the zeta potential (ζ) was higher (~ -41 mV) in the aqueous suspensions than in the ME medium in the presence of either fungal ecotype (Table 3.1).

Table 3.1 Hydrodynamic diameter (HDD), polydispersity index (Pdl) and zeta potential of AgNPs in ultrapure water (UPW) and ME medium before (T0) and after 3 days (T1) of exposure. Mean \pm SD, n = 3.

Sample	Zeta potential (mV)	Pdl	Peak 1		Peak 2	
			Average HDD (nm)	Area Intensity (%)	Average HDD (nm)	Area Intensity (%)
UPWT0	-40.7 \pm 0.5	0.29 \pm 0.00	31.9 \pm 0.1	100 \pm 0	-	-
UPWT1	-40.6 \pm 0.5	0.29 \pm 0.00	32.1 \pm 0.1	100 \pm 0	-	-
ME + At61T0	-27.7 \pm 0.8	0.53 \pm 0.09	295.9 \pm 48	83.6 \pm 4	41.7 \pm 11	16.4 \pm 4
ME + At61T1	-19.3 \pm 2	0.50 \pm 0.14	377.7 \pm 187	88.9 \pm 7	40.3 \pm 27	11.1 \pm 7
ME + At72T0	-25.3 \pm 0.3	0.46 \pm 0.21	295.8 \pm 43	76.9 \pm 2	37.8 \pm 4	23.1 \pm 2
ME + At72T1	-30.4 \pm 1.6	0.44 \pm 0.07	292.9 \pm 51	68.1 \pm 1	42.9 \pm 7	31.9 \pm 1

At T0 and at T1, two peaks of HDD were observed in the presence of At61 or At72. The zeta potential decreased during the experiment in the presence of At61 (-27.7 to -19.3 mV), indicating particle agglomeration (Table 3.1). At T1, the area intensity and HDD of larger particles increased in the presence of At61, supporting increased agglomeration of AgNPs with the exposure time. However, in the presence of At72, the intensity of the smaller sized nanoparticles was relatively higher (23.1%) and Pdl was relatively lower (<0.5) than in the presence of At61 at T0 (Table 3.1). Moreover, an opposite trend was observed in the presence of At72 at T1 (Table 3.1), indicating increased particle stability and lesser agglomeration with exposure time.

The silver quantification, by ICP-MS, revealed that at T0 the concentration of Ag⁺ from the dissolution of AgNPs (7.5 $\mu\text{g L}^{-1}$ and 158.9 $\mu\text{g L}^{-1}$ for At72 and At61, respectively) to ME

medium was below the limit of quantification ($<0.2 \mu\text{g L}^{-1}$; the detection limit was $0.06 \mu\text{g L}^{-1}$) and did not change with time. On the other hand, At72 and At61 adsorbed 0.62 ± 0.3 and $3.85 \pm 2.6 \mu\text{g of Ag}^+ \text{g}^{-1}$ fungal dry mass, respectively at T1, which corresponded to $5.7 \pm 3.2\%$ and $1.6 \pm 1.1\%$ of total Ag added per flask, respectively. In addition, the accumulated Ag in mycelia of At72 and At61 was 2.6 ± 1.0 and $107.4 \pm 18.4 \mu\text{g g}^{-1}$ fungal dry mass, respectively, after 3 days of exposure to EC_{20} of AgNPs.

3.3.2. Effects of AgNPs and Ag^+ on the fungal growth

The exposure of both *A. tetracladia* ecotypes to Ag^+ or AgNPs resulted in a dose-dependent reduction in their specific growth rates (Appendix 7). The At72 was the most sensitive ecotype to AgNPs (EC_{20} : $7.5 \mu\text{g L}^{-1}$ for At72, and $158.9 \mu\text{g L}^{-1}$ for AT61, respectively; Table 3.2). In contrast, the EC_{20} of Ag^+ was ca. 6-fold higher in At72 than in At61 (Table 3.2).

Table 3.2 Concentrations of AgNPs and Ag^+ inhibiting 20% (EC_{20}) of the growth of two aquatic fungal ecotypes of *A. tetracladia* collected from a non-polluted stream (At72) and from a metal-polluted stream (At61). Fungi were grown in ME 1% for 3 days. (in parenthesis is 95% C.I.)

Ecotype	EC_{20} ($\mu\text{g L}^{-1}$)	
	AgNP	Ag^+
At72	7.5 (0.1-39.4)	117.4 (97.7-135.8)
At61	158.9 (81.7-246.5)	18.7 (0.5-41.0)

3.3.3. Effects of AgNPs and Ag^+ on antioxidant enzymatic biomarkers

In the absence of AgNPs or Ag^+ , the activity of CAT was higher in At72 ($45.0 \pm 1.4 \mu\text{mol min}^{-1} \text{mg}^{-1}$ of protein) than in At61, whereas activities of SOD, GST or GPx were similar (Appendix 9). Both forms of Ag (i.e. AgNPs and Ag^+) either at EC_{20} or at a concentration of AgNPs corresponding to EC_{20} of Ag^+ led to a significant increase in the activities of all enzymes in both ecotypes (one-way ANOVA, $P < 0.05$) (Fig. 3.1). In At72, the EC_{20} of Ag^+ led to the highest increase in the activity of GST (384.0%), followed by CAT (379.6%), SOD (349.8%) and GPx (224.7%) (Fig. 3.1A), whereas the exposure to EC_{20} of AgNPs led to a higher stimulation of CAT (261.5%), followed by SOD (244.4%), GST (211.1%) and GPx (171.5%) (Fig. 3.1A). In At61, the activity of CAT was the highest at EC_{20} of either form of Ag (Ag^+ : 257.1%, AgNPs: 239.9%), followed by SOD (Ag^+ : 240.9%, AgNPs: 233.9%), GST (195.1%, AgNPs: 192.0%) and GPx (Ag^+ :

162.3%, AgNPs: 155.3%) (Fig. 3.1B). In At72, at the concentration of AgNPs corresponding to EC₂₀ of Ag⁺ (117.4 μg L⁻¹), the activity of CAT was the highest, increasing to 415% (Fig. 3.1C), whereas the increased activities of the other three enzymes were slightly lower (Fig. 3.1A). In At61, the enzyme activities were considerably lower at the concentration of AgNPs corresponding to EC₂₀ of Ag⁺ (18.7 μg L⁻¹, Fig. 3.1D) than that observed at the same concentration of Ag⁺ (Fig. 3.1B).

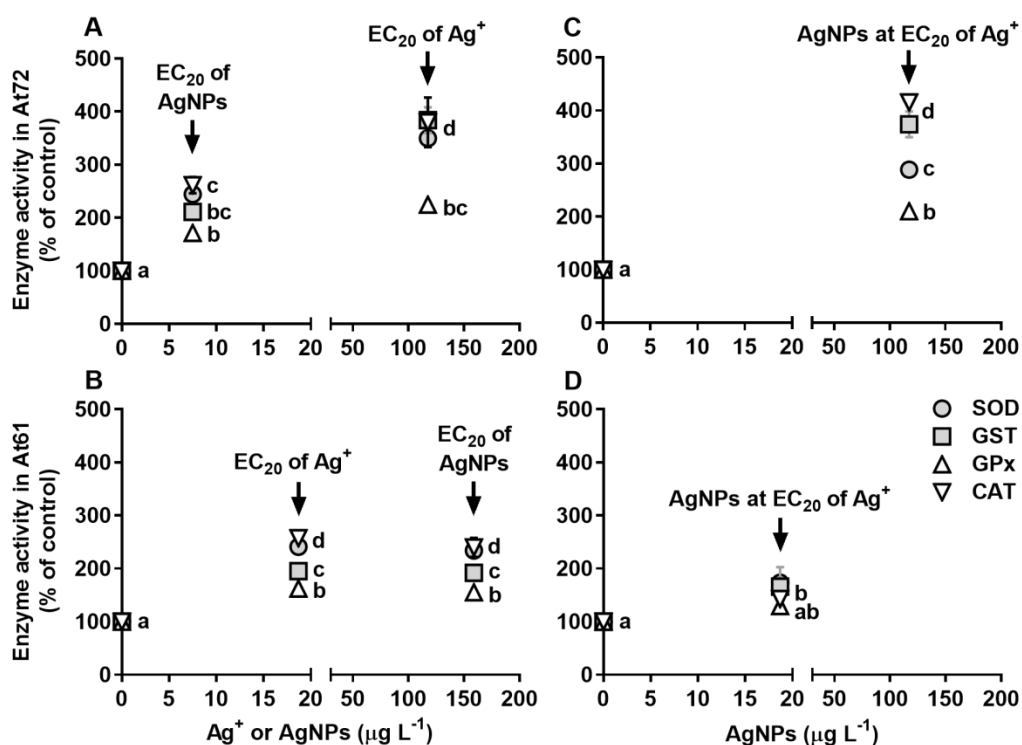


Figure 3.1 Activities of superoxide dismutase (SOD), glutathione S-transferase (GST), glutathione peroxidase (GPx) and catalase (CAT) in two ecotypes of *A. tetracladia* collected from a non-polluted stream (At72) and from a metal-polluted stream (At61) at EC₂₀ of AgNPs and Ag⁺ for At72 (A) and At61 (B), and at the concentration of AgNPs corresponding to the EC₂₀ of Ag⁺ for At72 (C) and At61 (D). Values are in percentage of respective control. Mean ± SEM, n = 3. Different letters indicate significant differences (P < 0.05).

3.3.4. Effects of AgNPs and Ag⁺ on fungal proteomes

A total of 358 and 516 proteins were quantified by SWATH-MS in At72 and At61 after exposure to EC₂₀ of Ag⁺ and AgNPs, respectively (Appendices 11 and 12). However, only 172 proteins of At72 and 260 proteins of At61 showed significant alteration in quantity (one-way ANOVA, P < 0.05) upon exposure to either or both forms of silver (Appendices 11 and 12).

Out of these, 71 proteins were common to both ecotypes (Fig. 3.2A). Among the altered proteins in At72, 51.7% and 58.1% showed increased levels by Ag⁺ and AgNP exposure, respectively; while in At61 those percentages were higher (77.7% and 76.5%, respectively; Fig. 3.2B). Clearly, the percentages of increased proteins upon exposure to EC₂₀ of Ag⁺ and AgNPs were much higher (26.0% and 18.4%, respectively) in At61 than in At72.

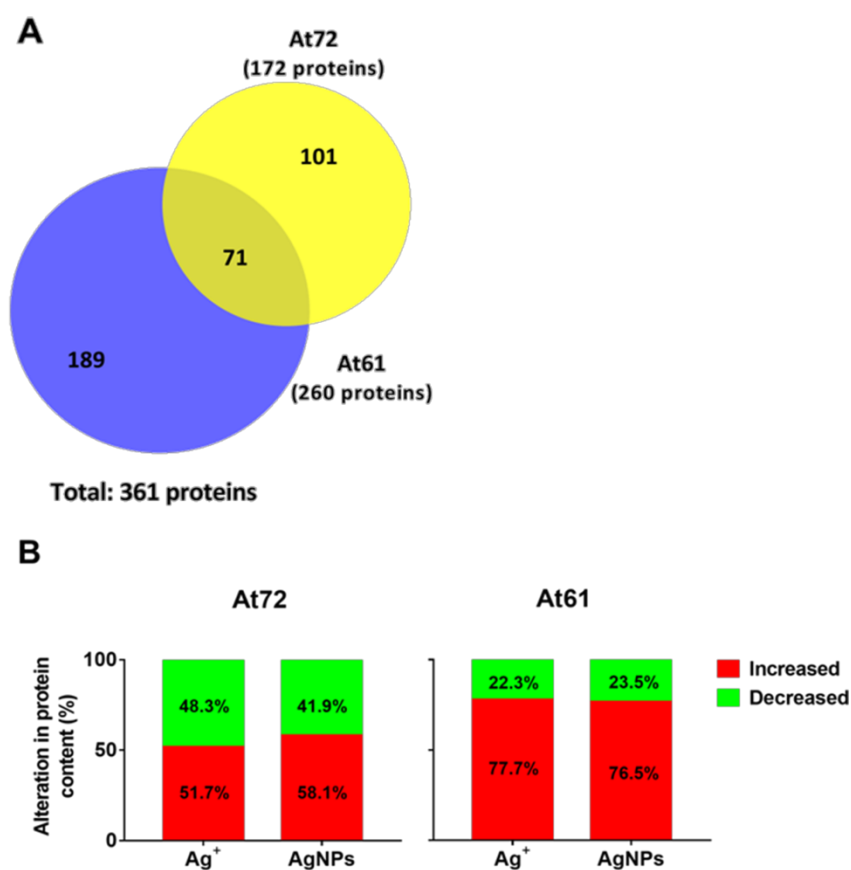
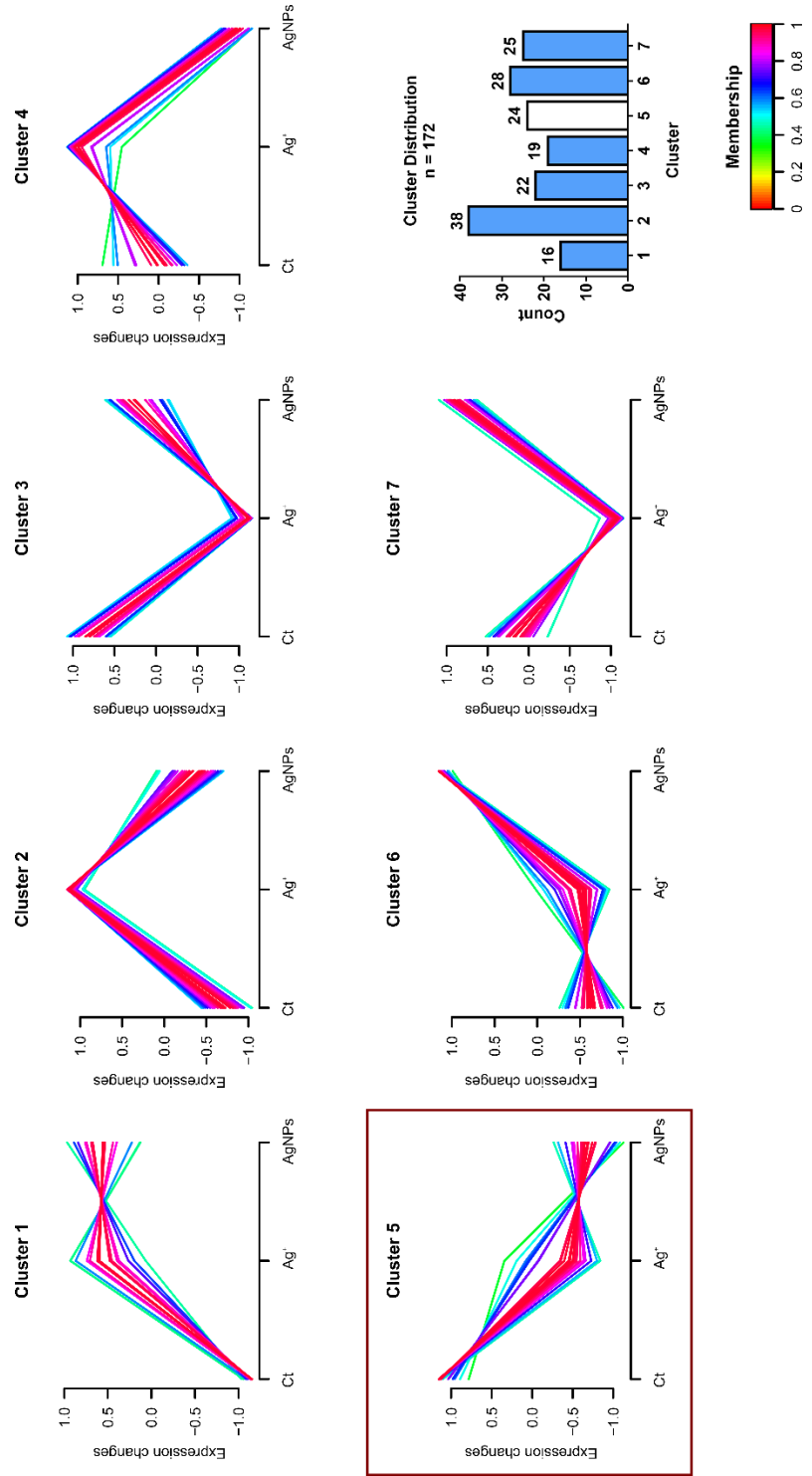
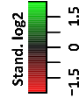
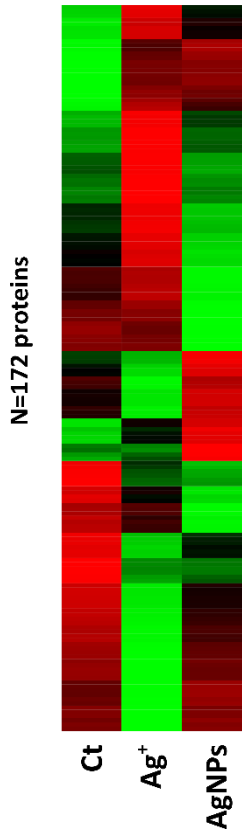


Figure 3.2 Venn diagram comparing the number of proteins significantly altered in the fungal ecotype At72 (172 proteins; in yellow) and the fungal ecotype At61 (260 proteins; in blue) and the proteins common to both ecotypes (71 proteins) (A). Percentage of significantly altered proteins, which content increased (in red) or decreased (in green), was calculated in relation to the total number of identified proteins (172 proteins for At72 and 260 proteins for At61) under exposure to Ag⁺ or AgNPs (B). Ecotypes of *A. tetracladia* were collected from a non-polluted stream (At72) or a metal-polluted stream (At61).

Moreover, the average fold changes of altered proteins upon exposure to AgNPs were also higher in At61 than in At72 (At61 vs At72: 2.62 vs 0.57-fold, and -1.45 vs -0.59-fold, respectively for increased and decreased proteins). A similar trend was observed upon exposure to Ag⁺, but only for the increased proteins (1.72 and 0.79-fold for At61 and At72,

respectively). The heatmap analyses showed the dynamic profiles that exhibited the alteration in protein levels under different exposure conditions in At72 and At61 (Fig. 3.3A and 3.4A). Based on these, proteins were clustered according to their behavioural profiles resulting in the generation of 7 clusters for At72 and 6 clusters for At61 (Fig. 3.3B and 3.4B). Due to lack of the existence of a specific database for *A. tetracladia*, other (related) species were considered in order to make the identification and functional characterization of the proteins. In At72, the levels of proteins in the cluster 1 (16 proteins) increased (average fold change: 0.88 for each Ag form) upon exposure to Ag⁺ or AgNPs (Appendix 11). Cluster 2 included 38 proteins, all of which increased considerably (average: 1.14-fold) upon exposure to Ag⁺, while the content of 9 proteins decreased (average fold change -0.17) and the remaining proteins increased moderately (average: 0.36-fold) upon exposure to AgNPs. In cluster 3 (22 proteins), the contents of all proteins decreased strongly (average: -1.16-fold) upon exposure to Ag⁺ and moderately (average: -0.26-fold) upon exposure to AgNPs, with the exception of aldehyde dehydrogenase and ATP-dependent RNA helicase sub2. All of the 19 proteins in cluster 4 decreased upon exposure to AgNPs (average fold change: -0.6), but increased (average: 0.46-fold) upon exposure to Ag⁺, except for methylthioribose-1-phosphate isomerase. A total of 24 proteins were included in cluster 5, most of which decreased strongly upon exposure to both Ag forms (average: -0.94- and -1.01-fold by Ag⁺ and AgNPs, respectively). The protein contents in cluster 6 (28 proteins) increased considerably upon exposure to AgNPs (average fold change: 0.89), while under exposure to Ag⁺ only few proteins increased moderately. All proteins in cluster 7 (29 proteins) increased moderately (average: 0.29-fold) upon exposure to AgNPs but decreased (average: -0.7-fold) upon exposure to Ag⁺ (Appendix 11).

In At61, all proteins from cluster 1 (75 proteins) increased considerably under exposure to AgNPs (average fold change: 2.53); under exposure to Ag⁺, 68 of those proteins increased slightly (average fold change: 1.11), while 4 decreased strongly (transaldolase, 50S ribosomal protein L15, dCTP deaminase and 30S ribosomal protein S16) (Appendix 12).



A

B

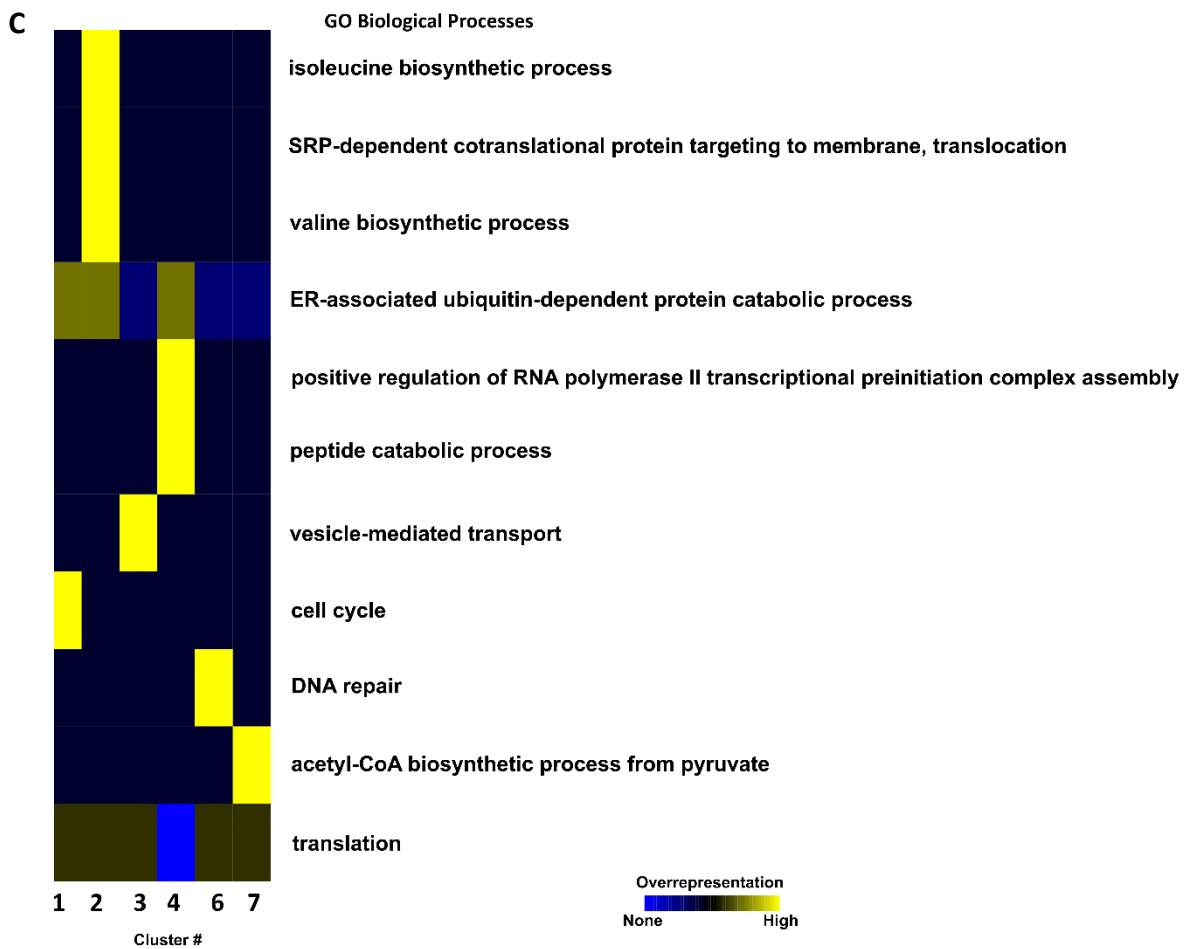
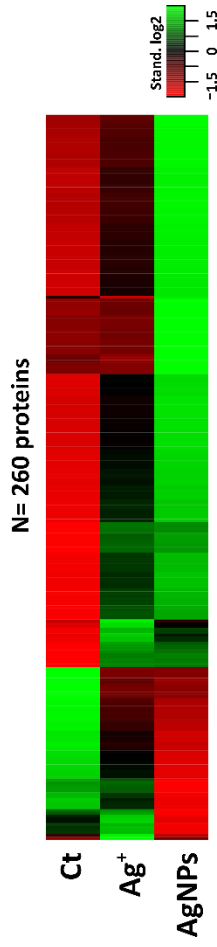
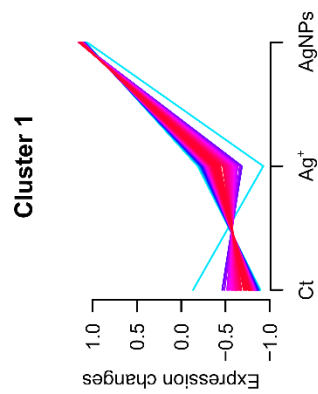
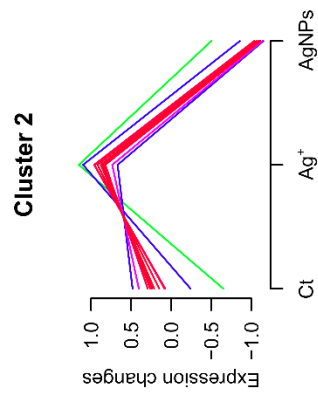
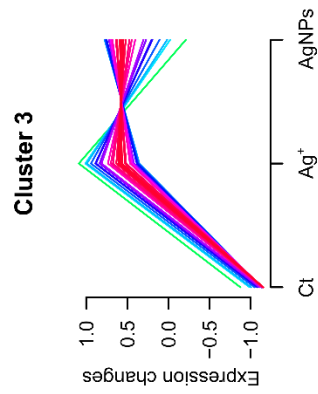
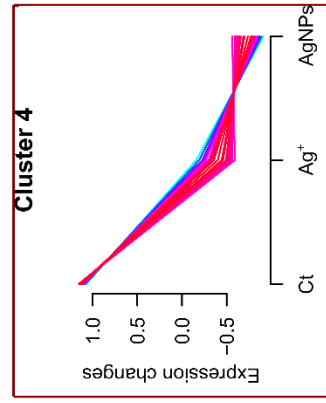


Figure 3.3 Heatmap (A) and clustering analysis (B) of the proteins with significant variation and Gene Ontology (GO) enrichment analysis (C) in the ecotype of *A. tetracladia*: At72, collected from a non-polluted stream, under exposure to Ag⁺ and AgNPs. Unsupervised clustering was performed for the standardized protein of the 172 altered proteins. An upper and lower ratio limit of log₂ (2) and log₂ (0.5) was used for inclusion into a cluster. Membership value represents how well the protein profile fit the average cluster profile (B). Overrepresented biological processes (C) of each cluster (B). Each cluster from (B) was tested for overrepresented GO compared with the cluster 5, using a Binomial statistical test with Benjamini-Hochberg adjustment ($P < 0.05$). Ct: Control.

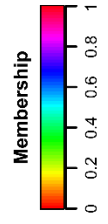
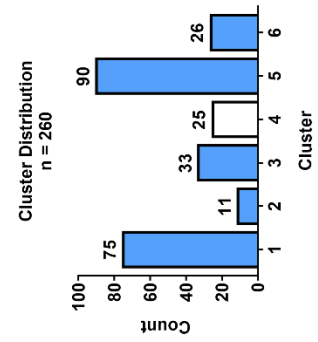
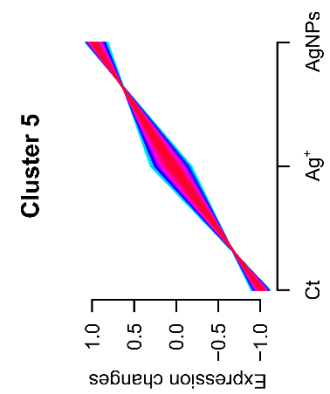
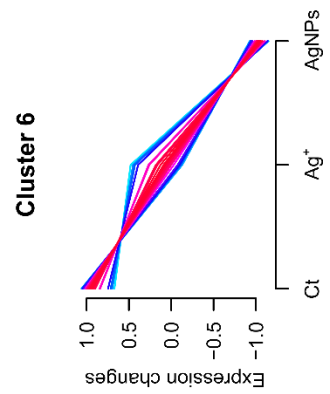
In cluster 2 (11 proteins), all protein levels increased moderately (average: 0.42-fold) under exposure to Ag⁺, but decreased (average: -0.7-fold) under exposure to AgNPs, except for protein RecA. The content of all proteins in cluster 3 (33 proteins) increased significantly upon exposure to both forms of Ag (average: 2.43-fold by Ag⁺ and 2.39-fold by AgNPs). Cluster 4 was composed of 25 proteins, the levels of which decreased strongly upon exposure to Ag⁺ (average: -1.21-fold) and AgNPs (average: -1.6-fold).



A



B



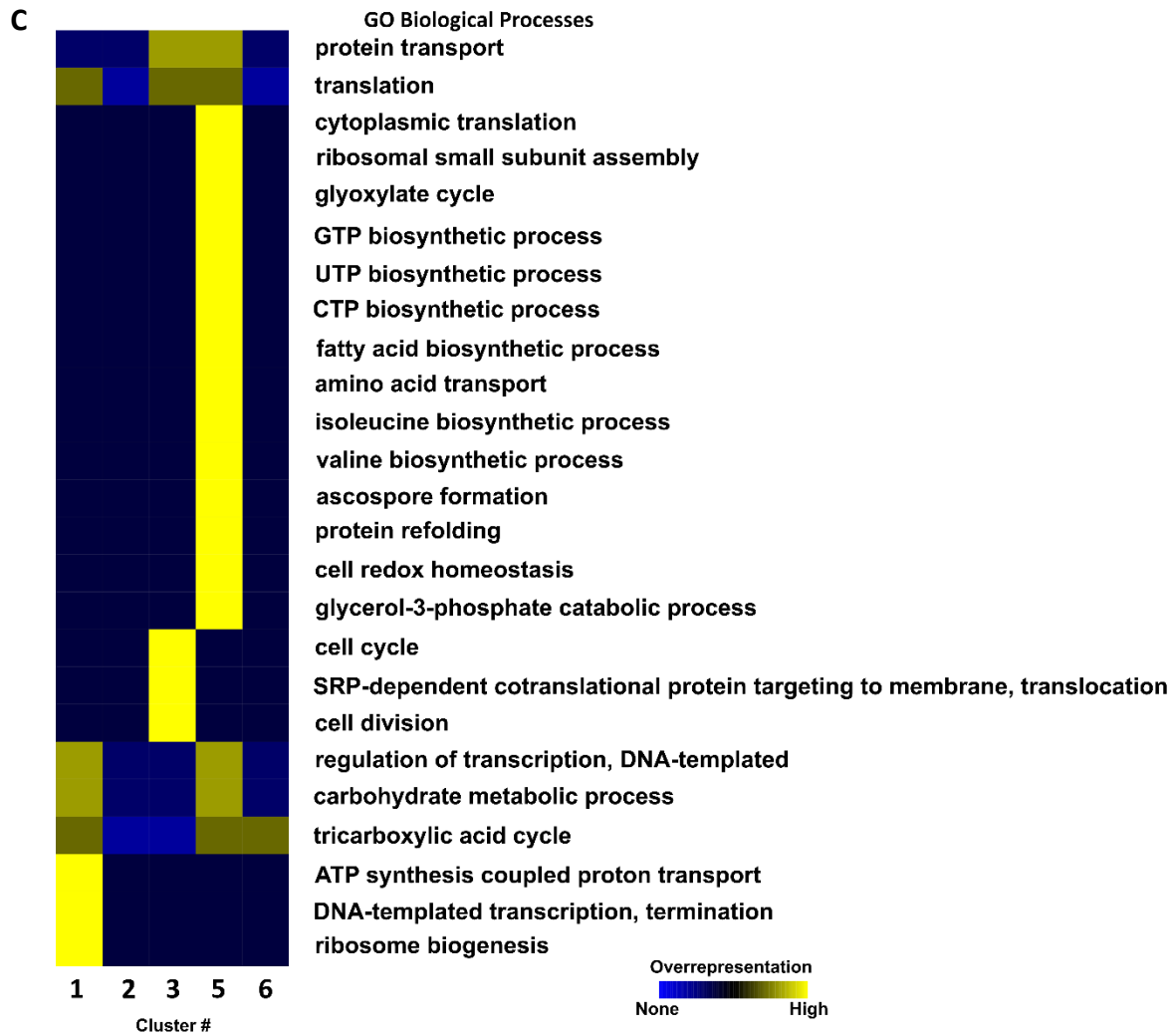


Figure 3.4 Heatmap (A) and clustering analysis (B) of the proteins with significant variation and Gene Ontology (GO) enrichment analysis (C) in the ecotype of *A. tetracladia*: At61, collected from a metal-polluted stream, under exposure to Ag^+ and AgNPs. Unsupervised clustering was performed for the standardized protein of the 260 altered proteins. An upper and lower ratio limit of $\log_2(2)$ and $\log_2(0.5)$ was used for inclusion into a cluster. Membership value represents how well the protein profile fit the average cluster profile (B). Overrepresented biological processes (C) of each cluster (B). Each cluster from (B) was tested for overrepresented GO compared with the cluster 4 using a Binomial statistical test with Benjamini-Hochberg adjustment ($P < 0.05$). Ct: Control.

Both silver forms considerably stimulated (average: 2.09-fold by Ag^+ and 2.8-fold by AgNPs) the protein levels from cluster 5 (90 proteins). All of the 26 proteins belonging to cluster 6 decreased strongly (average fold change: -1.6) upon exposure to AgNPs and most proteins decreased moderately (average fold change: -0.44) upon exposure to Ag^+ .

3.3.5. Relationship between proteomic and enzymatic responses to oxidative stress

The overall responses of antioxidant enzymes and proteins involved in antioxidant activities in At72 or At61 under exposure to Ag⁺ and AgNPs at concentrations corresponding to EC₂₀ were analysed by PCA (Fig. 3.5). The exposure of At72 or At61 to Ag⁺ and AgNPs showed significant effects on the activities of antioxidant enzymes and on the contents of proteins involved in defense against oxidative stress (PERMANOVA, $P < 0.05$). The PC1 explained 77.5% and 73.9% of the total variance for At72 (Fig. 3.5A) and At61 (Fig. 3.5B). In At72, the controls and treatments with Ag⁺ and AgNPs were clearly separated along the PC1 based on the responses of antioxidant biomarkers and related proteins (Fig. 3.5A). For At61, the segregation between Ag⁺ and AgNPs treatments was less pronounced (Fig. 3.5B). In At72, all antioxidant enzymatic biomarkers and the contents of the related proteins considered for PCA (both the KATGs, SOD_BOTFU, SOD, CAT, GPx and GST) were positively associated with Ag⁺ (Fig. 3.5A). In At61, the activities of the antioxidant enzymes (SOD, CAT, GPx and GST) were positively associated with Ag⁺ exposure, whereas the contents of the proteins involved in antioxidant activities were mostly associated with AgNP exposure (Fig. 3.5B).

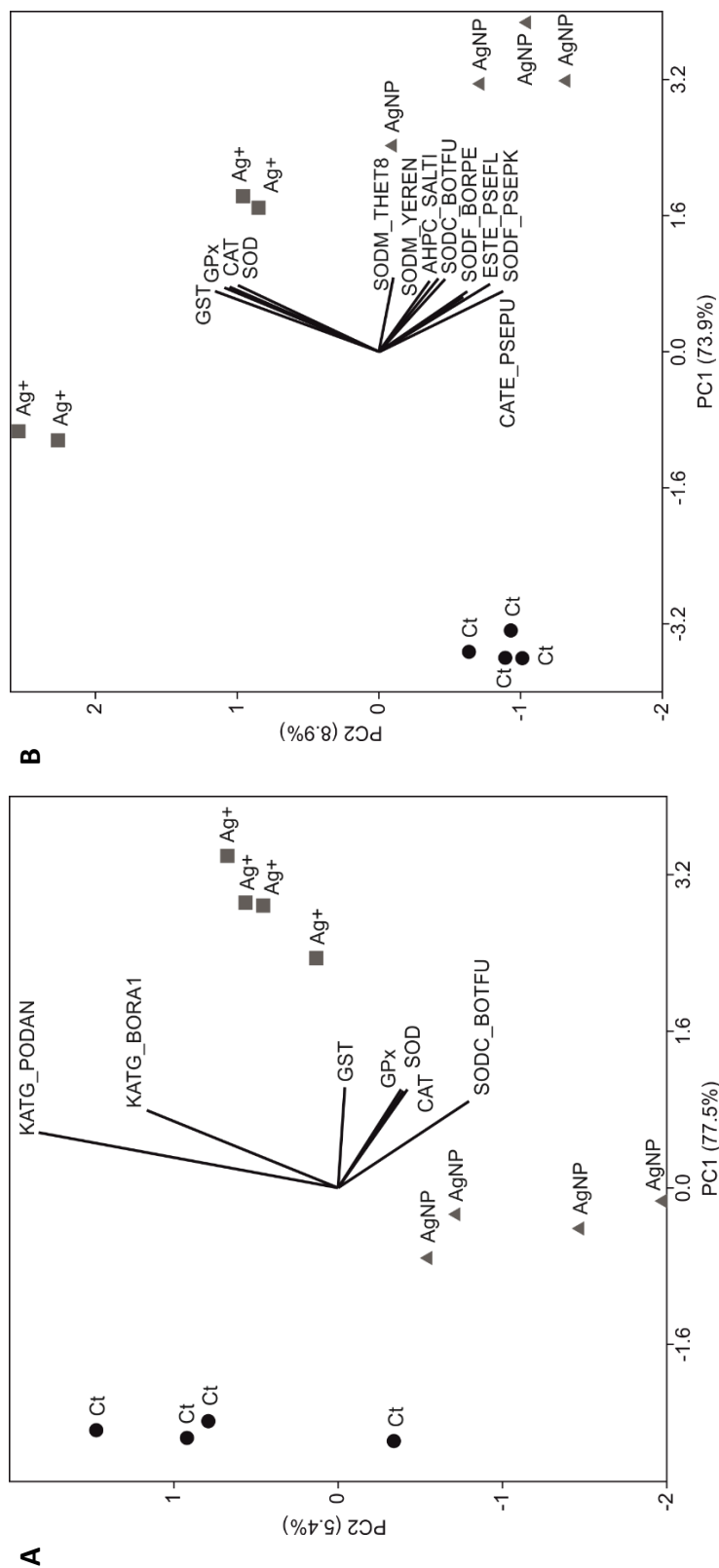


Figure 3.5. Principal component analysis (PCA) of overall responses of proteins involved in antioxidant activities (KATG_PODAN, KAT_BORA1, AHPC_SALTI, ESTE_PSEFL, SODC_BOTFU, SODF_BORPE, SODF_PSEPK, SODM_THET8 and SODM_YEREN) and activities of antioxidant enzymes in two ecotypes of *A. tetracladia*: At72 collected from a non-polluted stream (A), and At61 collected from a metal-polluted stream (B) unexposed (Ct) or exposed for 3 days to EC₂₀ of AgNPs and Ag⁺. KATG_PODAN: catalase-peroxidase (*Podospora anserina*); KAT_BORA1: catalase-peroxidase (*Bordetella avium*); CATE_PSEPU: catalase HPII (*Pseudomonas putida*); AHPC_SALTI: alkyl hydroperoxide reductase C (*Salmonella typhi*); ESTE_PSEFL: arylesterase (*Pseudomonas fluorescens*); SODC_BOTFU: superoxide dismutase [Cu-Zn] (*Botryotinia fuckeliana*); SODF_BORPE: superoxide dismutase [Fe] (*Bordetella pertussis*); SODF_PSEPK: superoxide dismutase [Fe] (*Pseudomonas putida*); SODM_THET8: superoxide dismutase [Mn] (*Thermus thermophilus*) and SODM_YEREN: superoxide dismutase [Mn] (*Yersinia enterocolitica*). SOD: superoxide dismutase; GST: glutathione S-transferase; GPx: glutathione peroxidase and CAT: catalase. Ct: control.

3.4. Discussion

In our study, the ecotype *A. tetracladia* from the polluted stream was more tolerant to AgNPs than the ecotype from the non-polluted stream (EC_{20} for the growth of At72 < At61). However, an opposite trend was observed for the effects of Ag^+ . The absence of silver in the metal-polluted stream from which At61 was isolated may contribute to explain the low tolerance of this ecotype to Ag^+ . Different sensitivity of aquatic fungi to different metals has been shown earlier (e.g. Azevedo et al 2009). Similarl to what reported for stream microbial decomposer communities (Tlili et al 2016), we found that the impacts of AgNPs were higher than those of Ag^+ in At72. In our study, the negligible amount of dissolved Ag^+ released from AgNPs, suggests that toxicity can be mainly attributed to the nanoparticulate form.

Also, fungi are sensitive to inorganic nutrients (e.g. NO_3^- , Fernandes et al 2014). In a complementary test, we found that the two ecotypes were differentially affected by nitrate; exposure to the lowest tested concentration of nitrate led to an increase in fungal biomass of At72 ecotype (ca. 15%, $P < 0.05$; Appendix 8), but At61 remained unaffected. This suggests that this nutrient, released from the dissolution of $AgNO_3$, might have alleviated the toxic effects of Ag^+ on At72 and contributed to explain the higher EC_{20} on the growth of At72 than of At61 for Ag^+ .

The aggregation state of nanoparticles can play a critical role in their toxicity, as dispersed AgNPs exhibit greater negative effects over aggregated ones (Dorjnamjin et al 2008, Kvittek et al 2008). In our study, DLS and zeta potential supported these findings because the particle stability increased and the average HDD remained smaller along the exposure period for At72, the ecotype highly sensitive to AgNPs. In contrast, we found higher agglomeration and relatively lesser stability of nanoparticles in the presence of At61, contributing to alleviate the impacts of AgNPs in this fungal ecotype. Moreover, at EC_{20} , the bioaccumulation of Ag from AgNPs per unit biomass of At61 was much higher (>40 times) and the intake of total Ag was almost twice than that of At72, reflecting the higher tolerance of At61 to AgNPs. Bioaccumulation may depend on the metabolic energy and can occur in microbes inhabiting metal-polluted ecosystems to facilitate their survival in such harsh environments (Habi and Daba 2009, Zolgharnein et al 2010).

The exposure to AgNPs or Ag^+ triggered oxidative stress defenses as revealed by the enhanced activities of the antioxidant enzymes in both fungal ecotypes. The crucial role of

antioxidant enzymes to overcome the oxidative stress promoted by the toxicants was previously observed for other metal ions or nanoparticles (Azevedo et al 2009, Pradhan et al 2016). Both Ag forms stimulated the activities of CAT in both ecotypes. Although GPx had been less stimulated, the increased activity of CAT may have been efficient to deal with the oxidative stress triggered by AgNPs and Ag⁺. This is consistent with the compensatory roles of these two enzymes (Lubrano and Balzan 2015). GPx mostly catalyses the reduction of a variety of organic hydroperoxides, while CAT is considered the most efficient enzyme since it is not saturated by H₂O₂ (Lledías et al 1998). Moreover, CAT also possesses peroxidase activity. In At61, both Ag forms stimulated the SOD activity, pinpointing the efficiency of this enzyme to counteract the superoxide anions and convert those into less reactive H₂O₂ (Lubrano and Balzan 2015). In At72, the activity of GST was also stimulated, suggesting an elevated intracellular accumulation of ROS. Moreover, the lower negative effects of Ag⁺ than of AgNPs on the growth of At72 may indicate high efficiency of CAT, SOD and GST to deal with the oxidative stress induced by Ag⁺.

Gene Ontology enrichment analysis based on protein clustering predicted that different biological processes are likely to be associated with the responses of *A. tetracladia* ecotypes to Ag⁺ or AgNPs (Fig. 3.3C and 3.4C). Some of the predicted processes were common in response to both stressors and in both fungal ecotypes. Both ecotypes showed alterations in processes related to protein homeostasis, most of which were common upon exposure to both Ag forms. Specifically, in At72, the levels of proteins involved in transcription (positive regulation of RNA polymerase II transcriptional preinitiation complex assembly) and peptide catabolism increased under exposure to Ag⁺ more than to AgNPs (clusters 4; Fig. 3.3C); proteins involved in α amino acid (isoleucine and valine) biosynthesis and signal recognition particle (SRP)-dependent protein translocation increased moderately upon Ag⁺ exposure, but decreased under exposure to AgNPs (clusters 2; Fig. 3.3C). This indicated that protein homeostasis was strongly affected by AgNPs in At72. In At61, protein homeostasis was dependent on transcription (DNA-templated regulation and termination), ribosomal subunit assembly and biogenesis, (SRP)-dependent protein translocation, α -amino acid biosynthesis and transport, and protein refolding and transport, as the related protein levels increased more under exposure to AgNPs than to Ag⁺ (clusters 1, 3 and 5; Fig. 3.4C). Moreover, the GO enrichment analysis predicted that 23.9% of the common proteins in both ecotypes were related to protein biosynthesis (translation). In At72, both Ag forms led to a

considerable increase in proteins associated with translation (all except cluster 4; Fig. 3.3C), although the number of increased proteins was higher under exposure to AgNPs. In At61, the translation related proteins (cluster 1, 3 and 5; Fig. 3.4C) were stimulated by both Ag forms, particularly under AgNPs exposure. This supported the higher efficiency of At61 than At72 in maintaining protein homeostasis under AgNP-induced stress. These findings are in agreement with other proteomic studies showing alterations in protein biosynthesis, transcription and translation in bacteria (Yuan et al 2013, Mirzajani et al 2014) and human cell lines (Miethling-Graff et al 2014) by AgNPs.

Another highly overrepresented process in both ecotypes (cluster 1 in At72; cluster 3 in At61) was related to cell cycle (Fig. 3.3C and 3.4C), as the proteins (*e.g.* fimbriin) likely to be involved in this process increased in both ecotypes under exposure to both Ag forms, consistently to that found in other biological systems (plants, Nair and Chung 2014; in zebra fish larvae, Kang et al 2016).

Protein degradation is crucial for cell protection (Zhu et al 2006). A highly overrepresentation of the ubiquitin-dependent endoplasmic reticulum-associated protein degradation (ERAD, Lemus and Goder 2014) was observed in At72 in response to Ag⁺ (cluster 1, 2 and 4; Fig. 3.3C). However, this trend was not observed for AgNPs, suggesting that ERAD was possibly more responsive to Ag⁺ than to AgNPs at least in the ecotype from the non-polluted stream. In our study, the protein level expressed by *CDC48* increased in At72 particularly under exposure to Ag⁺. The *CDC48* gene is essential to ERAD pathways, and its mutation is linked to apoptosis in yeast (Braun et al 2006). Moreover, neither the overrepresentation of ERAD nor this protein was observed in At61 under exposure to either Ag form.

Vesicle-mediated transport was highly overrepresented in At72 (cluster 3; Fig. 3.3C). In fungi, vesicles are involved in exporting macromolecules across cell wall (Casadevall et al 2009) and this is an important mechanism to protect cells from self-toxicity by sequestering secondary metabolites (Sirikantaramas et al 2008). In At72, the decreased levels of proteins likely to be involved in vesicle-mediated transport (cluster 3; Fig. 3.3C) were more pronounced upon exposure to Ag⁺ than AgNPs, suggesting a particular toxicity mode of Ag⁺ by impairing this pathway in this fungal ecotype.

Several metabolic processes involved in energy production were also highlighted by the GO enrichment analysis although differently in each fungal ecotype. In At72, proteins involved

in the synthesis of acetyl-CoA from pyruvate (e.g. pyruvate dehydrogenase, cluster 7; Fig. 3.3C) increased under exposure to AgNPs but decreased under Ag⁺ exposure. For At61 (Fig. 3.4C), the featured processes were ATP synthesis coupled with proton transport (cluster 1), carbohydrate metabolism (clusters 1 and 5), tricarboxylic acid cycle (clusters 1, 5 and 6) and glyoxylate cycle (cluster 5). The majority of proteins involved in these metabolic processes (e.g. ATP synthase, pyruvate kinase, glycogen phosphorylase and isocitrate dehydrogenase) increased under exposure to both stressors but protein levels were higher under AgNP exposure, suggesting increased need of energy in fungal cells to compensate the stress induced by silver, particularly by the nanoparticulate form. Also, the increase in the levels of these proteins was much higher in At61 than in At72, which may help to explain the higher tolerance of At61 to AgNPs than the ecotype from clean stream.

Both forms of Ag can increase cell membrane permeability by progressive release of lipopolysaccharides and membrane proteins, leading to cell death (Amro et al 2000, Sondi and Salopek-Sondi 2004). In At61, all the proteins in cluster 5 were significantly stimulated by both Ag forms, mainly by AgNPs (Appendix 12); hence, the overrepresentation of fatty acids biosynthesis in cluster 5 might be recognized as a recovery mechanism for damaged membrane lipids (e.g. ergosterol; Gessner 2005) promoted by both forms of Ag. Sporulation of freshwater fungi is a sensitive endpoint to both Ag forms (Pradhan et al 2011, Batista et al 2017), potentially compromising the survival of fungi in streams. However, some studies reported an increase in fungal reproduction under low doses of AgNPs (Kasprowicz et al 2010, Tlili et al 2016). In our study, the overrepresentation of ascospore formation (Fig. 3.4C) can be envisaged as a survival strategy under the stress induced by both Ag forms considering that: i) ascospores have thick cell-walls, energy reserves and low metabolic rates (Moore-Landecker 2002) and ii) the production of asexual spores often decrease under stress conditions (Pradhan et al 2011, Batista et al 2017). Proteins likely to be involved in cell division process were stimulated in At61 under exposure to either form of Ag (cluster 3; Fig. 3.4C), corroborating the previous findings in bacteria exposed to AgNPs (Mirzajani et al 2014).

The process of cell redox homeostasis was also featured by GO enrichment analysis in At61 (cluster 5; Fig. 3.4C). This is crucial for the preservation of several cellular processes including responses to ROS, signalling and the removal of xenobiotics (Chiu and Dawes 2012, Ayer et al 2014). The contents of alkyl hydroperoxide reductase increased in At61 under exposure

to either form of Ag, supporting the role of peroxiredoxin activity as the first line of defense against peroxides (Ayer et al 2014). Cellular stress responses may vary according to the levels of ROS accumulation. The antioxidant systems that are triggered by accumulation of ROS can be repressed in the cells adapted to ROS (Temple et al 2005). The levels of proteins with antioxidant activities (*e.g.* superoxide dismutase) in At61 were higher under exposure to AgNPs compared to Ag⁺. A similar trend was observed for arylesterase, which reduces the oxidative stress by hydrolysing lipid peroxidases in oxidized lipoproteins (Aslan et al 2008). At61 also exhibited increased levels of glutathione synthetase under exposure to Ag⁺ and AgNPs, suggesting a crucial role of glutathione in maintaining cellular redox homeostasis (Schafer and Buettner 2001). Furthermore, in At61, the levels of glycerol-3-phosphate catabolism related proteins (*e.g.* glycerol-3-phosphate dehydrogenase) increased under exposure to both stressors, but protein levels were higher under AgNPs exposure. Apart from its involvement as a precursor in carbohydrate and lipid biosyntheses (Mugabo et al 2016), the glycerol-3-phosphate or its primary metabolites can also play a crucial role in stress responses as observed in plants and algae (Chanda et al 2008; Lai et al 2015). This suggests the higher efficiency of At61 to combat the oxidative stress induced by AgNPs that can be further supported by the correlation between the responses of antioxidant enzymes and related proteins (Fig. 3.5).

In At72, the most overrepresented process belonging to cluster 6 seemed to be associated with DNA repair. Indeed, RuvB-like helicase 1 and Casein kinase I homolog hhp2 are two proteins involved in DNA damage response (Dhillon and Hoekstra 1994; Peterson and Côté 2004); both of these proteins considerably increased under exposure to AgNPs, indicating DNA damage induced by AgNPs in At72. In At61, the biosynthesis of nucleosides triphosphate (NTPs) was also overrepresented (cluster 5; Fig. 3.4C); NTPs are the building blocks of DNA and RNA and are involved in energy supply to several cellular reactions. In At61, proteins related to the biosynthesis of NTPs including nucleoside diphosphate kinase (Ndk), an evolutionarily conserved and ubiquitously expressed protein involved in balancing cellular NTP-pools (Ray and Mathews 1992), increased under exposure to both Ag forms, particularly to AgNPs. This can also contribute to explain the greater tolerance of At61 to AgNPs than At72.

References

- Amro NA, Kotra LP, Wadu-Mesthrige K, Bulychev A, Mobashery S, Liu G. 2000. High-resolution atomic force microscopy studies of the *Escherichia coli* outer membrane: structural basis for permeability. *Langmuir*. 16: 2789-2796.
- Anjo SI, C Santa and B Manadas. 2014. Short GeLC-SWATH: a fast and reliable quantitative approach for proteomic screenings. *Proteomics*. 15: 757-62.
- Aslan M, Nazligul Y, Horoz M, Bolukbas C, Bolukbas FF, Gur M, Celik H, Erel O. 2008. Serum paraoxonase-1 activity in *Helicobacter pylori* infected subjects. *Atherosclerosis*. 196: 270-274.
- Ayer A, Gourlay CW and Dawes IW. 2014. Cellular redox homeostasis, reactive oxygen species and replicative ageing in *Saccharomyces cerevisiae*. *FEMS YeastRes*. 14: 60-72.
- Azevedo MM, Almeida B, Ludovico P, Cássio F. 2009. Metal stress induces programmed cell death in aquatic fungi. *Aquat Toxicol*. 92: 264-270.
- Bai Z, Harvey LM and McNeil B. 2003. Oxidative stress in submerged cultures of fungi. *Crit. Rev. Biotechnol*. 23: 267-302.
- Barros D, Pradhan A, Mendes VM, Manadas B, Santos PM, Pascoal C, Cássio F. 2019. Proteomics and antioxidant enzymes reveal different mechanisms of toxicity induced by ionic and nanoparticulate silver in bacteria. *Environ Sci Nano*. DOI: 10.1039/c8en01067f.
- Batista D, Pascoal C, Cássio F. 2017. Temperature modulates AgNP impacts on microbial decomposer activity. *Sci. Total Environ*. 601-602: 1324-1332.
- Behra R, Sigg L, Clift MJ, Herzog F, Minghetti M, Johnston B, Petri-Fink A, Rothen-Rutishauser B. 2013. Bioavailability of silver nanoparticles and ions: from a chemical and biochemical perspective. *J R Soc Interface*. 10(87): 20130396.
- Blaser SA, Scheringer M, MacLeod M, Hungerbühler K. 2008. Estimation of cumulative aquatic exposure and risk due to silver: contribution of nano-functionalized plastics and textiles. *Sci Total Environ*. 390: 396-409.
- Bouatra S, Aziat E, Mandal R, Guo AC, Wilson MR, Knox C, Bjorn Dahl TC, Krishnamurthy R, Saleem F, Liu P, Dame ZT, Poelzer J, Huynh J, Yallou FS, Psychogios N, Dong E, Bogumil R, Roehring C, Wishart DS. 2013. The human urine metabolome. *PloS One*. 8: e73076.
- Boxall, ABA. 2012. New and emerging water pollutants arising from agriculture. Paris, OECD (Organisation for Economic Co-Operation and Development). <https://www.oecd.org/tad/sustainable-agriculture/49848768.pdf>
- Braun RJ, Zischka H, Madeo F, Eisenberg T, Wissing S, Buttner S, Engelhardt SM, Buringer D, Ueffing M. 2006. Crucial mitochondrial impairment upon *CDC48* mutation in apoptotic yeast. *J Biol Chem*. 281: 25757-25767.
- Casadevall A, Nosanchuk JD, Williamson P, Rodrigues ML. 2009. Vesicular transport across the fungal cell wall. *Trends Microbiol*. 17: 158-162.
- Chanda B, Venugopal SC, Kulshrestha S, Navarre DA, Downie B, Vaillancourt L, Kachroo A, Kachroo P. 2008. Glycerol-3-phosphate levels are associated with basal resistance to the hemibiotrophic fungus *Colletotrichum higginsianum* in *Arabidopsis*. *Plant Physiol*. 147: 2017-2029.
- Chiu J and Dawes IW. 2012. Redox control of cell proliferation. *Trends Cell Biol*. 22: 592-601.
- Clairborne A. 1985. Catalase activity. In: Greenwald, R.A. (Ed.), *CRC Handbook of Methods in Oxygen Radical Research*. CRC Press, Boca Raton, FL.

- Collins BC, Gillet LC, Rosenberger G, Röst HL, Vichalkovski A, Gstaiger M, Aebersold R. 2013. Quantifying protein interaction dynamics by SWATH mass spectrometry: application to the 14-3-3 system. *Nat. Methods*. 10: 1246-53.
- Dhillon N and Hoekstra MF. 1994. Characterization of two protein kinases from *Schizosaccharomyces pombe* involved in the regulation of DNA repair. *EMBO J*. 13: 2777-2788.
- Dorjnamjin D, Ariunaa M and Shim YK. 2008. Synthesis of silver nanoparticles using hydroxyl functionalized ionic liquids and their antimicrobial activity. *Int J Mol Sci*. 9: 807-819.
- European Commission. 2012. Commission staff working paper. Types and uses of nanomaterials, including safety aspects. Accompanying the Communication from the Commission to the European Parliament, The Council and the European Economic and Social Committee on the Second Regulatory Review on Nanomaterials.
- Fernandes I, Seena S, Pascoal C, Cássio F. 2014. Elevated temperature may intensify the positive effects of nutrients on microbial decomposition in streams. *Freshwater Biol*. 59: 2390-2399.
- Flohé L and Günzler WA. 1984. Assays of glutathione peroxidase. *Methods Enzymol*. 105: 114-121.
- Gessner MO. 2005. Ergosterol as a measure of fungal biomass. In Graça MAS, Bärlocher F, Gessner MO (Eds) *Methods to study litter decomposition: a practical guide*, Springer, Dordrecht, The Netherlands, pp 171-176.
- Gottschalk F, Kost E, Nowack B. 2013. Engineered nanomaterials in water and soils: a risk quantification based on probabilistic exposure and effect modeling. *Environ Toxicol Chem*. 32(6): 1278-1287.
- Guimarães-Soares L, Pascoal C, Cássio F. 2007. Effects of heavy metals on the production of thiol compounds by the aquatic fungi *Fontanospora fusiformis* and *Flagellospora curta*. *Ecotoxicol Environ Saf*. 66: 36-43.
- Habi S and Daba H. 2009. Plasmid Incidence, Antibiotic and Metal Resistance among Enterobacteriaceae Isolated from Algerian Streams. *Pak J Biol Sci*. 12: 1474-1482.
- Habig WH, Pabst MJ, Jakoby WB. 1974. Glutathione S-transferases – first enzymatic step in mercapturic acid formation. *J. Biol. Chem*. 249: 7130-7139.
- Hammer Ø, Harper DAT, Ryan PD. 2001. PAST: paleontological statistics software package for education and data analysis. *Palaeontol. Electron*. 4 (1): 9pp.
- He D, Dorantes-Aranda JJ and Waite TD. 2012. Silver Nanoparticle-Algae Interactions: Oxidative Dissolution, Reactive Oxygen Species Generation and Synergistic Toxic Effects. *Environ. Sci. Technol*. 46: 8731-8738.
- Huang GY, Wang YS, Sun CC, Dong JD, Sun ZX. 2010. The effect of multiple heavy metals on ascorbate, glutathione and related enzymes in two mangrove plant seedlings (*Kandelia candel* and *Bruguiera gymnorrhiza*). *Oceanol. Hydrobiol. Stud*. 39: 11-25.
- Jo HJ, Choi JW, Lee SH, Hong SW. 2012. Acute toxicity of Ag and CuO nanoparticle suspensions against *Daphnia magna*: the importance of their dissolved fraction varying with preparation methods. *J Hazard Mater*. 227-228: 301-308.
- Kaegi R, Sinnet B, Zuleeg S, Hagendorfer H, Mueller E, Vonbank R, Boller M, Burkhardt M. 2010. Release of silver nanoparticles from outdoor facades. *Environmental Pollution* 158: 2900-2905.
- Kang JS, Bong J, Choi J-S, Henry TB, Park J-W. 2016. Differentially transcriptional regulation on cell cycle pathway by silver nanoparticles from ionic silver in larval zebrafish (*Danio rerio*). *Biochem Biophys Res Commun*. 479: 753-758.

- Kasprowicz MJ, Koziol M and Gorczyca A. 2010. The effect of silver nanoparticles on phytopathogenic spores of *Fusarium culmorum*. *Can J Microbiol.* 56: 247-253.
- Kültz D. 2005. Molecular and evolutionary basis of the cellular stress response. *Annu. Rev. Physiol.* 67: 225-257.
- Kumar L and Futschik ME. 2007. Mfuzz: a software package for soft clustering of microarray data. *Bioinformatics.* 2: 5-7.
- Kvitek L, Panacek A, Soukupova J, Kolar M, Vecerova R, Pucek R, Holecova M, Zboril R. 2008. Effect of surfactants and polymerson stability and antibacterial activity of silver nanoparticles (NPs). *J Phys Chem C.* 112: 5825-5834.
- Lai XJ, Yang R, Luo QJ, Chen JJ, Chen HM, Yan XJ. 2015. Glycerol-3-phosphatemetabolism plays a role in stress response in red alga *Pyropia haitanensis*. *J Phycol.* 51: 321-331.
- Lemus L and Goder V. 2014. Regulation of endoplasmic reticulum-associated protein degradation (ERAD) by ubiquitin. *Cells.* 3: 824-847.
- Liu HH, Cohen Y. 2014. Multimedia environmental distribution of engineered nanomaterials. *Environ Sci Technol.* 48(6):3281-3292.
- Lledías F, Rangel P and Hansberg W. 1998. Oxidation of catalase by singlet oxygen. *J Biol Chem.* 273: 10630-10637.
- Lubrano V and Balzan S. 2015. Enzymatic antioxidant system in vascular inflammation and coronary artery disease. *World J Exp Med.* 5: 218-224.
- Marambio-Jones C, Hoek EMV. 2010. A review of the antibacterial effects of silver nanomaterials and the potential implications for human health and the environment. *J Nanoparticle Research* 12: 1531-1551.
- Miethling-Graff R, Rumpker R, Richter M, Verano-Braga T, Kjeldsen F, Brewer J, Hoyland J, Rubahn HG, Erdmann H. 2014. Exposure to silver nanoparticles induces size- and dose-dependent oxidative stress and cytotoxicity in human colon carcinoma cells. *Toxicol In Vitro.* 28: 1280-1289.
- Minden JS. 2012. Two-dimensional difference gel electrophoresis. *Methods Mol. Biol.* 869: 287-304.
- Mirzajani F, Askari H, Hamzelou S, Schober Y, Römpf A, Ghassempour A, Spengler B. 2014. Proteomics study of silver nanoparticles toxicity on *Bacillus thuringiensis*. *Ecotoxicol and Environ Safety.* 100: 122-130.
- Moore-Landecker E. 2002. Fungal Spores. In: *Encyclopedia of life sciences (eLS)*. John Wiley & Sons Ltd, Chichester.
- Mugabo Y, Zhao S, Seifried A, Gezzar S, Al-Mass A, Zhang D, Lamontagne J, Attane C, Poursharifi P, Iglesias J, Joly E, Peyot ML, Gohla A, Madiraju SRM, Prentki, M. 2016. Identification of a mammalian glycerol-3-phosphate phosphatase: Role in metabolism and signaling in pancreatic β -cells and hepatocytes. *Proc Natl Acad Sci USA.* 113: E430-E439.
- Mueller NC, Nowack B. 2008. Exposure modeling of engineered nanoparticles in the environment. *Environ Sci Technol.* 42: 4447-4453.
- Nair PMG and Chung I-M. 2014. Cell cycle and mismatch repair genes as potential biomarkers in *Arabidopsis thaliana* seedlings exposed to silver nanoparticles. *Bull Environ Contam Toxicol.* 92: 719-725.
- Navarro E, Piccapietra F, Wagner B, Marconi F, Kaegi R, OdzakN, Sigg L, Behra R. 2008. Toxicity of silver nanoparticles to *Chlamydomonas reinhardtii*. *Environ Sci Technol.* 42: 8959-8964.

- OECD. 2014. Ecotoxicology and environmental fate of manufactured nanomaterials: test guidelines. Series on the Safety of Manufactured Nanomaterials. No. 40, ENV/JM/MONO Organisation for Economic Co-operation and Development, Paris.
- Pascoal C, Cássio F, Marcotegui BS, Gomes P. 2005a. Role of fungi, bacteria, and invertebrates in leaf litter breakdown in a polluted river. *J N Am Benthol Soc.* 24: 784-797.
- Pascoal C, Marvanová L, Cássio F. 2005b. Aquatic hyphomycete diversity in streams of Northwest Portugal. *Fung. Divers.* 19: 109-128.
- Peterson GL. 1983. Determination of total protein. *Meth. Enzymol.* 91: 95-121.
- Peterson CL and Côté J. 2004. Cellular machineries for chromosomal DNA repair. *Genes Dev.* 18: 602-616.
- Petrak J, Ivanek R, Toman O, Cmejla R, Cmejlova J, Vyoral D, Zivny J, Vulpe CD. 2008. Deja vu in proteomics. A hit parade of repeatedly identified differentially expressed proteins. *Proteomics.* 8: 1744-1749.
- Poynton HC, Lazorchak JM, Impellitteri CA, Blalock BJ, Rogers K, Allen HJ, Loguinov A, Govindaswamy S. 2012. Toxicogenomic responses of nanotoxicity in *Daphnia magna* exposed to silver nitrate and coated silver nanoparticles. *Environ Sci Technol.* 46: 6288-6296.
- Pradhan A, Seena S, Pascoal C, Cássio F. 2011. Can metal nanoparticles be a threat to microbial decomposers of plant litter in streams? *Microb. Ecol.* 62: 58-68.
- Pradhan A, Seena S, Schlosser D, Gerth K, Helm S, Dobritsch M, Krauss G-J, Dobritsch D, Pascoal C, Cássio F. 2015. Fungi from metal-polluted streams may have high ability to cope with the oxidative stress induced by copper oxide nanoparticles. *Environ Toxicol Chem.* 34: 923-930.
- Pradhan A, Silva CO, Silva C, Pascoal C, Cássio F. 2016. Enzymatic biomarkers can portray nanoCuO-induced oxidative and neuronal stress in freshwater shredders. *Aquat Toxicol.* 180: 227-235.
- Ray NB and Mathews CK. 1992. Nucleoside diphosphokinase: a functional link between intermediary metabolism and nucleic acid synthesis. *Curr Top Cell Regul.* 33: 343-357.
- Rigbolt KT, Vanselow JT and Blagoev B. 2011. GProX, a user-friendly platform for bioinformatics analysis and visualization of quantitative proteomics data. *Mol Cell Proteomics.* 10: O110-007450.
- Salata OV. 2004. Applications of nanoparticles in biology and medicine. *J Nanobiotechnol.* 2 (6 pp)
- Schafer FQ and Buettner GR. 2001. Redox environment of the cell as viewed through the redox state of the glutathione disulfide/glutathione couple. *Free Radic Biol Med.* 30:1191-1212.
- Sirikantaramas S, Yamazaki M and Saito K. 2008. Mechanisms of resistance to self-produced toxic secondary metabolites in plants. *Phytochem Rev.* 7: 467-477.
- Soares HMVM, Boaventura RAR, Machado AASC, Esteves da Silva JCG. 1999. Sediments as monitors of heavy metal contamination in the Ave river basin (Portugal): multivariate analysis of data. *Environ. Pollut.* 105: 311-323.
- Sondi I and Salopek-Sondi B. 2004. Silver nanoparticles as antimicrobial agent: a case study on *E. coli* as a model for Gram-negative bacteria. *J Colloid Interface Sci.* 275:177-182.
- Temple MD, Perrone GG and Dawes IW. 2005. Complex cellular responses to reactive oxygen species. *Trends Cell. Biol.* 15: 319-326.
- Tiede K, Boxall ABA, Wang X, Gore D, Tiede D, Baxter M, David H, Tear SP and Lewis J. 2010. Application of hydrodynamic chromatography-ICP-MS to investigate the fate of silver nanoparticles in activated sludge, *J Anal At Spectrom.* 25: 1149-1154.
- Tlili A, Cornut J, Behra R, Gil-Allué C, Gessner MO. 2016. Harmful effects of silver nanoparticles on a complex detrital model system. *Nanotoxicology.* 10: 728-735.

- van Aerle R, Lange A, Moorhouse A, Paszkiewicz K, Ball K, Johnston BD, de-Bastos E, Booth T, Tyler CR, Santos EM. 2013. Molecular Mechanisms of Toxicity of Silver Nanoparticles in Zebrafish Embryos. *Environ. Sci. Technol.* 47: 8005-8014.
- Wang P, Bouwman FG and Mariman EC. 2009. Generally detected proteins in comparative proteomics - A matter of cellular stress response? *Proteomics.* 9: 2955-2966.
- Yuan Z, Li J, Cui L, Xu B, Zhang H, Yu CP. 2013. Interaction of silver nanoparticles with pure nitrifying bacteria. *Chemosphere* 90: 1404-1411.
- Zhang F, Wu X, Chen Y and Lin H. 2009. Application of silver nanoparticles to cotton fabric as an antibacterial textile finish. *Fibers Polym.* 10: 496-50.
- Zhu JY, Huang HQ, Bao XD, Lin QM, Cai ZW. 2006. Acute toxicity profile of cadmium revealed by proteomics in brain tissue of *Paralichthys olivaceus*: potential role of transferrin in cadmium toxicity. *AquatToxicol.* 78: 127-135.
- Zolgharnein H, Karami K, Assadi MM, Sohrab AD. 2010. Investigation of Heavy Metals Biosorption on *Pseudomonas aeruginosa* Strain MCCB 102 Isolated from the Persian Gulf. *Asian J. Biotechnol.* 2: 99-109.

Chapter 4

Transcriptomics reveal different mechanisms of toxicity to nanoparticulate and ionic silver in aquatic fungi

Abstract

The mechanisms of toxicity of silver nanoparticles (AgNPs) are not clear, and the role of Ag^+ released from the nanoparticulated form in the overall toxicity requires further attention. With the advance of omics, new avenues are open to explore specific responses to stressors. In this study, we assessed whole transcriptome alterations in a worldwide aquatic fungal species to understand the toxicity of AgNPs and Ag^+ . A total of 1056 genes were differentially expressed: 448 were up-regulated and 84 were down-regulated upon exposure to Ag^+ , and 258 genes were up-regulated and 162 were down-regulated upon exposure to AgNPs. The major cellular component likely to be affected by both silver forms was the membrane. However, differential expression patterns suggested different mechanisms of action of Ag^+ and AgNPs. GO-based biological processes indicated that AgNPs promoted the up-regulation of genes involved in the transport, nucleobase metabolism and generation of energy, while genes associated with redox and carbohydrate metabolism were down-regulated. In contrast, Ag^+ led to the up-regulation of genes involved in carbohydrate and steroid metabolism, whereas genes involved in localization and transport were down-regulated. Our results showed, for the first time, distinct profiles of gene expression in fungi exposed to Ag^+ and AgNPs, supporting different modes of toxicity for each form of silver.

Key words: AgNPs and Ag^+ , high-throughput RNA sequencing, aquatic fungus, ecotoxicity.

4.1. Introduction

Aquatic hyphomycetes are a group of phylogenetically heterogeneous fungi that are the key microbial decomposers of plant litter in freshwater ecosystems worldwide (Bärlocher 2005, Shearer et al 2007). The adaptations of these fungi to aquatic environments include their ability to produce extracellular enzymes for the degradation of recalcitrant polymers of plant cell walls, the capacity to remain active, grow and reproduce at relatively low temperatures and the efficient conidial attachment to substrata (Suberkropp 1998). However, the activity of aquatic hyphomycetes as decomposers depends on several factors, such as the physicochemical properties of stream water (Dangles et al 2004, Duarte et al 2009), the riparian vegetation (Fernandes et al 2013) and the presence of stressors (Duarte et al 2008, Pradhan et al 2011, Tlili et al 2016). Because aquatic hyphomycetes are at the bottom of the detrital food webs, alterations in its physiology may affect the associated ecological functions with potential implications to ecosystem services in freshwaters.

Over the last few years, metal nanoparticles (MNPs) have raised concern for aquatic ecosystems as emerging chemical contaminants. MNPs are non-biodegradable, hence they persist in the environment and can accumulate into organisms leading to biomagnification along food webs. In addition, MNPs have unique inherent properties due to their high surface-to-volume ratio resulting in high surface reactivity. Silver nanoparticles (AgNPs) are currently among the most widespread MNPs due to the antimicrobial properties of silver (Swathy et al 2014). AgNPs exhibit toxicity to several freshwater organisms, including bacteria and fungi involved in plant litter decomposition (Pradhan et al 2011, Tlili et al 2016). Although the mode of AgNPs toxicity is still unclear, some studies reported that toxicity can be related to the release of Ag ions from nanoparticles (Navarro et al 2008, Jo et al 2012) or to the nanoparticle itself (Poynton et al 2012). Molecular markers may be useful in differentiating the effects of each form of silver. Unlike the classical endpoints (growth, reproduction or survival) used to assess the impacts of contaminants, omics can be a useful approach for monitoring subtle changes in organisms related to toxicity or adaptive responses (Lemos et al 2010, Van Aggelen et al 2010, Schirmer et al 2010). Because omics can screen alterations in biological pathways at genome-level, they can be helpful to ascertain the mechanisms underlying the effects of environmental stressors.

High-throughput RNA sequencing (RNA-seq) is a powerful tool for transcriptome profiling that provides a precise quantitative measurement of the transcript levels (Wang et al 2009, Lowe et al 2017), and it has been employed even in non-model organisms whose reference genome is not available (Grabherr et al 2011).

In this study, we assessed the effects of AgNPs and Ag⁺ on gene expression profiles by transcriptomic analyses aiming to provide mechanistic insights into the AgNP toxicity in aquatic hyphomycetes. We hypothesized that i) the toxicity induced by AgNPs would be due to the nanoparticle itself and independent of the release of Ag⁺ from nanoparticles; ii) the transcriptomic profiles would allow us to identify specific modes of action of AgNPs; and iii) the responses of cells to AgNPs and Ag⁺ would be different.

4.2. Materials and methods

4.2.1. Preparation of AgNPs

Citrate-coated AgNPs (~20 nm, 1 g L⁻¹) were purchased from NanoSys GmbH (Wolfhalden, Switzerland) and the stock suspension was prepared in filtered (0.2- μ m pore-size membrane; Millipore, Billerica, MA) ultrapure water (Milli-Q, 18.2 M Ω -cm) and stored in the dark. The stock solution of AgNO₃ (AgNO₃, >99%; Sigma) was prepared by suspending the powder in autoclaved (121°C, 20 min) ultrapure water.

4.2.2. Fungal growth

The aquatic fungal strain, *Articulospora tetracladia* UMB-072.01 (At72), was isolated from foam in Maceira stream, a non-polluted stream at Peneda-Gerês National Park, Portugal (Pascoal et al 2005 for details about the sampling site). The strain was maintained on malt extract agar (MEA; malt extract 1% w/v, agar, 1% w/v).

For assessing the transcriptomic responses of At72 to AgNPs and Ag⁺, mycelia were exposed to concentrations inhibiting 20% (EC₂₀) of biomass production (EC₂₀ of AgNPs: 7.5 μ g L⁻¹; EC₂₀ of Ag⁺: 117.4 μ g L⁻¹) in triplicates. One agar plug (5-mm diameter, 5-mm depth; MEA) of 20 day-old culture was homogenized (Ultraturrax, IKA, Staufen, Germany) in 1 mL sterile liquid malt extract medium (ME 1%), and 1 mL of the fungal homogenate was transferred aseptically to 250-mL Erlenmeyer flasks containing 100 mL of sterile ME 1%. The flasks were kept under shaking (140 rpm) at 18°C, and after 48h of fungal growth the

stressors were added. The flasks containing growing fungal cultures were incubated for additional 3 days (to reach mid-exponential growth phase).

4.2.3. RNA extraction

Samples for RNA extraction were collected by centrifugation (5000 × g for 5 min at 4°C), kept in cooled RNA later (Sigma-Aldrich) and stored at 4°C until used for RNA extraction.

Total RNA samples were obtained using the RNA/DNA purification kit (Norgen Biotek Corp, Thorold, Canada) according to the manufacturer's protocol, except the lysis that was conducted in the FastPrep FP120 (velocity 5.5, duration 10''; Qbiogene, Heidelberg, Germany). This step was done in lysing matrix E 2 mL tubes (MP Biomedicals, Solon OH, USA) containing 300 µL of lysis buffer SK. RNA samples were quantified with a NanoDrop™ 1000 Spectrophotometer (Thermo Scientific, Lisbon, Portugal). For extraction of RNA, RNase-free disposable plasticware was used. All glassware, solutions and ultrapure water for RNA extraction were treated with 0.1 % diethylpyrocarbonate (DEPC) overnight at 37°C and autoclaved (121°C, 60 min) to inactivate DEPC, and nondisposable plasticware were cleaned with RNaseZap® Solution (Ambion).

4.2.4. Library preparation and sequencing

The integrity of the extracted RNA was verified (Agilent 2100 Bioanalyzer) and only samples with RNA Integrity Number (RIN) over 8.0 were used in RNA-seq. The RNA library for transcriptome sequencing was prepared from high quality mRNA with the Truseq RNA Library Prep Kit V2 (Illumina, San Diego, USA) and sequenced using paired-end 2x150 bp on the HiSeq 4000® Illumina® platform at BGI (Hong Kong). All procedures were performed according to standard manufacturer's protocols.

4.2.5. Transcriptome assembly and annotation

The sequenced reads were quality-filtered with Trimmomatic version 0.30 (Bolger et al 2014) using the following parameters: i) bases with average quality lower than Q25 in a window of 5 bases were trimmed, and ii) reads with less than 100 bases were discarded. Reads were checked for rRNA using ribopicker version 0.4.3 (Schmieder et al 2012). High quality reads were assembled with Trinity, version 2.2.0 (Haas et al 2013) using the default parameters. Read-counts and normalised expression values in Fragments Per Kilobase

Million (FPKM) units were obtained using RSEM version 1.2.11 (Li and Dewey 2011). The expression values were then applied to evaluate the biological replicates using a correlation matrix and to perform differential expression analysis using edgeR package (Robinson et al 2010). Transcript annotation was performed with Trinotate version 3.1.1 (<http://trinotate.github.io>). Transcript sequences, expression values and differential expression analysis were organized on a web platform based on the TrinotateWeb platform.

Differentially expressed genes were clustered using hierarchical clustering method to retrieve expression profiles. Results of gene expression (FPKM) were reported as centered log₂ (FPKM +1). For each expression profile, goseq software (Young et al. 2012) was used to perform gene ontology (GO) enrichment analysis. Furthermore, goseq was also used to perform enrichment on the differentially expressed genes between tested conditions.

4.3. Results and discussion

4.3.1. Transcriptome sequencing and assembly

In our study, a total of 9 cDNA libraries were constructed from the total RNA of the aquatic fungus *A. tetracladia*, unexposed or exposed to Ag⁺ or AgNPs at EC₂₀ of fungal growth. Illumina HiSeq-based sequencing of these libraries resulted in a total reads of i) 52,114,634; 39,831,882 and 28,135,965 for controls, ii) 38,534,012; 40,169,209 and 44,530,178 for treatments with Ag⁺, and iii) 38,760,656; 37,031,764 and 46,290,763 for treatments with AgNPs (Appendix 13). RNA-seq is an effective technology for quantification of the expression levels of transcripts under different conditions (Jiang et al 2016, Zhu et al 2018). Due to the lack of reference genomic sequences for *A. tetracladia*, the transcripts were constructed using *de novo* assembly based on Trinity, which has shown high efficiency in *de novo* reconstruction of transcripts (Haas et al 2013). A total of 81,521 transcripts were obtained belonging to 73,445 genes, which sequencing, filtering and rRNA reads metrics are in Table S4.1 (Appendix 13). The total number of assembled bases was 94,408,678, the average contig length was 1158.09 bp and the N50 length was 3406 bp. The G+C content found for the Ascomycota *A. tetracladia* was 48.79%, which agrees with that reported for Ascomycetes (Storck and Alexopoulos 1970, Shearer et al 2007).

4.3.2. Transcriptional responses to AgNPs and Ag⁺

To explore the mode of action of AgNPs and Ag⁺ on fungi, the transcriptional profiles in the absence and presence of Ag⁺ or AgNPs at EC₂₀ of growth (117.4 µg L⁻¹ for Ag⁺ and 7.5 µg L⁻¹ for AgNPs) were examined. Because the genome of *A. tetracladia* is not sequenced, other organisms were considered for the identification and prediction of functional characterization of genes. Exposure of *A. tetracladia* to AgNPs or Ag⁺ resulted in a total of 1056 differentially expressed genes (false discovery rate < 0.05). Moreover, a distinct expression profile between the treatments (AgNPs, Ag⁺ and control) was observed suggesting different action mechanisms for each silver form (Fig. 4.1).

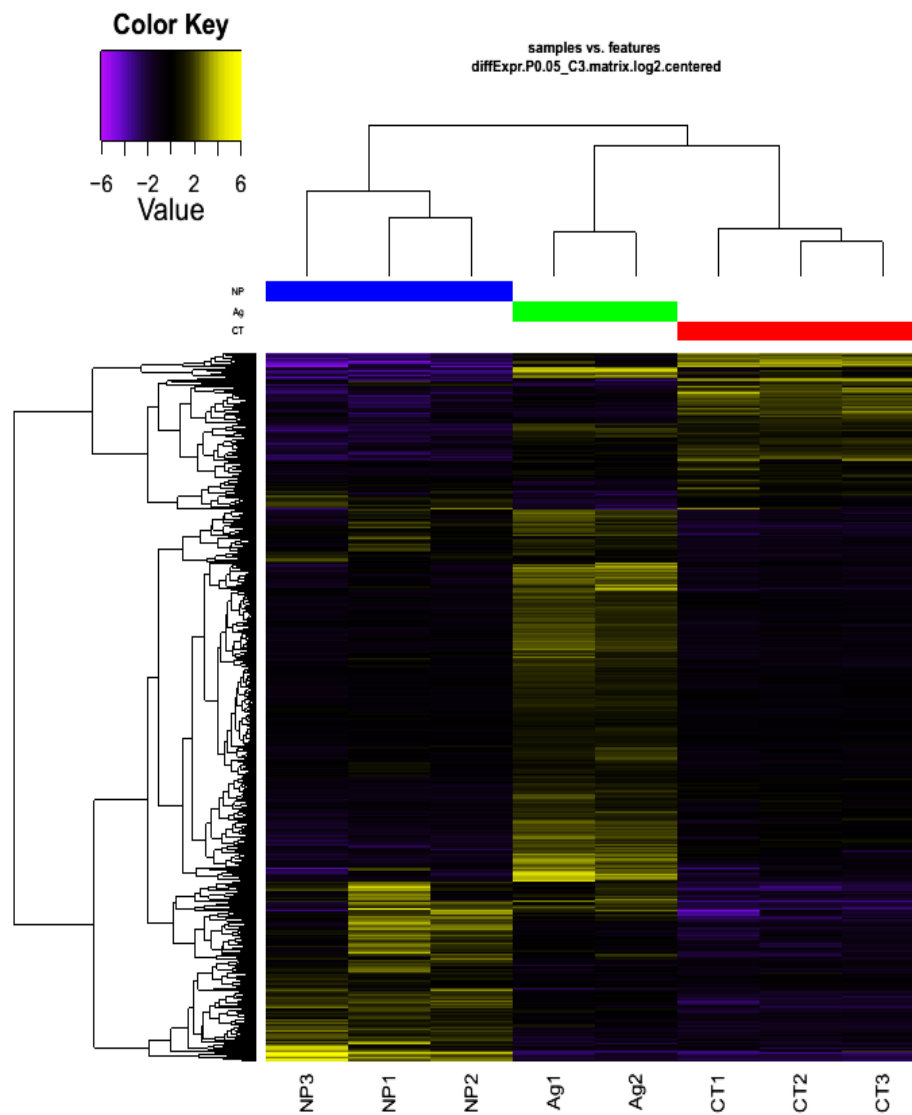
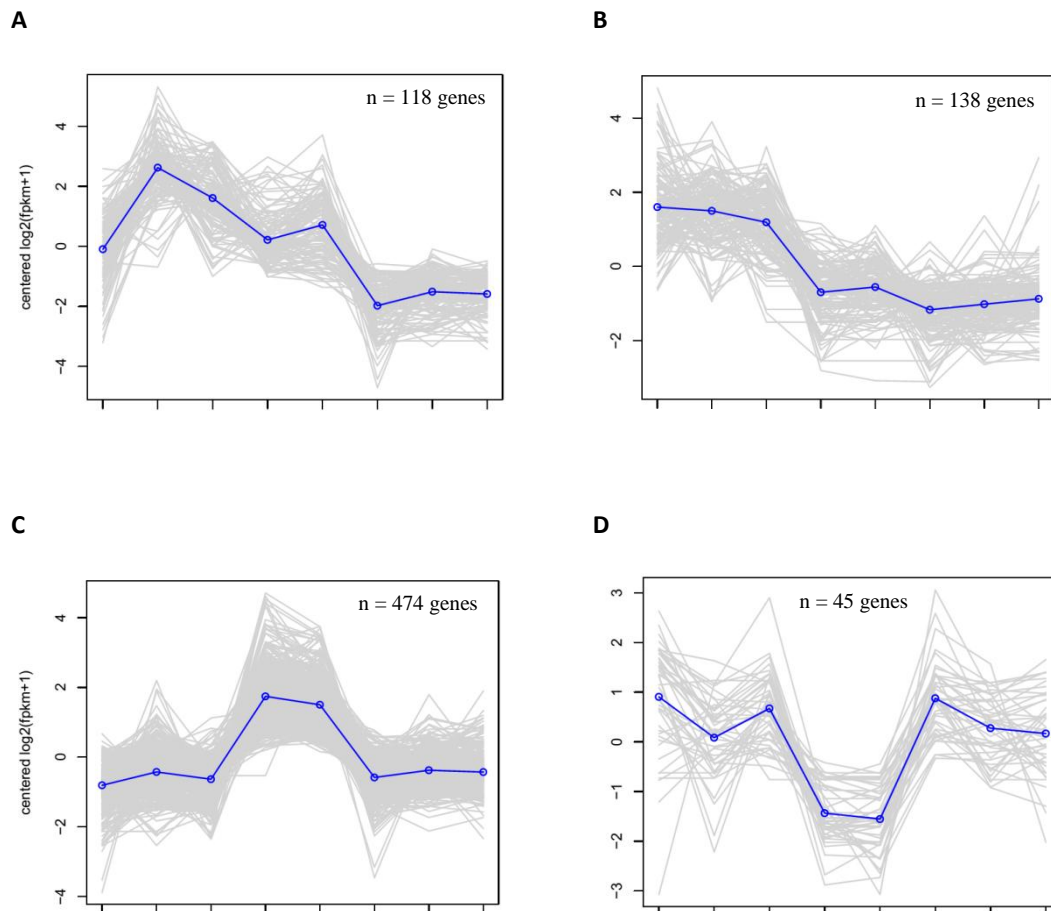


Figure 4.1 Differential gene expression profile of control (CT) versus Ag⁺ and AgNPs. N = 1056 genes.

Of the 1056 differentially expressed genes, 532 genes ($\approx 50\%$; 448 up- and 84 down-regulated) were expressed upon exposure to Ag^+ and 420 genes ($\approx 40\%$; 258 up- and 162 down-regulated) were expressed upon exposure to AgNPs. On the other hand, after comparing both treatments, 533 genes were differentially expressed ($\approx 50\%$ of total), of which 415 and 118 genes were up-regulated upon exposure to Ag^+ and AgNPs, respectively.

Hierarchical clustering analysis grouped the genes with similar expression profiles in 10 patterns of expression (Fig. 4.2A-J, see Appendix 14 for cluster description).



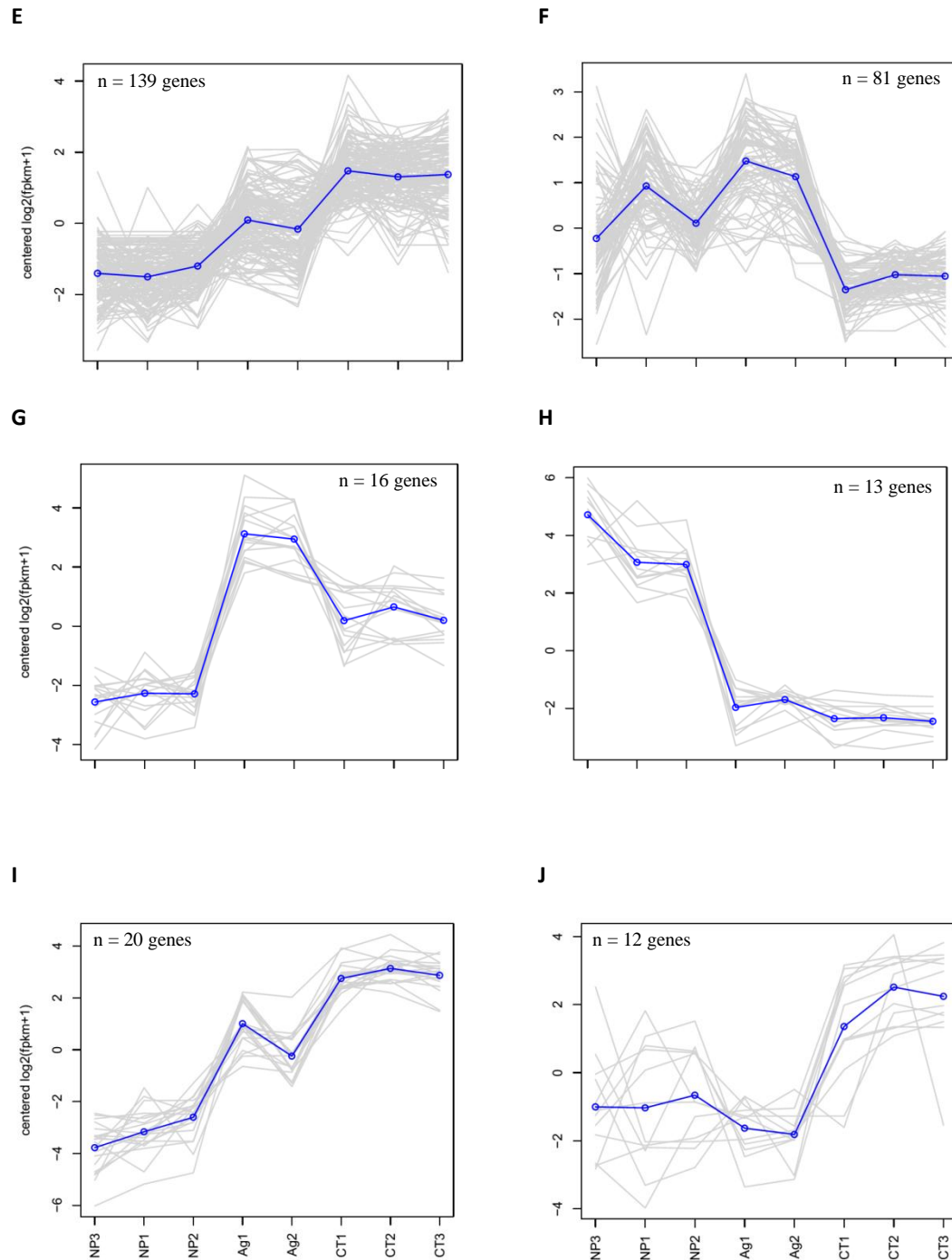


Figure 4.2 Clusters (A to J) of differential expressed genes in the different experimental conditions (Control: CT; Ag⁺: Ag; AgNPs: NP). The average expressions of clustered genes are presented in blue lines. N = 1056 genes.

Differentially expressed genes were further organized into three categories, namely cellular component, biological process and molecular function based on closely related protein homologues as predicted by GO terms. A total of 183 GO terms were attributed to

differentially expressed genes of which 73 were related to biological processes, 25 to cellular components and 85 to molecular functions (Appendix 15). A heatmap analysis was performed according to the enrichment of GO terms which included 347 differentially expressed genes and 139 GO terms; the analysis revealed different patterns of gene expression, reiterating different mechanisms of action of AgNPs and Ag⁺ in the fungus (Appendix 16).

The analysis of the most frequent biological processes and cellular components associated with differentially expressed genes upon exposure to Ag⁺ (Fig. 4.3A) or AgNPs (Fig. 4.3B) provided further insight into the putative mechanisms of action of each form of silver.

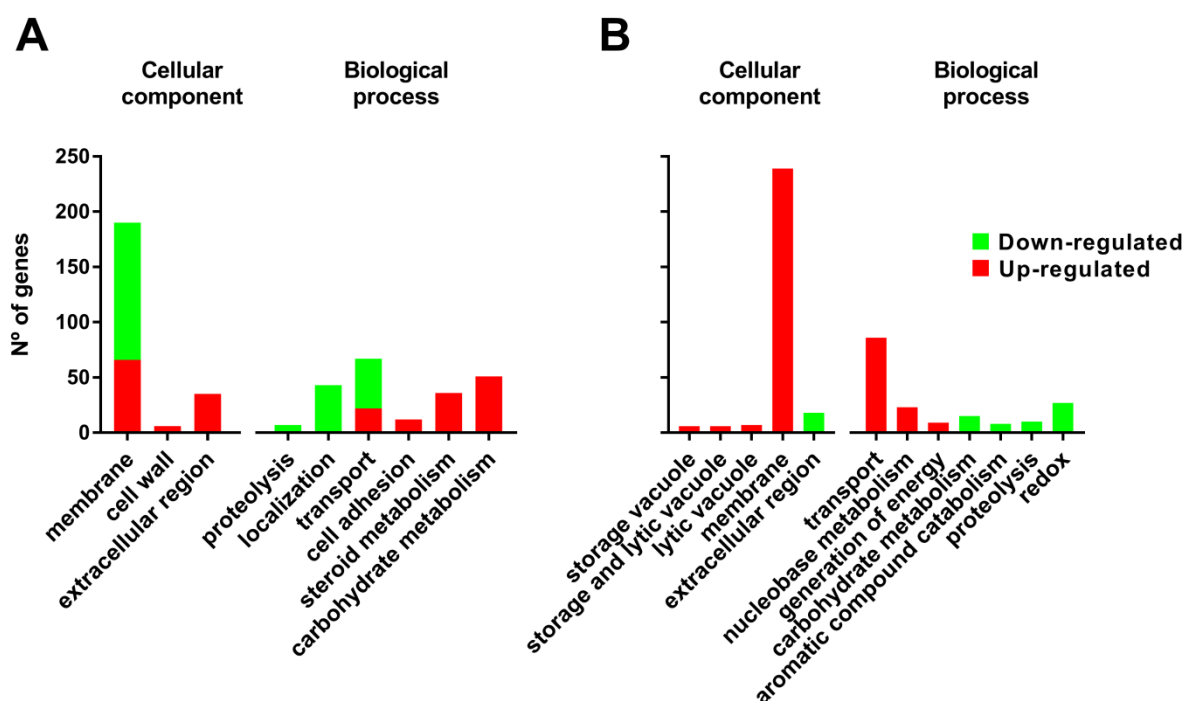


Figure 4.3 Histograms of gene ontology (GO) classification. The results are summarized in two main categories: cellular component and biological process. The y-axis indicates the number of genes in a category and the x-axis indicates the subcategories. A) corresponds to Ag⁺ vs Ct, B) corresponds to AgNPs vs Ct. Up-regulation and down-regulation are indicated by red and green, respectively. Only the GO terms with more than 5 genes were considered.

Indeed, the major GO-based term under cellular component category was the membrane, because the expression of related genes was affected by both forms of silver (Fig. 4.3A and 4.3B). Effects of AgNP exposure on membrane were clear since all 239 related genes were up-regulated (Fig. 4.3B). Particularly, annotations regarding the membrane comprised the

genes related to intrinsic component (67 genes, GO:0031224; 14 genes, GO:0031224), integral component (62 genes, GO:0016021; 14 genes, GO:0016021) and other membrane parts (68 genes, GO:0044425; 14 genes, GO:0044459). This suggests that AgNPs affected the plasma membrane including all the components consisting of the protein complexes having at least some part of their peptides embedded in the hydrophobic region of plasma membrane, as well as the constituents (e.g. phospholipids and proteins) of other lipid bilayer membranes of organelles. The effects of Ag⁺ on membranes were different since related genes were down- (124 genes) and up-regulated (66 genes; Fig. 4.3A). Moreover, the up-regulated genes were likely to be associated with the plasma membranes only, while the down-regulated genes were likely to be associated with all type of cellular membranes. This suggests that cellular membranes and their intrinsic or integral components can be the major targets of both silver forms. However, the effects of AgNPs appeared to be more severe because the GO term membrane was overrepresented only under AgNP-exposure compared to Ag⁺ exposure (Appendix 17).

The extracellular region (GO:0005576) consisting of gene products that are not attached to the cell surface was affected differently by the silver form, since 35 genes were up-regulated upon exposure to Ag⁺ (Fig. 4.3A), while 18 genes were down-regulated upon AgNP-exposure (Fig. 4.3B). Also, the GO term extracellular region was only overrepresentative of Ag⁺ exposure (Appendix 17), suggesting that effects of ionic form of silver on the outer surface of fungal mycelia were stronger than the effects of AgNPs which can be related to the ability of fungi to control the entering of ions. This is consistent with the reported ion extracellular sequestration by the cell wall through exopolysaccharides and other extracellular metabolites (Fomina et al 2005, Van Acker et al 2014). The fungal cell wall (GO:0009277), consisting of extensively cross-linked glycoproteins and carbohydrates, is a rigid hitherto dynamic structure surrounding the plasma membrane that offers protection from stressors and contributes to cell morphogenesis (Walker and White 2005, Gow et al 2017). Exposure to Ag⁺ increased the expression of 6 genes related to the cell wall (Fig. 4.3A). On the other hand, the exposure to AgNPs also up-regulated 19 genes related to storage and lytic vacuole (6 genes with GO:0000322, 6 genes with GO:0000324 and 7 genes with GO:0000323). Fungal vacuoles can function as reservoirs for the storage of materials (including nutrients, pigments, waste products and small molecules) or as primary acidic compartments for degradation of compounds by enzymes,

including acid hydrolases (Klionsky et al 1990, Weber 2002, Richards et al 2010). These organelles can be a possible route of AgNPs entry into the fungal cells, causing increased membrane damage and, in turn, inducing the expression of genes related to protective responses. Similar organelles, namely lysosomes, were preferential targets for many types of NPs, in mammalian cells because these compartments have been implicated in the intake of NPs via endocytosis (Goya et al 2008, Faklaris et al 2009).

Considering the GO-based predicted biological process, the genes associated with the transport were highly represented under exposure to both forms of silver. The transport comprises the movement of substances or cellular components (macromolecules, small molecules, ions, complexes, organelles, etc.) into cell, out of cell, or within a cell, or between cells through *e.g.* transporters, pores or motor proteins (GO:0006810). However, the genes associated with transport were differentially regulated by both silver forms. Exposure to AgNPs increased the expression of all genes related to transport (Fig. 4.3B), namely those involved in carbohydrate transport (7 genes, GO:0008643), cation transmembrane transport (8 genes, GO:0098655), ion transmembrane transport (12 genes, GO:0034220), ion transport (20 genes, GO:0006811) and transmembrane transport (39 genes, GO:0055085). The up-regulation of these genes might be related to the annotation of the storage and lytic vacuoles as cellular components representative of AgNP exposure due to their role in transporting molecules across cell wall (Casadevall et al 2009) and protecting cells by sequestering toxic molecules (Sirikantaramas et al 2008). The responses to Ag⁺ exposure were different: 22 and 45 genes related to transport were up- and down-regulated, respectively (Fig. 4.3A). The up-regulated genes were predicted to be involved in amino acid transport (6 genes, GO:0006865) and cation transport (16 genes, GO:0006812), while down-regulated genes were likely to be associated with ion transmembrane transport (6 genes, GO:0034220) and transmembrane transport (18 genes, GO:0055085; 21 genes, GO:0006810).

The GO analysis also predicted that carbohydrate metabolism was another key biological process affected by both silver forms. However, the carbohydrate metabolism was regulated in opposite ways (Fig. 4.3A and 4.3B). Upon exposure to Ag⁺, up-regulated genes were associated with polysaccharide (17 genes, GO:0005976) and carbohydrate metabolic processes (34 genes, GO:0005975). This might be associated with the additional energy needed to compensate the Ag⁺-induced stress since aquatic fungi mainly obtain energy

from enzymatic degradation of submerged plant materials releasing sugars from structural carbohydrates (Wurzbacher et al 2011). In addition, carbohydrates are also structural cell wall components, and the related genes were up-regulated under exposure to Ag^+ . The exposure to AgNPs decreased the expression of genes associated with polysaccharide metabolic processes (8 genes, GO:0005976) and polysaccharide catabolic processes (7 genes, GO:0000272). Moreover, the exposure to AgNPs increased the expression of genes associated with generation of energy (9 genes, GO:0006091) indicating that *A. tetracladia* might have also constrains in obtaining energy under AgNP-stress.

Another GO-predicted biological process affected by silver was proteolysis, because several related genes were down-regulated under exposure to both silver forms (7 genes for Ag^+ , Fig. 4.3A; 10 genes for AgNPs, Fig. 4.3B). This process (GO:0006508) involves the hydrolysis of proteins into smaller polypeptides and/or amino acids as provision of amino acids as sources of energy, production of new and active proteins, removal of damaged and abnormal proteins, cell cycle regulation or apoptosis mainly by activating or deactivating enzymes, transcription factors and receptors (Glotzer et al 1991; Creighton 1993; Hengartner 2000). The down-regulation of genes associated with proteolysis indicates that both silver forms were responsible for affecting this process in *A. tetracladia*. Other three biological processes, namely steroid metabolism, cell adhesion and localization were predicted to be representative of the stress induced by Ag^+ (Fig. 4.3A). Genes likely to be involved in steroid metabolism, including sterol (9 genes, GO:0016125) and steroid (12 genes, GO:0008202) metabolic and biosynthetic processes (sterol: 6 genes, GO:0016126; steroid: 9 genes, GO:0006694) were up-regulated. Fungal steroids, including ergosterol, which is present in fungal membranes, contributes to maintain its integrity (Walker and White 2005) and fungi can alter their ergosterol content to develop resistance against drugs (Abu-Elteen and Hamad 2005). Accordingly, up-regulation of genes likely to be involved in steroid metabolism in *A. tetracladia* exposed to Ag^+ might be related to a mechanism of defense against this stressor. In addition, the increased expression of lipid metabolism genes under exposure to Ag^+ (cluster C, Fig. 4.2C), indicates that this toxicant induced more membrane damage than AgNPs in *A. tetracladia*.

Cell adhesion was a less representative process (cell adhesion, 6 genes, GO:0007155 and biological adhesion, 6 genes, GO:0022610) that refers to the attachment of cells, spores or fungal mycelia to another cell, organism or substrates, and may also include the

intracellular attachment between membrane regions. Since this process can be involved in cellular signal transduction for detection and response to changes in the environment (Gumbiner 1996), the up-regulation of genes related to this process might also be involved in the protection of *A. tetracladia* against Ag^+ .

The process of localization (establishment of localization, 21 genes, GO:0051234 and localization, 22 genes, GO:0051179) refers to any process in which a cell, a substance, or a cellular entity (e.g. protein complex or organelle) is transported, tethered to or otherwise maintained in a specific location. Genes likely to be associated with this process were down-regulated upon Ag^+ exposure. Other three biological processes were putatively representative of exposure to AgNPs, namely redox (27 genes, GO:0055114) and aromatic compound catabolism (8 genes, GO:0019439), whose genes were down-regulated, and nucleobase metabolism (23 genes; GO:0006144, GO:0009112 and GO:0072521), whose genes were up-regulated (Fig. 4.3B). Many important biological processes involve redox reactions with removal or addition of one or more electrons from or to a substance, with or without the concomitant removal or addition of protons. Redox reactions are intimately associated with the process of cellular respiration, i.e. oxidation of carbohydrates. Redox also includes free radical reactions that occur as part of homeostasis, indicating that exposure to AgNPs had probably compromised the stability of fungal mycelia. Like carbohydrates, the aromatic compounds constitute well known common carbon sources in the environment. It seems that AgNP exposure had a negative effect on the catabolism of such molecules which probably reduced the ability of *A. tetracladia* to protect against AgNPs, at least in comparison with Ag^+ due to the lack of energy supply; this may further provide the mechanistic explanation for the lower EC_{20} of AgNPs than Ag^+ . In addition, the increase in the expression of genes associated with the metabolism of nucleobases supports that AgNPs induce nucleic acids damage in aquatic hyphomycetes (Pradhan et al 2015).

References

- Abu-Elteen KH and Hamad M. 2005. Antifungal Agents for Use in Human Therapy. In: Kavanagh K (Eds) Fungi: Biology and Applications. John Wiley & Sons Ltd, England, pp. 1-34.

- Bärlocher F. 2005. Freshwater fungal communities. In: Deighton J, Oudemans P, White J (Eds) *The fungal community: its organization and role in the ecosystem*, 3rd ed, Taylor and Francis, CRC Press, Boca Raton, Florida, pp. 39-59.
- Bolger AM, Lohse M and Usadel B. 2014. Trimmomatic: a flexible trimmer for Illumina sequence data. *Bioinformatics*. 30: 2114-2120.
- Casadevall A, Nosanchuk JD, Williamson P, Rodrigues ML. 2009. Vesicular transport across the fungal cell wall. *Trends Microbiol*. 17: 158-162.
- Creighton TE. 1993. *Proteins: Structures and Molecular Properties* (2nd ed.). W H Freeman and Company. pp. 78-86.
- Dangles O, Gessner MO, Guérol F and Chauvet E. 2004. Impacts of stream acidification on litter breakdown: implications for assessing ecosystem functioning. *J. Appl. Ecol*. 41: 365-378.
- Deng Y, Yang F and Naqvi NI. 2015. The role of nutrients in fungal development and pathogenesis. In: Gupta VK, Mach RL, Sreenivasaprasad S (Eds) *Fungal Biomolecules: Sources, Applications and Recent Developments*. John Wiley & Sons, UK. pp 203-212.
- Duarte S, Pascoal C and Cássio F. 2009. Functional stability of stream-dwelling microbial decomposers to copper and zinc stress. *Freshwater Biology*. 54: 1683-1691.
- Duarte S, Pascoal C, Alves A, Correia A, Cássio F. 2008. Copper and zinc mixtures induce shifts in microbial communities and reduce leaf litter decomposition in streams. *Freshwater Biol*. 53: 91-101.
- Faklaris O, Joshi V, Irinopoulou T, Tauc P, Girard H, Gesset C, Sennour M, Thorel A, Arnault JC, Boudou JP, Curmi PA and Treussart F. 2009. Photoluminescent diamond nanoparticles for cell labelling: study of the uptake mechanism in mammalian cells. *ACS Nano*. 3: 3955-3962.
- Fernandes I, Duarte S, Cássio F and Pascoal C. 2013. Effects of riparian plant diversity loss on aquatic microbial decomposers become more pronounced with increasing time. *Microb. Ecol*. 4: 763-772.
- Fomina M, Burford EP, Gadd GM. 2005. Toxic Metals and Fungal Communities. In Dighton J, White JF, Oudemans P (Eds), *The Fungal Community: Its Organization and Role in the Ecosystem* (3rd edition). Taylor & Francis, Boca Raton, pp. 733-759.
- Glutzer M, Murray AW, Kirschner MW. 1991. Cyclin is degraded by the ubiquitin pathway. *Nature*. 349: 132-138.
- Gow NAR, Latge JP, Munro CA. 2017. The fungal cell wall: Structure, biosynthesis, and function. *Microbiol. Spectr*. 5: 1-25.
- Goya GF, Marcos-Campos I, Fernandez-Pacheco R, Saez B, Godino J, Asin L, Lambea J, Tabuenca P, Mayordomo JI, Larrad L, Ibarra MR and Tres A. 2008. Dendritic cell uptake of iron-based magnetic nanoparticles. *Cell. Biol. Int*. 32: 1001-1005.
- Grabherr MG, Haas BJ, Yassour M, Levin JZ, Thompson DA, Amit I, Adiconis X, Fan L, Raychowdhury R, Zeng Q, Chen Z, Mauceli E, Hacohen N, Gnirke A, Rhind N, di Palma F, Birren BW, Nusbaum C, Lindblad-Toh K, Friedman N and Regev A. 2011. Full-length

- transcriptome assembly from RNA-Seq data without a reference genome. *Nat. Biotechnol.* 29: 644-652.
- Gumbiner BM. 1996. Cell Adhesion: The Molecular Basis of Tissue Architecture and Morphogenesis. *Cell.* 84: 345-357.
- Haas BJ, Papanicolaou A, Yassour M, Grabherr M, Blood PD, Bowden J, Couger MB, Eccles D, Li B, Lieber M, MacManes MD, Ott M, Orvis J, Pochet N, Strozzi F, Weeks N, Westerman R, William T, Dewey CN, Henschel R, LeDuc RD, Friedman N and Regev A. 2013. De novo transcript sequence reconstruction from RNA-seq using the Trinity platform for reference generation and analysis. *Nature Protocols.* 8: 1494-1512.
- Hengartner MO. 2000. The biochemistry of apoptosis. *Nature.* 407: 770-776.
- Jiang X, Qiu LG, Zhao HW, Song QQ, Zhou HL, Han Q, Diao XP. 2016. Transcriptomic responses of *Perna viridis* embryo to Benzo(a)pyrene exposure elucidated by RNA sequencing. *Chemosphere.* 163: 125-132.
- Jo HJ, Choi JW, Lee SH and Hong SW. 2012. Acute toxicity of Ag and CuO nanoparticle suspensions against *Daphnia magna*: the importance of their dissolved fraction varying with preparation methods. *J. Hazard Mater.* 227-228: 301-308.
- Klionsky DJ, Herman PK and Emr SD. 1990. The fungal vacuole: composition, function, and biogenesis. *Microbiol. Rev.* 54: 266-292.
- Lemos MFL, Soares AMVM, Correia AC, Esteves AC. 2010. Proteins in ecotoxicology – how, why and why not? *Proteomics.* 10: 873-887.
- Li B and Dewey CN. 2011. RSEM: accurate transcript quantification from RNA-Seq data with or without a reference genome. *BMC Bioinformatics.* 12: 323.
- Lowe R, Shirley N, Bleackley M, Dolan S and Shafee T. 2017. Transcriptomics technologies. *PLoS Comput. Biol.* 13: e1005457.
- Navarro E, Piccapietra F, Wagner B, Marconi F, Kaegi R, OdzakN, Sigg L and Behra R. 2008. Toxicity of silver nanoparticles to *Chlamydomonas reinhardtii*. *Environ. Sci. Technol.* 42: 8959-8964.
- Pascoal C, Marvanová L and Cássio F. 2005. Aquatic hyphomycete diversity in streams of Northwest Portugal. *Fung. Divers.* 19: 109-128.
- Poynton HC, Lazorchak JM, Impellitteri CA, Blalock BJ, Rogers K, Allen HJ, Loguinov A, Heckman JL, Govindasmaw S. 2012. Toxicogenomic responses of nanotoxicity in *Daphnia magna* exposed to silver nitrate and coated silver nanoparticles. *Environ. Sci. and Technol.* 46: 6288-6296.
- Pradhan A, Seena S, Schlosser D, Gerth K, Helm S, Dobritsch M, Krauss G-J, Dobritsch D, Pascoal C and Cássio F. 2015. Fungi from metal-polluted streams may have high ability to cope with the oxidative stress induced by copper oxide nanoparticles. *Environ. Toxicol. Chem.* 34: 923-930.
- Pradhan A, Seena S, Pascoal C, Cássio F. 2011. Can Metal Nanoparticles Be a Threat to Microbial Decomposers of Plant Litter in Streams? *Microb. Ecol.* 62: 58-68.
- Richards A, Veses V and Gow NAR. 2010. Vacuole dynamics in fungi. *Fungal Biol. Rev.* 24: 93-105.

- Robinson MD, McCarthy DJ and Smyth GK. 2010. edgeR: a Bioconductor package for differential expression analysis of digital gene expression data. *Bioinformatics*. 26: 139-40.
- Schirmer K, Fischer BB, Madureira DJ, Pillai S. 2010. Transcriptomics in ecotoxicology. *Anal. Bioanal. Chem.* 397: 917-923.
- Schmieder R, Lim YW and Edwards R. 2012. Identification and removal of ribosomal RNA sequences from metatranscriptomes. *Bioinformatics*. 28: 433-435.
- Shearer CA, Descals E, Kohlmeyer B, Kohlmeyer J, Marvanová L, Padgett D, Porter D, Raja HA, Schmit JP, Thorton HA and Voglymayr H. 2007. Fungal biodiversity in aquatic habitats. *Biodiversity and Conservation*. 16: 49-67.
- Sirikantaramas S, Yamazaki M and Saito K. 2008. Mechanisms of resistance to self-produced toxic secondary metabolites in plants. *Phytochem. Rev.* 7: 467-477.
- Storck R and Alexopoulos CJ. 1970. Deoxyribonucleic acid of fungi. *Bacteriol. Rev.* 34: 126-154.
- Suberkropp KF. 1998. Microorganisms and organic matter decomposition. In Naiman RJ, Bilby RE (Eds), *River Ecology and Management: Lessons from the Pacific Coastal Ecoregion*. Springer, New York, pp. 120-143.
- Swathy JR, Udhaya Sankar M, Chaudhary A, Aigal S and Pradeep T. 2014. Antimicrobial silver: an unprecedented anion effect. *Sci. Rep.* 4: 1. doi:10.1038/srep07161.
- Tlili A, Cornut J, Behra R, Gil-Allué C and Gessner MO. 2016. Harmful effects of silver nanoparticles on a complex detrital model system. *Nanotoxicology*. 10: 728-735.
- Van Acker H, Van Dijck P, Coenye T. 2014. Molecular mechanisms of antimicrobial tolerance and resistance in bacterial and fungal biofilms. *Trends Microbiol.* 22: 326-333.
- Van Aggelen G, Ankley GT, Baldwin WS, Bearden DW, Benson WH, Chipman JK, Collette TW, Craft JA, Denslow ND, Embry MR, Falciani F, George SG, Helbing CC, Hoekstra PF, Iguchi T, Kagami Y, Katsiadaki I, Kille P, Liu L, Lord PG, McIntyre T, O'Neill A, Osachoff H, Perkins EJ, Santos EM, Skirrow RC, Snape JR, Tyler CR, Versteeg D, Viant MR, Volz DC, Williams TD, Yu L. 2010. Integrating omic technologies into aquatic ecological risk assessment and environmental monitoring: Hurdles, achievements, and future outlook. *Environ. Health Perspect.* 118: 1-5.
- Walker GM and White NA. 2005. Introduction to Fungal Physiology. In: Kavanagh K (Eds) *Fungi: Biology and Applications*. John Wiley & Sons Ltd, England, pp. 1-34.
- Wang Z, Gerstein M and Snyder M. 2009. RNA-Seq: A revolutionary tool for transcriptomics. *Nat. Rev. Genet.* 10: 57-63.
- Weber RWS. 2002. Vacuoles and the fungal lifestyle. *Mycologist*. 16: 10-20
- Wurzbacher C, Kerr J, Grossart H-P. 2011. Aquatic fungi. In: Grillo O and Venora G (Eds) *The Dynamic Processes of Biodiversity – Case Studies of Evolution and Spatial Distribution*. InTech Press, Rijeka. pp. 227-258.
- Young MD, Wakefield MJ, Smyth GK and Oshlack A. 2010. Gene ontology analysis for RNA-seq: accounting for selection bias. *Genome Biol.* 11: R14.

Zhu HH, Ai HL, Cao LW, Sui R, Ye HP, Du DY, Sun J, Yao J, Chen K, Chen L. 2018. Transcriptome analysis providing novel insights for Cd-resistant tall fescue responses to Cd stress. *Ecotoxicol Environ Saf.* 160: 349-356.

Chapter 5

General discussion and future perspectives

General discussion and future perspectives

Water connects all Earth's ecosystems sustaining agriculture, households and industries; however, concern about the future supplies of freshwaters to meet human demands is becoming a priority among the global societal issues. Essential goods and services provided by aquatic ecosystems include food, water and waste removal, but evidence of anthropogenic threats to the environment is raising awareness of the rapid degradation of natural environments at the globe scale. In fact, aquatic ecosystems play key roles as sentinels of environmental change in the terrestrial surroundings (Williamson et al 2008). One major threat to these ecosystems is water pollution (Dudgeon et al 2006), being pollution by metals of great concern due to their non-degradability, accumulation in the biota and biomagnification along food webs. This concern could be extended to metal-based NPs that are among the most used ENMs due to the development of nanotechnology industries (Fabrega et al 2011). AgNPs are currently among the most used NMs, mainly due to the Ag⁺ antimicrobial properties, increasing the possibility of their release into aquatic ecosystems and raising concern about the risks to non-target organisms and their ecological functions. A wide range of organisms, including bacteria, algae and fungi are affected by the toxic effects of AgNPs (Kumar et al 2014, Navarro et al 2015), thus, there is a need to understand their interaction with biota, especially in aquatic ecosystems, where NPs will most likely end up. As many studies draw attention to their potential toxicity (Poynton et al 2012, Angel et al 2013, Blinova et al 2013), one question that remains unclear is whether toxicity is exclusively related to NP properties or also mediated by the released Ag⁺ from AgNPs, and so efforts to discern their mechanism of action are becoming urgent.

To better understand AgNP toxicity to aquatic organisms, we investigated the effects of citrate-coated AgNPs and its ionic precursor under environmentally realistic concentrations on bacteria (Chapter 2) and aquatic fungi (Chapter 3 and 4) that play key ecological roles in freshwater ecosystems. Responses were further compared at similar effect concentrations of both silver forms. Since distinct species and populations may present different biological responses to stressors, we selected microbes with different background, namely a bacterial strain collected from a

polluted stream (*Pseudomonas* sp. M1) and two aquatic fungal ecotypes of *Articulospora tetracladia*, one isolated from a clean stream (At72) and the other from a metal-polluted stream (At61) to ascertain differences in the susceptibility to these toxicants. Since NP bioavailability can affect its toxicity, the characterization of AgNPs and quantification of silver were also performed in different experimental conditions. Some studies show that the toxicity of some NPs is due to the released ions and not to NPs themselves (Gil-Allué et al 2015, Völker et al 2015), while other studies show opposite findings (Nair et al 2013, Tlili et al 2016). To uncover if toxicity of AgNPs was due to Ag^+ dissolution from AgNPs or was particle specific, the effects of Ag^+ (as AgNO_3) were compared to those of AgNPs. Effects of AgNPs on fungal growth revealed that the ecotype from the non-polluted stream (At72) was the most sensitive, whereas *Pseudomonas* sp. M1 was the most tolerant one ($\text{EC of At72} < \text{EC of At61} < \text{EC of } Pseudomonas \text{ sp. M1}$). Results from nanoparticles characterization supported these findings, since particle stability increased along the exposure period in the presence of At72. On the other hand, for At61 and *Pseudomonas* sp. M1, a higher agglomeration and relatively lesser stability of AgNPs was found, particularly for *Pseudomonas* sp. M1 whose tolerance (higher EC) to AgNPs was higher than that of At61. It is known that dispersed AgNPs contribute to greater negative effects over aggregated ones (Dorjnamjin et al 2008, Kvitek et al 2008), supporting the importance of characterizing AgNPs under exposure conditions when ascertaining its toxicity. In contrast, the fungal ecotype from the metal-polluted stream (At61) was more susceptible to Ag^+ , whereas At72 and *Pseudomonas* sp. M1 were more tolerant ($\text{EC of At61} < \text{EC of } Pseudomonas \text{ sp M1} \approx \text{EC of At72}$). The higher EC of Ag^+ in At72 compared to At61 might be explained by the influence of the nitrate from AgNO_3 which might have alleviated the toxic effects of Ag^+ on At72, as demonstrated by the increase in fungal biomass of At72 (ca. 15%) but not that of At61 upon exposure to the lowest tested concentration of NO_3^- . The sensitivity of fungi to inorganic nutrients (e.g. NO_3^-) was previously shown by Fernandes et al (2014) who reported an increase in biomass of fungi grown in the presence of increasing concentrations of nitrogen.

The analysis of silver content in fungal mycelium revealed that At61 accumulated more silver from AgNPs per unit biomass (>40 times) and the intake of total Ag was almost twice than that in At72, which could be representative of the higher tolerance of At61

to AgNPs (EC of At61 > EC of At72). Moreover, the negligible amount of dissolved Ag^+ released from AgNPs to the media, for both fungi and *Pseudomonas* sp. M1, suggests that the toxicity of AgNPs was mainly particle specific. In the case of *Pseudomonas* sp. M1, a complementary test with cysteine, a strong Ag^+ ligand, further supported that AgNPs induce a direct toxicity on the bacterium, although possible interactions between Cl^- from the medium and Ag^+ released from AgNPs or AgNO_3 cannot be discarded (Behra et al 2013). Although the collection sites of *Pseudomonas* sp. M1 and At61 were polluted (At61 from the Este River: Soares et al 1999; *Pseudomonas* sp. M1 from the Rhine river: Middelkoop 2000, Vega and Weng 2013), contamination by silver was not found in those environments. Therefore, adaptive mechanisms of microbes might or might not be specific to the existing stressors (e.g. copper, lead and cadmium) and the occurrence of co-tolerance mechanisms (Soldo and Behra 2000, Tlili et al 2011) between the metals present at the origin sites and AgNPs is a possibility. Consistently, fungi isolated from metal polluted streams were reported to be more resistant to CuONPs than fungi from non-polluted streams (Pradhan et al 2015).

Because NPs can induce oxidative stress by generating ROS, we examined the ability of AgNPs and Ag^+ to promote changes in the antioxidant enzymatic responses to further understand the resistance/tolerance of microbes to the stress induced by these Ag forms. Our results suggested that the tolerance of these microbes to AgNPs and Ag^+ might depend on their ability to initiate an efficient antioxidant defense system since most activities of the tested enzymes (SOD, GPx, GST and CAT) increased after exposure to AgNPs or Ag^+ in all tested microorganisms. However, at similar effective concentrations of AgNPs or Ag^+ , the activities increased more in At72 than in At61, indicating induction of higher stress in the fungal ecotype collected from the non-polluted stream. In addition, enzymatic activities were higher under exposure to Ag^+ than to AgNPs suggesting that the ionic form of Ag promoted higher levels of oxidative stress in all microbes. The activity of CAT was the highest in both fungal ecotypes under exposure to both forms of Ag suggesting that the formation of H_2O_2 was primarily detoxified by CAT and not by GPx, which has a compensatory role in catalysing the reduction of hydroperoxides (Lubrano and Balzan 2015) and had the lowest activity under similar exposure conditions. Moreover, CAT was also the primary antioxidant enzyme with greater role in alleviating the stress induced in fungi exposed

to metals (Zn and Cu, Azevedo et al 2007). In *Pseudomonas* sp. M1, the exposure to both stressors led to higher stimulation of GPx and SOD indicating greater involvement of these enzymes in alleviating the oxidative stress induced by both forms of Ag.

The mode of action of AgNPs was explored by proteomic and transcriptomic approaches which have been useful in examining the molecular mechanisms underlying the tolerance/sensitivity of bacteria and fungi to stressors (Mirzajani et al 2014, Huang et al 2018, Zheng et al 2018) and may help to better explain the action mechanisms of AgNPs and Ag⁺. Moreover, gene and/or protein expression profiling can be used to develop robust molecular biomarkers that will allow the early detection of environmental stressors.

In our study, proteomic responses of exposure to AgNPs or Ag⁺ revealed that the total number of quantified proteins was higher in At61 and lower in *Pseudomonas* sp. M1 (both collected from metal polluted streams, with 516 and 166 proteins, respectively) which was concordant with the number of responsive proteins (higher for At61 ≈ 50% and lesser for *Pseudomonas* sp. M1 ≈ 35%; Fig. 5.1).

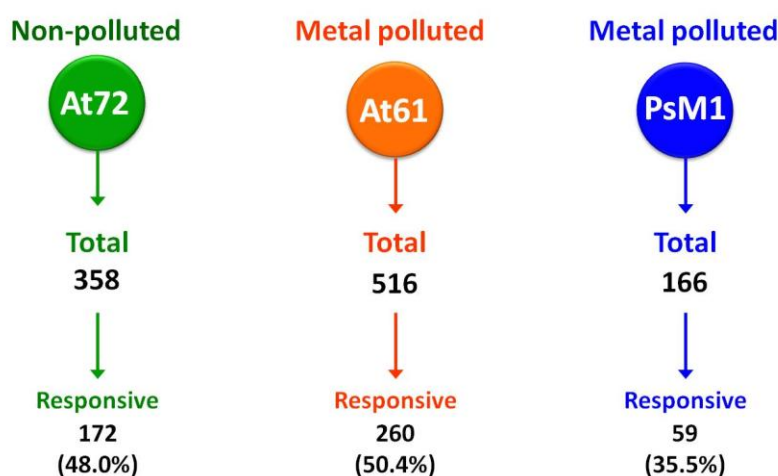


Figure 5.1 Total number of identified and significantly altered proteins in two ecotypes of *A. tetracladia* collected from a non-polluted stream (At72) and from a metal-polluted stream (At61) and in *Pseudomonas* sp. M1 from a metal-polluted stream (PsM1) under exposure to Ag⁺ or AgNPs.

In our study, the fungal ecotypes seemed to display distinct responses to Ag⁺ and AgNPs since only 20% of the total number of responsive proteins was common to both ecotypes. Moreover, a higher number of proteins with opposite response under exposure to each silver form was found in At72 (37.8%) compared to At61 (6.5%).

These results indicate that At61 had a more similar response than At72 to both forms of silver, which may be attributed to developed mechanisms of co-tolerance to metals present in At61 collection site. Three main hypotheses have been proposed to explain the toxicity caused by AgNPs: 1) AgNPs exert toxicity through released Ag ions (Kim J et al 2011, Zhao and Wang 2011); 2) AgNPs exert toxicity through a mechanism independent of their correspondent metal ions (Shoults-Wilson et al 2011, Bilberg et al 2011); and 3) AgNPs remain intact (with unaltered structure/composition) but once inside the cells, they release Ag ions that exert toxicity (Park et al 2010, Meyer et al 2010). However, such experimental studies do not provide the mechanistic explanation on how AgNPs exert their toxicity. Omic studies often point to distinct mechanisms of toxicity of NPs with different expression profiles among NPs and their ionic counterparts (Poynton et al 2012, Nair and Chung 2015, Su et al 2015). In our study, the analysis of the dynamic profiles of the responsive proteins of each microorganism allowed us to verify, at least visually, that each silver form promoted different proteomic responses (Fig. 5.2).

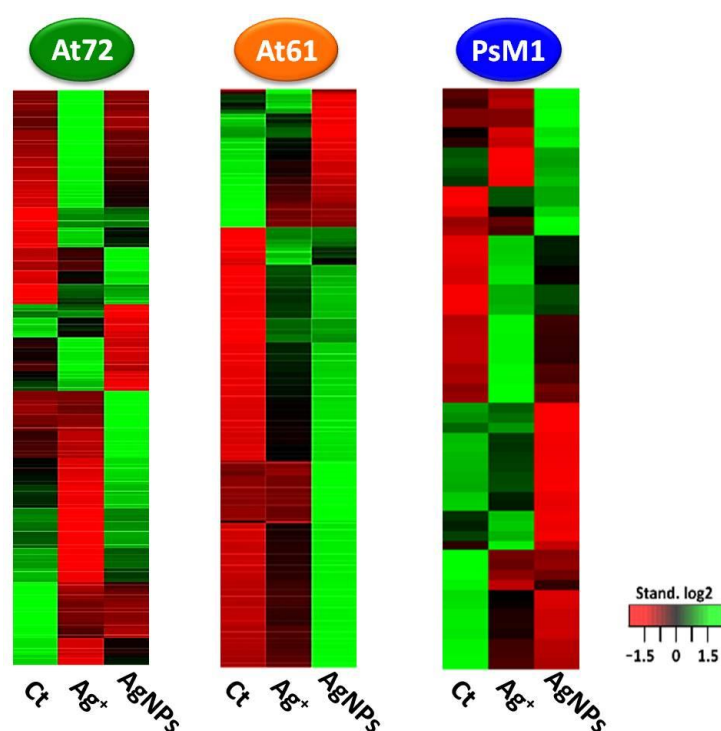


Figure 5.2 Heatmaps of the proteins with significant variation in two ecotypes of *A. tetracladia* collected from a non-polluted stream (At72) and from a metal-polluted stream (At61) and in *Pseudomonas* sp. M1 from a metal-polluted stream (PsM1) under exposure to Ag⁺ or AgNPs.

This assumption was then supported by GO enrichment analysis of responsive proteins in which the most relevant biological processes associated with exposure to AgNPs and/or Ag⁺ were disclosed highlighting different responses between the selected microbes (Fig. 5.3). Particularly, in *Pseudomonas* sp. M1, the processes of protein folding and transmembrane transport were associated with proteins that increased under Ag⁺ exposure more strongly than under AgNP exposure, indicating that these proteins were mainly targeted by Ag⁺. Disturbance of transmembrane transport can in turn have implication in the stressors intake into bacterial cells, increasing cellular damage or, on the contrary, in the stressors export to protect cells. Increase in protein folding suggests damage to proteins which in turn required the prevention of misfolding and promotion of refolding and proper assembly of unfolded polypeptides generated under these stress conditions. Additionally, the processes (negative regulation) of biofilm formation as well as of pathogenesis were also positively affected by both forms of silver, however no designation related to these processes (as biological processes annotated in UniProt) was attributed to any differentially expressed protein. The formation of biofilm was previously reported to be a process affected by AgNPs in other *Pseudomonas* species (Kalishwaralal et al 2010, Singh et al 2015). In the case of pathogenesis, despite *Pseudomonas* sp. M1 is an environmental strain whose pathogenicity is unknown, there is evidence that virulence factors related to pathogenesis can also be encoded in the genomes of non-pathogenic bacteria (Niu et al 2013). Moreover, virulence activation was correlated to metal resistance (Pitondo-Silva et al 2016). Because these defense processes require considerable amount of energy, the prioritization of one process over the other may have been a strategy of *Pseudomonas* sp. M1 to save energy to deal with the stress induced by both silver forms. The process of translation was the most overrepresented and was associated with proteins whose content increased under exposure to AgNPs and decreased upon exposure to Ag⁺, indicating that ionic and nanoparticulate forms of Ag affected differently this process. Translation was also highlighted in At61 (also collected from a metal-polluted stream) but related proteins were only affected by AgNPs.

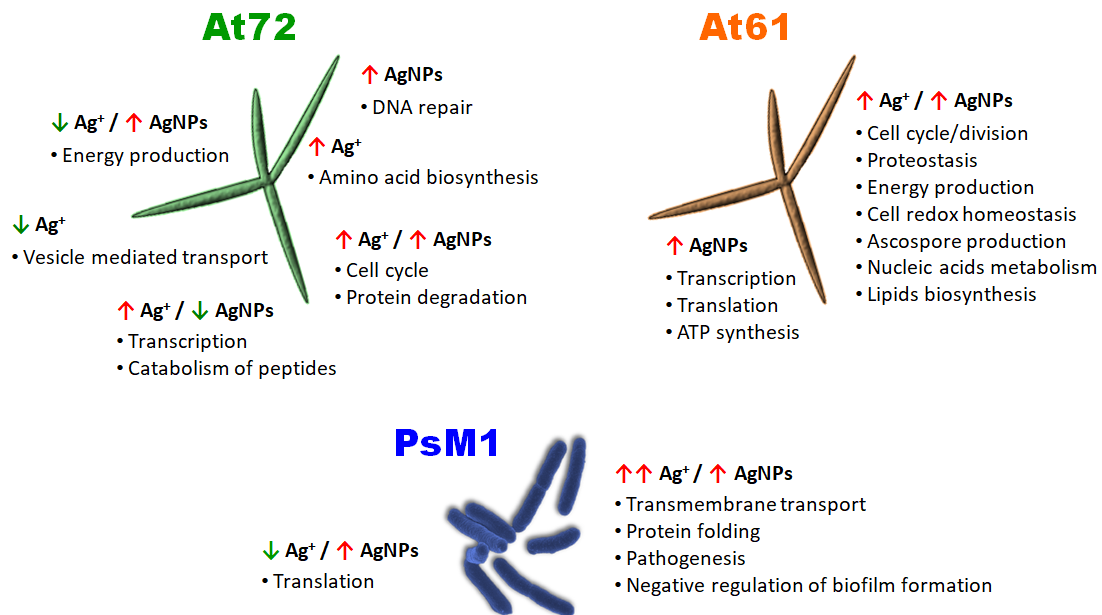


Figure 5.3 Most relevant biological processes highlighted by GO enrichment analysis of the proteins with significant variation (↑ up-regulation and ↓ down-regulation) in two ecotypes of *A. tetracladia* collected from a non-polluted stream (At72) and from a metal-polluted stream (At61) and in *Pseudomonas* sp. M1 from a metal-polluted stream (PsM1) under exposure to Ag⁺ or AgNPs.

Regarding fungal ecotypes, GO enrichment analysis disclosed common processes (e.g. transcription and amino acid biosynthesis) to both silver forms and to both fungal ecotypes; however, most of the processes associated with altered proteins were distinct and, therefore, valuable in differentiating fungal ecotypes. Specifically, proteome analysis of At72 under exposure to AgNPs or Ag⁺ revealed multiple groups of processes possibly indicative of its non-polluted background. For instance, DNA repair was representative of proteins whose content increased exclusively under AgNP exposure, suggesting DNA damage by AgNPs. This supports previous findings by Pradhan et al (2015) who showed DNA-strand breaks in fungal mycelia exposed to CuNPs. On the other hand, the process of amino acids biosynthesis was only highlighted under exposure to Ag⁺, whereas the transport mediated by vesicles was only representative of proteins decreased upon exposure to Ag⁺. Energy production was induced by AgNPs (as in At61 and *Pseudomonas* sp. M1) but repressed by Ag⁺ indicating opposite effects of AgNPs and Ag⁺. Both silver forms increased the content of proteins involved in cell cycle in both ecotypes, indicating disturbance of events that take place in cells leading to cellular reproduction by both forms of silver. The process

of protein degradation, which is crucial for cell protection, was also positively regulated by AgNPs and Ag⁺.

The last group of overrepresented processes included the transcription and peptide catabolism whose related proteins increased under Ag⁺ exposure but decreased upon exposure to AgNPs. Similarly to that found in *Pseudomonas* sp. M1, proteomic responses of At61 were less complex since only two groups of processes were disclosed. The majority of the overrepresented processes including cell cycle/division, cell-redox and protein homeostasis, fatty acid biosynthesis and nucleic acids metabolism were induced under exposure to both silver forms. A particular process was highlighted in At61 also under exposure to both silver forms, namely ascospore formation. Considering that ascospores have thick cell-walls, energy reserves and low metabolic activity (Moore-Landecker 2002), the induction of proteins related to their production by both Ag forms can be envisaged as a survival strategy since asexual reproduction is often decreased under stressful conditions (Pradhan et al 2011, Batista et al 2017), while sexual reproduction is considered evolutionarily advantageous (Ram and Hadany 2016). Moreover, the processes of transcription and energy production were related to proteins whose content increased solely under exposure to AgNPs.

The transcriptomic approach also supported different modes of toxicity of Ag⁺ and AgNPs in At72 since, as in the proteomic analysis, distinct profiles of gene expression were unveiled. GO enrichment analysis evidenced that membrane is the main cellular component likely to be affected by both silver forms strongly suggesting that cellular membranes are the major targets of AgNPs and Ag⁺. The process of energy production whose genes were up-regulated under exposure to AgNPs was also highlighted in the proteomic analysis revealing concordance between these two approaches. More importantly, since this process was induced by AgNPs in all three microorganisms, we deduce that coping with AgNP stress requires an increased supply of energy. Furthermore, genes associated with the metabolism of steroids were up-regulated under exposure to Ag⁺ suggesting potential protection against fungal cell membrane damage.

Transport processes were highly represented; however genes likely to be associated with this process were up-regulated under AgNP exposure, while under Ag⁺ exposure some genes were up- and other were down-regulated, suggesting distinct regulation

by both silver forms. The metabolism of carbohydrates was also oppositely regulated by both silver forms. As part of cell wall composition, increased expression of genes related to the metabolism of carbohydrates under exposure to Ag^+ may be indicative of damage to cell wall by ionic silver. On the other hand, carbohydrates can be used as energy sources indicating that these molecules may have been used for different purposes depending on cellular needs under exposure to AgNPs or Ag^+ . The metabolism of nucleobases was representative of genes whose expression increased under exposure to AgNPs, possibly indicating damage to nucleic acids since nucleobases are essential building blocks of DNA and RNA. Indeed, previous studies indicate that metal nanoparticles promote genotoxicity (Kim HR et al 2011, Sharma et al 2011, Pradhan et al 2015). In contrast, in our study, AgNPs led to the down-regulation of genes associated with redox processes suggesting compromised cellular redox homeostasis in fungal mycelia which is consistent with alterations in biomarkers of oxidative stress in response to other metal nanoparticles in freshwater organisms (Pradhan et al 2015, Pradhan et al 2016).

Overall, our systems toxicology approach included biochemical, proteomic and transcriptomic responses to AgNPs and was proven successful to unravel several processes associated with different target molecules (i.e. enzymes/proteins/genes). Although some of the processes were common to the responses of all studied microorganisms under exposure to AgNPs and Ag^+ , the majority were distinct. Furthermore, our results allowed us to differentiate the effects of AgNPs from those of Ag^+ providing detailed insights into the molecular mechanisms of equitoxic levels of AgNPs and Ag^+ in microbes. If AgNPs are a source of Ag^+ , it would be reasonable to assume that the molecular mechanisms of these silver forms would be analogous. However, in our study, the amount of dissolved Ag^+ released from AgNPs to the media was irrelevant, suggesting that the toxicity of AgNPs was mainly particle specific. Hence, it is likely that different mechanisms of toxicity to different silver forms may exist. Our results support precisely this, since each form of silver induced different adaptive responses. However, the variety of silver nanoforms with different physico-chemical properties (i.e. size, shape, coating, etc) instigates that every product with AgNPs should be individually considered due to different modes of action and consequently different toxicities. On the other hand, in aquatic environments, the

transformation and fate of AgNPs and the consequent silver ions release must be adequately evaluated taking into consideration physical and chemical properties of water (e.g. pH, conductivity and organic matter). Likewise, the presence of other toxicants and even the presence and interaction with living organisms should be considered. After taking these aspects into consideration, we believe that the next step should be the application of omic approaches to entire communities. This will allow us to gain insight on the consequences of AgNPs to ecological functions and the services provided by the biological communities, and will provide of better understanding of the potential impacts of AgNPs on freshwater ecosystems. In future omic studies, more profound approaches should be applied to look beyond and confirm specific biomarkers. Additionally, genome sequencing of non-model organisms becomes critical since that data acquired for protein identification is only meaningful after database searching which makes proteomics largely dependent on the content of protein databases.

References

- Angel BM, Batley GE, Jarolimek CV, Rogers NJ. 2013. The impact of size on the fate and toxicity of nanoparticulate silver in aquatic systems. *Chemosphere*. 93: 359-365.
- Batista D, Pascoal C, Cássio F. 2017. Temperature modulates AgNP impacts on microbial decomposer activity. *Sci. Total Environ*. 601-602: 1324-1332.
- Behra R, Sigg L, Clift MJ, Herzog F, Minghetti M, Johnston B, Petri-Fink A, Rothen-Rutishauser B. 2013. Bioavailability of silver nanoparticles and ions: from a chemical and biochemical perspective. *J. R. Soc. Interface*. 10: 20130396.
- Bilberg K, Doving KB, Beedholm K, Baatrup E. 2011. Silver nanoparticles disrupt olfaction in Crucian carp (*Carassius carassius*) and Eurasian perch (*Perca fluviatilis*). *Aquat. Toxicol*. 104: 145-152.
- Blinova I, Niskanen J, Kajankari P, Kanarvik L, Käkinen A, Tenhu h, Penttinen O-P, Kahru A. 2013. Toxicity of two types of silver nanoparticles to aquatic crustaceans *Daphnia magna* and *Thamnocephalus platyurus*. *Environ. Sci. Pollut. Res*. 20: 3456-3463.
- Dorjnamjin D, Ariunaa M and Shim YK. 2008. Synthesis of silvernanoparticles using hydroxyl functionalized ionic liquids and their antimicrobial activity. *Int. J. Mol. Sci*. 9: 807-819.
- Dudgeon D, Arthington AH, Gessner MO, Kawabata Z-I, Knowler DJ, Lévêque C, Naiman RJ, Prieur-Richard A-H, Soto D, Stiassny MLJ, Sullivan CA. 2006. Freshwater biodiversity: importance, threats, status and conservation challenges. *Biol. Rev*. 81: 163-182.
- Fabrega J, Luoma SN, Tyler CR, Galloway TS, Lead JR. 2011. Silver nanoparticles: Behaviour and effects in the aquatic environment. *Environment International*. 37: 517-531.

- Fernandes I, Seena S, Pascoal C, Cássio F. 2014. Elevated temperature may intensify the positive effects of nutrients on microbial decomposition in streams. *Freshwater Biol.* 59: 2390-2399.
- Gil-Allué C, Schirmer K, Tlili A, Gessner MO and Behra R. 2015. Silver nanoparticle effects on stream periphyton during short-term exposures. *Environ. Sci. Technol.* 49: 1165-1172.
- Huang C, Wang R, Zeng G, Huang D, Lai C, Zhang J, Xiao Z, Wan J, Xu P, Gong X, Xue W, Ren X. 2018. Transcriptome analysis reveals novel insights into the response to Pb exposure in *Phanerochaete chrysosporium*. *Chemosphere.* 194: 657-665.
- Kalishwaralal K, BarathManiKanth S, Pandian SRK, Deepak V, Gurunathan S. 2010. Silver nanoparticles impede the biofilm formation by *Pseudomonas aeruginosa* and *Staphylococcus epidermidis*. *Colloids Surf. B.* 79: 340-344.
- Kim HR, Kim MJ, Lee SY, Oh SM and Chung KH. 2011. Genotoxic effects of silver nanoparticles stimulated by oxidative stress in human normal bronchial epithelial (BEAS-2B) cells. *Mutat. Res.* 726: 129-135.
- Kim J, Kim S, Lee S. 2011. Differentiation of the toxicities of silver nanoparticles and silver ions to the Japanese medaka (*Oryzias latipes*) and the cladoceran *Daphnia magna*. *Nanotoxicology.* 5: 208-214.
- Kumar N, Palmer GR, Shah V, Walker VK. 2014. The effect of silver nanoparticles on seasonal change in arctic tundra bacterial and fungal assemblages. *PLoS One* 9: e99953-10.
- Kvitek L, Panacek A, Soukupova J, Kolar M, Vecerova R, Pucek R, Holecova M, Zboril R. 2008. Effect of surfactants and polymers on stability and antibacterial activity of silver nanoparticles (NPs). *J. Phys. Chem. C.* 112: 5825-5834.
- Lubrano V and Balzan S. 2015. Enzymatic antioxidant system in vascular inflammation and coronary artery disease. *World J. Exp. Med.* 5: 218-224.
- Meyer JN, Lord CA, Yang XY, Turner EA, Badireddy AR, Marinakos SM, Chilkoti A, Wiesner MR, Auffan M. 2010. Intracellular uptake and associated toxicity of silver nanoparticles in *Caenorhabditis elegans*. *Aquat. Toxicol.* 100: 140-150.
- Middelkoop H. 2000. Heavy metal pollution of the river Rhine and Meuse floodplains in the Netherlands. *Neth. J. Geosci.* 79: 411-428.
- Mirzajani F, Askari H, Hamzelou S, Schober Y, Römpf A, Ghassempour A, Spengler B. 2014. Proteomics study of silver nanoparticles toxicity on *Bacillus thuringiensis*. *Ecotoxicol. and Environ. Safety.* 100: 122-130.
- Moore-Landecker E. 2002. Fungal Spores. In: *Encyclopedia of life sciences (eLS)*. John Wiley & Sons Ltd, Chichester.
- Nair PMG and Chung IM. 2015. Alteration in the expression of antioxidant and detoxification genes in *Chironomus riparius* exposed to zinc oxide nanoparticles. *Comp. Biochem. Phys. B.* 190: 1-7.
- Nair PMG, Park SY and Choi J. 2013. Evaluation of the effect of silver nanoparticles and silver ions using stress responsive gene expression in *Chironomus riparius*. *Chemosphere.* 92: 592-599.
- Navarro E, Wagner B, Odzak N, Sigg L, Behra R. 2015. Effects of differently coated silver nanoparticles on the photosynthesis of *Chlamydomonas reinhardtii*. *Environ. Sci. Technol.* 49: 8041-8047.

- Niu C, Yu D, Wang Y, Ren H, Jin Y, Zhou W, Li B, Cheng Y, Yue J, Gao Z and Liang L. 2013. Common and pathogen-specific virulence factors are different in function and structure. *Virulence*. 4: 473-482.
- Park EJ, Yi J, Kim Y, Choi K, Park K. 2010. Silver nanoparticles induce cytotoxicity by a Trojan-horse type mechanism. *Toxicol. In Vitro*. 24: 872-878.
- Poynton HC, Lazorchak JM, Impellitteri CA, Blalock BJ, Rogers K, Allen HJ, Loguinov A, Heckman JM, Govindasmawly S. 2012. Toxicogenomic responses of nanotoxicity in *Daphnia magna* exposed to silver nitrate and coated silver nanoparticles. *Environ. Sci. Technol.* 46: 6288-6296.
- Pradhan A, Silva CO, Silva C, Pascoal C, Cássio F. 2016. Enzymatic biomarkers can portray nanoCuO-induced oxidative and neuronal stress in freshwater shredders. *Aquat Toxicol.* 180: 227-235.
- Pradhan A, Seena S, Schlosser D, Gerth K, Helm S, Dobritzsch M, Krauss G-J, Dobritzsch D, Pascoal C and Cássio F. 2015. Fungi from metal-polluted streams may have high ability to cope with the oxidative stress induced by copper oxide nanoparticles. *Environ. Toxicol. Chem.* 34: 923-930.
- Pradhan A, Seena S, Pascoal C, Cássio F. 2011. Can metal nanoparticles be a threat to microbial decomposers of plant litter in streams? *Microb. Ecol.* 62: 58-68.
- Ram Y and Hadany L. 2016. Condition-dependent sex: who does it, when and why? *Phil. Trans. R. Soc. B.* 371: 20150539.
- Santos PM, Roma V, Benndorf D, von Bergen M, Harms H, Sá-Correia I. 2007. Mechanistic insights into the global response to phenol in the phenol-biodegrading strain *Pseudomonas* sp. M1, revealed by quantitative proteomics. *OMICS*. 11: 233-251.
- Santos PM, Simões T, Sá-Correia I. 2009. Insights into yeast adaptive response to the agricultural fungicide mancozeb: a toxicoproteomics approach. *Proteomics*. 9: 657-670.
- Sharma V, Anderson D and Dhawan A. 2011. Zinc oxide nanoparticles induce oxidative stress and genotoxicity in human liver cells (HepG2). *J. Biomed. Nanotechnol.* 7: 98-99.
- Singh BR, Singh BN, Singh A, Khan W, Naqvi AH and Singh HB. 2015. Mycofabricated biosilver nanoparticles interrupt *Pseudomonas aeruginosa* quorum sensing systems. *Sci. Rep.* 5:13719.
- Soares HMVM, Boaventura RAR, Machado AASC, Esteves da Silva JCG. 1999. Sediments as monitors of heavy metal contamination in the Ave river basin (Portugal): multivariate analysis of data. *Environ. Pollut.* 105: 311-323.
- Soldo D and Behra R. 2000. Long-term effects of copper on the structure of freshwater periphyton communities and their tolerance to copper, zinc, nickel and silver. *Aquat. Toxicol.* 47: 181-189.
- Su GY, Zhang XW, Giesy JP, Musarrat J, Saquib Q, Alkhedhairi AA and Yu HX. 2015. Comparison on the molecular response profiles between nano zinc oxide (ZnO) particles and free zinc ion using a genome-wide toxicogenomics approach. *Environ. Sci. Pollut. Res.* 22: 17434-17442.
- Teixeira MC, Santos PM, Fernandes AR, Sá-Correia I. 2005. Proteome analysis of the yeast response to the herbicide 2,4-dichlorophenoxyacetic acid. *Proteomics*. 5: 1889-1901.
- Tlili A, Cornut J, Behra R, Gil-Allué C and Gessner MO. 2016. Harmful effects of silver nanoparticles on a complex detrital model system. *Nanotoxicology*. 10: 728-735.

- Tlili A, Marechal M, Berard A, Volat B and Montuelle B. 2011. Enhanced co-tolerance and co-sensitivity from long-term metal exposures of heterotrophic and autotrophic components of fluvial biofilms. *Sci. Total Environ.* 409: 4335-4343.
- Vega FA and Weng LP. 2013. Speciation of heavy metals in River Rhine. *Water Res.* 47: 363-372.
- Völker C, Kampken I, Boedicker C, Oehlmann J and Oetken M. 2015. Toxicity of silver nanoparticles and ionic silver: comparison of adverse effects and potential toxicity mechanisms in the freshwater clam *Sphaerium corneum*. *Nanotoxicology.* 9: 677-685.
- Williamson CE, Dodds W, Kratz TK, Palmer MA. 2008. Lakes and streams as sentinels of environmental change in terrestrial and atmospheric processes. *Front. Ecol. Environ.* 6: 247-254.
- Zhao CM and Wang WX. 2011. Comparison of acute and chronic toxicity of silver nanoparticles and silver nitrate to *Daphnia magna*. *Environ. Toxicol. Chem.* 30: 885-892.
- Zheng H, Wang J, Chen Y, Wei Y. 2018. Comprehensive analysis of transcriptional and proteomic profiling reveals silver nanoparticles-induced toxicity to bacterial denitrification. *J. Hazard Mater.* 344: 291-298.

Appendix

Appendix 1_Chapter 2

Table S2.1. Enzyme activity fold-changes (with respect to control) of superoxide dismutase (SOD), glutathione S-transferase (GST), glutathione peroxidase (GPx) and catalase (CAT) in *Pseudomonas* sp. M1 exposed or not to Ag⁺ or AgNPs for 90 minutes.

Enzyme	Concentration ($\mu\text{g L}^{-1}$)	Enzyme activity in fold-change	
		Ag ⁺	AgNPs
SOD	50	3.04*	1.52
	100	6.67*	1.94*
	200	-	2.83*
	300	-	5.83*
GST	50	1.35	1.14
	100	1.76	1.23
	200	-	1.38
	300	-	1.59
GPx	50	2.95*	1.59
	100	4.18*	2.51*
	200	-	3.11*
	300	-	4.34*
CAT	50	1.13	1.16
	100	2.74*	1.99*
	200	-	2.69*
	300	-	1.36

-. not determined; *. treatments that differ significantly from the respective control (Dunnett's test. $P < 0.05$).

Appendix 2_Chapter 2

Protein identification by mass spectrometry

In gel Digestion/Sample Preparation

After denaturation, the proteins were alkylated with acrylamide and subjected to in gel digestion by using the short-GeLC approach (Anjo et al 2014). Briefly, gel pieces were destained using the destaining solution (50 mM ammonium bicarbonate and 30% acetonitrile) following by a washing step with water. Gel pieces were dehydrated on Concentrador Plus/Vacufuge® Plus (Eppendorf). Trypsin (0.01 µg/µL solution in 10 mM ammonium bicarbonate) was added to the dried gel bands and left for 15 min on ice to rehydrate the gel pieces. After this, 10 mM ammonium bicarbonate were added to cover the rehydrated bands and in-gel digestion was performed overnight at room temperature in the dark. The excess solution from gel pieces were collected to in a low binding microcentrifuge tube (LoBind®, Eppendorf) and peptides were extracted from the gel pieces by sequential addition of acetonitrile (ACN) in 1% formic acid (FA) (30%, 50%, and 98% of ACN). Then, the tubes were shaken in the thermomixer (Eppendorf) at 1050 rpm for 15 min and solutions were collected to the tube containing the previous fraction. All the peptide mixtures were dried (not completely) by rotary evaporation under vacuum.

Before performing the LC-MS/MS, analysis the peptide mixtures were subjected to SPE using OMIX tips with C18 stationary phase (Agilent Technologies) as recommended by the manufacture. Eluates were dried by rotator evaporation, avoiding to totally evaporate the samples, and peptide mixtures were resuspended in 30 µL of 2% ACN and 0.1% FA containing iRT peptides (Biognosys AG) as internal standards, followed by vortex, spin and sonication in a water bath (2 min; pulses of 1 sec sonication followed by 1 sec resting, at 20% intensity, in a sonicatorVibraCell 750 watts, Sonics®; Sonics & Materials). In order to remove insoluble material, the peptide mixtures were centrifuged for 5 min at 14000 × *g* and collected into proper vials for LC-MS injection. Five µL of each replicate sample was combined to obtain one pooled sample per experimental condition (in a total of four pools), to be used for protein identification and SWATH-library generation.

SWATH acquisition

Samples were analyzed on a Triple TOF™ 5600 System (ABSciex®) in two phases: information-dependent acquisition (IDA) of the pooled samples, and SWATH (Sequential Windowed data independent Acquisition of the Total High-resolution Mass Spectra) acquisition of each individual sample. Peptides were resolved by liquid chromatography (nanoLC Ultra 2D, Eksigent®) on a MicroLC column ChromXP™ C18CL (300 µm ID × 15cm length, 3 µm particles, 120 Å pore size, Eksigent®) at 5 µL min⁻¹ with a multistep gradient: 0-1 min of 2% acetonitrile in 0.1 % FA and, 2-45 min linear gradient from 2 % to 30 % of acetonitrile in 0.1 % FA. Peptides were eluted into the mass spectrometer using an

electrospray ionization source (DuoSpray™ Source. ABSciex®) with a 50 µm internal diameter (ID) stainless steel emitter (NewObjective).

Information dependent acquisition (IDA) experiments were performed for each pooled sample. The mass spectrometer was set for IDA scanning full spectra (350-1250 m/z) for 250 ms. followed by up to 20 MS/MS scans (100-1500 m/z for 100 ms each). Candidate ions with a charge state between +2 and +5 and counts above 70 counts per sec were isolated for fragmentation. and 1 MS/MS spectra was collected before adding the ions to the exclusion list for 20 sec (mass spectrometer operated by Analyst® TF 1.6. AB Sciex). Rolling collision energy was used with a collision energy spread of 5. Peptide identification and library generation were performed with Protein Pilot software (v5.1. ABSciex®). using the following parameters: i) search against a database composed by the genus *Pseudomonas* from the SwissProt database (release at June 2015); ii) acrylamide alkylated cysteines as fixed modification; iii) trypsin as digestion type. and iv) allowing biological modifications. An independent False Discovery Rate (FDR) analysis using the target-decoy approach provided with Protein Pilot software was used to assess the quality of the identifications and positive identifications were considered when identified proteins and peptides reached a 5% local FDR (Tang et al 2008. Sennels et al 2009).

For SWATH-MS based experiments. the mass spectrometer was operated in a looped product ion mode (Gillet et al 2012) and the same chromatographic conditions used as in the IDA run described above. The instrument was specifically tuned to allow a quadrupole resolution of 25-m z⁻¹ mass selection. Using an isolation width of 26 m z⁻¹ (containing 1 m z⁻¹ for the window overlap). a set of 30 overlapping windows was constructed covering the precursor mass range of 350-1100 m z⁻¹. A 50 ms survey scan (350-1250 m z⁻¹) was acquired at the beginning of each cycle for instrument calibration and SWATH-MS/MS spectra were collected from 100-1500 m z⁻¹ for 100 ms resulting in a cycle time of 3.25 sec from the precursors ranging from 350 to 1100 m z⁻¹. The collision energy for each window was determined according to the calculation for a charge 2+ ion centred upon the window with a collision energy spread of 15.

A specific library of precursor masses and fragment ions was created by combining all files from the IDA experiments. and used for subsequent SWATH processing. Libraries were obtained using Protein Pilot™ software (v5.1. ABSciex®) with the same parameters as described above. Data processing was performed using SWATH™ processing plug-in for PeakView™ (v2.0.01. ABSciex®). Briefly. peptides were selected automatically from the library using the following criteria: i) the unique peptides for a specific targeted protein were ranked by the intensity of the precursor ion from the IDA analysis as estimated by the ProteinPilot™ software. and ii) peptides that shared different protein entries/isoforms were excluded from selection. Up to 15 peptides were chosen per protein. and SWATH™ quantitation was attempted for all proteins in the library file that were identified below 5% local FDR from ProteinPilot™ searches. In SWATH™ Acquisition data. peptides were confirmed by finding and scoring peak groups. which are a set of fragment ions for the peptide.

Target fragment ions, up to 5, were automatically selected and peak groups were scored following the criteria described by Lambert et al (2013). Peak group confidence threshold was determined based on a FDR analysis using the target-decoy approach and 1% extraction FDR threshold was used for all the analyses. Peptide that met 1% FDR threshold in at three of the four biological replicates were retained, and the peak areas of the target fragment ions of those peptides were extracted across the experiments using an extracted-ion chromatogram (XIC) window of 5 minutes with 20 mDa XIC width. The levels of the proteins were estimated by summing all transitions from all the filtered peptides for a given protein (an adaptation of Collins et al 2013) and normalized to the total intensity.

Appendix 3_Chapter 2

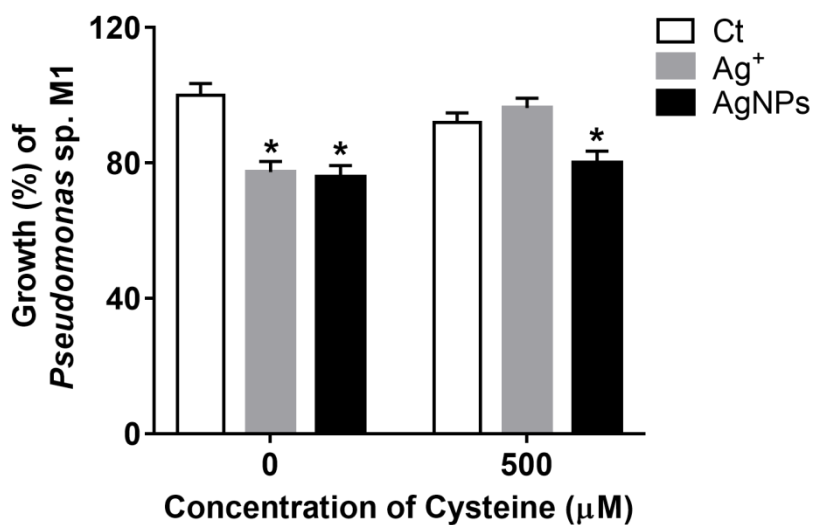


Figure S2.1 Effects of the Ag⁺-ligand cysteine on growth of *Pseudomonas sp. M1* in MM medium with 0.4% lactate at 30°C for 90 minutes in the absence (Ct) or presence of Ag⁺ (at EC₂₀) or AgNPs (at EC₂₀). Results are expressed as percentage of the unexposed control (unexposed to cysteine or either form of silver). Asterisks indicate significant differences from the unexposed control according to post-hoc Dunnett's multiple comparisons test ($P < 0.01$). Mean \pm SEM. $n = 3$.

Appendix 4_Chapter 2

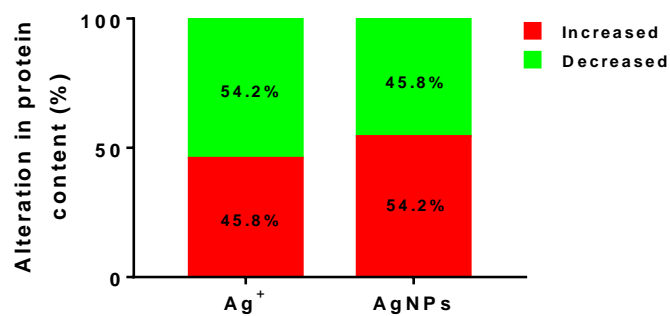


Figure S2.2. Percentages of significantly altered proteins in exposure to Ag⁺ or AgNPs. The contents of proteins increased (in red) or decreased (in green) were calculated in relation to the total number of identified proteins (59 proteins).

Appendix 5_Chapter 2

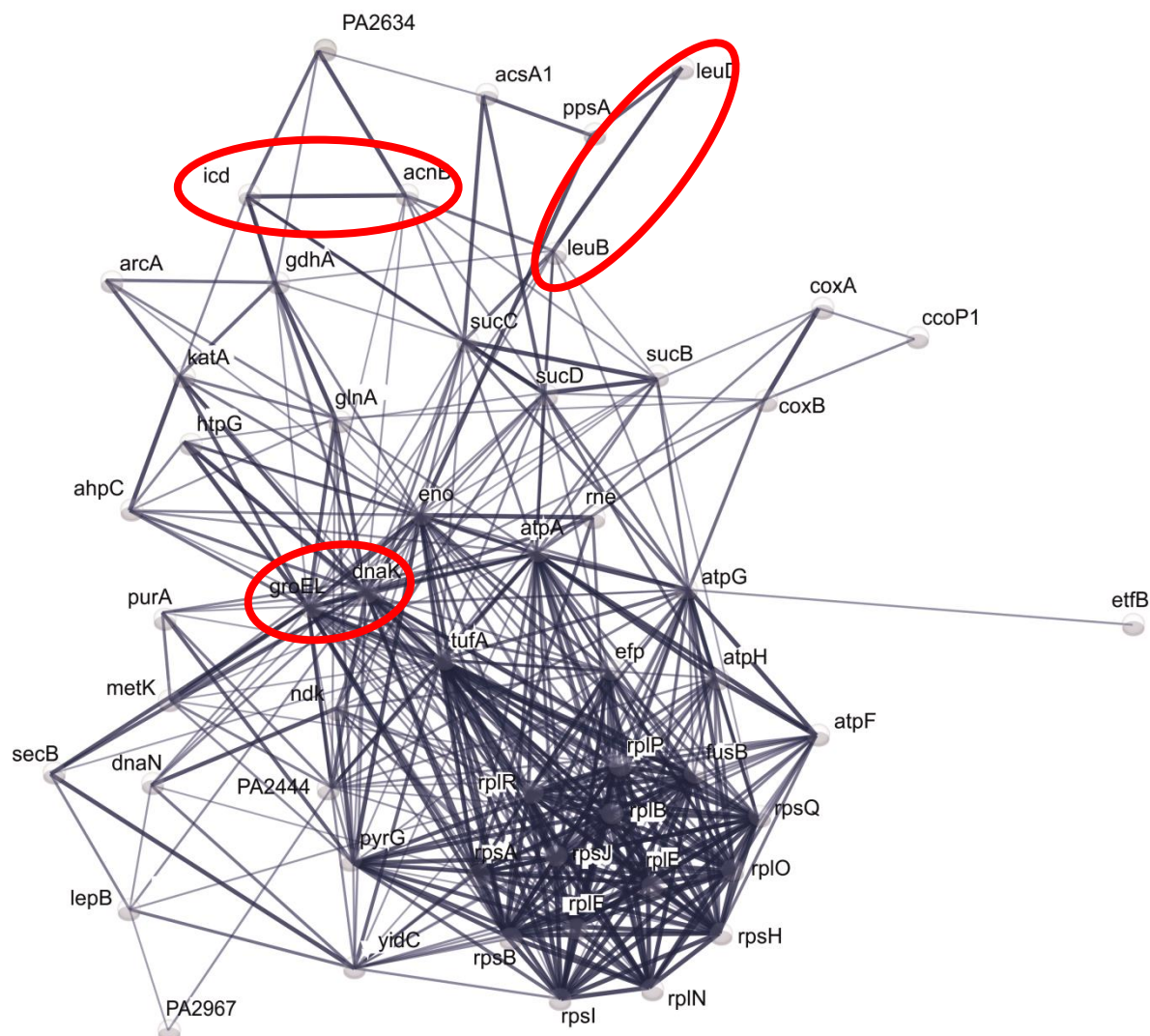






Figure S2.3 Protein networks in *Pseudomonas aeruginosa* adapted from STRING database. The network includes the proteins altered by Ag^+ and AgNPs in *Pseudomonas* sp. M1 and identified in *P. aeruginosa*. Stronger associations among the proteins are represented by thicker lines. Databases. experiments. textmining. co-expression. neighbourhood. gene fusion and co-occurrence were selected as active interaction sources. Edge confidence: low (0.15) , medium (0.40) , high (0.70) , highest (0.90) . The associations between key proteins were highlighted in red.

Appendix 6_Chapter 2

Table S2.2. Total identified proteins by SWATH-MS/MS from SDS-PAGE gels with (protein crude) extracts from cells of *Pseudomonas* sp. M1 grown in lactate supplemented mineral medium (MM; as described by Hartmans et al. 1989) in presence or absence of Ag⁺ or AgNPs for 90 minutes. Relative alteration of protein content (average fold change relative to control) of statistically significant proteins ($P < 0.05$) and respective cluster inclusion group are shaded in light grey. Positive and negative fold changes suggest increase and decrease in the protein content. respectively.

Accession number	Protein Name	ANOVA (<i>P</i> -value)	Average fold change ^a		Cluster ^b
			Ag ⁺	AgNPs	
ETM69128.1	30S ribosomal protein S8 RpsH	0.003	-1.077	0.317	1
ETM69126.1	50S ribosomal protein L5	0.003	-0.083	0.210	1
ETM66430.1	30S ribosomal protein S1	0.006	-0.085	0.343	1
ETM69113.1	30S ribosomal protein S10 RpsJ	0.007	-0.254	0.375	1
ETM64203.1	transcriptional regulator	0.007	0.446	1.320	1
ETM69123.1	30S ribosomal protein S17	0.010	-0.336	0.056	1
ETM65842.1	30S ribosomal protein S9	0.015	-0.310	0.067	1
ETM66170.1	membrane protein	0.018	1.648	2.324	1
ETM69133.1	50S ribosomal protein L15	0.018	-0.489	0.124	1
ETM67937.1	30S ribosomal protein S2	0.027	-0.151	0.151	1
ETM64865.1	S-adenosylmethionine synthase	0.045	-0.067	1.450	1
ETM66535.1	transcriptional regulator	0.046	0.139	0.789	1
ETM64930.1	glutamine synthetase	0.046	-0.008	0.454	1
ETM69112.1	elongation factor Tu Tuf	0.000	-0.424	-2.080	2
ETM68814.1	isocitrate dehydrogenase	0.000	0.951	-1.041	2
ETM65642.1	serine hydroxymethyltransferase	0.000	0.142	-2.218	2
ETM67938.1	elongation factor Ts Tsf	0.001	-0.301	-2.539	2
ETM66843.1	succinyl-CoA synthetase subunit alpha	0.001	-0.240	-0.675	2
ETM66664.1	aconitate hydratase B AcnB	0.001	0.370	-0.899	2
ETM64607.1	alkyl hydroperoxide reductase subunit C AhpC	0.002	-0.384	-2.682	2

Accession number	Protein Name	ANOVA (<i>P</i> -value)	Average fold change ^a		Cluster ^b
			Ag ⁺	AgNPs	
ETM65247.1	L-lactate permease	0.005	0.266	-0.759	2
ETM65393.1	purine biosynthesis protein purH	0.005	-0.076	-1.470	2
ETM64939.1	preprotein translocase subunit SecB	0.014	-0.141	-0.515	2
ETM63932.1	electron transfer flavoprotein subunit beta	0.019	-0.350	-1.962	2
ETM63915.1	3-ketoacyl-ACP reductase	0.026	-0.150	-1.397	2
ETM65886.1	molecular chaperone GroES	0.027	-0.173	-0.899	2
ETM67957.1	CTP synthetase	0.032	0.153	-0.507	2
ETM65487.1	adenylosuccinate synthetase	0.037	-0.499	-2.017	2
ETM66453.1	isopropylmalate isomerase LeuC	0.000	-1.473	-3.010	3
ETM66454.1	3-isopropylmalate dehydratase small subunit LeuD	0.000	-2.260	-3.138	3
ETM66206.1	hypothetical protein PM1_Q208385	0.000	-2.121	-1.807	3
ETM67686.1	nucleoside diphosphate kinase	0.000	-0.730	-1.943	3
ETM69111.1	elongation factor G	0.000	-0.772	-1.733	3
ETM66456.1	3-isopropylmalate dehydrogenase LeuB	0.000	-1.488	-2.606	3
ETM66285.1	acetyl-CoA synthetase	0.002	-1.797	-1.987	3
ETM67959.1	Enolase	0.004	-0.635	-1.752	3
ETM65137.1	Endoribonuclease	0.017	-1.066	-2.689	3
ETM63983.1	elongation factor P	0.023	-1.170	-3.568	3
ETM65645.1	glutamate dehydrogenase	0.036	-2.063	-1.048	3
ETM69050.1	spermidine/putrescine ABC transporter substrate-binding protein	0.037	-1.549	-3.454	3
ETM66840.1	dihydrolipoamide succinyltransferase	0.001	0.403	0.492	4
ETM65239.1	molecular chaperone DnaK	0.001	1.168	0.454	4
ETM69176.1	outer membrane protein W	0.001	1.230	0.226	4
ETM63384.1	cytochrome CBB3	0.001	1.287	0.560	4
ETM68644.1	phosphoenolpyruvate synthase	0.003	1.157	0.365	4
ETM64990.1	arginine deiminase	0.003	0.981	0.534	4

Accession number	Protein Name	ANOVA (<i>P</i> -value)	Average fold change ^a		Cluster ^b
			Ag ⁺	AgNPs	
ETM66534.1	Peptidase	0.005	1.165	0.780	4
ETM67390.1	H-NS histone	0.005	0.741	0.598	4
ETM68804.1	isocitrate lyase	0.008	1.960	0.848	4
ETM65887.1	molecular chaperone GroEL	0.008	0.761	0.407	4
ETM68650.1	Porin	0.009	0.936	0.379	4
ETM68113.1	Porin	0.009	0.846	0.218	4
ETM65223.1	peptidase M54	0.012	0.336	0.264	4
ETM63387.1	cytochrome oxidase subunit I	0.015	1.021	0.700	4
ETM69141.1	catalase/hydroperoxidase HPI(I) KatG	0.017	1.578	0.739	4
ETM68466.1	membrane protein	0.021	1.791	1.300	4
ETM64574.1	FOF1 ATP synthase subunit alpha	0.024	0.499	0.373	4
ETM64558.1	DNA polymerase III subunit beta	0.042	1.039	1.218	4
ETM66851.1	heat shock protein 90	0.043	1.145	0.102	4
ETM65482.1	30S ribosomal protein S18	0.056			
ETM67796.1	30S ribosomal protein S16	0.061			
ETM66001.1	adenine methyltransferase	0.061			
ETM66837.1	succinate dehydrogenase flavoprotein subunit	0.061			
ETM69130.1	50S ribosomal protein L18	0.066			
ETM69124.1	50S ribosomal protein L14	0.067			
ETM69119.1	50S ribosomal protein L22	0.073			
ETM66842.1	malate--CoA ligase subunit beta	0.075			
ETM63981.1	Major outer membrane lipoprotein	0.077			
ETM64891.1	glucan biosynthesis protein D	0.080			
ETM69106.1	50S ribosomal protein L7/L12	0.081			
ETM64287.1	pyruvate carboxylase	0.085			
ETM64571.1	FOF1 ATP synthase subunit C	0.087			
ETM63916.1	acyl carrier protein	0.088			

Accession number	Protein Name	ANOVA (<i>P</i> -value)	Average fold change ^a		Cluster ^b
			Ag ⁺	AgNPs	
ETM69116.1	50S ribosomal protein L23	0.093			
ETM65599.1	50S ribosomal protein L25	0.099			
ETM65822.1	UDP-N-acetylglucosamine 1-carboxyvinyltransferase	0.099			
ETM64991.1	ornithine carbamoyltransferase	0.100			
ETM65218.1	polynucleotide phosphorylase/polyadenylase	0.105			
ETM67644.1	DNA-binding protein	0.106			
ETM65600.1	ribose-phosphate pyrophosphokinase	0.110			
ETM64998.1	dihydroxy-acid dehydratase	0.111			
ETM66300.1	alanyl-tRNA synthetase	0.113			
ETM64556.1	DNA gyrase subunit B	0.113			
ETM68177.1	peptidyl-prolyl cis-trans isomerase	0.114			
ETM67711.1	inosine 5'-monophosphate dehydrogenase	0.124			
ETM66531.1	trigger factor	0.133			
ETM65234.1	carbamoyl phosphate synthase large subunit	0.135			
ETM65177.1	ketol-acid reductoisomerase	0.148			
ETM69137.1	30S ribosomal protein S4	0.160			
ETM67799.1	50S ribosomal protein L19	0.162			
ETM65249.1	4Fe-4S ferredoxin	0.162			
ETM69121.1	50S ribosomal protein L16	0.166			
ETM63881.1	glyceraldehyde-3-phosphate dehydrogenase	0.167			
ETM67675.1	inositol monophosphatase	0.171			
ETM69125.1	50S ribosomal protein L24	0.194			
ETM69139.1	50S ribosomal protein L17	0.195			
ETM65841.1	50S ribosomal protein L13	0.197			
ETM65818.1	organic solvent ABC transporter substrate-binding protein	0.201			
ETM69136.1	30S ribosomal protein S11	0.205			
ETM64827.1	pyruvate dehydrogenase	0.209			

Accession number	Protein Name	ANOVA (<i>P</i> -value)	Average fold change ^a		Cluster ^b
			Ag ⁺	AgNPs	
ETM64889.1	amino acid ABC transporter substrate-binding protein	0.211			
ETM69135.1	30S ribosomal protein S13	0.217			
ETM64267.1	phosphoenolpyruvate carboxykinase	0.217			
ETM63814.1	glutamate dehydrogenase	0.222			
ETM64575.1	F0F1 ATP synthase subunit gamma	0.233			
ETM63869.1	topoisomerase I	0.233			
ETM69108.1	DNA-directed RNA polymerase subunit beta'	0.241			
ETM69189.1	6.7-dimethyl-8-ribityllumazine synthase	0.275			
ETM69022.1	RNA polymerase sigma factor RpoD	0.276			
ETM69127.1	30S ribosomal protein S14	0.276			
ETM68777.1	type III restriction endonuclease subunit R	0.279			
ETM69144.1	single-stranded DNA-binding protein	0.283			
ETM65248.1	L-lactate dehydrogenase	0.301			
ETM67464.1	hypothetical protein PM1_0214880	0.307			
ETM69138.1	DNA-directed RNA polymerase subunit alpha	0.318			
ETM69115.1	50S ribosomal protein L4	0.320			
ETM68502.1	50S ribosomal protein L20	0.336			
ETM69109.1	30S ribosomal protein S12	0.341			
ETM64576.1	F0F1 ATP synthase subunit beta	0.341			
ETM67783.1	phosphoribosylformylglycinamide synthase	0.341			
ETM65236.1	carbamoyl phosphate synthase small subunit	0.343			
ETM64846.1	glutamate synthase subunit alpha	0.352			
ETM65543.1	leucyl-tRNA synthetase	0.364			
ETM69103.1	50S ribosomal protein L11	0.365			
ETM65788.1	glutamyl-tRNA(Gln) amidotransferase	0.375			
ETM64828.1	dihydrolipoamide acetyltransferase	0.384			
ETM69107.1	DNA-directed RNA polymerase subunit beta	0.396			

Accession number	Protein Name	ANOVA (<i>P</i> -value)	Average fold change ^a		Cluster ^b
			Ag ⁺	AgNPs	
ETM63386.1	peptidase S41	0.403			
ETM68119.1	aspartyl-tRNA synthetase	0.421			
ETM65222.1	translation initiation factor IF-2	0.430			
ETM69105.1	50S ribosomal protein L10	0.453			
ETM69117.1	50S ribosomal protein L2	0.456			
ETM66131.1	argininosuccinate synthase	0.462			
ETM69023.1	30S ribosomal protein S21	0.477			
ETM69101.1	preprotein translocase subunit SecE	0.524			
ETM65480.1	50S ribosomal protein L9	0.532			
ETM66834.1	type II citrate synthase	0.539			
ETM65120.1	50S ribosomal protein L28	0.541			
ETM69131.1	30S ribosomal protein S5	0.597			
ETM65488.1	ATP phosphoribosyltransferase	0.601			
ETM65031.1	3-phosphoglycerate dehydrogenase	0.616			
ETM68813.1	isocitrate dehydrogenase	0.635			
ETM64886.1	DEAD/DEAH box helicase	0.673			
ETM66836.1	succinate dehydrogenase	0.712			
ETM69129.1	50S ribosomal protein L6	0.748			
ETM65870.1	preprotein translocase subunit SecA	0.754			
ETM66301.1	aspartokinase	0.785			
ETM66838.1	succinate dehydrogenase iron-sulfur subunit	0.796			
ETM65179.1	acetolactate synthase	0.803			
ETM64288.1	acetyl-CoA carboxylase subunit alpha	0.821			
ETM65706.1	competence protein	0.836			
ETM69120.1	30S ribosomal protein S3	0.838			
ETM67463.1	hypothetical protein PM1_0214875	0.859			
ETM69102.1	transcription antitermination protein NusG	0.863			

Accession number	Protein Name	ANOVA (<i>P</i> -value)	Average fold change ^a		Cluster ^b
			Ag ⁺	AgNPs	
ETM64572.1	FOF1 ATP synthase subunit B	0.863			
ETM66841.1	dihydrolipoamide dehydrogenase	0.867			
ETM64208.1	uroporphyrin-III C-methyltransferase	0.889			
ETM69110.1	30S ribosomal protein S7	0.912			
ETM67885.1	lysyl-tRNA synthetase	0.917			
ETM69104.1	50S ribosomal protein L1	0.924			
ETM65658.1	50S ribosomal protein L21	0.934			
ETM68450.1	ribonucleotide-diphosphate reductase subunit alpha	0.945			
ETM65219.1	30S ribosomal protein S15	0.953			
ETM69114.1	50S ribosomal protein L3	0.988			
ETM66839.1	2-oxoglutarate dehydrogenase E1	0.991			
ETM64883.1	adenosylhomocysteinase	0.992			

^a Values were calculated as the average data from at least four independent experiments. Fold changes of statistically significant proteins (ANOVA, $P < 0.05$) were determined by Log₂ transformation of the ratio values of normalized protein levels obtained using crude protein extracts from cells of *Pseudomonas* sp. M1 after 90 minutes of exposure to Ag⁺ or AgNPs at concentrations similar to EC₂₀ versus cells grown in control medium.

^b The unsupervised clustering analysis was performed considering standardization and the 59 statistically significant proteins across the different experimental conditions (Control. Ct; silver ions. Ag⁺ and silver nanoparticles. AgNPs) were partitioned into 4 clusters.

Appendix 7_Chapter 3

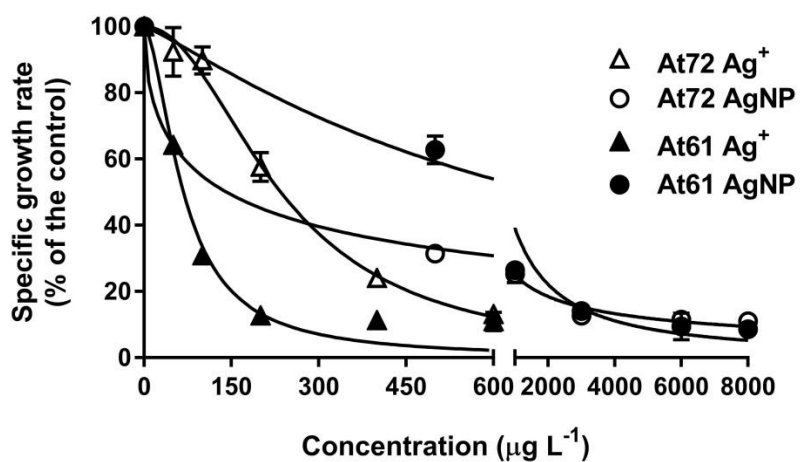


Figure S3.1. Effects of AgNPs (circles) or Ag⁺ (triangles) on the specific growth rate of *A. tetracladia* (strains At72 and At61). Data are percentage of the specific growth rate of the control culture (grown in the absence of AgNPs or Ag⁺) in malt extract liquid media (1% w/v). Specific growth rates are median values of three independent growth experiments. Mean \pm SEM.

Appendix 8_Chapter 3

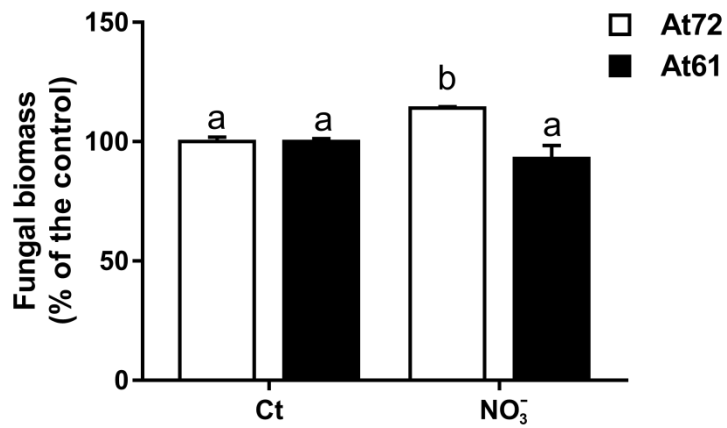


Figure S3.2. Fungal biomass produced by *A. tetracladia* (strains At72 and At61) after 3 days of growth followed by 3 days of growth with 18 $\mu\text{g L}^{-1}$ of nitrate as NaNO_3 (equivalent to the lowest tested AgNO_3 concentration in determination of ECs). Values are in % of respective control. Mean \pm SEM. $n = 3$. Different letters indicate significant differences ($P < 0.05$).

Appendix 9_Chapter 3

Table S3.1. Specific activities of catalase (CAT), superoxide dismutase (SOD), glutathione peroxidase (GPx) and glutathione S-transferase (GST) in *A. tetracladia* (strains At72 and At61) grown 6 days without addition of stressors (Ag⁺ or AgNPs). Mean \pm SEM. n = 3.

Fungal strain	Enzyme Activity (nanomol ⁻¹ min ⁻¹ mg ⁻¹ protein)			
	CAT	SOD	GPx	GST
At72	45.0 \pm 1.4	35.3 \pm 0.7	45.0 \pm 1.4	4.3 \pm 0.4
At61	31.5 \pm 2.9	34.8 \pm 2.0	47.7 \pm 1.1	4.6 \pm 0.3

Annex 10_Chapter 3

In gel Digestion/Sample Preparation

After denaturation, proteins were alkylated with acrylamide and subjected to in gel digestion by using the short-GeLC approach (Anjo et al 2015). Briefly, gel pieces were destained using the destaining solution (50 mM ammonium bicarbonate and 30% acetonitrile) following by a washing step with water. Gel pieces were dehydrated on Concentrador Plus/Vacufuge® Plus (Eppendorf). Four hundred μL of trypsin (0.01 $\mu\text{g}/\mu\text{L}$ solution in 10 mM ammonium bicarbonate) were added to the dried gel bands and left for 15 min. on ice. to rehydrate de gel pieces. After this, 100 μL of 10 mM ammonium bicarbonate were added and in-gel digestion was performed overnight at room temperature in the dark. After the digestion, the excess solution from gel pieces was collected in a low binding microcentrifuge tube (LoBind®, Eppendorf) and peptides were extracted from the gel pieces by sequential addition of three solutions of acetonitrile (ACN) in 1% formic acid (FA) (30%, 50%, and 98% of ACN, respectively). After the addition of each solution, the tubes were shaken in the thermomixer (Eppendorf) at 1050 rpm for 15 min and the solution was collected to the tube containing the previous fraction. All the peptides mixtures were dried (preferentially not completely) by rotary evaporation under vacuum.

Before performing the LC-MS/MS, analysis the peptide mixtures were subjected to SPE using OMIX tips with C18 stationary phase (Agilent Technologies) as recommended by the manufacture. Eluates were dried by rotator evaporation, avoiding to totally evaporate the samples and peptides mixtures were resuspended in 40 μL of 2% ACN and 0.1% FA containing iRT peptides (Biognosys AG) as internal standards, followed by vortex, spin and sonication in a water bath [(2 min; pulses of 1 sec sonication followed by 1 sec resting, at 20% intensity, in a sonicator VibraCell 750 watts, Sonics® (Sonics & Materials)]. In order to remove insoluble material, the peptide mixtures were centrifuged for 5 min at 14 000 $\times g$ and collected into proper vial for LC-MS injection. Ten μL of each biological replicate was combined to obtained one pooled sample per experimental condition (in a total of four pools), to be used for protein identification and SWATH-library generation.

SWATH acquisition

Samples were analyzed on a Triple TOF™ 5600 System (ABSciex®) in two phases: information-dependent acquisition (IDA) of the pooled samples and, SWATH (Sequential Windowed data independent Acquisition of the Total High-resolution Mass Spectra) acquisition of each individual sample. Peptides were resolved by liquid chromatography (nanoLC Ultra 2D, Eksigent®) on a MicroLC column ChromXP™ C18CL (300 μm ID \times 15cm length, 3 μm particles, 120 Å pore size, Eksigent®) at 5 $\mu\text{L min}^{-1}$ with a multistep gradient: 0-2 min linear gradient from 5 to 10 %, 2-45 min linear gradient from 10 % to 30 % and, 45-46 min to 35 % of acetonitrile in 0.1 % FA. Peptides were eluted into the mass spectrometer

using an electrospray ionization source (DuoSpray™ Source, ABSciex®) with a 50 µm internal diameter (ID) stainless steel emitter (NewObjective).

Information dependent acquisition (IDA) experiments were performed for each pooled sample. The mass spectrometer was set to scanning full spectra (350-1250 m/z) for 250 ms, followed by up to 100 MS/MS scans (100-1500 m/z from a dynamic accumulation time – minimum 30 ms for precursor above the intensity threshold of 1000 – in order to maintain a cycle time of 3.3 sec). Candidate ions with a charge state between +2 and +5 and counts above a minimum threshold of 10 counts per sec were isolated for fragmentation and 1 MS/MS spectra was collected before adding those ions to the exclusion list for 25 sec (mass spectrometer operated by Analyst® TF 1.7, ABSciex®). Rolling collision was used with a collision energy spread of 5. Peptide identification and library generation were performed with Protein Pilot software (v5.1, ABSciex®), using the following parameters: i) search against the SwissProt database (release at March 2016); ii) acrylamide alkylated cysteines as fixed modification; iii) trypsin as digestion type. An independent False Discovery Rate (FDR) analysis using the target-decoy approach provided with Protein Pilot software was used to assess the quality of the identifications and positive identifications were considered when identified proteins and peptides reached a 5% local FDR (Tang et al 2008, Sennels et al 2009). For SWATH-MS based experiments, the mass spectrometer was operated in a looped product ion mode (Gillet et al 2012) and the same chromatographic conditions used as in the IDA run described above. The SWATH-MS setup was designed specifically for the samples to be analyzed (Table S2), in order to adapt the SWATH windows to the complexity of the set of samples to be analyzed. A set of 60 windows of variable width (containing 1 m/z for the window overlap) was constructed covering the precursor mass range of 350-1250 m/z. A 250 ms survey scan (350-1500 m/z) was acquired at the beginning of each cycle for instrument calibration and SWATH MS/MS spectra were collected from 100–1500 m/z for 50 ms resulting in a cycle time of 3.25 sec from the precursors ranging from 350 to 1250 m/z. The collision energy for each window was determined according to the calculation for a charge +2 ion centered upon the window with variable collision energy spread (CES) according with the window.

A specific library of precursor masses and fragment ions was created by combining all files from the IDA experiments, and used for subsequent SWATH processing. Libraries were obtained using Protein Pilot™ software (v5.1, ABSciex®) with the same parameters as described above. Data processing was performed using SWATH™ processing plug-in for PeakView™ (v2.0.01, ABSciex®). Briefly, peptides were selected automatically from the library using the following criteria: (i) the unique peptides for a specific targeted protein were ranked by the intensity of the precursor ion from the IDA analysis as estimated by the ProteinPilot™ software, and (ii) peptides that contained biological modifications and/or were shared between different protein entries/isoforms were excluded from selection. Up to 15 peptides were chosen per protein, and SWATH™ quantitation was attempted for all proteins in library file that were identified below 5% local FDR from ProteinPilot™ searches.

In SWATH™ Acquisition data, peptides were confirmed by finding and scoring peak groups, which are a set of fragment ions for the peptide.

Target fragment ions, up to 5, were automatically selected and peak groups were scored following the criteria described in Lambert et al (2013). Peak group confidence threshold was determined based on a FDR analysis using the target-decoy approach and 1% extraction FDR threshold was used for all the analyses. Peptide that met the 1% FDR threshold in at three of the four biological replicates were retained, and the peak areas of the target fragment ions of those peptides were extracted across the experiments using an extracted-ion chromatogram (XIC) window of 5 min with 100 ppm XIC width. The levels of the proteins were estimated by summing all transitions from all the filtered peptides for a given protein (an adaptation of Collins et al 2013) and normalized to the total intensity.

References

- Anjo SI, Santa C and Manadas B. 2015. Short GeLC-SWATH: a fast and reliable quantitative approach for proteomic screenings. *Proteomics*. 15: 757-62.
- Tang WH, Shilov IV and Seymour SL. 2008. Nonlinear fitting method for determining local false discovery rates from decoy database searches. *J Proteome Res*. 7(9): p. 3661-7.
- Sennels L, Bukowski-Wills JC and Rappsilber J. 2009. Improved results in proteomics by use of local and peptide-class specific false discovery rates. *BMC Bioinformatics*. 10: p. 179.
- Gillet LC, Navarro P, Tate S, Röst H, Selevsek N, Reiter L, Bonner R, Aebersold R. 2012. Targeted data extraction of the MS/MS spectra generated by data-independent acquisition: a new concept for consistent and accurate proteome analysis. *Mol. Cell Proteomics*. 11(6).
- Lambert JP, Ivosev G, Couzens AL, Larsen B, Taipale M, Lin ZY, Zhong Q, Lindquist S, Vidal M, Aebersold R, Pawson T, Bonner R, Tate S and Gingras AC. 2013. Mapping differential interactomes by affinity purification coupled with data-independent mass spectrometry acquisition. *Nat Methods*. 10(12): 1239-45.
- Collins BC, Gillet LC, Rosenberger G, Röst HL, Vichalkovski A, Gstaiger M, Aebersold R. 2013. Quantifying protein interaction dynamics by SWATH mass spectrometry: application to the 14-3-3 system. *Nat Methods*. 10(12): 1246-53.

Appendix 11_Chapter 3

Table S3.2 Total identified proteins by SWATH-MS/MS from SDS-PAGE gels with (protein crude) extracts from mycelia of *A. tetracladia* (strain At72) grown in malt extract medium (ME 1%) in presence or absence of Ag⁺ or AgNPs for 3 days. Relative alteration of protein content (average fold change relative to control) of statistically significant proteins ($P < 0.05$) and respective cluster inclusion group are shaded in light grey. Positive and negative fold changes suggest increase and decrease in the protein content, respectively.

Accession no.	UniProt recommended Protein name	Fold change ^a		ANOVA p-value	Cluster ^b	Common to At61
		Ag ⁺	AgNPs			
Q4K7C1	Protein translocase subunit SecA	0.60	0.96	0.00	1	
Q03134	Formate dehydrogenase (FDH) (EC 1.2.1.2) (Acetate inducible protein A) (NAD-dependent formate dehydrogenase)	0.91	0.90	0.00	1	
G5EB89	Importin subunit alpha (Karyopherin alpha)	0.89	1.05	0.00	1	
P32936	Alpha-amylase/trypsin inhibitor CMb (Chloroform/methanol-soluble protein CMb)	0.86	0.95	0.00	1	
Q9C3Z6	60S acidic ribosomal protein P0	1.30	0.99	0.00	1	y
Q5R9Y4	Ras-related protein Rab-7a	1.02	0.99	0.00	1	y
Q9ZP06	Malate dehydrogenase 1, mitochondrial (EC 1.1.1.37) (Mitochondrial MDH1) (mMDH1) (Mitochondrial NAD-dependent malate dehydrogenase 1) (mNAD-MDH 1) (mtNAD-MDH1)	1.24	0.86	0.00	1	y
P26518	Glyceraldehyde-3-phosphate dehydrogenase, cytosolic (EC 1.2.1.12)	0.73	0.48	0.00	1	y
A7F1L5	Cyanate hydratase (Cyanase) (EC 4.2.1.104) (Cyanate hydrolase) (Cyanate lyase)	0.62	0.60	0.00	1	y
Q5B4R3	Peptidyl-prolyl cis-trans isomerase B (PPlase B) (EC 5.2.1.8) (Rotamase B)	1.60	1.72	0.01	1	y
P11593	V-type proton ATPase subunit B (V-ATPase subunit B) (V-ATPase 57 kDa subunit) (Vacuolar proton pump subunit B)	0.50	0.44	0.01	1	
P60764	Ras-related C3 botulinum toxin substrate 3 (p21-Rac3)	0.52	0.74	0.01	1	
O59948	Eukaryotic peptide chain release factor subunit 1 (Eukaryotic release factor 1) (eRF1)	0.62	0.82	0.03	1	

Accession no.	UniProt recommended Protein name	Fold change ^a		ANOVA p-value	Cluster ^b	Common to At61
		Ag ⁺	AgNPs			
A7EHP6	ATPase get3 (EC 3.6.-.-) (Arsenical pump-driving ATPase) (Arsenite-stimulated ATPase) (Golgi to ER traffic protein 3) (Guided entry of tail-anchored proteins 3)	1.16	1.12	0.03	1	
P48347	14-3-3-like protein GF14 epsilon (General regulatory factor 10)	0.82	0.70	0.03	1	y
P40233	Casein kinase I homolog 1 (EC 2.7.11.1)	0.66	0.77	0.05	1	
O24653	Guanosine nucleotide diphosphate dissociation inhibitor 2 (AtGDI2)	1.45	0.25	0.00	2	y
Q1DWN4	NADH-cytochrome b5 reductase 1 (EC 1.6.2.2) (Microsomal cytochrome b reductase)	1.72	-0.41	0.00	2	
P14228	Phosphoglycerate kinase (EC 2.7.2.3)	0.71	0.23	0.00	2	
O42943	Uncharacterized ABC transporter ATP-binding protein C16H5.08c	1.42	0.25	0.00	2	
P34727	ADP-ribosylation factor	0.86	-0.20	0.00	2	y
P34731	Fatty acid synthase subunit beta (EC 2.3.1.86) [Includes: 3-hydroxyacyl-[acyl-carrier-protein] dehydratase (EC 4.2.1.59); Enoyl-[acyl-carrier-protein] reductase [NADH] (EC 1.3.1.9); [Acyl-carrier-protein] acetyltransferase (EC 2.3.1.38); [Acyl-carrier-protein] malonyltransferase (EC 2.3.1.39); S-acyl fatty acid synthase thioesterase (EC 3.1.2.14)]	1.42	0.54	0.00	2	
Q2U6P7	ATP-dependent RNA helicase sub2 (EC 3.6.4.13)	1.42	0.64	0.00	2	
Q9P7U2	Putative aryl-alcohol dehydrogenase C977.14c (EC 1.1.1.-)	1.58	0.28	0.00	2	
Q59QD6	Elongation factor 1-alpha 2 (EF-1-alpha 2)	1.52	0.33	0.00	2	y
Q9C413	Tubulin alpha chain (Alpha-tubulin)	1.34	0.70	0.00	2	
Q4U3E8	Mannose-1-phosphate guanylyltransferase (EC 2.7.7.13) (GDP-mannose pyrophosphorylase) (GTP-mannose-1-phosphate guanylyltransferase)	0.50	0.04	0.00	2	
Q5ZJN2	Ras-related protein Rab-11A	3.00	-0.10	0.00	2	y
O59945	Fimbrin	1.01	0.31	0.00	2	y
P00761	Trypsin (EC 3.4.21.4)	1.03	-0.12	0.00	2	y
Q6BZH1	78 kDa glucose-regulated protein homolog (GRP-78) (Immunoglobulin heavy chain-binding protein homolog) (BIP)	2.00	0.97	0.00	2	y

Accession no.	UniProt recommended Protein name	Fold change ^a		ANOVA p-value	Cluster ^b	Common to At61
		Ag ⁺	AgNPs			
Q07103	Formate dehydrogenase (FDH) (EC 1.2.1.2) (NAD-dependent formate dehydrogenase)	0.96	-0.23	0.00	2	y
Q5B0C0	Heat shock 70 kDa protein	0.81	0.03	0.00	2	
L7IK19	40S ribosomal protein S1	0.88	-0.17	0.00	2	y
P28814	Barwin	1.23	0.66	0.00	2	
P41836	26S protease regulatory subunit 8 homolog (Protein let1)	2.32	0.74	0.00	2	
Q2UPZ7	Aspartyl aminopeptidase (DAP) (EC 3.4.11.21)	1.42	0.32	0.00	2	y
P79089	Isocitrate dehydrogenase [NADP]. mitochondrial (IDH) (EC 1.1.1.42) (IDP) (NADP(+)-specific ICDH) (Oxalosuccinate decarboxylase)	2.89	0.08	0.00	2	y
Q9SF40	60S ribosomal protein L4-1 (L1)	0.53	-0.11	0.00	2	y
A6SFQ6	Eukaryotic translation initiation factor 3 subunit B (eIF3b) (Eukaryotic translation initiation factor 3 90 kDa subunit homolog) (eIF3 p90) (Translation initiation factor eIF3. p90 subunit homolog)	0.59	0.16	0.00	2	y
Q00955	Acetyl-CoA carboxylase (ACC) (EC 6.4.1.2) (Fatty acid synthetase 3) (mRNA transport-defective protein 7) [Includes: Biotin carboxylase (EC 6.3.4.14)]	0.97	0.47	0.00	2	y
Q5AWS6	Cell division control protein 48	0.49	0.21	0.00	2	
P34825	Elongation factor 1-alpha (EF-1-alpha)	0.57	0.33	0.00	2	y
P23301	Eukaryotic translation initiation factor 5A-1 (eIF-5A-1) (Hypusine-containing protein HP2) (eIF-4D)	0.94	0.61	0.01	2	
Q70Q35	Superoxide dismutase [Cu-Zn] (EC 1.15.1.1)	0.57	0.34	0.01	2	y
C1GUB6	40S ribosomal protein S0	0.33	0.14	0.01	2	y
P53596	Succinate--CoA ligase [ADP/GDP-forming] subunit alpha. mitochondrial (EC 6.2.1.4) (EC 6.2.1.5) (Succinyl-CoA synthetase subunit alpha) (SCS-alpha)	1.53	0.72	0.01	2	
Q874J6	Histone H3-like centromeric protein CSE4 (CENP-A homolog)	1.02	-0.06	0.01	2	y
Q7Z8E7	Glycerol-3-phosphate dehydrogenase [NAD(+)] (EC 1.1.1.8)	0.79	0.29	0.02	2	y
A7F4H5	Carboxypeptidase Y homolog A (EC 3.4.16.5)	1.21	0.64	0.02	2	

Accession no.	UniProt recommended Protein name	Fold change ^a		ANOVA p-value	Cluster ^b	Common to At61
		Ag ⁺	AgNPs			
P38078	V-type proton ATPase catalytic subunit A (V-ATPase subunit A) (EC 3.6.3.14) (Vacuolar proton pump subunit A) [Cleaved into: Endonuclease PI-Ctrl (EC 3.1.-.-) (Ctr VMA intein) (VMA1-derived endonuclease) (VDE)]	0.61	-0.12	0.02	2	y
P38999	Saccharopine dehydrogenase [NADP(+), L-glutamate-forming] (EC 1.5.1.10) (Saccharopine reductase)	0.46	0.07	0.02	2	
P48826	Glucose-6-phosphate 1-dehydrogenase (G6PD) (EC 1.1.1.49)	0.33	0.00	0.02	2	y
P37833	Aspartate aminotransferase, cytoplasmic (EC 2.6.1.1) (Transaminase A)	0.71	0.09	0.02	2	
Q9HES8	Pyruvate carboxylase (EC 6.4.1.1) (Pyruvic carboxylase) (PCB)	-1.02	-0.23	0.00	3	y
A0B6Y9	Dihydroxy-acid dehydratase (DAD) (EC 4.2.1.9)	-1.52	-0.02	0.00	3	y
P10592	Heat shock protein SSA2	-0.83	-0.12	0.00	3	y
P38720	6-phosphogluconate dehydrogenase, decarboxylating 1 (EC 1.1.1.44)	-1.95	-0.13	0.00	3	y
Q6FW50	78 kDa glucose-regulated protein homolog (GRP-78) (Immunoglobulin heavy chain-binding protein homolog) (BIP)	-1.14	-0.13	0.00	3	
P69061	Ubiquitin-40S ribosomal protein S27a [Cleaved into: Ubiquitin; 40S ribosomal protein S27a]	-1.56	-0.74	0.00	3	y
Q873C7	RuvB-like helicase 2 (EC 3.6.4.12)	-0.72	-0.27	0.00	3	
P32637	Glyceraldehyde-3-phosphate dehydrogenase (GAPDH) (EC 1.2.1.12)	-0.90	-0.41	0.00	3	y
P33297	26S protease regulatory subunit 6A (Tat-binding protein homolog 1) (TBP-1)	-0.31	-0.14	0.00	3	
O74225	Heat shock protein hsp88	-1.05	-0.34	0.00	3	
Q9P3T6	40S ribosomal protein S5-B	-0.69	-0.02	0.00	3	
Q05425	Guanine nucleotide-binding protein alpha-1 subunit (GP1-alpha)	-1.97	-0.21	0.00	3	y
P40108	Aldehyde dehydrogenase (ALDDH) (ALDH) (EC 1.2.1.3) (Allergen Cla h 3) (Allergen Cla h III) (allergen Cla h 10)	-0.65	0.02	0.00	3	
O93934	NADP-specific glutamate dehydrogenase (NADP-GDH) (EC 1.4.1.4) (NADP-dependent glutamate dehydrogenase)	-0.96	-0.52	0.01	3	y
Q10318	Putative dihydroxy-acid dehydratase, mitochondrial (DAD) (EC 4.2.1.9) (2,3-dihydroxy acid hydrolyase)	-2.43	-0.16	0.01	3	

Accession no.	UniProt recommended Protein name	Fold change ^a		ANOVA p-value	Cluster ^b	Common to At61
		Ag ⁺	AgNPs			
P26521	Glyceraldehyde-3-phosphate dehydrogenase. cytosolic (EC 1.2.1.12)	-1.41	-0.61	0.01	3	y
Q876L8	NAD(P)H-dependent D-xylose reductase xyl1 (XR) (EC 1.1.1.-)	-0.70	-0.18	0.01	3	y
P40941	ADP.ATP carrier protein 2. mitochondrial (ADP/ATP translocase 2) (Adenine nucleotide translocator 2) (ANT 2)	-0.89	-0.43	0.02	3	
A7EIX7	ATP-dependent RNA helicase sub2 (EC 3.6.4.13)	-0.75	0.01	0.02	3	y
P87222	Heat shock protein SSB1	-1.45	-0.24	0.03	3	y
Q6C354	2-methylcitrate dehydratase. mitochondrial (EC 4.2.1.79)	-1.71	-0.13	0.04	3	
O42772	Succinate dehydrogenase [ubiquinone] iron-sulfur subunit. mitochondrial (EC 1.3.5.1) (Iron-sulfur subunit of complex II) (Ip)	-0.85	-0.20	0.04	3	y
A7EGL7	ATP-dependent RNA helicase eIF4A (EC 3.6.4.13) (Eukaryotic initiation factor 4A) (eIF-4A) (Translation initiation factor 1)	0.46	-0.48	0.00	4	y
P51996	GTP-binding protein YPT32/YPT11 (Rab GTPase YPT32)	0.75	-0.38	0.00	4	
Q8X034	60S ribosomal protein L15	1.13	-0.86	0.00	4	y
Q7RV75	40S ribosomal protein S22 (Cytoplasmic ribosomal protein 27)	0.61	-0.54	0.00	4	
Q92T12	Methylthioribose-1-phosphate isomerase (M1Pi) (MTR-1-P isomerase) (EC 5.3.1.23) (S-methyl-5-thioribose-1-phosphate isomerase)	-0.10	-1.00	0.00	4	
A7E4H3	40S ribosomal protein S1	0.70	-0.52	0.00	4	y
A4R935	NADH-cytochrome b5 reductase 1 (EC 1.6.2.2) (Microsomal cytochrome b reductase)	0.26	-1.02	0.00	4	y
Q00251	Elongation factor 1-alpha (EF-1-alpha)	0.01	-0.61	0.00	4	y
O43105	40S ribosomal protein S7 (Cytoplasmic ribosomal protein 15)	0.63	-0.79	0.00	4	
P36017	Vacuolar protein sorting-associated protein 21 (GTP-binding protein YPT51) (Vacuolar protein-targeting protein 12)	0.58	-0.21	0.00	4	
P0CM17	ADP-ribosylation factor	0.16	-0.53	0.00	4	y
Q8X1X3	Glyceraldehyde-3-phosphate dehydrogenase (GAPDH) (EC 1.2.1.12)	0.38	-0.54	0.00	4	y
Q9UVR2	Ubiquitin-conjugating enzyme E2-16 kDa (EC 2.3.2.23) (E2 ubiquitin-conjugating enzyme 1) (Ubiquitin carrier protein) (Ubiquitin-protein ligase)	0.42	-0.65	0.01	4	

Accession no.	UniProt recommended Protein name	Fold change ^a		ANOVA p-value	Cluster ^b	Common to At61
		Ag ⁺	AgNPs			
Q41346	Cytochrome c	0.73	-0.74	0.01	4	
Q9SEX2	Katanin p60 ATPase-containing subunit A1 (Katanin p60 subunit A1) (EC 3.6.4.3) (CAD ATPase) (Katanin-1) (Atp60) (Protein BOTERO 1) (Protein ECTOPIC ROOT HAIR 3) (Protein FAT ROOT) (Protein FRAGILE FIBER 2) (AtAAA1) (p60 katanin)	0.25	-0.41	0.01	4	
P06738	Glycogen phosphorylase (EC 2.4.1.1)	0.60	-0.78	0.03	4	y
Q4WY53	Phosphoglucomutase (PGM) (EC 5.4.2.2) (Glucose phosphomutase)	0.03	-0.41	0.03	4	y
B2ASU5	Catalase-peroxidase (CP) (EC 1.11.1.21) (Peroxidase/catalase)	0.28	-0.24	0.03	4	
P40292	Heat shock protein 90 (65 kDa IgE-binding protein) (Heat shock protein hsp1) (allergen Asp f 12)	0.21	-0.72	0.05	4	
Q7S8R8	26S proteasome regulatory subunit rpn-1	-0.75	-0.83	0.00	5	
O14018	Serine--tRNA ligase. cytoplasmic (EC 6.1.1.11) (Seryl-tRNA synthetase) (SerRS) (Seryl-tRNA(Ser/Sec) synthetase)	-1.21	-1.30	0.00	5	
Q0US25	Protein transport protein SEC23	-0.86	-1.26	0.00	5	
A6LE80	DNA-directed RNA polymerase subunit beta' (RNAP subunit beta') (EC 2.7.7.6) (RNA polymerase subunit beta') (Transcriptase subunit beta')	-0.82	-0.99	0.00	5	y
P31411	V-type proton ATPase subunit B (V-ATPase subunit B) (V-ATPase 57 kDa subunit) (Vacuolar proton pump subunit B)	-1.23	-1.06	0.00	5	
Q2KIW6	26S protease regulatory subunit 10B (26S proteasome AAA-ATPase subunit RPT4) (Proteasome 26S subunit ATPase 6)	-2.35	-1.33	0.00	5	
P50125	Homocysteine synthase (EC 2.5.1.49) (O-acetylhomoserine sulfhydrylase) (OAH SHL) (OAH sulfhydrylase)	-1.68	-1.79	0.00	5	
P40327	26S protease regulatory subunit 4 homolog (Tat-binding homolog 5)	-1.38	-1.48	0.00	5	
P51044	Citrate synthase. mitochondrial (EC 2.3.3.16)	-1.44	-1.39	0.00	5	y
Q27032	Cell division control protein 2 homolog (EC 2.7.11.22) (EC 2.7.11.23)	-1.30	-1.88	0.00	5	
P25997	Elongation factor 3 (EF-3)	-1.16	-1.27	0.00	5	
Q96X45	Elongation factor 2 (EF-2) (Colonial temperature-sensitive 3)	-0.40	-0.82	0.00	5	y

Accession no.	UniProt recommended Protein name	Fold change ^a		ANOVA p-value	Cluster ^b	Common to At61
		Ag ⁺	AgNPs			
Q01369	Guanine nucleotide-binding protein subunit beta-like protein (Cross-pathway control WD-repeat protein cpc-2)	-0.78	-0.71	0.00	5	
A6S043	Eukaryotic translation initiation factor 3 subunit C (eIF3c) (Eukaryotic translation initiation factor 3 93 kDa subunit homolog) (eIF3 p93) (Translation initiation factor eIF3. p93 subunit homolog)	-0.32	-0.63	0.00	5	
Q76KF9	Enolase (EC 4.2.1.11) (2-phospho-D-glycerate hydro-lyase) (2-phosphoglycerate dehydratase)	-0.21	-0.28	0.01	5	
P22515	Ubiquitin-activating enzyme E1 1 (EC 6.2.1.45)	-2.23	-1.17	0.01	5	
Q8ZNV7	Zinc import ATP-binding protein ZnuC (EC 3.6.3.-)	-0.28	-0.73	0.01	5	y
P38674	Ketol-acid reductoisomerase. mitochondrial (EC 1.1.1.86) (Acetohydroxy-acid reductoisomerase) (Alpha-keto-beta-hydroxylacyl reductoisomerase)	-0.23	-0.55	0.01	5	
Q6GZR2	Putative deoxyuridine 5'-triphosphate nucleotidohydrolase (dUTPase) (EC 3.6.1.23)	-0.28	-0.67	0.01	5	
Q7SCP4	F-actin-capping protein subunit beta (F-actin capping protein 2)	-0.90	-1.01	0.02	5	y
A4RD35	Protein transport protein SEC31	-0.10	-0.31	0.03	5	
A7EJL9	Leukotriene A-4 hydrolase homolog (LTA-4 hydrolase) (EC 3.3.2.6) (Leukotriene A(4) hydrolase)	-0.11	-0.57	0.04	5	y
Q7SE75	Sulfate adenylyltransferase (EC 2.7.7.4) (ATP-sulfurylase) (Sulfate adenylyl transferase) (SAT)	-0.70	-0.83	0.04	5	
P32599	Fimbrin (ABP67)	-1.82	-1.31	0.05	5	
P53731	Actin-related protein 2/3 complex subunit 2 (Arp2/3 complex 34 kDa subunit) (p34-ARC)	-0.52	0.86	0.00	6	
P87018	Ras-like protein	0.20	0.78	0.00	6	y
P40236	Casein kinase I homolog hhp2 (EC 2.7.11.1)	0.01	0.98	0.00	6	
Q7RVX9	Repressible high-affinity phosphate permease	-0.19	0.48	0.00	6	
Q9HGY8	Triosephosphate isomerase (TIM) (EC 5.3.1.1) (Triose-phosphate isomerase)	-0.04	0.58	0.00	6	
Q9C2L8	Probable Ras-related protein Rab7	0.46	0.88	0.00	6	

Accession no.	UniProt recommended Protein name	Fold change ^a		ANOVA p-value	Cluster ^b	Common to At61
		Ag ⁺	AgNPs			
Q4ICA8	RuvB-like helicase 1 (EC 3.6.4.12)	0.50	1.00	0.00	6	
Q39994	Calnexin homolog	0.67	1.68	0.00	6	
Q6FRB7	Inorganic pyrophosphatase (EC 3.6.1.1) (Pyrophosphate phosphohydrolase) (PPase)	0.07	0.97	0.00	6	y
P24000	60S ribosomal protein L24-B (L30) (RP29) (YL21)	0.29	1.05	0.00	6	
P22137	Clathrin heavy chain	0.44	1.13	0.00	6	
P52015	Peptidyl-prolyl cis-trans isomerase 7 (PPIase 7) (EC 5.2.1.8) (Cyclophilin-7) (Rotamase 7)	-0.14	0.66	0.00	6	
Q4L7Z4	Serine hydroxymethyltransferase (SHMT) (Serine methylase) (EC 2.1.2.1)	0.02	0.98	0.00	6	y
P13228	Tryptophan synthase (EC 4.2.1.20)	0.10	0.71	0.00	6	
P07597	Non-specific lipid-transfer protein 1 (LTP 1) (Probable amylase/protease inhibitor)	0.11	0.94	0.00	6	
Q1E4I8	Adenylate kinase (EC 2.7.4.3) (ATP-AMP transphosphorylase) (ATP:AMP phosphotransferase) (Adenylate kinase cytosolic and mitochondrial) (Adenylate monophosphate kinase)	-0.27	0.71	0.00	6	
Q975H9	Isoleucine--tRNA ligase (EC 6.1.1.5) (Isoleucyl-tRNA synthetase) (IleRS)	0.19	0.55	0.00	6	
Q9ZKD8	NADP-specific glutamate dehydrogenase (NADP-GDH) (EC 1.4.1.4)	-0.27	0.48	0.01	6	y
Q9XEK8	60S ribosomal protein L23 (L17)	-0.19	0.47	0.01	6	
Q92407	Glucokinase (EC 2.7.1.2) (Glucose kinase) (GLK)	-0.22	0.52	0.01	6	
Q9KZM1	Adenosylhomocysteinase (EC 3.3.1.1) (S-adenosyl-L-homocysteine hydrolase) (AdoHcyase)	-0.20	0.88	0.01	6	y
A7EF03	Eukaryotic translation initiation factor 3 subunit I (eIF3i) (Eukaryotic translation initiation factor 3 39 kDa subunit homolog) (eIF-3 39 kDa subunit homolog)	-0.06	1.04	0.01	6	y
Q8HXX7	Rab GDP dissociation inhibitor alpha (Rab GDI alpha) (Guanosine diphosphate dissociation inhibitor 1) (GDI-1)	-0.09	0.94	0.01	6	

Accession no.	UniProt recommended Protein name	Fold change ^a		ANOVA p-value	Cluster ^b	Common to At61
		Ag ⁺	AgNPs			
P33282	Uricase (EC 1.7.3.3) (Urate oxidase)	0.07	1.08	0.01	6	y
P32379	Proteasome subunit alpha type-5 (EC 3.4.25.1) (Macropain subunit PUP2) (Multicatalytic endopeptidase complex subunit PUP2) (Proteinase YSCE subunit PUP2)	0.22	1.31	0.02	6	
P42040	Enolase (EC 4.2.1.11) (2-phospho-D-glycerate hydro-lyase) (2-phosphoglycerate dehydratase) (Allergen Cla h VI) (allergen Cla h 6)	0.26	0.65	0.02	6	
P46598	Heat shock protein 90 homolog	0.61	1.93	0.03	6	
O04630	Threonine--tRNA ligase. mitochondrial 1 (EC 6.1.1.3) (AtSYT1) (Threonyl-tRNA synthetase) (ThrRS)	0.34	0.61	0.04	6	
Q9JMB1	Testicular haploid expressed gene protein	-0.75	0.51	0.00	7	
A7EY76	ATP-dependent RNA helicase dbp5 (EC 3.6.4.13)	-0.57	0.38	0.00	7	y
P49376	ATP synthase subunit beta. mitochondrial (EC 3.6.3.14)	-0.91	0.54	0.00	7	
Q0CFZ0	Probable Xaa-Pro aminopeptidase pepP (EC 3.4.11.9) (Aminoacylproline aminopeptidase) (Prolidase)	-0.64	0.34	0.00	7	
Q09171	Pyruvate dehydrogenase E1 component subunit beta. mitochondrial (PDHE1-B) (EC 1.2.4.1)	-0.82	0.27	0.00	7	
Q9NW08	DNA-directed RNA polymerase III subunit RPC2 (RNA polymerase III subunit C2) (EC 2.7.7.6) (C128) (DNA-directed RNA polymerase III 127.6 kDa polypeptide) (DNA-directed RNA polymerase III subunit B)	-0.78	0.31	0.00	7	y
Q5BCG1	3'(2').5'-bisphosphate nucleotidase (EC 3.1.3.7) (3'(2').5-bisphosphonucleoside 3'(2')-phosphohydrolase) (DPNPase)	-0.68	0.84	0.00	7	y
Q2KT14	Catalase-peroxidase (CP) (EC 1.11.1.21) (Peroxidase/catalase)	-0.97	0.38	0.00	7	
Q9P720	60S ribosomal protein L16 (Cytoplasmic ribosomal protein 46)	-0.96	0.28	0.00	7	
O14460	Elongation factor 2 (EF-2)	-0.65	0.52	0.00	7	y

Accession no.	UniProt recommended Protein name	Fold change ^a		ANOVA p-value	Cluster ^b	Common to At61
		Ag ⁺	AgNPs			
P49601	3-isopropylmalate dehydratase (EC 4.2.1.33) (Alpha-IPM isomerase) (IPMI) (Isopropylmalate isomerase)	-0.89	0.11	0.00	7	
Q43492	Serpin-Z7 (BSZ7) (HorvuZ7)	-0.70	0.39	0.00	7	y
Q52813	General L-amino acid transport system permease protein AapQ	-0.27	0.45	0.00	7	
O93937	Protein pyrABCN [Includes: Glutamine-dependent carbamoyl-phosphate (EC 6.3.5.5); Aspartate carbamoyltransferase (EC 2.1.3.2)]	-0.59	0.09	0.01	7	
P78820	Acetyl-CoA carboxylase (ACC) (EC 6.4.1.2) (Cell untimely torn protein 6) [Includes: Biotin carboxylase (EC 6.3.4.14)]	-1.04	0.05	0.01	7	
O43109	Heat shock protein 90 homolog (Suppressor of vegetative incompatibility MOD-E)	-0.42	0.25	0.01	7	y
Q54BC8	Proteasome subunit beta type-5 (EC 3.4.25.1)	-0.54	0.09	0.01	7	
P25457	60S ribosomal protein L7-B	-0.63	0.06	0.01	7	
Q59PT0	V-type proton ATPase subunit B (V-ATPase subunit B) (Vacuolar proton pump subunit B)	-0.45	0.30	0.01	7	y
P55059	Protein disulfide-isomerase (PDI) (EC 5.3.4.1)	-0.95	0.26	0.03	7	
Q7RZS0	60S ribosomal protein L10a (Cytoplasmic ribosomal protein 74)	-0.44	0.09	0.03	7	y
P24487	ATP synthase subunit alpha. mitochondrial	-0.56	0.25	0.03	7	
P83617	78 kDa glucose-regulated protein homolog (GRP-78) (Immunoglobulin heavy chain-binding protein homolog) (BiP)	-0.82	0.33	0.03	7	
Q9ZJQ9	Fumarate hydratase class II (Fumarase C) (EC 4.2.1.2)	-1.05	0.06	0.03	7	
O13366	Pyruvate dehydrogenase E1 component subunit alpha. mitochondrial (PDHE1-A) (EC 1.2.4.1)	-0.43	0.10	0.04	7	
P34085	Citrate synthase. mitochondrial (EC 2.3.3.16)	-0.75	-0.04	0.05		
D7PHZ1	Oxidoreductase vrtI (EC 1.14.-.-) (Viridicatumtoxin synthesis protein I)	-0.26	-0.08	0.05		
P38708	Putative proline--tRNA ligase YHR020W (EC 6.1.1.15) (Prolyl-tRNA synthetase) (ProRS)	-0.51	-0.63	0.05		
Q5AAG6	Mitogen-activated protein kinase MKC1 (MAP kinase MKC1) (EC 2.7.11.24)	0.25	0.13	0.05		
Q8TG13	Casein kinase II subunit alpha (CK II subunit alpha) (EC 2.7.11.1)	-1.67	-0.11	0.05		

Accession no.	UniProt recommended Protein name	Fold change ^a		ANOVA p-value	Cluster ^b	Common to At61
		Ag ⁺	AgNPs			
J9MJK9	Transaldolase (FoTal) (EC 2.2.1.2)	-0.26	-0.10	0.06		
P32381	Actin-related protein 2 (Actin-like protein ARP2) (Actin-like protein 2)	-0.37	-0.02	0.06		
P52810	40S ribosomal protein S9 (S7)	0.53	0.48	0.06		
Q4UK18	ATP synthase subunit beta (EC 3.6.3.14) (ATP synthase F1 sector subunit beta) (F-ATPase subunit beta)	-0.66	-1.04	0.06		
O94313	Carbamoyl-phosphate synthase arginine-specific large chain (EC 6.3.5.5) (Arginine-specific carbamoyl-phosphate synthetase. ammonia chain)	-0.47	-0.38	0.06		
Q99002	14-3-3 protein homolog (Th1433)	0.31	0.70	0.06		
P93422	Histidine--tRNA ligase. cytoplasmic (EC 6.1.1.21) (Histidyl-tRNA synthetase) (HisRS)	-0.90	0.59	0.06		
O42849	Phenylalanine--tRNA ligase beta subunit (EC 6.1.1.20) (Phenylalanyl-tRNA synthetase beta subunit) (PheRS)	0.16	-0.42	0.07		
Q88QM3	50S ribosomal protein L5	-0.25	0.40	0.07		
P32449	Phospho-2-dehydro-3-deoxyheptonate aldolase. tyrosine-inhibited (EC 2.5.1.54) (3-deoxy-D-arabino-heptulosonate 7-phosphate synthase) (DAHP synthase) (Phospho-2-keto-3-deoxyheptonate aldolase)	0.56	0.61	0.07		
Q0C9L8	ATP synthase subunit beta. mitochondrial (EC 3.6.3.14) (Citroviridin biosynthesis protein E)	0.00	0.54	0.07		
P78712	Actin-related protein 3 (Actin-like protein 3)	-0.27	-0.87	0.07		
P06293	Serpin-Z4 (BSZ4) (HorvuZ4) (Major endosperm albumin) (Protein Z4) (Protein Z)	0.04	-0.65	0.08		
Q00737	Chromosome segregation protein sudA (DA-box protein sudA)	0.83	1.01	0.08		
Q9SPB1	Leghemoglobin reductase (EC 1.6.2.6) (Ferric leghemoglobin reductase) (FLbR)	0.29	0.70	0.08		
PODKC4	Phosphoglycolate phosphatase 1B. chloroplastic (EC 3.1.3.18)	1.19	0.59	0.08		
P10819	Adenosylhomocysteinase (AdoHcyase) (EC 3.3.1.1) (S-adenosyl-L-homocysteine hydrolase)	-0.08	0.20	0.08		

Accession no.	UniProt recommended Protein name	Fold change ^a		ANOVA p-value	Cluster ^b	Common to At61
		Ag ⁺	AgNPs			
Q12335	Protoplast secreted protein 2	0.20	0.56	0.08		
Q875B7	Histone H2B	1.39	0.45	0.08		
Q6BJ25	Elongation factor 2 (EF-2)	0.23	0.78	0.08		
A7E8H8	Adenylate kinase (EC 2.7.4.3) (ATP-AMP transphosphorylase) (ATP:AMP phosphotransferase) (Adenylate kinase cytosolic and mitochondrial) (Adenylate monophosphate kinase)	0.38	-0.21	0.08		
P40915	NADH-ubiquinone oxidoreductase 24 kDa subunit. mitochondrial (EC 1.6.5.3) (EC 1.6.99.3)	-0.69	-0.44	0.08		
P27770	40S ribosomal protein S17 (CRP3)	-1.22	0.16	0.09		
P38624	Proteasome subunit beta type-1 (EC 3.4.25.1) (Macropain subunit PRE3) (Multicatalytic endopeptidase complex subunit PRE3) (Proteasome component PRE3) (Proteinase YSCE subunit PRE3)	-1.06	-0.98	0.09		
Q0CXB1	Probable dipeptidyl-aminopeptidase B (DPAP B) (EC 3.4.14.5)	-0.97	-0.08	0.09		
Q1CRI6	4-diphosphocytidyl-2-C-methyl-D-erythritol kinase (CMK) (EC 2.7.1.148) (4-(cytidine-5'-diphospho)-2-C-methyl-D-erythritol kinase)	0.30	-0.15	0.09		
Q1DXH0	Polyadenylate-binding protein. cytoplasmic and nuclear (PABP) (Poly(A)-binding protein) (Polyadenylate tail-binding protein)	-0.41	-0.38	0.09		
Q752U5	60S ribosomal protein L30	-0.17	-0.31	0.09		
Q7RVI1	40S ribosomal protein S5	-0.18	-0.57	0.10		
A5DI11	Elongation factor 2 (EF-2)	0.30	-0.42	0.10		
Q00217	Alpha.alpha-trehalose-phosphate synthase [UDP-forming] 2 (EC 2.4.1.15) (Trehalose-6-phosphate synthase) (UDP-glucose-glucosephosphate glucosyltransferase)	0.57	-0.06	0.10		
Q9Y8H7	Spermidine synthase (SPDSY) (EC 2.5.1.16) (Putrescine aminopropyltransferase)	-0.64	-0.28	0.10		
O74445	Probable 26S protease subunit rpt4	0.23	0.56	0.10		

Accession no.	UniProt recommended Protein name	Fold change ^a		ANOVA p-value	Cluster ^b	Common to At61
		Ag ⁺	AgNPs			
P87252	Woronin body major protein	0.20	0.36	0.10		
P31353	Phosphomannomutase (PMM) (EC 5.4.2.8)	0.58	0.35	0.10		
A4RM69	Eukaryotic translation initiation factor 3 subunit A (eIF3a) (Eukaryotic translation initiation factor 3 110 kDa subunit homolog) (eIF3 p110) (Translation initiation factor eIF3. p110 subunit homolog)	1.25	0.10	0.11		
Q00043	Heat shock 70 kDa protein	0.46	-0.56	0.11		
E4ZHQ5	Leucine aminopeptidase 1 (EC 3.4.11.-) (Leucyl aminopeptidase 1) (LAP1)	0.54	0.10	0.11		
P29497	Glyceraldehyde-3-phosphate dehydrogenase (GAPDH) (EC 1.2.1.12)	-0.58	0.49	0.11		
Q96564	40S ribosomal protein S27 (Manganese efficiency-related protein 1)	-1.15	-1.24	0.12		
Q00216	Protein disulfide-isomerase tlgA (EC 5.3.4.1)	-0.47	-0.33	0.12		
Q8NKF4	60S ribosomal protein L3 (allergen Asp f 23)	-0.28	-0.52	0.12		
Q00859	Mitogen-activated protein kinase (EC 2.7.11.24) (FsMAPK)	-2.55	-0.65	0.12		
C3K255	Polyribonucleotide nucleotidyltransferase (EC 2.7.7.8) (Polynucleotide phosphorylase) (PNPase)	0.32	0.49	0.12		
P29405	Phosphoglycerate kinase 1 (EC 2.7.2.3)	0.95	0.07	0.13		
P78615	Fatty acid synthase subunit alpha (EC 2.3.1.86) [Includes: Acyl carrier; 3-oxoacyl-[acyl-carrier-protein] reductase (EC 1.1.1.100) (Beta-ketoacyl reductase); 3-oxoacyl-[acyl-carrier-protein] synthase (EC 2.3.1.41) (Beta-ketoacyl synthase)]	1.05	0.09	0.13		
Q7LKT3	Histone H4	0.20	0.66	0.13		
Q0BW40	Adenosylhomocysteinase (EC 3.3.1.1) (S-adenosyl-L-homocysteine hydrolase) (AdoHcyase)	-0.37	-1.81	0.13		
A7EVF4	Molybdopterin synthase catalytic subunit (EC 2.8.1.12) (Common component for nitrate reductase and xanthine dehydrogenase protein H) (Molybdenum cofactor synthesis protein 2 large subunit) (Molybdenum cofactor synthesis protein 2B) (MOCS2B)	-0.57	0.07	0.14		
A9GP90	Urease accessory protein UreG	0.01	-0.42	0.14		

Accession no.	UniProt recommended Protein name	Fold change ^a		ANOVA p-value	Cluster ^b	Common to At61
		Ag ⁺	AgNPs			
Q7SBD5	60S ribosomal protein L7	-0.66	0.28	0.14		
O94225	Homocitrate synthase. mitochondrial (EC 2.3.3.14)	-0.04	-0.64	0.14		
P48580	Serine/threonine-protein phosphatase PP2A catalytic subunit (EC 3.1.3.16)	0.04	0.93	0.14		
Q9P6M8	mRNA export factor crp79 (Meiotic expression up-regulated protein 5) (Polyadenylate-binding protein crp79) (PABP) (Poly(A)-binding protein)	-0.30	0.02	0.14		
Q9UW86	Serine/threonine-protein phosphatase PP1 (EC 3.1.3.16) (Phosphoprotein phosphatase 1)	0.28	0.24	0.15		
POCX48	40S ribosomal protein S11-B (RP41) (S18) (YS12)	-1.07	-1.49	0.15		
P37211	ATP synthase subunit alpha. mitochondrial	-0.01	0.29	0.15		
Q09116	Septin homolog spn2	0.20	0.24	0.16		
P09041	Phosphoglycerate kinase 2 (EC 2.7.2.3) (Phosphoglycerate kinase. testis specific)	-0.78	-0.01	0.16		
P41756	Phosphoglycerate kinase (EC 2.7.2.3)	-0.24	0.04	0.16		
P11913	Mitochondrial-processing peptidase subunit beta (EC 3.4.24.64) (Beta-MPP) (Ubiquinol-cytochrome-c reductase complex core protein I)	0.35	1.21	0.16		
Q93HX6	Glucosaminiate ammonia-lyase (EC 4.3.1.9) (D-glucosaminiate dehydratase alpha-subunit) (GlcNA-DH alpha subunit) (GlcNADH-alpha)	0.61	0.41	0.17		
Q765N2	Fatty acid synthase subunit alpha (EC 2.3.1.86) (p190/210) [Includes: Acyl carrier; 3-oxoacyl-[acyl-carrier-protein] reductase (EC 1.1.1.100) (Beta-ketoacyl reductase); 3-oxoacyl-[acyl-carrier-protein] synthase (EC 2.3.1.41) (Beta-ketoacyl synthase)]	-0.47	-0.26	0.17		
Q00771	Calcium/calmodulin-dependent protein kinase (CMPK) (EC 2.7.11.17)	-0.35	0.43	0.17		
P39939	40S ribosomal protein S26-B	-0.57	0.15	0.18		
Q9P4E9	GTP-binding nuclear protein GSP1/Ran	-0.53	-0.10	0.18		
O13302	Isocitrate dehydrogenase [NAD] subunit 1. mitochondrial (EC 1.1.1.41) (Isocitric dehydrogenase) (NAD(+)-specific ICDH)	-0.19	0.77	0.18		
Q8TFN0	Nucleoside diphosphate kinase (NDP kinase) (EC 2.7.4.6) (AnNDK) (NDK)	-0.39	-0.27	0.18		
Q9Y7Z2	ADP-ribosylation factor 6	-0.29	0.97	0.19		

Accession no.	UniProt recommended Protein name	Fold change ^a		ANOVA p-value	Cluster ^b	Common to At61
		Ag ⁺	AgNPs			
P31865	Pyruvate kinase (PK) (EC 2.7.1.40)	-0.30	-0.34	0.19		
Q9UUE1	Pyruvate carboxylase (EC 6.4.1.1) (Pyruvic carboxylase) (PCB)	-0.56	-1.33	0.19		
P28295	Elongation factor 1-alpha (EF-1-alpha)	0.18	-0.14	0.20		
Q5B998	Homoserine dehydrogenase (HDH) (EC 1.1.1.3)	0.03	0.24	0.21		
Q9Y897	3-isopropylmalate dehydrogenase (3-IPM-DH) (IMDH) (EC 1.1.1.85) (Beta-IPM dehydrogenase)	-0.41	-0.41	0.22		
Q6FTK4	60S ribosomal protein L11	-0.45	-0.43	0.22		
POCT59	40S ribosomal protein S22-B	-0.30	-0.06	0.22		
Q96X46	Enolase (EC 4.2.1.11) (2-phospho-D-glycerate hydro-lyase) (2-phosphoglycerate dehydratase) (allergen Pen c 22)	-0.37	0.35	0.22		
Q7RZF5	Protein transport protein sec13 (Nucleoporin 20)	0.58	0.24	0.22		
Q4P112	RuvB-like helicase 1 (EC 3.6.4.12)	-1.56	-0.42	0.23		
A1AZF8	Glycine--tRNA ligase beta subunit (EC 6.1.1.14) (Glycyl-tRNA synthetase beta subunit) (GlyRS)	-0.54	0.04	0.23		
Q9C3Y4	GTP-binding protein rhoA (Rho1 protein homolog)	-0.26	-0.53	0.23		
P48466	S-adenosylmethionine synthase (AdoMet synthase) (EC 2.5.1.6) (Ethionine resistance protein 1) (Methionine adenosyltransferase) (MAT)	0.20	0.71	0.24		
P53228	Transaldolase NQM1 (EC 2.2.1.2) (Non-quiescent mutant protein 1)	0.28	-0.35	0.24		
Q8TGA9	Mitogen-activated protein kinase HOG1 (MAP kinase HOG1) (EC 2.7.11.24)	-0.02	0.11	0.25		
P40918	Heat shock 70 kDa protein (Allergen Cla h IV) (allergen Cla h 4)	-0.06	0.23	0.26		
P16928	Acetyl-coenzyme A synthetase (EC 6.2.1.1) (Acetate--CoA ligase) (Acyl-activating enzyme)	0.18	0.11	0.27		
Q8X9L0	ATP-dependent zinc metalloprotease FtsH (EC 3.4.24.-)	0.03	-0.30	0.27		
P80581	Hexokinase (EC 2.7.1.1)	-0.43	-1.72	0.27		
Q8X132	Histone H2A	-0.79	-0.01	0.28		

Accession no.	UniProt recommended Protein name	Fold change ^a		ANOVA p-value	Cluster ^b	Common to At61
		Ag ⁺	AgNPs			
Q9P567	Succinate--CoA ligase [ADP-forming] subunit beta. mitochondrial (EC 6.2.1.5) (Succinyl-CoA synthetase beta chain) (SCS-beta)	-0.02	-0.43	0.28		
P53385	Urocanate hydratase (Urocanase) (EC 4.2.1.49) (Imidazolonepropionate hydrolase)	-0.24	-0.22	0.28		
P78695	78 kDa glucose-regulated protein homolog (GRP-78) (Immunoglobulin heavy chain-binding protein homolog) (BiP)	-0.44	0.29	0.29		
O59936	40S ribosomal protein S12	-0.41	-0.27	0.29		
Q4WUR1	Serine/threonine-protein phosphatase 2B catalytic subunit (EC 3.1.3.16) (Calmodulin-dependent calcineurin A subunit)	-1.05	0.29	0.29		
Q9C285	60S ribosomal protein L12	0.96	0.89	0.30		
Q09668	60S ribosomal protein L22	-0.32	-0.24	0.31		
B2VVA8	Arginine biosynthesis bifunctional protein ArgJ. mitochondrial [Cleaved into: Arginine biosynthesis bifunctional protein ArgJ alpha chain; Arginine biosynthesis bifunctional protein ArgJ beta chain] [Includes: Glutamate N-acetyltransferase (GAT) (EC 2.3.1.35) (Ornithine acetyltransferase) (OATase) (Ornithine transacetylase); Amino-acid acetyltransferase (EC 2.3.1.1) (N-acetylglutamate synthase) (AGS)]	-0.97	0.11	0.31		
Q7SDV9	Cytochrome c peroxidase. mitochondrial (CCP) (EC 1.11.1.5)	0.13	0.33	0.31		
Q922D8	C-1-tetrahydrofolate synthase. cytoplasmic (C1-THF synthase) [Cleaved into: C-1-tetrahydrofolate synthase. cytoplasmic. N-terminally processed] [Includes: Methylenetetrahydrofolate dehydrogenase (EC 1.5.1.5); Methenyltetrahydrofolate cyclohydrolase (EC 3.5.4.9); Formyltetrahydrofolate synthetase (EC 6.3.4.3)]	-0.91	-0.25	0.31		
A8IW34	Adenylosuccinate synthetase. chloroplastic (AMPSase) (AdSS) (EC 6.3.4.4) (IMP--aspartate ligase)	-0.24	0.11	0.33		

Accession no.	UniProt recommended Protein name	Fold change ^a		ANOVA p-value	Cluster ^b	Common to At61
		Ag ⁺	AgNPs			
P50142	Heat shock protein 60. mitochondrial (Antigen HIS-62)	-0.77	-0.71	0.33		
B9EAH1	Enolase (EC 4.2.1.11) (2-phospho-D-glycerate hydro-lyase) (2-phosphoglycerate dehydratase)	0.65	0.23	0.34		
Q5BAX8	E3 ubiquitin ligase complex SCF subunit sconC (Sulfur controller C) (Sulfur metabolite repression control protein C)	0.21	-0.16	0.34		
Q4W9B8	ATP-dependent 6-phosphofructokinase (ATP-PFK) (Phosphofructokinase) (EC 2.7.1.11) (Phosphohexokinase)	-0.92	0.37	0.34		
Q7S6N6	Polyadenylate-binding protein. cytoplasmic and nuclear (PABP) (Poly(A)-binding protein) (Polyadenylate tail-binding protein)	-0.35	0.10	0.35		
P33723	GTP-binding protein ypt1	0.43	-0.23	0.35		
Q9XIE2	ABC transporter G family member 36 (ABC transporter ABCG.36) (AtABCG36) (Pleiotropic drug resistance protein 8) (Protein PENETRATION 3)	0.26	-0.10	0.36		
P13681	Serine/threonine-protein phosphatase PP1-1 (EC 3.1.3.16)	-0.81	-0.82	0.36		
Q6ZPE2	Myotubularin-related protein 5 (SET-binding factor 1) (Sbf1)	-0.52	-0.06	0.38		
P48081	ATP synthase subunit beta. cyanelle (EC 3.6.3.14) (ATP synthase F1 sector subunit beta) (F-ATPase subunit beta)	-0.44	0.04	0.38		
Q9HE25	60S ribosomal protein L17	0.10	0.62	0.39		
P02723	ADP.ATP carrier protein (ADP/ATP translocase) (Adenine nucleotide translocator) (ANT)	-0.01	-0.22	0.39		
P05694	5-methyltetrahydropteroyltriglutamate--homocysteine methyltransferase (EC 2.1.1.14) (Cobalamin-independent methionine synthase) (Delta-P8 protein) (Methionine synthase. vitamin-B12 independent isozyme)	0.65	0.21	0.41		
C5FS55	Vacuolar protease A (EC 3.4.23.25) (Aspartic endopeptidase PEP2) (Aspartic protease PEP2)	-0.20	-0.74	0.42		

Accession no.	UniProt recommended Protein name	Fold change ^a		ANOVA p-value	Cluster ^b	Common to At61
		Ag ⁺	AgNPs			
P53319	6-phosphogluconate dehydrogenase. decarboxylating 2 (EC 1.1.1.44)	0.35	0.17	0.42		
Q8X166	Peptidyl-prolyl cis-trans isomerase B (PPIase B) (EC 5.2.1.8) (Rotamase B)	0.68	0.38	0.42		
Q6MVH7	Inorganic pyrophosphatase (EC 3.6.1.1) (Pyrophosphate phosphohydrolase) (PPase)	0.11	0.44	0.43		
O93869	Glycogen [starch] synthase (EC 2.4.1.11)	-0.42	0.07	0.43		
B4EYR8	Glucose-6-phosphate isomerase (GPI) (EC 5.3.1.9) (Phosphoglucose isomerase) (PGI) (Phosphohexose isomerase) (PHI)	-0.26	0.31	0.44		
P82611	Aconitate hydratase. mitochondrial (Aconitase) (EC 4.2.1.3) (Citrate hydrolyase)	0.31	-0.04	0.44		
Q2NA62	NADH-quinone oxidoreductase subunit C (EC 1.6.5.11) (NADH dehydrogenase I subunit C) (NDH-1 subunit C)	0.25	0.26	0.45		
P19115	40S ribosomal protein S14 (CRP2)	-0.67	-0.52	0.46		
O93918	Pyruvate carboxylase (EC 6.4.1.1) (Pyruvic carboxylase) (PCB)	0.05	-0.14	0.46		
A7E449	ATP-dependent RNA helicase dbp2 (EC 3.6.4.13)	-0.04	-0.32	0.46		
A6SB28	Nascent polypeptide-associated complex subunit alpha (NAC-alpha) (Alpha-NAC)	-0.30	-0.11	0.48		
Q7RVA8	Pyruvate kinase (PK) (EC 2.7.1.40) (Acetate-requiring protein 8)	-1.03	-0.84	0.50		
P12709	Glucose-6-phosphate isomerase (GPI) (EC 5.3.1.9) (Phosphoglucose isomerase) (PGI) (Phosphohexose isomerase) (PHI)	0.32	-0.23	0.51		
POCT11	Glycerol-3-phosphate dehydrogenase [NAD(+)] (EC 1.1.1.8)	0.30	0.05	0.52		
POCB32	Heat shock 70 kDa protein 1-like (Heat shock 70 kDa protein 1L)	-0.75	-0.39	0.53		
B3E9Q7	Phosphoglycerate kinase (EC 2.7.2.3)	-0.21	-0.11	0.54		
Q2KJB1	Septin-10	0.51	0.04	0.54		
Q9UT19	Probable 5-methyltetrahydropteroyltriglutamate--homocysteine methyltransferase (EC 2.1.1.14) (Cobalamin-independent methionine synthase) (Methionine synthase. vitamin-B12 independent isozyme)	0.06	0.27	0.55		
P04264	Keratin. type II cytoskeletal 1 (67 kDa cytokeratin) (Cytokeratin-1) (CK-1) (Hair alpha protein) (Keratin-1) (K1) (Type-II keratin Kb1)	-0.01	0.27	0.55		

Accession no.	UniProt recommended Protein name	Fold change ^a		ANOVA p-value	Cluster ^b	Common to At61
		Ag ⁺	AgNPs			
Q7RV85	Enolase (EC 4.2.1.11) (2-phospho-D-glycerate hydro-lyase) (2-phosphoglycerate dehydratase) (Embden-meyerhof pathway protein 7)	0.22	0.05	0.57		
P0CP79	Peptidyl-prolyl cis-trans isomerase B (PPIase B) (EC 5.2.1.8) (Rotamase B)	-0.15	-0.06	0.57		
Q9HEP7	cAMP-dependent protein kinase regulatory subunit (PKA regulatory subunit)	-0.30	0.06	0.58		
P07144	Mitochondrial outer membrane protein porin	-0.06	0.07	0.58		
Q7RYE7	Galactose-1-phosphate uridylyltransferase (Gal-1-P uridylyltransferase) (EC 2.7.7.12) (UDP-glucose--hexose-1-phosphate uridylyltransferase)	0.59	0.65	0.58		
Q9ZJ71	Elongation factor Ts (EF-Ts)	-0.51	0.21	0.58		
O94489	Elongation factor 3 (EF-3)	0.52	0.01	0.59		
O76511	Thymidylate synthase (TS) (TSase) (EC 2.1.1.45)	-0.85	-0.06	0.59		
P39708	NADP-specific glutamate dehydrogenase 2 (NADP-GDH 2) (EC 1.4.1.4) (NADP-dependent glutamate dehydrogenase 2)	0.18	-0.02	0.60		
O93866	Heat shock 70 kDa protein	0.05	0.19	0.61		
A7EUB3	Probable Xaa-Pro aminopeptidase pepP (EC 3.4.11.9) (Aminoacylproline aminopeptidase) (Prolidase)	-0.88	-0.87	0.62		
Q9SCX3	Elongation factor 1-beta 2 (EF-1-beta 2) (Elongation factor 1-beta' 2) (EF-1-beta' 2) (Elongation factor 1B-alpha 2) (eEF-1B alpha 2)	0.40	0.19	0.62		
O13419	Actin	-0.12	0.03	0.63		
P22068	ATP synthase subunit beta. mitochondrial (EC 3.6.3.14)	-0.53	0.65	0.64		
Q96KP4	Cytosolic non-specific dipeptidase (EC 3.4.13.18) (CNDP dipeptidase 2) (Carnosine dipeptidase II) (Epididymis secretory protein Li 13) (Glutamate carboxypeptidase-like protein 1) (Peptidase A)	0.13	0.56	0.64		
Q9AT34	40S ribosomal protein S15a	-0.14	-0.33	0.64		
P38793	tRNA (guanine(37)-N1)-methyltransferase (EC 2.1.1.228) (M1G-methyltransferase) (tRNA [GM37] methyltransferase) (tRNA methyltransferase 5)	0.24	0.04	0.66		
P48164	40S ribosomal protein S7-B	-0.28	0.24	0.67		

Accession no.	UniProt recommended Protein name	Fold change ^a		ANOVA p-value	Cluster ^b	Common to At61
		Ag ⁺	AgNPs			
Q9P4R4	Saccharopine dehydrogenase [NADP(+). L-glutamate-forming] (EC 1.5.1.10) (Saccharopine reductase)	0.22	0.15	0.68		
Q7RVN0	60S ribosomal protein L11	-0.12	-0.19	0.69		
C5P4Z8	Subtilisin-like protease CPC735_031240 (EC 3.4.21.-)	-0.41	-0.64	0.70		
B3Q4F9	Catalase-peroxidase (CP) (EC 1.11.1.21) (Peroxidase/catalase)	0.13	0.19	0.71		
D4AT77	Aconitate hydratase. mitochondrial (Aconitase) (EC 4.2.1.3) (Citrate hydro-lyase)	-0.33	0.04	0.73		
Q2S936	30S ribosomal protein S4	0.09	-0.04	0.75		
C7C436	2-methylcitrate synthase. mitochondrial (Methylcitrate synthase) (EC 2.3.3.5) ((2S.3S)-2-methylcitrate synthase) (Citrate synthase 2) (EC 2.3.3.16)	-0.08	-0.23	0.75		
A7TMJ2	Very-long-chain 3-oxoacyl-CoA reductase (EC 1.1.1.330) (3-ketoacyl-CoA reductase) (3-ketoreductase) (KAR) (Microsomal beta-keto-reductase)	-0.11	-0.17	0.75		
Q9P727	Succinate--CoA ligase [ADP-forming] subunit alpha. mitochondrial (EC 6.2.1.5) (Succinyl-CoA synthetase subunit alpha) (SCS-alpha)	-0.14	-0.32	0.77		
Q8X077	Probable proteasome subunit alpha type-2 (EC 3.4.25.1)	-0.01	-0.15	0.77		
A7F8K7	Eukaryotic translation initiation factor 3 subunit D (eIF3d)	-0.17	-0.16	0.79		
Q8J112	Probable electron transfer flavoprotein subunit alpha. mitochondrial (Alpha-ETF)	0.15	0.04	0.79		
O77033	General transcriptional corepressor trfA	-0.24	-0.06	0.80		
P05750	40S ribosomal protein S3 (RP13) (YS3)	-0.02	-0.14	0.80		
P11592	V-type proton ATPase catalytic subunit A (V-ATPase subunit A) (EC 3.6.3.14) (V-ATPase 67 kDa subunit) (Vacuolar proton pump subunit alpha)	0.00	0.37	0.80		
Q7S045	Non-histone chromosomal protein 6	0.06	-0.02	0.81		
O94550	Prohibitin-2	-0.47	0.03	0.81		
P0CX56	40S ribosomal protein S18-B	0.14	0.24	0.83		
O94128	Tubulin alpha chain	-0.22	-0.05	0.85		
A7EWN6	Eukaryotic translation initiation factor 3 subunit G (eIF3g) (Eukaryotic translation initiation factor 3 RNA-binding subunit) (eIF-3 RNA-binding	-0.25	0.01	0.87		

Accession no.	UniProt recommended Protein name	Fold change ^a		ANOVA p-value	Cluster ^b	Common to At61
		Ag ⁺	AgNPs			
	subunit) (Translation initiation factor eIF3 p33 subunit homolog) (eIF3 p33 homolog)					
Q4WM67	NADPH--cytochrome P450 reductase (CPR) (P450R) (EC 1.6.2.4)	0.26	0.24	0.90		
G0SGU4	Formate dehydrogenase (FDH) (EC 1.2.1.2) (NAD-dependent formate dehydrogenase)	0.27	0.33	0.90		
Q9P4V2	Phosphoacetylglucosamine mutase (PAGM) (EC 5.4.2.3) (Acetylglucosamine phosphomutase) (N-acetylglucosamine-phosphate mutase)	0.13	0.00	0.91		
P20285	Dihydrolipoyllysine-residue acetyltransferase component of pyruvate dehydrogenase complex. mitochondrial (EC 2.3.1.12) (Dihydrolipoamide acetyltransferase component of pyruvate dehydrogenase complex)	0.07	-0.13	0.93		
Q8LAH7	12-oxophytodienoate reductase 1 (EC 1.3.1.42) (12-oxophytodienoate-10.11-reductase 1) (AtOPR1) (OPDA-reductase 1) (FS-AT-I)	-0.11	-0.07	0.93		
P15368	Fatty acid synthase subunit alpha (EC 2.3.1.86) [Includes: Acyl carrier; 3-oxoacyl-[acyl-carrier-protein] reductase (EC 1.1.1.100) (Beta-ketoacyl reductase)	0.07	0.08	0.94		
A6SEH9	ATP-dependent RNA helicase ded1 (EC 3.6.4.13)	0.79	0.21	0.94		
Q0U0H7	Clustered mitochondria protein homolog (Protein TIF31 homolog)	0.07	0.08	0.95		
O14435	Guanine nucleotide-binding protein subunit beta	-0.03	0.02	0.97		
Q8X097	Probable ATP-citrate synthase subunit 1 (EC 2.3.3.8) (ATP-citrate (pro-S)-lyase 1) (Citrate cleavage enzyme subunit 1)	0.00	0.01	1.00		

^a Values were calculated as the average data from. at least four independent experiments. Fold changes of statistically significant proteins (ANOVA. $P < 0.05$) were determined by Log2 transformation of the ratio values of normalized protein levels obtained using crude protein extracts from *A. tetracladia* after 3 days of exposure to Ag⁺ or AgNPs at concentrations similar to EC₂₀ versus mycelia grown in control medium.

^b The unsupervised clustering analysis was performed considering standardization and the 172 statistically significant proteins across the different experimental conditions (Control. Ct; silver ions. Ag⁺ and silver nanoparticles. AgNPs) were partitioned into 7 clusters.

Appendix 12_Chapter 3

Table S3.3 Total identified proteins by SWATH-MS/MS from SDS-PAGE gels with (protein crude) extracts from mycelia of *A. tetracladia* (strain At61) grown in malt extract medium (ME 1%) in presence or absence of Ag⁺ or AgNPs for 3 days. Relative alteration of protein content (average fold change relative to control) of statistically significant proteins ($P < 0.05$) and respective cluster inclusion group are shaded in light grey. Positive and negative fold changes suggest increase and decrease in the protein content, respectively.

Accession no.	Protein name (UNIPROT)	Fold Change to Ct		ANOVA p-value	Cluster No.	Common to At61
		Ag ⁺	AgNPs			
A6SZW5	RNA-binding protein Hfq	2.58	4.32	0.00	1	
A6T3L6	50S ribosomal protein L1	1.21	5.35	0.00	1	
P95539	Catalase HPII (EC 1.11.1.6)	0.20	1.60	0.00	1	
Q8Y1H8	6.7-dimethyl-8-ribityllumazine synthase (DMRL synthase) (LS) (Lumazine synthase) (EC 2.5.1.78)	2.38	4.38	0.00	1	
A4G5Z9	Malate dehydrogenase (EC 1.1.1.37)	0.53	3.38	0.00	1	
Q82X69	DNA-directed RNA polymerase subunit alpha (RNAP subunit alpha) (EC 2.7.7.6) (RNA polymerase subunit alpha) (Transcriptase subunit alpha)	3.20	4.63	0.00	1	
Q8PJ05	dCTP deaminase (EC 3.5.4.13) (Deoxycytidine triphosphate deaminase)	-0.43	2.25	0.00	1	
Q9KHS6	DNA-binding protein HU-beta	0.62	1.40	0.00	1	
A6SUN7	50S ribosomal protein L13	2.15	4.03	0.00	1	
Q4ZX09	GMP synthase [glutamine-hydrolyzing] (EC 6.3.5.2) (GMP synthetase) (Glutamine amidotransferase)	0.32	1.66	0.00	1	
Q8XV10	Elongation factor G 1 (EF-G 1)	1.37	2.64	0.00	1	
Q8Y0J1	Acyl carrier protein 1 (ACP 1)	2.77	4.23	0.00	1	
Q87TT4	ATP synthase subunit beta (EC 3.6.3.14) (ATP synthase F1 sector subunit beta) (F-ATPase subunit beta)	0.20	1.32	0.00	1	
A4G995	Protein-export protein SecB	1.75	5.24	0.00	1	
P0CP79	Peptidyl-prolyl cis-trans isomerase B (PPIase B) (EC 5.2.1.8) (Rotamase B)	3.98	5.79	0.00	1	
Q8Y0W0	30S ribosomal protein S16	-0.29	3.22	0.00	1	

Accession no.	Protein name (UNIPROT)	Fold Change to Ct		ANOVA p-value	Cluster No.	Common to At61
		Ag ⁺	AgNPs			
C3K2V4	30S ribosomal protein S13	0.32	1.71	0.00	1	
Q5B4R3	Peptidyl-prolyl cis-trans isomerase B (PPIase B) (EC 5.2.1.8) (Rotamase B)	1.86	3.60	0.00	1	y
P01086	Trypsin inhibitor CMe (Alpha-amylase/trypsin inhibitor) (BTI-CMe1) (BTI-CMe2.1) (BTI-CMe3.1) (Chloroform/methanol-soluble protein CMe)	2.07	3.43	0.00	1	
P37369	Superoxide dismutase [Fe] (EC 1.15.1.1)	0.82	3.49	0.00	1	
C3K3G6	Adenosylhomocysteinase (EC 3.3.1.1) (S-adenosyl-L-homocysteine hydrolase) (AdoHcyase)	0.02	1.51	0.00	1	
Q51567	Succinate--CoA ligase [ADP-forming] subunit alpha (EC 6.2.1.5) (Succinyl-CoA synthetase subunit alpha) (SCS-alpha)	0.12	1.29	0.00	1	
B1J254	Chaperone protein DnaK (HSP70) (Heat shock 70 kDa protein) (Heat shock protein 70)	0.35	1.54	0.00	1	
P22862	Arylesterase (EC 3.1.1.2) (Aryl-ester hydrolase) (PFE) (Putative bromoperoxidase) (EC 1.-.-.-)	1.53	3.11	0.00	1	
A4G9T3	50S ribosomal protein L22	1.53	4.26	0.00	1	
C3K1E8	ATP synthase subunit alpha (EC 3.6.3.14) (ATP synthase F1 sector subunit alpha) (F-ATPase subunit alpha)	1.97	3.20	0.00	1	
C3K8X4	UDP-N-acetylglucosamine 1-carboxyvinyltransferase (EC 2.5.1.7) (Enoylpyruvate transferase) (UDP-N-acetylglucosamine enolpyruvyl transferase) (EPT)	0.95	1.98	0.00	1	
P0A1P7	Glutamine synthetase (EC 6.3.1.2) (Glutamate--ammonia ligase)	1.26	2.58	0.00	1	
Q9HWC4	Transcription termination/antitermination protein NusG	2.21	3.53	0.00	1	
Q8Z7S0	Outer membrane protein A	2.10	3.47	0.00	1	
Q889U7	30S ribosomal protein S4	0.58	1.60	0.00	1	
Q59633	UTP--glucose-1-phosphate uridylyltransferase (EC 2.7.7.9) (Alpha-D-glucosyl-1-phosphate uridylyltransferase) (UDP-glucose pyrophosphorylase) (UDPGP) (Uridine diphosphoglucose pyrophosphorylase)	-0.01	0.62	0.00	1	
P24751	Glyceraldehyde-3-phosphate dehydrogenase (GAPDH) (EC 1.2.1.12) (NAD-dependent glyceraldehyde-3-phosphate dehydrogenase) (Fragment)	1.46	2.90	0.00	1	

Accession no.	Protein name (UNIPROT)	Fold Change to Ct		ANOVA p-value	Cluster No.	Common to At61
		Ag ⁺	AgNPs			
Q475T3	50S ribosomal protein L13	1.85	3.44	0.00	1	
A4SUV5	DNA-directed RNA polymerase subunit beta' (RNAP subunit beta') (EC 2.7.7.6) (RNA polymerase subunit beta') (Transcriptase subunit beta')	0.48	2.41	0.00	1	
A6UZJ8	50S ribosomal protein L14	0.15	2.61	0.01	1	
Q8XZJ1	30S ribosomal protein S2	0.84	3.21	0.01	1	
C6DKK7	Polyribonucleotide nucleotidyltransferase (EC 2.7.7.8) (Polynucleotide phosphorylase) (PNPase)	1.08	2.34	0.01	1	
C3K2X8	Elongation factor Tu (EF-Tu)	0.79	1.63	0.01	1	
Q88PD5	Superoxide dismutase [Fe] (EC 1.15.1.1)	2.33	4.21	0.01	1	
O42772	Succinate dehydrogenase [ubiquinone] iron-sulfur subunit. mitochondrial (EC 1.3.5.1) (Iron-sulfur subunit of complex II) (Ip)	0.85	2.07	0.01	1	y
Q4K3A8	ATP synthase gamma chain (ATP synthase F1 sector gamma subunit) (F-ATPase gamma subunit)	1.14	2.14	0.01	1	
Q4KF90	Transaldolase (EC 2.2.1.2)	-0.76	0.70	0.01	1	
Q88BD4	Phosphomannomutase/phosphoglucomutase (PMM / PGM) (EC 5.4.2.2) (EC 5.4.2.8)	1.02	2.38	0.01	1	
Q9HWE0	50S ribosomal protein L22	-0.16	1.70	0.01	1	
Q8X166	Peptidyl-prolyl cis-trans isomerase B (PPIase B) (EC 5.2.1.8) (Rotamase B)	2.23	4.53	0.01	1	
Q4ZMP7	50S ribosomal protein L2	1.46	3.04	0.01	1	
A6T1E5	60 kDa chaperonin (GroEL protein) (Protein Cpn60)	0.98	2.06	0.01	1	
Q9I2V5	Aconitate hydratase B (ACN) (Aconitase) (EC 4.2.1.3) ((2R.3S)-2-methylisocitrate dehydratase) ((2S.3R)-3-hydroxybutane-1.2.3-tricarboxylate dehydratase) (2-methyl-cis-aconitate hydratase) (EC 4.2.1.99) (Iron-responsive protein-like) (IRP-like) (RNA-binding protein)	1.28	2.31	0.01	1	
C3K2Y5	50S ribosomal protein L10	0.25	2.46	0.01	1	
A7EWN6	Eukaryotic translation initiation factor 3 subunit G (eIF3g) (Eukaryotic translation initiation factor 3 RNA-binding subunit) (eIF-3 RNA-binding	0.31	0.79	0.01	1	

Accession no.	Protein name (UNIPROT)	Fold Change to Ct		ANOVA p-value	Cluster No.	Common to At61
		Ag ⁺	AgNPs			
	subunit) (Translation initiation factor eIF3 p33 subunit homolog) (eIF3 p33 homolog)					
Q4K4K8	NAD/NADP-dependent betaine aldehyde dehydrogenase (BADH) (EC 1.2.1.8)	0.11	1.79	0.01	1	
Q88B43	Peptide deformylase 1 (PDF 1) (EC 3.5.1.88) (Polypeptide deformylase 1)	0.98	2.66	0.01	1	
C5B7L0	Transaldolase (EC 2.2.1.2)	0.92	1.99	0.01	1	
C5FS55	Vacuolar protease A (EC 3.4.23.25) (Aspartic endopeptidase PEP2) (Aspartic protease PEP2)	0.74	1.71	0.02	1	
Q9ZKD8	NADP-specific glutamate dehydrogenase (NADP-GDH) (EC 1.4.1.4)	0.05	0.63	0.02	1	y
Q9D6J6	NADH dehydrogenase [ubiquinone] flavoprotein 2, mitochondrial (EC 1.6.5.3) (EC 1.6.99.3) (NADH-ubiquinone oxidoreductase 24 kDa subunit)	0.81	2.09	0.02	1	
C3K6N0	Succinate--CoA ligase [ADP-forming] subunit beta (EC 6.2.1.5) (Succinyl-CoA synthetase subunit beta) (SCS-beta)	0.55	1.53	0.02	1	
Q752U5	60S ribosomal protein L30	2.27	3.68	0.02	1	
Q9Y7Z2	ADP-ribosylation factor 6	0.98	2.13	0.02	1	
Q4KIH1	Chaperone protein DnaK (HSP70) (Heat shock 70 kDa protein) (Heat shock protein 70)	0.35	2.57	0.02	1	
P33282	Uricase (EC 1.7.3.3) (Urate oxidase)	0.15	0.60	0.02	1	y
A4G1T2	50S ribosomal protein L13	1.52	2.66	0.02	1	
Q4K529	30S ribosomal protein S7	0.37	1.27	0.03	1	
O93934	NADP-specific glutamate dehydrogenase (NADP-GDH) (EC 1.4.1.4) (NADP-dependent glutamate dehydrogenase)	-0.08	0.56	0.03	1	y
Q3K5Y5	Elongation factor G (EF-G)	0.19	1.87	0.03	1	
C3JZN6	Translation initiation factor IF-3	0.70	2.03	0.03	1	
C3K2V7	50S ribosomal protein L15	-0.53	1.69	0.03	1	

Accession no.	Protein name (UNIPROT)	Fold Change to Ct		ANOVA p-value	Cluster No.	Common to At61
		Ag ⁺	AgNPs			
Q9UT19	Probable 5-methyltetrahydropteroyltriglutamate--homocysteine methyltransferase (EC 2.1.1.14) (Cobalamin-independent methionine synthase) (Methionine synthase, vitamin-B12 independent isozyme)	1.01	2.18	0.03	1	
A7EF03	Eukaryotic translation initiation factor 3 subunit I (eIF3i) (Eukaryotic translation initiation factor 3 39 kDa subunit homolog) (eIF-3 39 kDa subunit homolog)	0.10	1.81	0.04	1	y
C3K5Z6	Elongation factor Ts (EF-Ts)	1.37	2.50	0.04	1	
P52155	Transcription termination factor Rho (EC 3.6.4.-) (ATP-dependent helicase Rho)	0.52	1.55	0.04	1	
C1DAQ8	50S ribosomal protein L10	0.14	1.97	0.04	1	
B2VCA4	ATP synthase subunit beta (EC 3.6.3.14) (ATP synthase F1 sector subunit beta) (F-ATPase subunit beta)	1.51	2.98	0.05	1	
Q889U6	DNA-directed RNA polymerase subunit alpha (RNAP subunit alpha) (EC 2.7.7.6) (RNA polymerase subunit alpha) (Transcriptase subunit alpha)	0.67	2.35	0.05	1	
Q9KZM1	Adenosylhomocysteinase (EC 3.3.1.1) (S-adenosyl-L-homocysteine hydrolase) (AdoHcyase)	0.39	-0.74	0.00	2	y
O74445	Probable 26S protease subunit rpt4	0.23	-0.66	0.00	2	
O43109	Heat shock protein 90 homolog (Suppressor of vegetative incompatibility MOD-E)	0.36	-0.63	0.00	2	y
P52810	40S ribosomal protein S9 (S7)	0.30	-1.41	0.01	2	
Q5B998	Homoserine dehydrogenase (HDH) (EC 1.1.1.3)	0.49	-0.30	0.01	2	
Q477V3	Protein RecA (Recombinase A)	2.10	0.34	0.01	2	
P51044	Citrate synthase, mitochondrial (EC 2.3.3.16)	0.21	-0.68	0.01	2	y
P48164	40S ribosomal protein S7-B	0.10	-1.38	0.03	2	
Q875B7	Histone H2B	0.33	-0.74	0.03	2	
A7EGL7	ATP-dependent RNA helicase eIF4A (EC 3.6.4.13) (Eukaryotic initiation factor 4A) (eIF-4A) (Translation initiation factor 1)	0.06	-0.33	0.03	2	y
P29497	Glyceraldehyde-3-phosphate dehydrogenase (GAPDH) (EC 1.2.1.12)	0.07	-0.16	0.05	2	

Accession no.	Protein name (UNIPROT)	Fold Change to Ct		ANOVA p-value	Cluster No.	Common to At61
		Ag ⁺	AgNPs			
Q13TJ6	DNA-directed RNA polymerase subunit alpha (RNAP subunit alpha) (EC 2.7.7.6) (RNA polymerase subunit alpha) (Transcriptase subunit alpha)	3.96	3.40	0.00	3	
P48347	14-3-3-like protein GF14 epsilon (General regulatory factor 10)	0.96	0.40	0.00	3	y
P31865	Pyruvate kinase (PK) (EC 2.7.1.40)	0.87	0.97	0.00	3	
P0A2K8	UTP--glucose-1-phosphate uridylyltransferase (EC 2.7.7.9) (Alpha-D-glucosyl-1-phosphate uridylyltransferase) (UDP-glucose pyrophosphorylase) (UDPGP) (Uridine diphosphoglucose pyrophosphorylase)	2.17	2.18	0.00	3	
P58582	Glutathione synthetase (EC 6.3.2.3) (GSH synthetase) (GSH-S) (GSHase) (Glutathione synthase)	1.53	1.75	0.00	3	
Q96X45	Elongation factor 2 (EF-2) (Colonial temperature-sensitive 3)	1.15	0.70	0.00	3	y
Q8XV37	30S ribosomal protein S4	2.43	2.51	0.00	3	
Q9NW08	DNA-directed RNA polymerase III subunit RPC2 (RNA polymerase III subunit C2) (EC 2.7.7.6) (C128) (DNA-directed RNA polymerase III 127.6 kDa polypeptide) (DNA-directed RNA polymerase III subunit B)	3.06	3.05	0.00	3	y
Q0KBK5	Trigger factor (TF) (EC 5.2.1.8) (PPIase)	4.13	4.37	0.00	3	
A6SY73	Trigger factor (TF) (EC 5.2.1.8) (PPIase)	3.82	4.15	0.00	3	
O24653	Guanosine nucleotide diphosphate dissociation inhibitor 2 (AtGDI2)	3.66	3.57	0.00	3	y
B2T9P8	Malate dehydrogenase (EC 1.1.1.37)	2.55	2.74	0.00	3	
A6SVI7	50S ribosomal protein L19	4.17	4.25	0.01	3	
A5DI11	Elongation factor 2 (EF-2)	1.51	1.49	0.01	3	
P0CM17	ADP-ribosylation factor	2.33	2.60	0.01	3	y
Q4WY53	Phosphoglucomutase (PGM) (EC 5.4.2.2) (Glucose phosphomutase)	2.94	3.15	0.01	3	y
P26518	Glyceraldehyde-3-phosphate dehydrogenase, cytosolic (EC 1.2.1.12)	6.16	6.52	0.01	3	y
A4W7A7	Trigger factor (TF) (EC 5.2.1.8) (PPIase)	0.78	0.82	0.01	3	
Q2UPZ7	Aspartyl aminopeptidase (DAP) (EC 3.4.11.21)	2.17	2.31	0.01	3	y
A7EY76	ATP-dependent RNA helicase dbp5 (EC 3.6.4.13)	1.34	0.80	0.01	3	y
Q9UUE1	Pyruvate carboxylase (EC 6.4.1.1) (Pyruvic carboxylase) (PCB)	3.76	3.56	0.01	3	

Accession no.	Protein name (UNIPROT)	Fold Change to Ct		ANOVA p-value	Cluster No.	Common to At61
		Ag ⁺	AgNPs			
Q6BZH1	78 kDa glucose-regulated protein homolog (GRP-78) (Immunoglobulin heavy chain-binding protein homolog) (BIP)	3.31	3.50	0.02	3	y
Q9HEP7	cAMP-dependent protein kinase regulatory subunit (PKA regulatory subunit)	3.17	2.50	0.02	3	
P33723	GTP-binding protein ypt1	1.64	1.70	0.02	3	
A6SX19	Elongation factor P (EF-P)	3.22	3.17	0.02	3	
P48466	S-adenosylmethionine synthase (AdoMet synthase) (EC 2.5.1.6) (Ethionine resistance protein 1) (Methionine adenosyltransferase) (MAT)	1.74	1.97	0.02	3	
Q9C285	60S ribosomal protein L12	0.75	0.82	0.02	3	
Q7SCP4	F-actin-capping protein subunit beta (F-actin capping protein 2)	1.60	1.32	0.03	3	y
P10592	Heat shock protein SSA2	4.64	4.48	0.03	3	y
Q9Y8H7	Spermidine synthase (SPDSY) (EC 2.5.1.16) (Putrescine aminopropyltransferase)	0.62	0.46	0.03	3	
A4W5A0	Elongation factor Tu (EF-Tu)	2.20	1.73	0.04	3	
Q6BJ25	Elongation factor 2 (EF-2)	1.42	1.25	0.04	3	
C1GUB6	40S ribosomal protein S0	0.56	0.56	0.05	3	y
Q00955	Acetyl-CoA carboxylase (ACC) (EC 6.4.1.2) (Fatty acid synthetase 3) (mRNA transport-defective protein 7) [Includes: Biotin carboxylase (EC 6.3.4.14)]	-1.25	-2.28	0.00	4	y
P12709	Glucose-6-phosphate isomerase (GPI) (EC 5.3.1.9) (Phosphoglucose isomerase) (PGI) (Phosphohexose isomerase) (PHI)	-1.33	-1.73	0.00	4	
Q9HES8	Pyruvate carboxylase (EC 6.4.1.1) (Pyruvic carboxylase) (PCB)	-0.76	-1.14	0.00	4	y
B3E9Q7	Phosphoglycerate kinase (EC 2.7.2.3)	-0.51	-0.89	0.00	4	
P04264	Keratin, type II cytoskeletal 1 (67 kDa cytokeratin) (Cytokeratin-1) (CK-1) (Hair alpha protein) (Keratin-1) (K1) (Type-II keratin Kb1)	-2.34	-2.87	0.00	4	
A8IW34	Adenylosuccinate synthetase, chloroplastic (AMPSase) (AdSS) (EC 6.3.4.4) (IMP--aspartate ligase)	-0.54	-0.88	0.00	4	
Q05425	Guanine nucleotide-binding protein alpha-1 subunit (GP1-alpha)	-1.11	-1.54	0.00	4	y
Q874J6	Histone H3-like centromeric protein CSE4 (CENP-A homolog)	-0.54	-0.89	0.00	4	y

Accession no.	Protein name (UNIPROT)	Fold Change to Ct		ANOVA p-value	Cluster No.	Common to At61
		Ag ⁺	AgNPs			
Q650L7	S-adenosylmethionine:tRNA ribosyltransferase-isomerase (EC 2.4.99.17) (Queuosine biosynthesis protein QueA)	-3.05	-2.88	0.00	4	
P00761	Trypsin (EC 3.4.21.4)	-1.63	-3.40	0.00	4	y
O94550	Prohibitin-2	-3.01	-3.24	0.00	4	
Q886V7	Phosphoribosylglycinamide formyltransferase 2 (GART 2) (EC 2.1.2.-) (5'-phosphoribosylglycinamide transformylase 2) (Formate-dependent GAR transformylase) (GAR transformylase 2)	-0.56	-1.06	0.01	4	
Q59638	Dihydropyridyllysine-residue acetyltransferase component of pyruvate dehydrogenase complex (EC 2.3.1.12) (Dihydrolipoamide acetyltransferase component of pyruvate dehydrogenase complex) (E2)	-0.86	-0.90	0.01	4	
P37726	Outer membrane porin F (Root adhesin)	-2.38	-3.16	0.01	4	
P22068	ATP synthase subunit beta, mitochondrial (EC 3.6.3.14)	-0.87	-1.32	0.01	4	
Q48D34	Elongation factor Tu (EF-Tu)	-0.63	-0.90	0.01	4	
Q8XCJ6	Glucose-6-phosphate 1-dehydrogenase (G6PD) (EC 1.1.1.49)	-0.68	-0.80	0.01	4	
A4R935	NADH-cytochrome b5 reductase 1 (EC 1.6.2.2) (Microsomal cytochrome b reductase)	-1.28	-1.39	0.01	4	y
Q5AAG6	Mitogen-activated protein kinase MKC1 (MAP kinase MKC1) (EC 2.7.11.24)	-1.80	-1.87	0.01	4	
P87018	Ras-like protein	-0.48	-0.74	0.02	4	y
A9GP90	Urease accessory protein UreG	-0.59	-0.64	0.04	4	
A6LE80	DNA-directed RNA polymerase subunit beta' (RNAP subunit beta') (EC 2.7.7.6) (RNA polymerase subunit beta') (Transcriptase subunit beta')	-1.48	-1.62	0.04	4	y
A6SFQ6	Eukaryotic translation initiation factor 3 subunit B (eIF3b) (Eukaryotic translation initiation factor 3 90 kDa subunit homolog) (eIF3 p90) (Translation initiation factor eIF3, p90 subunit homolog)	-0.34	-0.53	0.04	4	y
Q9M4E3	Hordoindoline-A	-0.89	-1.27	0.04	4	
P87252	Woronin body major protein	-1.27	-2.06	0.04	4	
Q5BAX8	E3 ubiquitin ligase complex SCF subunit sconC (Sulfur controller C) (Sulfur metabolite repression control protein C)	3.39	4.28	0.00	5	

Accession no.	Protein name (UNIPROT)	Fold Change to Ct		ANOVA p-value	Cluster No.	Common to At61
		Ag ⁺	AgNPs			
P09551	Lysine/arginine/ornithine-binding periplasmic protein (LAO-binding protein)	3.36	4.56	0.00	5	
J9MJK9	Transaldolase (FoTal) (EC 2.2.1.2)	0.82	1.38	0.00	5	
P87222	Heat shock protein SSB1	1.33	2.15	0.00	5	y
P06738	Glycogen phosphorylase (EC 2.4.1.1)	1.22	1.50	0.00	5	y
Q5R9Y4	Ras-related protein Rab-7a	2.76	3.65	0.00	5	y
C3KE70	50S ribosomal protein L9	1.13	2.09	0.00	5	
Q4K542	30S ribosomal protein S17	1.13	2.09	0.00	5	
A4VHT4	6.7-dimethyl-8-ribityllumazine synthase (DMRL synthase) (LS) (Lumazine synthase) (EC 2.5.1.78)	1.97	3.14	0.00	5	
Q4K749	Argininosuccinate synthase (EC 6.3.4.5) (Citrulline--aspartate ligase)	1.42	2.35	0.00	5	
P79089	Isocitrate dehydrogenase [NADP]. mitochondrial (IDH) (EC 1.1.1.42) (IDP) (NADP(+)-specific ICDH) (Oxalosuccinate decarboxylase)	1.92	2.33	0.00	5	y
P69061	Ubiquitin-40S ribosomal protein S27a [Cleaved into: Ubiquitin; 40S ribosomal protein S27a]	1.02	1.78	0.00	5	y
Q2L2G6	Elongation factor Tu (EF-Tu)	4.02	4.78	0.00	5	
P11643	Alpha-amylase/trypsin inhibitor CMd (Chloroform/methanol-soluble protein CMd)	0.89	1.73	0.00	5	
Q3K8L1	Acyl carrier protein (ACP)	3.86	4.53	0.00	5	
Q4K608	Ketol-acid reductoisomerase (NADP(+)) (KARI) (EC 1.1.1.86) (Acetohydroxy-acid isomeroreductase) (AHIR) (Alpha-keto-beta-hydroxylacyl reductoisomerase) (Ketol-acid reductoisomerase type 1) (Ketol-acid reductoisomerase type I)	1.45	2.35	0.00	5	
A5FZW7	Elongation factor Tu (EF-Tu)	2.66	3.41	0.00	5	
C3K307	Indole-3-glycerol phosphate synthase (IGPS) (EC 4.1.1.48)	2.14	2.86	0.00	5	
A4G9T1	50S ribosomal protein L16	3.56	4.05	0.00	5	
P61503	Superoxide dismutase [Mn] (EC 1.15.1.1)	2.41	3.09	0.00	5	
Q9SF40	60S ribosomal protein L4-1 (L1)	1.93	2.47	0.00	5	y
P13691	Alpha-amylase inhibitor BDAI-1	1.50	2.52	0.00	5	

Accession no.	Protein name (UNIPROT)	Fold Change to Ct		ANOVA p-value	Cluster No.	Common to At61
		Ag ⁺	AgNPs			
Q99002	14-3-3 protein homolog (Th1433)	4.04	5.17	0.00	5	
Q7RZS0	60S ribosomal protein L10a (Cytoplasmic ribosomal protein 74)	2.62	3.29	0.00	5	y
Q02NB5	Isocitrate dehydrogenase [NADP] (IDH) (EC 1.1.1.42) (IDP) (NADP(+)-specific ICDH) (Oxalosuccinate decarboxylase)	3.98	4.81	0.00	5	
P31353	Phosphomannomutase (PMM) (EC 5.4.2.8)	2.05	2.99	0.01	5	
Q5BCG1	3'(2').5'-bisphosphate nucleotidase (EC 3.1.3.7) (3'(2').5-bisphosphonucleoside 3'(2')-phosphohydrolase) (DPNPase)	2.86	3.62	0.01	5	y
Q9P727	Succinate--CoA ligase [ADP-forming] subunit alpha. mitochondrial (EC 6.2.1.5) (Succinyl-CoA synthetase subunit alpha) (SCS-alpha)	4.27	5.23	0.01	5	
Q8XGZ0	Elongation factor Tu (EF-Tu)	2.42	2.86	0.01	5	
A6VB57	60 kDa chaperonin (GroEL protein) (Protein Cpn60)	2.74	3.80	0.01	5	
P52993	Dihydrolipoyllysine-residue succinyltransferase component of 2-oxoglutarate dehydrogenase complex (EC 2.3.1.61) (2-oxoglutarate dehydrogenase complex component E2) (OGDC-E2) (Dihydrolipoamide succinyltransferase component of 2-oxoglutarate dehydrogenase complex)	2.12	2.77	0.01	5	
C3K1L8	Nucleoside diphosphate kinase (NDK) (NDP kinase) (EC 2.7.4.6) (Nucleoside-2-P kinase)	1.78	2.92	0.01	5	
Q9SCX3	Elongation factor 1-beta 2 (EF-1-beta 2) (Elongation factor 1-beta' 2) (EF-1-beta' 2) (Elongation factor 1B-alpha 2) (eEF-1B alpha 2)	3.39	4.39	0.01	5	
Q8X034	60S ribosomal protein L15	1.97	2.48	0.01	5	y
C4K4F8	Elongation factor Tu (EF-Tu)	1.53	2.17	0.01	5	
Q7RVA8	Pyruvate kinase (PK) (EC 2.7.1.40) (Acetate-requiring protein 8)	1.71	2.76	0.01	5	
P40918	Heat shock 70 kDa protein (Allergen Cla h IV) (allergen Cla h 4)	2.08	2.85	0.01	5	
Q1CRI6	4-diphosphocytidyl-2-C-methyl-D-erythritol kinase (CMK) (EC 2.7.1.148) (4-(cytidine-5'-diphospho)-2-C-methyl-D-erythritol kinase)	0.92	1.41	0.01	5	
P05694	5-methyltetrahydropteroyltriglutamate--homocysteine methyltransferase (EC 2.1.1.14) (Cobalamin-independent methionine synthase) (Delta-P8 protein) (Methionine synthase. vitamin-B12 independent isozyme)	2.97	3.98	0.01	5	

Accession no.	Protein name (UNIPROT)	Fold Change to Ct		ANOVA p-value	Cluster No.	Common to At61
		Ag ⁺	AgNPs			
P0A252	Alkyl hydroperoxide reductase subunit C (EC 1.11.1.15) (Alkyl hydroperoxide reductase protein C22) (Peroxiredoxin) (Thioredoxin peroxidase)	3.31	4.33	0.01	5	
A1AZF8	Glycine--tRNA ligase beta subunit (EC 6.1.1.14) (Glycyl-tRNA synthetase beta subunit) (GlyRS)	2.09	2.46	0.01	5	
A7EIX7	ATP-dependent RNA helicase sub2 (EC 3.6.4.13)	1.73	2.64	0.01	5	y
A7EJL9	Leukotriene A-4 hydrolase homolog (LTA-4 hydrolase) (EC 3.3.2.6) (Leukotriene A(4) hydrolase)	3.25	3.95	0.01	5	y
Q8DCA2	Transketolase 1 (TK 1) (EC 2.2.1.1)	1.81	2.72	0.01	5	
P19115	40S ribosomal protein S14 (CRP2)	1.00	1.46	0.01	5	
Q98N18	Nitrogen regulatory protein P-II	1.27	1.66	0.01	5	
Q7RVN0	60S ribosomal protein L11	1.71	2.52	0.01	5	
P41577	6-phosphogluconate dehydrogenase. decarboxylating (EC 1.1.1.44) (Fragment)	2.12	2.99	0.01	5	
Q07103	Formate dehydrogenase (FDH) (EC 1.2.1.2) (NAD-dependent formate dehydrogenase)	1.83	2.22	0.01	5	y
A7F1L5	Cyanate hydratase (Cyanase) (EC 4.2.1.104) (Cyanate hydrolase) (Cyanate lyase)	2.71	3.91	0.01	5	y
Q7S045	Non-histone chromosomal protein 6	2.38	3.47	0.01	5	
Q4KGQ4	Probable periplasmic serine endoprotease DegP-like (EC 3.4.21.107) (Protease Do)	2.87	3.56	0.01	5	
Q87X14	60 kDa chaperonin (GroEL protein) (Protein Cpn60)	1.57	2.27	0.01	5	
Q00251	Elongation factor 1-alpha (EF-1-alpha)	2.53	3.05	0.01	5	y
O14460	Elongation factor 2 (EF-2)	2.59	3.06	0.01	5	y
Q9ZF60	Glutamate/aspartate import solute-binding protein	2.55	3.82	0.01	5	
Q70Q35	Superoxide dismutase [Cu-Zn] (EC 1.15.1.1)	3.47	4.69	0.02	5	y
O59945	Fimbrin	1.91	2.45	0.02	5	y

Accession no.	Protein name (UNIPROT)	Fold Change to Ct		ANOVA p-value	Cluster No.	Common to At61
		Ag ⁺	AgNPs			
P53655	Superoxide dismutase [Mn] (EC 1.15.1.1)	2.04	2.77	0.02	5	
Q93HX6	Glucosaminatase (EC 4.3.1.9) (D-glucosaminatase alpha-subunit) (GlcNA-DH alpha subunit) (GlcNADH-alpha)	1.30	2.06	0.02	5	
L7IK19	40S ribosomal protein S1	1.19	1.56	0.02	5	y
A0B6Y9	Dihydroxy-acid dehydratase (DAD) (EC 4.2.1.9)	3.90	4.35	0.02	5	y
D4AT77	Aconitate hydratase, mitochondrial (Aconitase) (EC 4.2.1.3) (Citrate hydro-lyase)	2.42	2.79	0.02	5	
Q11Q98	Elongation factor Tu (EF-Tu)	0.86	1.70	0.02	5	
Q6FRB7	Inorganic pyrophosphatase (EC 3.6.1.1) (Pyrophosphate phospho-hydrolase) (PPase)	2.61	3.53	0.02	5	y
P48580	Serine/threonine-protein phosphatase PP2A catalytic subunit (EC 3.1.3.16)	2.61	3.05	0.02	5	
Q9HZ71	30S ribosomal protein S1	0.84	1.61	0.03	5	
Q8ZNV7	Zinc import ATP-binding protein ZnuC (EC 3.6.3.-)	0.80	1.36	0.03	5	y
Q09668	60S ribosomal protein L22	0.41	0.77	0.03	5	
Q9UW86	Serine/threonine-protein phosphatase PP1 (EC 3.1.3.16) (Phosphoprotein phosphatase 1)	1.60	2.22	0.03	5	
P34727	ADP-ribosylation factor	2.96	3.61	0.03	5	y
Q0C9L8	ATP synthase subunit beta, mitochondrial (EC 3.6.3.14) (Citroviridin biosynthesis protein E)	3.80	4.34	0.03	5	
P38078	V-type proton ATPase catalytic subunit A (V-ATPase subunit A) (EC 3.6.3.14) (Vacuolar proton pump subunit A) [Cleaved into: Endonuclease PI-Ctrl (EC 3.1.-.-) (Ctr VMA intein) (VMA1-derived endonuclease) (VDE)]	1.91	2.83	0.03	5	y
C7C436	2-methylcitrate synthase, mitochondrial (Methylcitrate synthase) (EC 2.3.3.5) ((2S,3S)-2-methylcitrate synthase) (Citrate synthase 2) (EC 2.3.3.16)	0.87	1.24	0.03	5	
Q876L8	NAD(P)H-dependent D-xylose reductase xyl1 (XR) (EC 1.1.1.-)	1.79	2.19	0.03	5	y
Q5ZJN2	Ras-related protein Rab-11A	0.63	1.08	0.03	5	y
P0ABD4	Bacterioferritin (BFR) (EC 1.16.3.1) (Cytochrome b-1) (Cytochrome b-557)	2.88	3.53	0.03	5	

Accession no.	Protein name (UNIPROT)	Fold Change to Ct		ANOVA p-value	Cluster No.	Common to At61
		Ag ⁺	AgNPs			
Q8LAH7	12-oxophytodienoate reductase 1 (EC 1.3.1.42) (12-oxophytodienoate-10.11-reductase 1) (AtOPR1) (OPDA-reductase 1) (FS-AT-I) [Cleaved into: 12-oxophytodienoate reductase 1. N-terminally processed]	0.86	1.42	0.03	5	
Q765N2	Fatty acid synthase subunit alpha (EC 2.3.1.86) (p190/210) [Includes: Acyl carrier; 3-oxoacyl-[acyl-carrier-protein] reductase (EC 1.1.1.100) (Beta-ketoacyl reductase); 3-oxoacyl-[acyl-carrier-protein] synthase (EC 2.3.1.41) (Beta-ketoacyl synthase)]	2.05	2.40	0.04	5	
P28295	Elongation factor 1-alpha (EF-1-alpha)	1.54	2.31	0.04	5	
A1WCN6	Elongation factor Tu 2 (EF-Tu 2)	2.17	2.79	0.04	5	
B2VCV8	50S ribosomal protein L9	0.96	1.81	0.04	5	
A7E4H3	40S ribosomal protein S1	2.33	2.85	0.04	5	y
P0A9Z0	Cold shock-like protein CspC (CSP-C)	0.57	0.74	0.04	5	
Q00216	Protein disulfide-isomerase tigA (EC 5.3.4.1)	2.45	3.33	0.04	5	
Q9C3Z6	60S acidic ribosomal protein P0	0.26	0.52	0.04	5	y
Q8TFN0	Nucleoside diphosphate kinase (NDP kinase) (EC 2.7.4.6) (AnNDK) (NDK)	4.28	4.92	0.04	5	
P0CT11	Glycerol-3-phosphate dehydrogenase [NAD(+)] (EC 1.1.1.8)	1.08	1.47	0.04	5	
P32637	Glyceraldehyde-3-phosphate dehydrogenase (GAPDH) (EC 1.2.1.12)	0.44	0.63	0.04	5	y
Q7Z8E7	Glycerol-3-phosphate dehydrogenase [NAD(+)] (EC 1.1.1.8)	1.54	2.14	0.05	5	y
Q59PT0	V-type proton ATPase subunit B (V-ATPase subunit B) (Vacuolar proton pump subunit B)	-0.33	-1.21	0.00	6	y
Q59KI0	UTP--glucose-1-phosphate uridylyltransferase (EC 2.7.7.9) (UDP-glucose pyrophosphorylase) (UDPGP) (UGPase)	-0.24	-0.70	0.00	6	
Q9ZP06	Malate dehydrogenase 1. mitochondrial (EC 1.1.1.37) (Mitochondrial MDH1) (mMDH1) (Mitochondrial NAD-dependent malate dehydrogenase 1) (mNAD-MDH 1) (mtNAD-MDH1)	-0.47	-1.18	0.00	6	y
P02723	ADP.ATP carrier protein (ADP/ATP translocase) (Adenine nucleotide translocator) (ANT)	-0.73	-2.75	0.00	6	

Accession no.	Protein name (UNIPROT)	Fold Change to Ct		ANOVA p-value	Cluster No.	Common to At61
		Ag ⁺	AgNPs			
P20285	Dihydrolipoyllysine-residue acetyltransferase component of pyruvate dehydrogenase complex. mitochondrial (EC 2.3.1.12) (Dihydrolipoamide acetyltransferase component of pyruvate dehydrogenase complex) (MRP3) (Pyruvate dehydrogenase complex component E2) (PDC-E2) (PDCE2)	-0.74	-1.74	0.00	6	
Q00859	Mitogen-activated protein kinase (EC 2.7.11.24) (FsMAPK)	-0.48	-2.01	0.00	6	
P38720	6-phosphogluconate dehydrogenase. decarboxylating 1 (EC 1.1.1.44)	-0.20	-0.83	0.00	6	y
P48826	Glucose-6-phosphate 1-dehydrogenase (G6PD) (EC 1.1.1.49)	-0.35	-0.66	0.00	6	y
Q9P4R4	Saccharopine dehydrogenase [NADP(+). L-glutamate-forming] (EC 1.5.1.10) (Saccharopine reductase)	-0.11	-1.74	0.00	6	
P09812	Glycogen phosphorylase. muscle form (EC 2.4.1.1) (Myophosphorylase)	-0.69	-2.32	0.00	6	
Q0BW40	Adenosylhomocysteinase (EC 3.3.1.1) (S-adenosyl-L-homocysteine hydrolase) (AdoHcyase)	-0.09	-0.72	0.01	6	
Q00217	Alpha.alpha-trehalose-phosphate synthase [UDP-forming] 2 (EC 2.4.1.15) (Trehalose-6-phosphate synthase) (UDP-glucose-glucosephosphate glucosyltransferase)	-0.34	-0.92	0.01	6	
Q4L7Z4	Serine hydroxymethyltransferase (SHMT) (Serine methylase) (EC 2.1.2.1)	-0.69	-1.66	0.01	6	y
P34825	Elongation factor 1-alpha (EF-1-alpha)	-0.49	-0.96	0.01	6	y
Q59QD6	Elongation factor 1-alpha 2 (EF-1-alpha 2)	-0.73	-1.57	0.01	6	y
Q8X1X3	Glyceraldehyde-3-phosphate dehydrogenase (GAPDH) (EC 1.2.1.12)	-0.15	-1.04	0.01	6	y
O14435	Guanine nucleotide-binding protein subunit beta	-0.20	-0.62	0.01	6	
P26521	Glyceraldehyde-3-phosphate dehydrogenase. cytosolic (EC 1.2.1.12)	-0.90	-3.83	0.01	6	y
P11913	Mitochondrial-processing peptidase subunit beta (EC 3.4.24.64) (Beta-MPP) (Ubiquinol-cytochrome-c reductase complex core protein I)	-0.19	-0.47	0.01	6	
O94128	Tubulin alpha chain	-0.39	-0.96	0.02	6	
Q09508	Succinate dehydrogenase [ubiquinone] flavoprotein subunit. mitochondrial (EC 1.3.5.1) (Flavoprotein subunit of complex II) (FP)	-0.66	-2.73	0.02	6	
POCB32	Heat shock 70 kDa protein 1-like (Heat shock 70 kDa protein 1L)	-0.48	-3.96	0.02	6	

Accession no.	Protein name (UNIPROT)	Fold Change to Ct		ANOVA p-value	Cluster No.	Common to At61
		Ag ⁺	AgNPs			
P93422	Histidine--tRNA ligase. cytoplasmic (EC 6.1.1.21) (Histidyl-tRNA synthetase) (HisRS)	-0.61	-1.95	0.03	6	
Q43492	Serpin-Z7 (BSZ7) (HorvuZ7)	-0.83	-2.62	0.03	6	y
B4EYR8	Glucose-6-phosphate isomerase (GPI) (EC 5.3.1.9) (Phosphoglucose isomerase) (PGI) (Phosphohexose isomerase) (PHI)	-0.05	-0.44	0.04	6	
P06293	Serpin-Z4 (BSZ4) (HorvuZ4) (Major endosperm albumin) (Protein Z4) (Protein Z)	-0.18	-2.05	0.05	6	
Q09116	Septin homolog spn2	0.57	0.44	0.05		
Q10318	Putative dihydroxy-acid dehydratase. mitochondrial (DAD) (EC 4.2.1.9) (2,3-dihydroxy acid hydrolyase)	0.73	2.00	0.05		
O74225	Heat shock protein hsp88	0.61	0.95	0.05		
Q52813	General L-amino acid transport system permease protein AapQ	0.43	0.68	0.05		
Q9C2L8	Probable Ras-related protein Rab7	1.42	2.38	0.05		
Q7SBD5	60S ribosomal protein L7	1.44	1.40	0.05		
P11592	V-type proton ATPase catalytic subunit A (V-ATPase subunit A) (EC 3.6.3.14) (V-ATPase 67 kDa subunit) (Vacuolar proton pump subunit alpha)	1.28	1.54	0.05		
Q7LKT3	Histone H4	0.74	0.09	0.05		
P10819	Adenosylhomocysteinase (AdoHcyase) (EC 3.3.1.1) (S-adenosyl-L-homocysteine hydrolase)	2.94	3.27	0.06		
Q889W4	50S ribosomal protein L16	0.81	1.55	0.06		
Q59637	Pyruvate dehydrogenase E1 component (PDH E1 component) (EC 1.2.4.1)	-0.28	1.01	0.06		
P53319	6-phosphogluconate dehydrogenase. decarboxylating 2 (EC 1.1.1.44)	0.04	-1.55	0.06		
Q9JMB1	Testicular haploid expressed gene protein	1.48	2.52	0.06		
Q2NA62	NADH-quinone oxidoreductase subunit C (EC 1.6.5.11) (NADH dehydrogenase I subunit C) (NDH-1 subunit C)	-0.71	-0.74	0.06		
C3K6E1	50S ribosomal protein L13	1.26	1.34	0.06		

Accession no.	Protein name (UNIPROT)	Fold Change to Ct		ANOVA p-value	Cluster No.	Common to At61
		Ag ⁺	AgNPs			
Q2U6P7	ATP-dependent RNA helicase sub2 (EC 3.6.4.13)	1.70	2.42	0.06		
P74582	Aconitate hydratase B (ACN) (Aconitase) (EC 4.2.1.3) ((2R.3S)-2-methylisocitrate dehydratase) ((2S.3R)-3-hydroxybutane-1.2.3-tricarboxylate dehydratase) (2-methyl-cis-aconitate hydratase) (EC 4.2.1.99) (Iron-responsive protein-like) (IRP-like) (RNA-binding protein)	-0.50	1.05	0.06		
C6DFP4	Glucose-6-phosphate isomerase (GPI) (EC 5.3.1.9) (Phosphoglucose isomerase) (PGI) (Phosphohexose isomerase) (PHI)	-0.45	-0.40	0.06		
Q27032	Cell division control protein 2 homolog (EC 2.7.11.22) (EC 2.7.11.23)	1.51	1.92	0.06		
P40292	Heat shock protein 90 (65 kDa IgE-binding protein) (Heat shock protein hsp1) (allergen Asp f 12)	2.93	3.00	0.06		
P80581	Hexokinase (EC 2.7.1.1)	-0.58	-0.41	0.06		
Q9Y897	3-isopropylmalate dehydrogenase (3-IPM-DH) (IMDH) (EC 1.1.1.85) (Beta-IPM dehydrogenase)	0.25	0.43	0.06		
Q9P4V2	Phosphoacetylglucosamine mutase (PAGM) (EC 5.4.2.3) (Acetylglucosamine phosphomutase) (N-acetylglucosamine-phosphate mutase)	0.59	0.54	0.06		
P02768	Serum albumin	-3.74	-5.98	0.06		
Q7RVI1	40S ribosomal protein S5	0.12	-0.58	0.07		
Q41346	Cytochrome c	1.38	2.29	0.07		
Q39994	Calnexin homolog	1.53	1.88	0.07		
P24487	ATP synthase subunit alpha. mitochondrial	-0.22	-0.14	0.07		
Q75BV4	Saccharopine dehydrogenase [NAD(+), L-lysine-forming] (SDH) (EC 1.5.1.7) (Lysine--2-oxoglutarate reductase)	-0.58	-2.43	0.07		
Q54BC8	Proteasome subunit beta type-5 (EC 3.4.25.1)	0.35	-0.40	0.07		
Q88AZ4	Phosphoenolpyruvate carboxykinase [ATP] (PCK) (PEP carboxykinase) (PEPCK) (EC 4.1.1.49)	-0.58	0.76	0.07		
P10388	Glutenin. high molecular weight subunit DX5	-0.16	0.59	0.07		
Q5AWS6	Cell division control protein 48	0.37	0.76	0.07		

Accession no.	Protein name (UNIPROT)	Fold Change to Ct		ANOVA p-value	Cluster No.	Common to At61
		Ag ⁺	AgNPs			
O13302	Isocitrate dehydrogenase [NAD] subunit 1. mitochondrial (EC 1.1.1.41) (Isocitric dehydrogenase) (NAD(+)-specific ICDH)	0.44	0.48	0.07		
P32449	Phospho-2-dehydro-3-deoxyheptonate aldolase. tyrosine-inhibited (EC 2.5.1.54) (3-deoxy-D-arabino-heptulosonate 7-phosphate synthase) (DAHP synthase) (Phospho-2-keto-3-deoxyheptonate aldolase)	1.22	1.51	0.08		
P39708	NADP-specific glutamate dehydrogenase 2 (NADP-GDH 2) (EC 1.4.1.4) (NADP-dependent glutamate dehydrogenase 2)	0.36	0.89	0.08		
P40941	ADP.ATP carrier protein 2. mitochondrial (ADP/ATP translocase 2) (Adenine nucleotide translocator 2) (ANT 2)	2.14	2.18	0.08		
Q9I3F5	Aconitate hydratase A (ACN) (Aconitase) (EC 4.2.1.3) ((2R.3S)-2-methylisocitrate dehydratase) ((2S.3R)-3-hydroxybutane-1.2.3-tricarboxylate dehydratase) (Iron-responsive protein-like) (IRP-like) (Probable 2-methyl-cis-aconitate hydratase) (EC 4.2.1.99) (RNA-binding protein)	0.01	1.38	0.08		
Q141C9	Probable acetoacetate decarboxylase (AAD) (ADC) (EC 4.1.1.4)	0.79	-0.08	0.08		
Q8ZQU3	Succinate dehydrogenase flavoprotein subunit (EC 1.3.5.1)	0.72	1.47	0.08		
P53228	Transaldolase NQM1 (EC 2.2.1.2) (Non-quiescent mutant protein 1)	-0.09	0.35	0.08		
B3Q4F9	Catalase-peroxidase (CP) (EC 1.11.1.21) (Peroxidase/catalase)	1.81	1.96	0.09		
P37211	ATP synthase subunit alpha. mitochondrial	0.49	0.39	0.09		
Q88QM3	50S ribosomal protein L5	-0.41	-1.74	0.09		
Q9K5X4	ATP phosphoribosyltransferase (ATP-PRT) (ATP-PRTase) (EC 2.4.2.17)	-1.45	-0.75	0.09		
C3K5E6	30S ribosomal protein S2	0.87	1.03	0.09		
Q9C413	Tubulin alpha chain (Alpha-tubulin)	1.03	0.15	0.09		
C3K1E6	ATP synthase subunit beta (EC 3.6.3.14) (ATP synthase F1 sector subunit beta) (F-ATPase subunit beta)	0.87	1.54	0.09		
Q9KNJ2	Glutamine synthetase (EC 6.3.1.2) (Glutamate--ammonia ligase)	-0.44	-1.42	0.09		
Q0CXB1	Probable dipeptidyl-aminopeptidase B (DPAP B) (EC 3.4.14.5)	0.50	1.55	0.09		
P78695	78 kDa glucose-regulated protein homolog (GRP-78) (Immunoglobulin heavy chain-binding protein homolog) (BiP)	0.86	1.41	0.09		

Accession no.	Protein name (UNIPROT)	Fold Change to Ct		ANOVA p-value	Cluster No.	Common to At61
		Ag ⁺	AgNPs			
Q9FSI9	Hordoindoline-B1 (Puroindoline-B)	-1.21	-0.47	0.09		
Q3KE62	Catalase-peroxidase (CP) (EC 1.11.1.21) (Peroxidase/catalase)	0.94	2.35	0.09		
Q975H9	Isoleucine--tRNA ligase (EC 6.1.1.5) (Isoleucyl-tRNA synthetase) (IleRS)	-0.57	-0.67	0.09		
P0AG70	30S ribosomal protein S1	0.63	0.46	0.10		
Q6MVH7	Inorganic pyrophosphatase (EC 3.6.1.1) (Pyrophosphate phospho-hydrolase) (PPase)	0.61	0.88	0.10		
Q4WUR1	Serine/threonine-protein phosphatase 2B catalytic subunit (EC 3.1.3.16) (Calmodulin-dependent calcineurin A subunit)	0.08	-0.50	0.10		
P22759	Bacterioferritin (BFR) (EC 1.16.3.1) (Cytochrome b-557.5)	2.32	3.12	0.10		
P31052	Dihydrolipoyl dehydrogenase (EC 1.8.1.4) (Dihydrolipoamide dehydrogenase) (E3 component of 2-oxoglutarate dehydrogenase complex) (Glycine oxidation system L-factor) (LPD-GLC)	0.81	1.38	0.10		
P58068	Putative amino-acid ABC transporter-binding protein YhdW	0.97	0.97	0.10		
C3KAD2	Bifunctional polymyxin resistance protein ArnA [Includes: UDP-4-amino-4-deoxy-L-arabinose formyltransferase (EC 2.1.2.13) (ArnAFT) (UDP-L-Ara4N formyltransferase); UDP-glucuronic acid oxidase.	-0.53	-0.27	0.10		
Q886M5	CTP synthase (EC 6.3.4.2) (Cytidine 5'-triphosphate synthase) (Cytidine triphosphate synthetase) (CTP synthetase) (CTPS) (UTP--ammonia ligase)	-0.97	-0.24	0.10		
Q9HU65	Glutamine synthetase (EC 6.3.1.2) (Glutamate--ammonia ligase)	-0.38	0.47	0.11		
A6T226	Chaperone protein DnaK (HSP70) (Heat shock 70 kDa protein) (Heat shock protein 70)	2.85	2.73	0.11		
Q3V5W6	Glutamine synthetase (EC 6.3.1.2) (Glutamate--ammonia ligase)	-0.06	0.50	0.11		
Q96X46	Enolase (EC 4.2.1.11) (2-phospho-D-glycerate hydro-lyase) (2-phosphoglycerate dehydratase) (allergen Pen c 22)	2.13	2.50	0.11		
P49601	3-isopropylmalate dehydratase (EC 4.2.1.33) (Alpha-IPM isomerase) (IPMI) (Isopropylmalate isomerase)	1.71	2.15	0.11		
P0DKC4	Phosphoglycolate phosphatase 1B. chloroplastic (EC 3.1.3.18)	-0.53	0.61	0.11		
P0A106	Cold shock protein CapB (C8.0) (Cold acclimation protein B)	0.04	1.26	0.11		

Accession no.	Protein name (UNIPROT)	Fold Change to Ct		ANOVA p-value	Cluster No.	Common to At61
		Ag ⁺	AgNPs			
O66218	60 kDa chaperonin (GroEL protein) (Protein Cpn60) (Fragment)	0.26	0.77	0.11		
Q5QWA3	Elongation factor Tu (EF-Tu)	0.95	1.94	0.11		
P23301	Eukaryotic translation initiation factor 5A-1 (eIF-5A-1) (Hypusine-containing protein HP2) (eIF-4D)	-0.39	0.49	0.11		
O94225	Homocitrate synthase. mitochondrial (EC 2.3.3.14)	-0.23	1.22	0.12		
O14018	Serine--tRNA ligase. cytoplasmic (EC 6.1.1.11) (Seryl-tRNA synthetase) (SerRS) (Seryl-tRNA(Ser/Sec) synthetase)	1.93	2.20	0.12		
P18781	Tellurium resistance protein TerD	1.43	3.09	0.12		
Q9P3T6	40S ribosomal protein S5-B	0.60	0.52	0.12		
Q12335	Protoplast secreted protein 2	1.82	2.77	0.12		
P55059	Protein disulfide-isomerase (PDI) (EC 5.3.4.1)	0.61	0.18	0.12		
P82611	Aconitate hydratase. mitochondrial (Aconitase) (EC 4.2.1.3) (Citrate hydro-lyase)	-0.08	-0.28	0.12		
Q0US25	Protein transport protein SEC23	-1.78	-1.61	0.12		
P07597	Non-specific lipid-transfer protein 1 (LTP 1) (Probable amylase/protease inhibitor)	1.17	2.03	0.13		
Q5PIW3	Elongation factor G (EF-G)	0.18	0.60	0.13		
Q9P6M8	mRNA export factor crp79 (Meiotic expression up-regulated protein 5) (Polyadenylate-binding protein crp79) (PABP) (Poly(A)-binding protein)	-0.40	-0.62	0.13		
Q3K5F2	Phosphoglycerate kinase (EC 2.7.2.3)	-0.70	0.37	0.13		
Q1E4I8	Adenylate kinase (EC 2.7.4.3) (ATP-AMP transphosphorylase) (ATP:AMP phosphotransferase) (Adenylate kinase cytosolic and mitochondrial) (Adenylate monophosphate kinase)	0.92	1.55	0.13		
Q9UVR2	Ubiquitin-conjugating enzyme E2-16 kDa (EC 2.3.2.23) (E2 ubiquitin-conjugating enzyme 1) (Ubiquitin carrier protein) (Ubiquitin-protein ligase)	2.45	2.80	0.13		
P42040	Enolase (EC 4.2.1.11) (2-phospho-D-glycerate hydro-lyase) (2-phosphoglycerate dehydratase) (Allergen Cla h VI) (allergen Cla h 6)	1.25	1.88	0.13		

Accession no.	Protein name (UNIPROT)	Fold Change to Ct		ANOVA p-value	Cluster No.	Common to At61
		Ag ⁺	AgNPs			
Q6GZR2	Putative deoxyuridine 5'-triphosphate nucleotidohydrolase (dUTPase) (EC 3.6.1.23)	0.19	0.91	0.14		
A6SB28	Nascent polypeptide-associated complex subunit alpha (NAC-alpha) (Alpha-NAC)	1.76	1.61	0.14		
P13228	Tryptophan synthase (EC 4.2.1.20)	0.59	0.01	0.14		
P32381	Actin-related protein 2 (Actin-like protein ARP2) (Actin-like protein 2)	0.94	1.63	0.14		
P78712	Actin-related protein 3 (Actin-like protein 3)	1.17	1.21	0.14		
P38624	Proteasome subunit beta type-1 (EC 3.4.25.1) (Macropain subunit PRE3) (Multicatalytic endopeptidase complex subunit PRE3) (Proteasome component PRE3) (Proteinase YSCE subunit PRE3)	1.27	1.84	0.14		
O04630	Threonine--tRNA ligase, mitochondrial 1 (EC 6.1.1.3) (AtSYT1) (Threonyl-tRNA synthetase) (ThrRS)	-0.03	-0.89	0.14		
A7E8H8	Adenylate kinase (EC 2.7.4.3) (ATP-AMP transphosphorylase) (ATP:AMP phosphotransferase) (Adenylate kinase cytosolic and mitochondrial) (Adenylate monophosphate kinase)	0.61	0.63	0.15		
P50142	Heat shock protein 60, mitochondrial (Antigen HIS-62)	0.88	1.24	0.15		
P29458	DNA replication licensing factor mcm4 (EC 3.6.4.12) (Cell division control protein 21) (Minichromosome maintenance protein 4)	1.60	0.62	0.15		
P77983	Pyruvate kinase I (EC 2.7.1.40) (PK-1)	0.64	1.22	0.16		
P51996	GTP-binding protein YPT32/YPT11 (Rab GTPase YPT32)	0.19	0.48	0.16		
Q889Y1	50S ribosomal protein L1	-1.75	-2.02	0.16		
Q7RV75	40S ribosomal protein S22 (Cytoplasmic ribosomal protein 27)	-0.01	-0.98	0.16		
O93918	Pyruvate carboxylase (EC 6.4.1.1) (Pyruvic carboxylase) (PCB)	2.13	1.91	0.17		
Q4K550	30S ribosomal protein S5	-0.61	0.93	0.17		
Q9ZJ71	Elongation factor Ts (EF-Ts)	1.52	2.60	0.17		

Accession no.	Protein name (UNIPROT)	Fold Change to Ct		ANOVA p-value	Cluster No.	Common to At61
		Ag ⁺	AgNPs			
Q4KIF9	Triosephosphate isomerase (TIM) (TPI) (EC 5.3.1.1) (Triose-phosphate isomerase)	1.69	1.82	0.17		
P25457	60S ribosomal protein L7-B	1.74	1.59	0.17		
Q76KF9	Enolase (EC 4.2.1.11) (2-phospho-D-glycerate hydro-lyase) (2-phosphoglycerate dehydratase)	1.13	1.14	0.17		
P0A954	3-oxoacyl-[acyl-carrier-protein] synthase 1 (EC 2.3.1.41) (3-oxoacyl-[acyl-carrier-protein] synthase I) (Beta-ketoacyl-ACP synthase I) (KAS I)	-0.55	-0.65	0.18		
P72192	Temperature acclimation protein B (E8.0) (Fragment)	0.27	0.47	0.18		
C3KAH3	Arginine--tRNA ligase (EC 6.1.1.19) (Arginyl-tRNA synthetase) (ArgRS)	-0.47	0.68	0.19		
P0CT59	40S ribosomal protein S22-B	-0.03	-0.58	0.19		
A7TMJ2	Very-long-chain 3-oxoacyl-CoA reductase (EC 1.1.1.330) (3-ketoacyl-CoA reductase) (3-ketoreductase) (KAR) (Microsomal beta-keto-reductase)	-0.49	-1.70	0.19		
Q4ZXX3	50S ribosomal protein L25 (General stress protein CTC)	0.15	0.80	0.19		
A7F4H5	Carboxypeptidase Y homolog A (EC 3.4.16.5)	0.71	0.66	0.19		
P15368	Fatty acid synthase subunit alpha (EC 2.3.1.86) [Includes: Acyl carrier; 3-oxoacyl-[acyl-carrier-protein] reductase (EC 1.1.1.100) (Beta-ketoacyl reductase); 3-oxoacyl-[acyl-carrier-protein] synthase (EC 2.3.1.41) (Beta-ketoacyl synthase)]	1.61	1.14	0.20		
P0AEQ5	Glutamine-binding periplasmic protein (GlnBP)	0.06	1.10	0.20		
P40915	NADH-ubiquinone oxidoreductase 24 kDa subunit. mitochondrial (EC 1.6.5.3) (EC 1.6.99.3)	1.27	2.19	0.21		
P46598	Heat shock protein 90 homolog	0.58	0.78	0.22		
Q3KGI9	Phosphoribosylaminoimidazole-succinocarboxamide synthase (EC 6.3.2.6) (SAICAR synthetase)	-0.71	-0.71	0.23		
B5XN94	50S ribosomal protein L3	0.77	-1.18	0.23		
P04845	Outer membrane protein A	0.33	1.38	0.24		

Accession no.	Protein name (UNIPROT)	Fold Change to Ct		ANOVA p-value	Cluster No.	Common to At61
		Ag ⁺	AgNPs			
P14228	Phosphoglycerate kinase (EC 2.7.2.3)	-0.19	-0.35	0.24		
A4VKF5	Acetyl-coenzyme A carboxylase carboxyl transferase subunit beta (ACCCase subunit beta) (Acetyl-CoA carboxylase carboxyltransferase subunit beta) (EC 6.4.1.2)	0.21	1.27	0.24		
C3JYK1	Trigger factor (TF) (EC 5.2.1.8) (PPIase)	-0.56	-0.73	0.24		
Q3KFT8	Chaperone protein HtpG (Heat shock protein HtpG) (High temperature protein G)	0.39	-0.24	0.24		
Q09171	Pyruvate dehydrogenase E1 component subunit beta. mitochondrial (PDHE1-B) (EC 1.2.4.1)	1.10	0.63	0.24		
C3KDE0	UDP-3-O-acyl-N-acetylglucosamine deacetylase (UDP-3-O-acyl-GlcNAc deacetylase) (EC 3.5.1.108) (UDP-3-O-[R-3-hydroxymyristoyl]-N-acetylglucosamine deacetylase)	0.30	-0.78	0.25		
Q01369	Guanine nucleotide-binding protein subunit beta-like protein (Cross-pathway control WD-repeat protein cpc-2)	-0.16	-0.10	0.25		
P87025	Trihydroxynaphthalene reductase (EC 1.1.1.-) (T3HN reductase)	-0.91	0.13	0.25		
Q03134	Formate dehydrogenase (FDH) (EC 1.2.1.2) (Acetate inducible protein A) (NAD-dependent formate dehydrogenase)	1.06	0.20	0.25		
Q9XIE2	ABC transporter G family member 36 (ABC transporter ABCG.36) (AtABCG36) (Pleiotropic drug resistance protein 8) (Protein PENETRATION 3)	-0.70	-0.15	0.25		
Q4KKR7	Glycine--tRNA ligase alpha subunit (EC 6.1.1.14) (Glycyl-tRNA synthetase alpha subunit) (GlyRS)	-0.86	-0.96	0.25		
P05750	40S ribosomal protein S3 (RP13) (YS3)	0.21	-0.43	0.26		
C3K255	Polyribonucleotide nucleotidyltransferase (EC 2.7.7.8) (Polynucleotide phosphorylase) (PNPase)	-0.60	-1.62	0.26		
Q1Q9E4	Histidine ammonia-lyase (Histidase) (EC 4.3.1.3)	-1.73	-0.30	0.28		

Accession no.	Protein name (UNIPROT)	Fold Change to Ct		ANOVA p-value	Cluster No.	Common to At61
		Ag ⁺	AgNPs			
G5EB89	Importin subunit alpha (Karyopherin alpha)	0.98	0.70	0.28		
P0CX56	40S ribosomal protein S18-B	1.27	1.93	0.28		
O42943	Uncharacterized ABC transporter ATP-binding protein C16H5.08c	1.14	1.05	0.28		
Q9P7U2	Putative aryl-alcohol dehydrogenase C977.14c (EC 1.1.1.-)	-0.05	0.16	0.29		
Q8TGA9	Mitogen-activated protein kinase HOG1 (MAP kinase HOG1) (EC 2.7.11.24)	-0.06	-0.50	0.29		
P38674	Ketol-acid reductoisomerase, mitochondrial (EC 1.1.1.86) (Acetohydroxy-acid reductoisomerase) (Alpha-keto-beta-hydroxylacyl reductoisomerase)	0.07	0.30	0.29		
Q881X0	1.4-alpha-glucan branching enzyme GlgB (EC 2.4.1.18) (1.4-alpha-D-glucan:1.4-alpha-D-glucan 6-glucosyl-transferase) (Alpha-(1->4)-glucan branching enzyme) (Glycogen branching enzyme) (BE)	-0.72	-0.14	0.29		
B2ASU5	Catalase-peroxidase (CP) (EC 1.11.1.21) (Peroxidase/catalase)	0.65	0.33	0.29		
A7F8K7	Eukaryotic translation initiation factor 3 subunit D (eIF3d)	0.75	-0.08	0.30		
Q6D182	Enolase (EC 4.2.1.11) (2-phospho-D-glycerate hydro-lyase) (2-phosphoglycerate dehydratase)	0.07	0.87	0.30		
A7EUB3	Probable Xaa-Pro aminopeptidase pepP (EC 3.4.11.9) (Aminoacylproline aminopeptidase) (Prolidase)	-0.32	-0.75	0.30		
Q1QVJ7	60 kDa chaperonin (GroEL protein) (Protein Cpn60)	-0.33	-0.29	0.30		
P39939	40S ribosomal protein S26-B	0.11	-0.50	0.31		
P33297	26S protease regulatory subunit 6A (Tat-binding protein homolog 1) (TBP-1)	-0.05	-0.72	0.31		
C3K2Y6	50S ribosomal protein L1	-0.31	0.22	0.32		
P09041	Phosphoglycerate kinase 2 (EC 2.7.2.3) (Phosphoglycerate kinase, testis specific)	0.45	0.90	0.32		
P83617	78 kDa glucose-regulated protein homolog (GRP-78) (Immunoglobulin heavy chain-binding protein homolog) (BiP)	0.07	-0.25	0.33		
Q4KHH5	Elongation factor Ts (EF-Ts)	0.62	1.07	0.33		
Q3KHM4	Probable cytosol aminopeptidase (EC 3.4.11.1) (Leucine aminopeptidase) (LAP) (EC 3.4.11.10) (Leucyl aminopeptidase)	-0.35	0.64	0.33		
O93866	Heat shock 70 kDa protein	1.05	1.28	0.34		

Accession no.	Protein name (UNIPROT)	Fold Change to Ct		ANOVA p-value	Cluster No.	Common to At61
		Ag ⁺	AgNPs			
P22515	Ubiquitin-activating enzyme E1 1 (EC 6.2.1.45)	1.18	1.34	0.34		
Q889W5	30S ribosomal protein S3	-0.40	-0.40	0.34		
P53385	Urocanate hydratase (Urocanase) (EC 4.2.1.49) (Imidazolonepropionate hydrolase)	-0.76	-0.72	0.35		
Q4ICA8	RuvB-like helicase 1 (EC 3.6.4.12)	-0.52	-0.96	0.35		
P32379	Proteasome subunit alpha type-5 (EC 3.4.25.1) (Macropain subunit PUP2) (Multicatalytic endopeptidase complex subunit PUP2) (Proteasome component PUP2) (Proteinase YSCE subunit PUP2)	0.28	0.81	0.36		
P07144	Mitochondrial outer membrane protein porin	1.36	1.41	0.36		
P53731	Actin-related protein 2/3 complex subunit 2 (Arp2/3 complex 34 kDa subunit) (p34-ARC)	0.58	0.50	0.36		
P38708	Putative proline--tRNA ligase YHR020W (EC 6.1.1.15) (Prolyl-tRNA synthetase) (ProRS)	0.38	0.58	0.36		
Q9P720	60S ribosomal protein L16 (Cytoplasmic ribosomal protein 46)	0.20	-1.39	0.37		
P46796	Glyceraldehyde-3-phosphate dehydrogenase (GAPDH) (EC 1.2.1.12) (NAD-dependent glyceraldehyde-3-phosphate dehydrogenase) (Fragment)	-2.77	-6.73	0.38		
P23847	Periplasmic dipeptide transport protein (Dipeptide-binding protein) (DBP)	0.56	-0.51	0.38		
P32936	Alpha-amylase/trypsin inhibitor CMb (Chloroform/methanol-soluble protein CMb)	0.23	-0.97	0.39		
Q9XEK8	60S ribosomal protein L23 (L17)	-1.38	-0.42	0.39		
Q9HUX1	Biosynthetic arginine decarboxylase (ADC) (EC 4.1.1.19)	-0.70	-0.17	0.39		
Q9C3Y4	GTP-binding protein rhoA (Rho1 protein homolog)	0.40	0.54	0.40		
Q2KJB1	Septin-10	-0.02	0.22	0.40		
Q5B0C0	Heat shock 70 kDa protein	1.33	0.69	0.40		
Q3K9G4	NADPH-dependent 7-cyano-7-deazaguanine reductase (EC 1.7.1.13) (7-cyano-7-carbaguanine reductase) (NADPH-dependent nitrile oxidoreductase) (PreQ(0) reductase)	-0.56	-0.66	0.41		
Q9CG20	Glutamate decarboxylase (GAD) (EC 4.1.1.15)	0.55	0.89	0.41		

Accession no.	Protein name (UNIPROT)	Fold Change to Ct		ANOVA p-value	Cluster No.	Common to At61
		Ag ⁺	AgNPs			
Q39K12	Elongation factor Tu (EF-Tu)	1.31	1.51	0.42		
Q8Z1X4	30S ribosomal protein S4	0.81	1.76	0.42		
A4VPQ5	Chaperone protein DnaK (HSP70) (Heat shock 70 kDa protein) (Heat shock protein 70)	-0.30	-1.35	0.42		
C3K613	Fatty acid oxidation complex subunit alpha [Includes: Enoyl-CoA hydratase/Delta(3)-cis-Delta(2)-trans-enoyl-CoA isomerase/3-hydroxybutyryl-CoA epimerase (EC 4.2.1.17) (EC 5.1.2.3) (EC 5.3.3.8); 3-hydroxyacyl-CoA dehydrogenase (EC 1.1.1.35)]	-0.10	0.46	0.42		
P0AFH9	Osmotically-inducible protein Y	-0.25	0.60	0.43		
P38793	tRNA (guanine(37)-N1)-methyltransferase (EC 2.1.1.228) (M1G-methyltransferase) (tRNA [GM37] methyltransferase) (tRNA methyltransferase 5)	0.46	0.15	0.43		
Q3K5W5	N-acetyl-gamma-glutamyl-phosphate reductase (AGPR) (EC 1.2.1.38) (N-acetyl-glutamate semialdehyde dehydrogenase) (NAGSA dehydrogenase)	0.25	0.98	0.44		
P0A9Q4	Aerobic respiration control protein ArcA	-0.50	-0.07	0.45		
P41756	Phosphoglycerate kinase (EC 2.7.2.3)	-0.18	0.05	0.45		
C3K469	50S ribosomal protein L28	-0.19	-0.84	0.46		
Q96KP4	Cytosolic non-specific dipeptidase (EC 3.4.13.18) (CNDP dipeptidase 2) (Carnosine dipeptidase II) (Epididymis secretory protein Li 13) (Glutamate carboxypeptidase-like protein 1) (Peptidase A)	0.62	0.96	0.46		
P24000	60S ribosomal protein L24-B (L30) (RP29) (YL21)	0.40	-0.20	0.47		
Q9P4E9	GTP-binding nuclear protein GSP1/Ran	0.47	0.28	0.47		
Q8ZJ87	DNA-directed RNA polymerase subunit alpha (RNAP subunit alpha) (EC 2.7.7.6) (RNA polymerase subunit alpha) (Transcriptase subunit alpha)	-1.02	-0.43	0.47		
C3K5J5	Enoyl-[acyl-carrier-protein] reductase [NADH] (ENR) (EC 1.3.1.9)	0.06	0.54	0.47		
Q889X0	50S ribosomal protein L4	-0.89	-0.25	0.48		
Q4WM67	NADPH--cytochrome P450 reductase (CPR) (P450R) (EC 1.6.2.4)	-0.30	-0.93	0.48		
Q2KTI4	Catalase-peroxidase (CP) (EC 1.11.1.21) (Peroxidase/catalase)	-0.11	-0.52	0.48		

Accession no.	Protein name (UNIPROT)	Fold Change to Ct		ANOVA p-value	Cluster No.	Common to At61
		Ag ⁺	AgNPs			
Q7SE75	Sulfate adenylyltransferase (EC 2.7.7.4) (ATP-sulfurylase) (Sulfate adenylyltransferase) (SAT)	-0.29	-0.40	0.48		
A6SEH9	ATP-dependent RNA helicase ded1 (EC 3.6.4.13)	0.23	0.19	0.48		
Q13SQ2	ATP synthase subunit beta 2 (EC 3.6.3.14) (ATP synthase F1 sector subunit beta 2) (F-ATPase subunit beta 2)	0.03	0.30	0.49		
Q9LEH8	Hordoindoline-B2 (Puroindoline-B)	-1.79	-1.54	0.49		
P0ABK6	Cysteine synthase A (CSase A) (EC 2.5.1.47) (O-acetylserine (thiol)-lyase A) (OAS-TL A) (O-acetylserine sulfhydrylase A) (Sulfate starvation-induced protein 5) (SSI5)	0.80	0.74	0.49		
P29405	Phosphoglycerate kinase 1 (EC 2.7.2.3)	0.16	0.43	0.50		
E4ZHQ5	Leucine aminopeptidase 1 (EC 3.4.11.-) (Leucyl aminopeptidase 1) (LAP1)	-0.16	0.04	0.50		
Q88NF9	Probable malate:quinone oxidoreductase 2 (EC 1.1.5.4) (MQO 2) (Malate dehydrogenase [quinone] 2)	-0.20	-0.28	0.50		
A8GKH4	30S ribosomal protein S4	-0.63	-0.82	0.51		
P25997	Elongation factor 3 (EF-3)	0.28	0.58	0.52		
P36017	Vacuolar protein sorting-associated protein 21 (GTP-binding protein YPT51) (Vacuolar protein-targeting protein 12)	0.35	0.13	0.52		
Q21EF4	Argininosuccinate lyase (ASAL) (EC 4.3.2.1) (Argininosuccinase)	0.29	0.65	0.53		
Q9P567	Succinate--CoA ligase [ADP-forming] subunit beta. mitochondrial (EC 6.2.1.5) (Succinyl-CoA synthetase beta chain) (SCS-beta)	2.21	1.01	0.53		
D7PHZ1	Oxidoreductase vrtI (EC 1.14.-.-) (Viridicatumtoxin synthesis protein I)	0.06	-0.22	0.54		
C3K2W1	50S ribosomal protein L6	-0.22	0.35	0.55		
Q4U3E8	Mannose-1-phosphate guanyltransferase (EC 2.7.7.13) (GDP-mannose pyrophosphorylase) (GTP-mannose-1-phosphate guanylyltransferase)	0.22	0.20	0.56		
P52015	Peptidyl-prolyl cis-trans isomerase 7 (PPIase 7) (EC 5.2.1.8) (Cyclophilin-7) (Rotamase 7)	1.17	1.14	0.56		

Accession no.	Protein name (UNIPROT)	Fold Change to Ct		ANOVA p-value	Cluster No.	Common to At61
		Ag ⁺	AgNPs			
B5Y1K5	2.3.4.5-tetrahydropyridine-2.6-dicarboxylate N-succinyltransferase (EC 2.3.1.117) (Tetrahydrodipicolinate N-succinyltransferase) (THP succinyltransferase) (Tetrahydropicolinate succinylase)	1.35	0.45	0.56		
Q9HGY8	Triosephosphate isomerase (TIM) (EC 5.3.1.1) (Triose-phosphate isomerase)	-1.12	-0.91	0.57		
O59948	Eukaryotic peptide chain release factor subunit 1 (Eukaryotic release factor 1) (eRF1)	0.13	-0.17	0.57		
P31411	V-type proton ATPase subunit B (V-ATPase subunit B) (V-ATPase 57 kDa subunit) (Vacuolar proton pump subunit B)	0.57	-0.11	0.58		
Q6FW50	78 kDa glucose-regulated protein homolog (GRP-78) (Immunoglobulin heavy chain-binding protein homolog) (BIP)	0.18	-0.04	0.58		
P78615	Fatty acid synthase subunit alpha (EC 2.3.1.86)	1.01	0.72	0.59		
Q63Q38	50S ribosomal protein L17	1.76	2.33	0.60		
C3K6L0	Elongation factor P (EF-P)	-0.07	-0.44	0.60		
Q8X132	Histone H2A	-0.24	-0.09	0.61		
Q9SEX2	Katanin p60 ATPase-containing subunit A1 (Katanin p60 subunit A1) (EC 3.6.4.3)	-0.14	-0.27	0.61		
Q9ALA4	Cell division protein FtsZ	-0.43	-0.44	0.62		
Q6FTK4	60S ribosomal protein L11	0.16	0.15	0.62		
O13419	Actin	0.23	0.18	0.63		
C3K2Y2	DNA-directed RNA polymerase subunit beta' (RNAP subunit beta') (EC 2.7.7.6) (RNA polymerase subunit beta') (Transcriptase subunit beta')	-0.03	-0.35	0.63		
C3K7N8	Recombination-associated protein RdgC	-0.96	0.56	0.64		
O43105	40S ribosomal protein S7 (Cytoplasmic ribosomal protein 15)	0.31	-0.52	0.64		
P48081	ATP synthase subunit beta. cyanelle (EC 3.6.3.14) (ATP synthase F1 sector subunit beta) (F-ATPase subunit beta)	-0.32	-0.27	0.64		

Accession no.	Protein name (UNIPROT)	Fold Change to Ct		ANOVA p-value	Cluster No.	Common to At61
		Ag ⁺	AgNPs			
Q889X1	50S ribosomal protein L3	0.65	1.13	0.65		
Q83KZ1	Mannose-6-phosphate isomerase (EC 5.3.1.8) (Phosphohexomutase) (Phosphomannose isomerase) (PMI)	0.38	0.78	0.66		
Q3K9H0	Transaldolase (EC 2.2.1.2)	-0.46	0.05	0.66		
Q00043	Heat shock 70 kDa protein	0.12	0.25	0.68		
A1K436	60 kDa chaperonin 1 (GroEL protein 1) (Protein Cpn60 1)	0.13	1.35	0.68		
Q92407	Glucokinase (EC 2.7.1.2) (Glucose kinase) (GLK)	0.07	0.22	0.68		
P13499	Glutamine synthetase (EC 6.3.1.2) (Glutamate--ammonia ligase) (Fragment)	0.88	1.27	0.69		
Q4FTX2	Adenylosuccinate synthetase (AMPSase) (AdSS) (EC 6.3.4.4) (IMP--aspartate ligase)	-0.52	0.08	0.71		
O59936	40S ribosomal protein S12	-0.88	-0.79	0.71		
A1JRB6	Succinate--CoA ligase [ADP-forming] subunit beta (EC 6.2.1.5) (Succinyl-CoA synthetase subunit beta) (SCS-beta)	-0.52	-0.24	0.74		
P76108	Putative ABC transporter periplasmic-binding protein YdcS	-0.18	0.11	0.74		
Q4K7C1	Protein translocase subunit SecA	0.65	0.55	0.75		
B7LQ20	Glyceraldehyde-3-phosphate dehydrogenase (GAPDH) (EC 1.2.1.12) (NAD-dependent glyceraldehyde-3-phosphate dehydrogenase)	-0.18	-0.46	0.76		
A7E449	ATP-dependent RNA helicase dbp2 (EC 3.6.4.13)	-0.32	-0.08	0.81		
D1ZG64	Eukaryotic translation initiation factor 6 (eIF-6)	-0.05	0.61	0.82		
Q6ZPE2	Myotubularin-related protein 5 (SET-binding factor 1) (Sbf1)	0.57	0.32	0.83		
P27726	Glyceraldehyde-3-phosphate dehydrogenase (GAPDH) (EC 1.2.1.12) (NAD-dependent glyceraldehyde-3-phosphate dehydrogenase)	-0.49	-0.22	0.83		
P65765	FKBP-type peptidyl-prolyl cis-trans isomerase FkpA (PPIase) (EC 5.2.1.8) (Rotamase)	-0.25	-0.27	0.83		
O94313	Carbamoyl-phosphate synthase arginine-specific large chain (EC 6.3.5.5) (Arginine-specific carbamoyl-phosphate synthetase. ammonia chain)	0.05	0.11	0.84		

Accession no.	Protein name (UNIPROT)	Fold Change to Ct		ANOVA p-value	Cluster No.	Common to At61
		Ag ⁺	AgNPs			
B9EAH1	Enolase (EC 4.2.1.11) (2-phospho-D-glycerate hydro-lyase) (2-phosphoglycerate dehydratase)	0.49	0.42	0.85		
P42656	DNA damage checkpoint protein rad24	0.32	-0.46	0.89		
Q8X097	Probable ATP-citrate synthase subunit 1 (EC 2.3.3.8) (ATP-citrate (pro-S)-lyase 1) (Citrate cleavage enzyme subunit 1)	0.48	-0.06	0.92		
Q8XAS6	Iron uptake system component EfeO	-0.35	-0.67	0.93		
Q4KKP4	Tryptophan synthase beta chain (EC 4.2.1.20)	0.13	0.20	0.94		
Q7SDV9	Cytochrome c peroxidase. mitochondrial (CCP) (EC 1.11.1.5)	0.40	0.14	0.94		
Q7RV85	Enolase (EC 4.2.1.11) (2-phospho-D-glycerate hydro-lyase) (2-phosphoglycerate dehydratase) (Embden-meyerhof pathway protein 7)	0.04	-0.23	0.96		
Q4K4P6	Serine hydroxymethyltransferase 2 (SHMT 2) (Serine methylase 2) (EC 2.1.2.1)	0.05	1.16	0.97		
Q1DXH0	Polyadenylate-binding protein. cytoplasmic and nuclear (PABP) (Poly(A)-binding protein) (Polyadenylate tail-binding protein)	0.10	0.17	0.99		
A7EHP6	ATPase get3 (EC 3.6.-.-) (Arsenical pump-driving ATPase) (Arsenite-stimulated ATPase) (Golgi to ER traffic protein 3) (Guided entry of tail-anchored proteins 3)	-0.17	-0.60	0.99		
P16968	Alpha-amylase inhibitor BMAI-1 (Alpha-amylase flour inhibitor) (allergen Hor v 1) (Fragment)	0.14	0.20	1.00		

^a Values were calculated as the average data from. at least four independent experiments. Fold changes of statistically significant proteins (ANOVA. $P < 0.05$) were determined by Log₂ transformation of the ratio values of normalized protein levels obtained using crude protein extracts from *A. tetracladia* after 3 days of exposure to Ag⁺ or AgNPs at concentrations similar to EC₂₀ versus mycelia grown in control medium.

^b The unsupervised clustering analysis was performed considering standardization and the 260 statistically significant proteins across the different experimental conditions (Control. Ct; silver ions. Ag⁺ and silver nanoparticles. AgNPs) were partitioned into 6 clusters.

Appendix 13_Chapter 4

Table S4.1. Transcriptome sequencing, filtering and rRNA reads metrics in the different experimental conditions (Control, CT; Ag⁺ or AgNPs, NP).

Samples	Total Reads sequenced (#)	Paired Reads after filter (#)	Unpaired Reads after filter (#)	rRNA Reads (#) (RiboPicker)
CT 1	52.114.634	51.075.571	1.023.571	375.252
CT 2	39.831.882	39.082.622	737.905	95.201
CT 3	28.135.965	27.796.121	334.646	68.954
Ag ⁺ 1	38.534.012	37.874.504	648.408	374.073
Ag ⁺ 2	40.169.209	39.592.986	566.600	424.523
Ag ⁺ 3	44.530.178	43.920.518	598.630	211.382
NP 1	38.760.656	38.148.689	601.804	168.320
NP 2	37.031.764	36.500.656	521.927	85.387
NP 3	46.290.763	45.572.610	707.008	219.629

Appendix 14_Chapter 4

Description of clusters from Figure 4.2

Cluster A was represented by 118 genes, which expression increased upon AgNP-exposure (average fpkm = 1.38), while only 80 genes increased by Ag⁺ exposure (average fpkm = 0.47). In cluster B, the expression of all 138 genes increased upon AgNP-exposure (average fpkm = 1.43), but the gene expression under Ag⁺-exposure remained similar to the control. In the cluster C, the expression of all 474 genes increased under Ag⁺-exposure (average fpkm = 1.62) while under AgNP-exposure remained unchanged. Cluster D showed that the expression of all 45 genes decreased upon Ag⁺-exposure (average fpkm = -1.49) while under AgNP-exposure was similar to control. Cluster E was represented by 139 genes whose expression decreased upon exposure to AgNPs (average fpkm = -1.37) while under Ag⁺-exposure the expression of 73 genes decreased and of 66 increased. In cluster F (81 genes), the exposure to Ag⁺ or AgNPs increased the expression of 75 (average fpkm = 1.31) and of 58 genes (average fpkm = 0.27), respectively. The cluster G was represented by 16 genes, whose expression was increased by Ag⁺ (average fpkm = 3.03) and decreased by AgNPs (average fpkm = -2.37). The expression of all genes (13) in cluster H increased upon exposure to AgNPs (average fpkm = 3.59) but did not differ from control upon exposure to Ag⁺. Cluster I was represented by 20 genes, whose expression decreased by AgNPs (average fpkm = -3.18); however, exposure to Ag⁺ led to an up-regulation of 13 genes and to a down-regulation of the remaining genes (average fpkm = 0.38). In cluster J, expression of all 12 genes decreased upon exposure to Ag⁺ (average fpkm = -1.72) whereas expression of 9 of those genes decreased upon AgNP-exposure (average fpkm = -0.90).

Appendix 15_Chapter 4

Table S4.2. Gene ontology enrichment of differentially expressed genes of control versus Ag⁺ and AgNPs (BP: Biological Process, CC: Cellular Component; p<0.01).

Category	term	ontology	p-value
GO:0072488	ammonium transmembrane transport	BP	0.0002
GO:0000272	polysaccharide catabolic process	BP	0.0003
GO:1902047	polyamine transmembrane transport	BP	0.0004
GO:1903710	spermine transmembrane transport	BP	0.0004
GO:0015846	polyamine transport	BP	0.0004
GO:0015848	spermidine transport	BP	0.0004
GO:1903711	spermidine transmembrane transport	BP	0.0005
GO:0042791	5S class rRNA transcription by RNA polymerase III	BP	0.0005
GO:0005976	polysaccharide metabolic process	BP	0.0005
GO:0042773	ATP synthesis coupled electron transport	BP	0.0007
GO:0043335	protein unfolding	BP	0.0009
GO:0000296	spermine transport	BP	0.0010
GO:0003333	amino acid transmembrane transport	BP	0.0013
GO:0015695	organic cation transport	BP	0.0014
GO:0015696	ammonium transport	BP	0.0016
GO:0015695	organic cation transport	BP	0.0016
GO:0006422	aspartyl-tRNA aminoacylation	BP	0.0016
GO:0015696	ammonium transport	BP	0.0016
GO:0009251	glucan catabolic process	BP	0.0018
GO:0010383	cell wall polysaccharide metabolic process	BP	0.0019
GO:0098704	carbohydrate import across plasma membrane	BP	0.0022
GO:0030245	cellulose catabolic process	BP	0.0026
GO:0034219	carbohydrate transmembrane transport	BP	0.0026
GO:0051275	beta-glucan catabolic process	BP	0.0026
GO:0034605	cellular response to heat	BP	0.0029
GO:0010410	hemicellulose metabolic process	BP	0.0032
GO:0006658	phosphatidylserine metabolic process	BP	0.0032
GO:0030243	cellulose metabolic process	BP	0.0033
GO:0042026	protein refolding	BP	0.0034
GO:0055085	transmembrane transport	BP	0.0036
GO:0070086	ubiquitin-dependent endocytosis	BP	0.0037
GO:0015871	choline transport	BP	0.0043
GO:0031460	glycine betaine transport	BP	0.0043
GO:0034229	ethanolamine transport	BP	0.0043
GO:1900749	(R)-carnitine transport	BP	0.0043
GO:0006660	phosphatidylserine catabolic process	BP	0.0044
GO:0010996	response to auditory stimulus	BP	0.0044
GO:0046462	monoacylglycerol metabolic process	BP	0.0044
GO:0052651	monoacylglycerol catabolic process	BP	0.0044
GO:0006865	amino acid transport	BP	0.0046
GO:0046292	formaldehyde metabolic process	BP	0.0047
GO:0046294	formaldehyde catabolic process	BP	0.0047
GO:0006660	phosphatidylserine catabolic process	BP	0.0049

GO:0010996	response to auditory stimulus	BP	0.0049
GO:0046462	monoacylglycerol metabolic process	BP	0.0049
GO:0052651	monoacylglycerol catabolic process	BP	0.0049
GO:0044036	cell wall macromolecule metabolic process	BP	0.0049
GO:0018890	cyanamide metabolic process	BP	0.0051
GO:0044247	cellular polysaccharide catabolic process	BP	0.0054
GO:0055085	transmembrane transport	BP	0.0054
GO:0006145	purine nucleobase catabolic process	BP	0.0058
GO:0051273	beta-glucan metabolic process	BP	0.0059
GO:0043090	amino acid import	BP	0.0062
GO:0071966	fungus-type cell wall polysaccharide metabolic process	BP	0.0064
GO:0051348	negative regulation of transferase activity	BP	0.0067
GO:0043327	chemotaxis to cAMP	BP	0.0070
GO:0009698	phenylpropanoid metabolic process	BP	0.0070
GO:0045491	xylan metabolic process	BP	0.0075
GO:0045493	xylan catabolic process	BP	0.0075
GO:0015804	neutral amino acid transport	BP	0.0076
GO:0043335	protein unfolding	BP	0.0078
GO:0015824	proline transport	BP	0.0081
GO:0015969	guanosine tetraphosphate metabolic process	BP	0.0083
GO:0034035	purine ribonucleoside bisphosphate metabolic process	BP	0.0083
GO:0015696	ammonium transport	BP	0.0084
GO:0006073	cellular glucan metabolic process	BP	0.0085
GO:0015697	quaternary ammonium group transport	BP	0.0088
GO:0015838	amino-acid betaine transport	BP	0.0088
GO:0015879	carnitine transport	BP	0.0088
GO:0010383	cell wall polysaccharide metabolic process	BP	0.0093
GO:0055114	oxidation-reduction process	BP	0.0094
GO:0015695	organic cation transport	BP	0.0098
GO:0044042	glucan metabolic process	BP	0.0099
GO:0005576	extracellular region	CC	0.0000
GO:0005887	integral component of plasma membrane	CC	0.0000
GO:0005887	integral component of plasma membrane	CC	0.0001
GO:0031226	intrinsic component of plasma membrane	CC	0.0001
GO:0031226	intrinsic component of plasma membrane	CC	0.0006
GO:0005886	plasma membrane	CC	0.0009
GO:0005576	extracellular region	CC	0.0010
GO:0005887	integral component of plasma membrane	CC	0.0019
GO:0044459	plasma membrane part	CC	0.0024
GO:0010339	external side of cell wall	CC	0.0032
GO:0008328	ionotropic glutamate receptor complex	CC	0.0044
GO:0032281	AMPA glutamate receptor complex	CC	0.0044
GO:0032839	dendrite cytoplasm	CC	0.0044
GO:0098878	neurotransmitter receptor complex	CC	0.0044
GO:0000127	transcription factor TFIIC complex	CC	0.0046
GO:0008328	ionotropic glutamate receptor complex	CC	0.0049
GO:0032281	AMPA glutamate receptor complex	CC	0.0049
GO:0032839	dendrite cytoplasm	CC	0.0049
GO:0098878	neurotransmitter receptor complex	CC	0.0049
GO:0031224	intrinsic component of membrane	CC	0.0065

GO:0034703	cation channel complex	CC	0.0070
GO:0034703	cation channel complex	CC	0.0071
GO:0031226	intrinsic component of plasma membrane	CC	0.0083
GO:0031520	plasma membrane of cell tip	CC	0.0086
GO:0044426	cell wall part	CC	0.0096

Appendix 16_Chapter 4

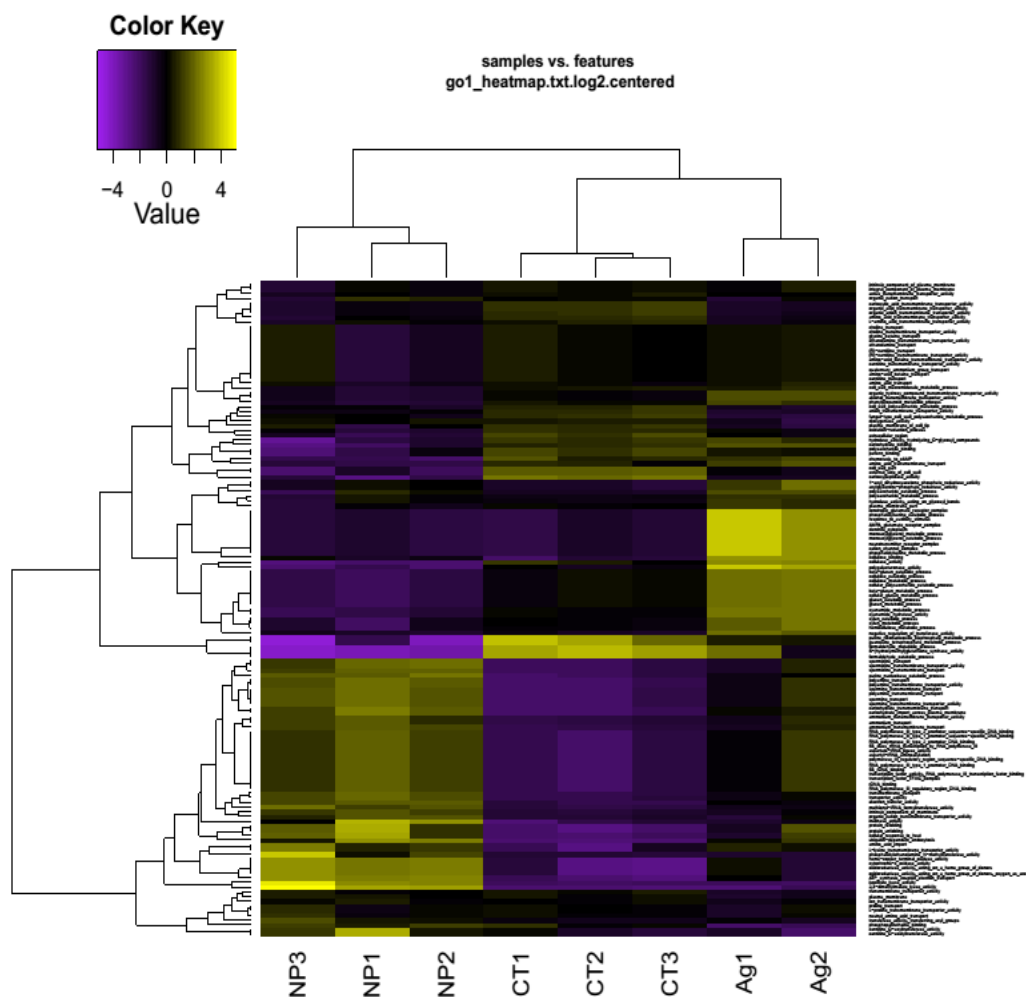


Figure S4.1. Gene ontology enrichment of differentially expressed genes of control (CT) versus Ag⁺ (Ag) and AgNPs (NP). Heatmap showing the expression sum of gene related to each GO term. Enrichment GO terms with a p-value lower than 0.01. This analysis involved 347 genes and 139 GO terms.

Appendix 17_Chapter 4

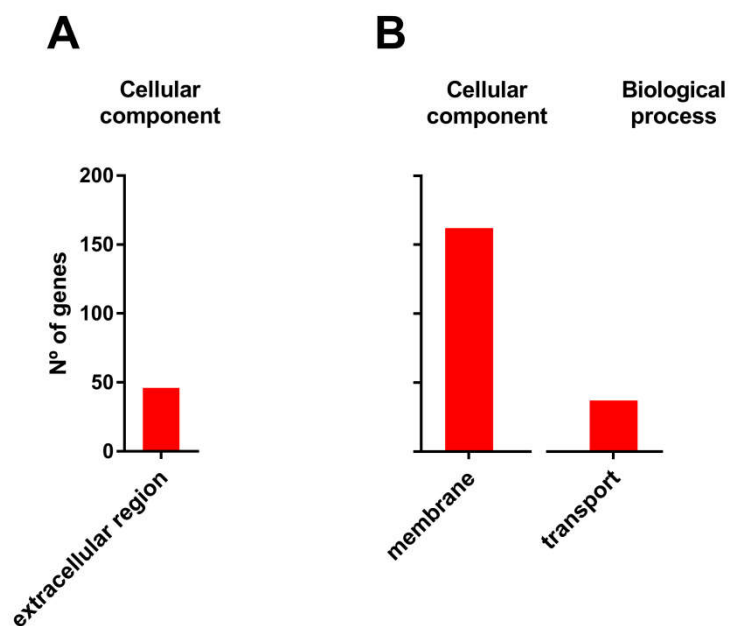


Figure S4.2 Histograms of gene ontology (GO) classification. The results are summarized in two main categories: cellular component and biological process. The y-axis indicates the number of up-regulated genes in a category and the x-axis indicates the subcategories. A) and B) correspond to Ag^+ vs AgNPs, where A) represent the up-regulated genes under exposure to Ag^+ and B) the up-regulated genes under exposure to AgNPs. Only GO terms with more than 5 genes were considered in each category.